Evaluating the interaction between curved coastline and beach width by using long waves

A case study of the Hondsbossche Dunes

A. Giezen

TU Delft

SVASEK HYDRAULICS
COASTAL, HARBOUR AND RIVER CONSULTANTS

Evaluating the interaction between curved coastline and beach width by using long waves

A case study of the Hondsbossche Dunes

by

A. Giezen

to obtain the degree of

Master of Science
in Civil Engineering

at the Delft University of Technology,

to be defended publicly on Wednesday August 28, 2024 at 11:00 AM.

Student number:	4940814	
Project duration:	November, 2023 - August, 2024	
Thesis committee:	Dr. ir. M.A. de Schipper	TU Delft
	Dr. ir. J. Kroon	Svašek Hydraulics
	Dr. ir. A.J.H.M. Reniers	TU Delft
	Dr. ing. M.Z. Voorendt	TU Delft

TU Delft

SVAŠEK HYDRAULICS
COASTAL, HARBOUR AND RIVER CONSULTANTS

Acknowledgement

This Master's thesis marks the end of my Master's degree in Civil Engineering at the Delft University of Technology. I followed the Hydraulic engineering track with the specialisation of Coastal Engineering. This thesis also marks the end of my study time in Delft. For me this has been a very pleasant time in which I met a lot of new people and made new friends. In this acknowledgement I would like to express my thanks to the people who helped me during the writing of the thesis, but also to the people who supported me during the past years.

I would like to thank my thesis committee members, Dr. ir. M.A. de Schipper, dr. ir. J. Kroon, dr. ir. A.J.H.M. Reniers and dr. ing. M.Z. Voorendt, for their support and input over the past few months. Matthieu de Schipper, the chair of my committee, whose critical questions and comments made me think about the results and how I could improve the content of the thesis every time. I would also like to thank Matthieu de Schipper for his enthusiasm on the subject and the knowledge he has with which he helped me. Next, I want to thank Ad Reniers who has a lot of knowledge about XBeach and was always enthusiastic during the meetings. With his feedback and tips, he managed to keep me motivated and ensure a better result from the thesis. I want to thank Mark Voorendt for his academic point of view on the report and tips on writing a thesis.

I performed this research in collaboration with Svašek Hydraulics in Rotterdam. I want to give a special thanks to Anna who guided me throughout the thesis and provided me with a lot of help. She has been closely involved in my research. She has helped me learn to understand XBeach and set up the model simulations in XBeach. I would also like to thank her for the feedback I received in the weekly meetings which provided more and better results. I would like to thank Ype for his help in setting up the XBeach model of the Hondsbossche Dunes and for his guidance during the period when Anna was on vacation. Furthermore, I would like to thank all the other colleagues at Svašek Hydraulics for the great time I had, all the help, the feedback and of course the fun activities outside of working hours. I would also like to thank Svašek Hydraulics for facilitating a working environment over the past few months.

Last, but not least, I would like to thank my family for the support I received from them throughout my studies. I also would like to thank my friends for all their support and enthusiasm throughout the study.

A. Giezen
Delft, August 2024

Abstract

Safety assessments are taken every five years to examine whether the coast is safe enough. After investigation, it was found that one of the weak spots is the Hondsbossche and Pettemer Sea defence (from hereafter referred to as HPZ) which required reinforcement at this location. Therefore, a mega nourishment was implemented in 2015 to ensure the safety of the hinterland. The implementation of this mega nourishment created the Hondsbossche Dunes (from hereafter referred to as HD). After the implementation of the mega nourishment, it was soon found that the width of the beach decreased. The beach width is defined as the horizontal distance between the waterline and the dune foot position which is defined at elevation NAP + 3.0 m. The decrease in beach width occurred mainly on the edges where there is a stronger curvature, so more change in shoreline orientation, compared to the other parts of the nourishment. As a result of the decrease in beach width, an additional nourishment was implemented in 2018 to meet the requirements. These are not the safety requirements but the beach width is important for recreation so the beach cannot be too narrow.

The aim of this research is to improve understanding of beach width reducing processes at curved coastlines to improve predictions of beach width on a scale of ~5 years after implementing a nourishment at the HD. The relationship between the curved coastline and long waves and its influence on the change in beach width was investigated. Special attention is given to the role of infragravity waves. Hereto the numerical model XBeach is used which can simulate morphodynamics with and without infragravity forcing. From the literature review, it follows that long waves, also called infragravity waves, are formed from small waves. A difference between infragravity waves and short waves is that the processes of the infragravity waves take place mainly in the surf zone and swash zone, while most of the short waves are dissipated in the surf zone and swash zone.

To determine the influence of coastline curvature and infragravity waves on beach width change, two types of models were run. The first model was a schematic model where an alongshore uniform coast is applied in the model to neglect the influence of alongshore variability in cross-shore profiles. In addition, multiple runs were performed varying the strength of the curvature and the mode (stationary mode, so without infragravity waves and groupiness, or surfbeat with infragravity waves) so that the results could be compared. This study showed that including infragravity waves results in a different predicted beach width change. In addition, stronger curvature leads to larger gradients in longshore sediment transport and thus the change in beach width.

The second model run was the HD's complex model where the conditions as present in reality were applied, i.e., bathymetry and wave conditions. Based on the XBeach model of the HD, it can be concluded that the prediction is reasonably similar for the first year of the simulation. The first year of the simulation is the second year after the nourishment is implemented, i.e. 2016, so initial effects are not included in the result of the measurements. However, the predictions and measurements hardly match in the other years resulting in a very low correlation which follows from the validation.

Contents

Nomenclature

Abbreviations

Abbreviation	Definition
HD	Hondsbossche Dunes (”Hondsbossche Duinen” in Dutch)
HPZ	Hondsbossche and Pettemer sea defence (”Hondsbossche en Pettemer Zeewering” in Dutch)
JARKUS	Yearly Coastal Measurements (”Jaarlijkse Kustmetingen” in Dutch)
MHW	Mean High Water
MHWS	Mean High Water Spring
MKL	Momentary Coastline Position (”Momentane Kustlijn” in Dutch)
MLW	Mean Low Water
MLWS	Mean Low Water Spring
Morfac	Morphological Acceleration Factor
NAP	Amsterdam Ordnance Datum (”Normaal Amsterdams Peil” in Dutch)
RSP	Reference system of Rijkswaterstaat (”Rijksstrandpaal” in Dutch)
UTM	Universal Transverse Mercator-stelsel

1

Introduction

1.1. Motivation for this research

A large part of the Dutch coast, approximately 75 per cent, consists of sandy beaches and dunes. These sandy beaches and dunes play an important role in protecting the low-lying hinterland of the Netherlands from flooding. As a result, the sandy beaches and dunes function as a primary flood defence system (Muller et al., 2012). The Dutch coast is subject to erosion, which is why beach and shoreface nourishments have been carried out since 1990 so that the damage from erosion is limited (Luijendijk et al., 2017). When a nourishment is implemented in the Netherlands, much attention is paid to improving safety and maintaining the total volume of sand, while less attention is paid to the width of the beach. Abroad, often more attention is paid to the width of the beach and less to improving safety (Brand et al., 2022). The beach width is important for recreation (Broer et al., 2011). It is calculated by measuring the horizontal distance between the waterline and the dune foot position, which is defined at NAP + 3.0 m (Kroon et al., 2022).

The safety of the hinterland is reviewed every five years by an assessment and from this, the so-called weak spots along the Dutch coast are identified. One of these weak spots turned out to be the Hondsbossche and Pettemer Sea defence ("Hondsbossche and Pettemer Zeewering" in Dutch; from hereafter referred to as HPZ). This sea defence consisted of a hard sea dike with a stone revetment, as shown in Figure 1.1. The HPZ is located on the North-Holland coast between Camperduin and Petten. A safety assessment showed that the HPZ was no longer safe enough and therefore it was needed to be reinforced. This reinforcement was performed in 2015.

Figure 1.1: The Hondsbossche and Pettemer Sea defence before the implementation of the nourishment and thus the Hondsbossche Dunes (Rijkswaterstaat, 1985).

In 2015, the HPZ was strengthened by implementing a foreshore, beach and dune nourishment in front of the old sea defence. The total volume of sand which was used for this nourishment is 35 million m^3. This created the Hondsbossche Dunes (”Hondsbossche Duinen” in Dutch; from hereafter referred to as HD), a nourishment which is twelve kilometres long. As a result of the nourishment, safety has been increased and space has been created for nature and recreation.

Figure 1.2: The Hondsbossche and Pettemer Sea defence after the implementation of the nourishment; the Hondsbossche Dunes (Bechauf et al., 2021).

The nourishment of the HD is seen as a mega nourishment. In both the Netherlands and abroad, not many nourishments of this size have yet been implemented. In the Netherlands, an example of another mega nourishment is the Sand Engine located at the coast of Delfland (Teixeira et al., 2024). Also in the United Kingdom, there is a mega nourishment implemented which is inspired by the Sand Engine in the Netherlands (Johnson et al., 2020).

After the nourishment was implemented in 2015, the width of the beach decreased rapidly. The decrease in beach width is mainly seen at the curved edges of the nourishment in the north and south. The losses in sediment are higher than what was expected based on predictions which are made during the design phase of the HD. These are also the locations where beach pavilions and recreation are present (Leenders et al., 2018). This report attempts to increase the understanding of the development of nourishments over time.

1.2. Problem analysis

The reduction in beach width at the HD is larger than what was predicted in advance during the design phase. These predictions were performed using the depth-averaged FINEL 2D model. During the design phase, it was assumed that dune volume would be the controlling parameter for determining when new maintenance was needed. However, in reality, it turns out that not only the dune volume is a controlling parameter, but also the beach width. The dune volume can meet the requirements while there is a large reduction in beach width. This results in the need to perform more maintenance because otherwise, the beach becomes too narrow for recreation. For this reason, an additional nourishment was implemented in 2018 (Leenders et al., 2018).

To figure out the cause and consequences of the reduction in beach width, a model is needed that predicts the development of the HD in the coming years. With the knowledge currently available, it is not possible to make predictions and to get an answer to the question of what causes there to be a difference between the predictions based on the model and the reality. Several models have been tested, but so far they have not been able to make accurate predictions relative to reality.

Several studies have been performed in the past on the relationship between shoreline curvature and beach width development (Ashton & Murray, 2006a; Den Heijer, 2013; Lauzon et al., 2019; Lazarus & Murray, 2007; Valvo et al., 2006). Den Heijer (2013) conducted his research using XBeach taking into account long waves. However, the results of his study were not compared with results where only short waves are considered with which it is not possible to conclude the influence of long waves. The other studies also did not specifically consider the effect of long waves on beach width development.

Arends (2018) performed a study of nourishment development using the numerical model FINEL 2D. This study did not consider infragravity waves, this type of wave is not implemented in FINEL 2D. It follows from the study that the results based on FINEL 2D lead to an underestimation compared to the measured results. This underestimation can be caused by several factors, one of which is the absence of long waves.

1.3. Research objective and research questions

This research project aims to improve understanding of beach width reducing processes at curved coastlines to improve predictions of beach width on a scale of ~5 years after placing a nourishment at the HD. This research therefore focuses on the following main question:

To what extent can the interaction between the curved coastline and the beach width of a mega nourishment, with a focus on the Hondsbossche Dunes, be predicted using a numerical model including long waves?

To answer this research question, the following sub-questions will need to be answered. The processes contributing to the development of the mega nourishment at the HD must be known. The sub-questions are as follows:

- What is the development of the mega nourishment of the Hondsbossche Dunes in the first years after the nourishment was implemented? Can differences be seen between development over the years and processes?
- What is the impact of long waves and coastal curvature on the reduction in beach width when tested in an idealised coastal setting?
- To what extent is the 2DH model, XBeach, able to predict the reduction in beach width of the Hondsbossche Dunes?

The second sub-question is divided into two sub-questions:

- What is the effect of the strength of coastal curvature on the change in beach width?
- What is the difference between the change in beach width when the simulation is run in stationary mode and in surfbeat mode?

1.4. Approach

This section discusses the stages taken to conduct the research. The first stage to perform is the literature review. The purpose of the literature review is to explain relevant concepts and the processes that influence beach width development. Furthermore, this chapter also discusses other studies on coastline curvature which can be used later in the discussion to compare whether the results agree with each other.

To answer the main question and sub-questions, the research is divided into two parts, namely a data study and numerical modelling. For numerical modelling, the numerical model XBeach is used. A detailed description of this numerical model is given in Section 3.2.

The second stage in the research is performed using a data study that allows the first sub-question, *"What is the development of the mega-supplementation of the Hondsbossche Dunes in the first years after the suppletion was built? Can differences be seen between the development over the years and the processes?"*, can be answered. This data study compares beach developments over the different years based on bathymetric data from the JARKUS data. For example, the development of the beach width and the development of the orientation of the coastline are examined. Furthermore, an analysis

of hydrodynamic data was performed to investigate whether these processes have a relationship with beach developments.

The other two sub-questions are answered by numerical modelling. Based on the literature review performed in stage one, sub-question 2 is formulated, *"What is the impact of waves and coastal curvature on the reduction in beach width when tested in an idealised coastal setting?"* and in order to answer this sub-question, a schematic model is built, this is stage three of the research. The schematic model is discussed in more detail in Section 3.3.

In stage four, the final sub-question is answered. The final sub-question, *"To what extent is the 2DH model, XBeach, able to predict the reduction in beach width of the Hondsbossche Dunes?"*, is answered by using the numerical model XBeach simulating reality as closely as possible. To answer this sub-question, bathymetry is applied to the HD which can be obtained from both the Vaklodingen surveys and the JARKUS data and a representative wave climate is applied. A more detailed description of the XBeach model can be found in Section 3.2. In this stage, validation of the XBeach model is also performed by comparing the simulation results with the measurement results.

1.5. Thesis outline

Chapter 2 contains stage 1, the literature review, where the relevant processes that may influence the change in beach width are discussed. The knowledge gained from the literature review can be used in the schematic model, Chapter 5. This model examines the influence of coastline curvature and long waves but also performs a sensitivity analysis describing what parameters have a major influence on the results. The literature review also includes studies previously performed that can be used in the discussion so that results can be compared.

The literature review is followed by the methodology. The methodology contains the data study. The data study can be used as input parameters in the models run in Chapter 5 and Chapter 6. Furthermore, this chapter explains why XBeach was chosen and discusses the settings of the two different models. Thus, this chapter provides a preliminary introduction to stages three and four.

Chapter 4 gives the data analysis of the development of the HD, so this is stage two. In this chapter, the development of relevant parameters is given and correlations between them are examined. This chapter is based on measured JARKUS data. The results of this chapter can be used to compare model outcomes with measured data.

The results of the schematic XBeach model are presented in Chapter 5 and the results of the complex XBeach model of the HD are presented in Chapter 6. In Chapter 6, validation of the model is also performed.

The study concludes with the discussion in Chapter 7 which compares the results from the previous two chapters, Chapter 5 and Chapter 6, with the results from previous studies.

The report concludes with the conclusion and recommendations in Chapter 8. The conclusion first answers the sub-questions and then answers the research question. The recommendations discuss what can be done differently in a subsequent study.

2

Literature Review

This chapter, stage one of the research, aims to discuss relevant processes and concepts for this study. Section 2.1 discusses the most important definitions from the beach profile, including beach width. Section 2.2 discusses what short waves are and what long waves are. Section 2.3 discusses the important processes that can lead to coastline changes. Here, cross-shore sediment transport and longshore sediment transport are discussed. The last section, Section 2.4 gives the definition of coastal curvature. In addition, this section also discusses the results of previously performed studies.

2.1. Introduction of the beach profile

This section discusses some relevant definitions and terms used in this research. The most important term in this research, beach width, is discussed in Subsection 2.1.2 where is explained how the beach width can be determined.

2.1.1. Depth of closure

The depth of closure is the depth at which repeated observations over a certain period of time, for instance one year, show no (significant) changes in the bottom elevation (Morang & Birkemeier, 2019). This depth is relevant to determine the active profile because the depth of closure is the lowest depth where the profile is active. In the figure below, Figure 2.1, the beach profile measured at different times shows at which depths varieties still occur. The depth of closure is indicated by d_i and is also called the inner depth of closure or the closure depth. Besides the inner depth of closure, the outer depth of closure, d_l, is shown in the figure. The outer depth of closure is the depth at which transition is made from the continental shelf to the lower shoreface. At depths larger than the outer depth of closure, waves do not play a significant role in sediment transport (Kraus et al., 1998).

The littoral zone is the zone closest to the beach, i.e. the zone where the water depth is lower than the inner depth limit. In the littoral zone, most of the bottom dynamics take place which can be seen in the figure because the grey zone, indicating the seasonal ranges, is present in the littoral zone. There is a seasonal range because the wave conditions, and thus the hydraulic forces, during summer and winter are different which leads to a variation in the bottom level. The average wave conditions during the summer allow the sand to settle and thus the bottom level is higher. During the winter, generally, there are more storms which leads to erosion and thus a lower bottom level. Due to the different conditions during the years, the profile measurements which determine the depth of closure should include periods with storm conditions and calm conditions (Bosboom & Stive, 2023; Hinton & Nicholls, 2015).

The offshore zone and shoaling zone are also shown in Figure 2.1. The shoreface in the beach profile is the part of the profile where waves will influence the profile. Generally, the shoreface begins at depths between 10 and 20 m. The shoreface (upper shoreface and lower shoreface) is the part that will be focused on in this research. In the lower shoreface, the waves are between the positions where the waves begin to feel the bottom, at d_i, and where the waves will break, at d_l. In this zone, the waves will begin to shoal with the amplitude increasing. In the upper shoreface, the waves will break so this zone

is morphologically the active zone (Anthony & Aagaard, 2020; Elgar & Guza, 1985).

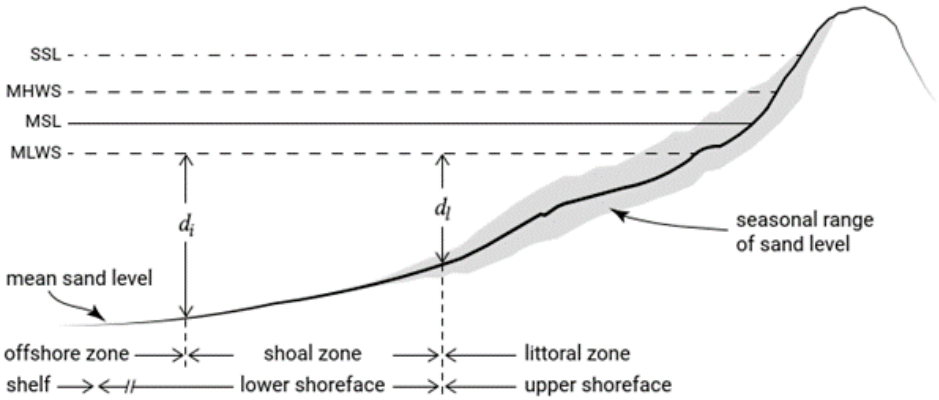

Figure 2.1: Depth of closure, d_l, according to Hallermeier (Bosboom & Stive, 2023). The outer depth limit is indicated with d_i and the inner depth limit is indicated with d_l. The tidal levels are indicated with MHWS (Mean High Water Spring) and MLWS (Mean Low Water Spring).

2.1.2. Beach width

In this report, one of the most important parameters is the beach width. The beach width is defined as the distance between the waterline position and the dune foot position. Here, the waterline position x_{WL} is defined as the average position of the intersection with the Mean High Water Level (MHWL) and the Mean Low Water Level (MLWL) (De Vries et al., 2012). The elevations of these water levels are also shown in Figure 2.2.

The dune foot position, which is the most seaward position of the dune, of the Dutch coast is generally assumed to be equal to NAP + 3.0 m, where NAP is the Dutch reference level (Van IJzendoorn et al., 2021). The HD is located in the Netherlands and therefore in this report, the dune foot position is assumed to be at NAP + 3.0 m.

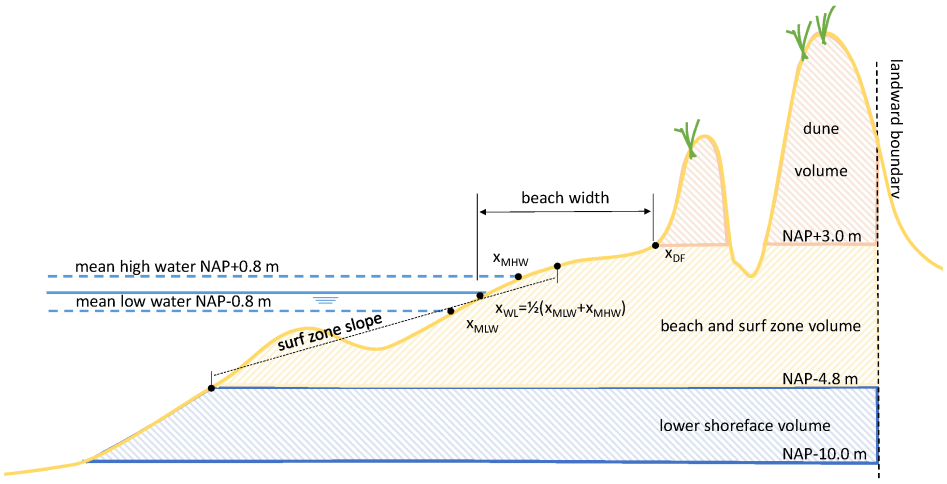

Figure 2.2: Cross-shore profile of a beach, including the beach width (Kroon et al., 2022).

2.1.3. Momentary Coastline position

The Momentary Coastline Position ("Momentane Kustlijn" in Dutch; from hereafter referred to as MKL) is the location of the coastline for a specific year and can be calculated from the yearly coastal measurements ("Jaarlijkse Kustmetingen" in Dutch; from hereafter referred to as JARKUS). An annual calculation of the MKL is made to determine if there is (annual) erosion. There is a correlation between the MKL and beach width where an increase in beach width leads to a seaward shift of the MKL and hence there is accretion rather than erosion (Damsma, 2009). The MKL can be defined by the following equation (Hillen et al., 1991):

$$MKL = \frac{A}{2H} + x_{dunefoot} \tag{2.1}$$

where:

A	area between the dune foot position and the position that is 2H below the dune foot	[m^2]
H	vertical distance between dune foot and the Mean Low Water Level	[m]
$x_{dune\ foot}$	horizontal distance between the dune foot and the location of the Rijksstrandpaal	[m]

As described in Subsection 2.1.2, the position of the dune foot is assumed to be NAP + 3.0 m. This makes the lower limit for determining the MKL position equal to NAP - 4.6 m (Kroon et al., 2020).

The position of the MKL is compared with the Basal Coast Line ("Basis Kustlijn" in Dutch; from hereafter referred to as BKL) (Taal et al., 2006). The BKL is the 1990 low water line which is used for reference. If the MKL lies behind the BKL, i.e. if the position of the MKL is more landward than the position of the BKL, then intervention is required which usually means the implementation of a nourishment (De Ruig & Hillen, 1997; Hillen & Roelse, 1995).

2.1.4. Equilibrium profile

Morphological changes occur when the morphological system is not in equilibrium with the forcing, such as currents, waves and tides. In general, the system reacts quickly immediately after a change and reacts more slowly as the system moves toward the new equilibrium. Thus, in the case of the nourishment of the HD, this would imply that the greatest changes and possible reduction in beach width occur in the first few years after the nourishment is implemented (Eichentopf et al., 2019).

The coastal profile attempts to balance each moment due to different conditions. This means, for example, that if the water level rises due to sea level rise, the coastal profile will adjust accordingly. Not only does the water level affect the change in the coastal profile, but waves also play a role. It is discussed in Section 2.3 that higher waves generally lead to more sediment transport. The coastline tries to adjust to the conditions present, which are not constant over time. The average profile from these changes is called the dynamic equilibrium profile (Dean, 1995; Jara et al., 2015).

2.2. Coastal hydrodynamics

This section explains the definitions of both short waves and long waves. By explaining the definition of both types of waves, the difference between them can be investigated.

2.2.1. Short waves

Short waves are waves generated by wind. These waves are generated in deep water and propagate towards the shore. The waves are also called sea waves if they are created by wind and they are called swell waves if they continue to propagate to areas other than where they were created. Short waves are called short waves because these types of waves have a short period with an associated frequency of between 0.04 and 1 Hz (Bertin et al., 2018; Van Dongeren et al., 2007).

In deep water, waves have a sinusoidal shape. This shape of the waves changes when the waves enter shallower water as a result of processes that lead to a transformation of the waves. Examples of these types of processes are refraction and shoaling (Van der Zanden, 2016). If waves are affected by the bottom because they have entered shallow water, the propagation velocity of the waves decreases.

Besides the propagation velocity, the wavelength also decreases, while the wave height increases and the wave energy remains constant. Moreover, the waves are no longer symmetrical and there is asymmetry about the horizontal axis. The periods of the peaks become smaller, while the periods of the troughs become longer. The phenomenon described above is called skewness. This is also depicted in Figure 2.3. The waves will propagate further towards the coast eventually creating a steep front face and a gentle rear face. This phenomenon is called wave asymmetry and, over time, will lead to the breaking of waves (Bosboom & Stive, 2023).

Once waves break, because the wave height is too high compared to the water depth, the waves will continue to propagate as a roller. A roller continues to propagate in the surf zone towards the shore, but it dissipates energy during propagation (see Figure 2.3). When the roller reaches the shore, it will up run on the beach with a decreasing speed due to e.g. the friction present on the beach. The zone in which this happens is called the swash zone and this zone is also shown in the figure below. In this zone, all short waves are already broken and mainly the infragravity waves can become dominant (Bertin et al., 2018; Van der Zanden, 2016).

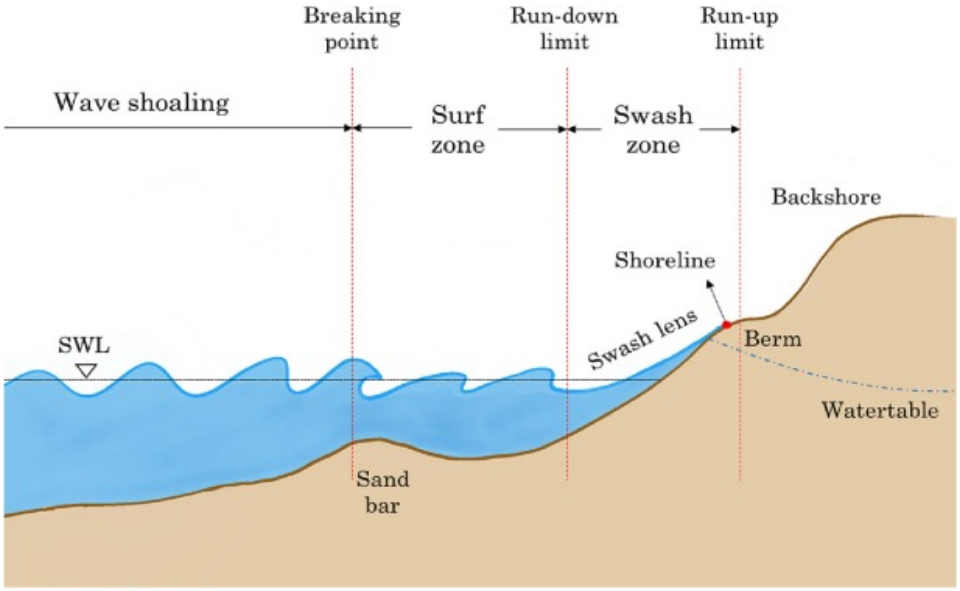

Figure 2.3: A beach profile including the different zones (Chen et al., 2023).

2.2.2. Infragravity waves

Infragravity waves play an important role in the nearshore processes that take place (Roelvink et al., 2009). This type of wave is formed by sea and swell waves, or short waves. The frequency of infragravity waves is generally between 0.004 Hz and 0.04 Hz (Bertin et al., 2018).

Figure 2.4 shows the bound long wave phenomenon compared to the short waves. The larger waves in the short wave group transport more momentum than the lower waves. As a result, most of the radiation stress occurs under the large waves and there is a decrease in the water level under the large waves and an increase in the water level under the small waves because there needs to be a balance between the pressure force and the radiation stress. The resulting wave is called a bound long wave because the infragravity wave propagates with the group velocity. This bound long wave is 180 degrees (π rad) out of phase with respect to the short wave group (Rossouw et al., 2013).

Due to a variation in wave height within the short wave group, waves will break at different locations. Higher waves break more offshore than lower waves. A consequence of breaking waves is that the bound long waves no longer propagate as a bound wave but as free waves (Munk, 1949; Ruessink, 1998).

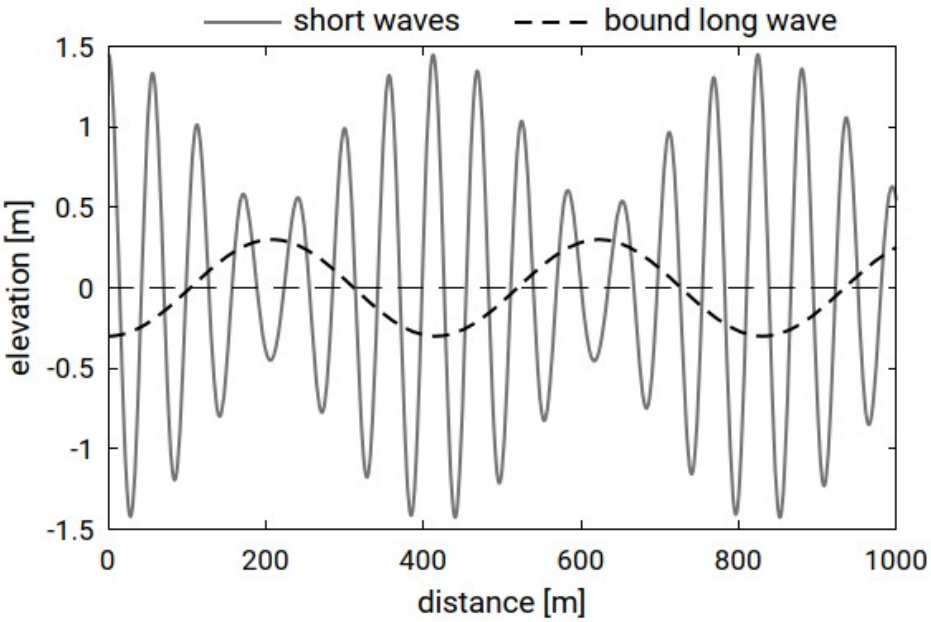

Figure 2.4: A bound long wave. This bound long wave is perfectly out of phase with the group of the short waves (Bosboom & Stive, 2023).

Wave run-up is the maximum height that waves reach in the beach profile. During storms, there are higher waves which results in a higher wave run-up. There is a positive correlation between wave height and wave run-up. A larger wave run-up leads to more erosion of the beach and dune resulting in a decrease in beach width. Besides a positive correlation between wave height and wave run-up, there is also a positive correlation between wave run-up and beach slope. On a steeper beach, erosion takes place more rapidly and hence a change in beach width (Marra et al., 2001; Mather et al., 2010).

2.3. Causes of coastline changes

This section discusses important processes that affect the morphological development of the HD and hence the reduction of beach width. The transport processes, longshore sediment transport and cross-shore sediment transport are discussed because these parameters contribute to the morphological changes of a nourishment. Hereby, the parameters that affect the magnitude of sediment transport are discussed.

Sediment transport is often described as a process consisting of both cross-shore transport processes and longshore transport processes. These two processes are described in this section.

2.3.1. Cross-shore transport

Cross-shore sediment transport is the transport of sediment perpendicular to the shoreline. This transport is caused by wave activity, tides and other hydrodynamic forces present (Seymour, 2005a). In general, sedimentation is referred to when there is an increase in bed level and erosion is referred to when there is a decrease in bed level. This means that we speak of sedimentation when there is a net inflow of sediment and we speak of erosion when this occurs the other way around (Bosboom & Stive, 2023).

There is transport in the shoreward direction when the beach volume increases while there is offshore transport when there is a decrease in the amount of sand above the mean sea level and an increase in the amount of sand below the mean sea level. During a storm, the cross-shore sediment transport has a major impact on erosion and therefore cross-shore transport also affects the development of beach width in the HD. An example of this is the summer and winter profiles of the beach during the year. In a summer profile, the beaches are wider and have fewer bars nearshore, while the winter profile consists of narrow beaches with bars present more offshore. These profiles imply that differences in

beach width can occur during the year due to cross-shore transport. The difference in these profiles is caused by waves, as higher waves lead to higher net sediment transport than lower waves (Seymour, 2005a).

The reason why there are narrower beaches during winter and the bars present are more offshore is related to the undertow. Due to storm conditions and the associated higher waves, sediment will be transported in the offshore direction by undertow. Undertow can be described as a return flow in the offshore direction. The return flow is small in waves that do not break. For breaking waves, the return flow is called undertow. The undertow causes sediment to be transported in an offshore direction because the current is directed offshore and this flow takes place in an area of high sediment concentration due to breaking waves (Bosboom & Stive, 2023).

Asymmetry leads to an onshore directed sediment transport because the larger peaks produce more suspended sediment and these waves are onshore directed (Grasso et al., 2011; Roelvink & Stive, 1989). As a result of wave skewness, the crests of the wave propagate faster than the troughs. The waves start leaning forward creating an asymmetric shape of the waves which is called wave asymmetry. The waves break as the waves become increasingly asymmetric (De Wit, 2022).

The energy of infragravity waves, with their longer wave periods and higher wave energy, plays a more substantial role in sediment transport than short waves, leading to larger changes in the beach morphology when infragravity waves are present (Power & Hughes, 2008). The direction, as well as the magnitude, of cross-shore sediment transport due to infragravity waves, depends on the ratio of these waves to short waves. In the outer surf zone, sediment is suspended by the breaking short waves. The largest short waves occur during the troughs of the infragravity waves and hence the sediment transport is offshore directed. In the inner surf zone, most of the infragravity waves are free waves and the largest short waves take place at the crests of the infragravity waves making the cross-shore sediment transport onshore directed. As the height of the infragravity wave increases relative to the height of the short wave, infragravity waves can also stir sand from the bottom. This sand is transported offshore (Bertin et al., 2018; de Bakker et al., 2016).

2.3.2. Longshore transport

Longshore transport is when the sediment is transported along the coast (Seymour, 2005b). Here the sediment transport occurs mainly in the surf zone. Coastal changes occur when there is a gradient in longshore sediment transport. There is a stable coast and no changes occurring once the sediment output and sediment input are equal to each other (Bosboom & Stive, 2023).

To calculate longshore sediment transport, there are several formulas that can be used, for example, the formula of Kamphuis. The formula for Kamphuis (1991) is as follows (Van Rijn, 2014):

$$Q_{t,im} = 2.33(T_p)^{1.5}(tan\beta)^{0.75}(d_{50})^{-0.25}(H_{s,br})^2[sin(2\theta_{br}]^{0.6} \tag{2.2}$$

where:

$Q_{t,im}$	the longshore sediment (immersed mass) transport	[kg/s]
T_p	the peak wave period	[s]
tanβ	the beach slope	[-]
d_{50}	the median particle size in the surfzone	[m]
$H_{s,br}$	the significant wave height at breaker line	[m]
ϑ_{br}	the wave angle at breaker line	[°]

From the equation, it can be concluded that wave height, wave period and wave angle have an influence on the amount of longshore sediment transport. In general, there is a strong correlation between wave height and wave period, which implies that higher waves correspond to waves with a higher wave period (Sánchez-Arcilla et al., 2016).

The angle of incidence can play a role in the HD because there is a curvature. As the coastline has a curvature, the angle of incidence at the beginning of the curve differs from the angle of incidence at the end of the curve, even if the offshore waves approach the coast at the same angle along the entire coast. This therefore means that if variations occur in the coastline orientation, this leads to a variation in the angle of incidence on the coast and hence a variation in sediment transport. In general,

the relationship between the amount of longshore sediment transport and the angle of incidence of the wave can be represented by a (S, φ)-curve, as shown below in Figure 2.5. It follows that no longshore sediment transport occurs if the angle of incidence is equal to 0 degrees, a normal incident wave, or if the angle of incidence is equal to 90 degrees. The maximum longshore sediment transport occurs around an angle of incidence of 45 degrees (Ashton & Murray, 2006b). This can also be deduced from Equation 2.2. The sine is calculated from twice the angle, here the sine of 90 degrees is maximum and therefore maximum longshore sediment transport takes place around an angle of incidence of 45 degrees.

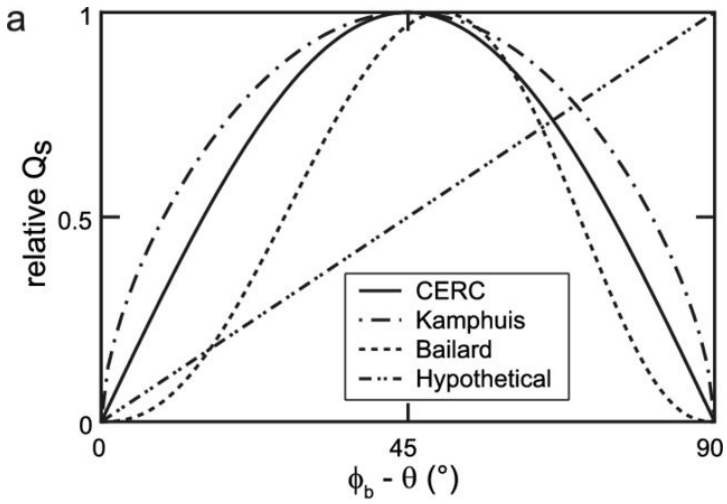

Figure 2.5: (S, φ)-curve (Ashton & Murray, 2006b).

2.4. Coastal curvature

Coastal curvature is defined as the gradient in the orientation of the curvature of the coastline. It can be obtained by connecting the cross-shore transects along the coast, i.e., the transects perpendicular to the coast (Kroon et al., 2022).

Due to coastal curvature, wave convergence can occur along a convex-shaped coast, leading to increased wave height and potentially higher rates of coastal erosion (Lauzon et al., 2019). The varying orientation of the shoreline causes waves to approach different locations at different angles. This variation in the angle of wave incidence can result in differences in the amount of erosion, as discussed earlier in Subsection 2.3.2. Radermacher (2018) studied that a stronger curvature of the shoreline affects the safety of swimmers. In fact, stronger curvature causes greater variations in the development of the beach width.

Den Heijer (2013) investigated the role of coastal curvature on dune erosion. This study was conducted by applying an alongshore uniform coast in the 2DH mode of XBeach. Constant hydraulic boundary conditions were applied while the coastline curvature is a varying parameter.

The study found that more erosion occurs at a wave angle of incidence of 45 degrees compared to a normal incident wave. It shows a relationship between the curvature and gradient in the longshore sediment transport, a stronger curvature leads to a larger gradient in the longshore sediment transport and a negative sediment balance. For the cross-shore sediment transport, differences due to curvature were small, but differences due to the angle of incidence were more significant. Most (negative) cross-shore sediment transport occurs around an angle of 50 degrees to 70 degrees. The resulting erosion pattern depends primarily on the wave angle of incidence and to a lesser extent on the shoreline curvature.

Lazarus and Murray (2007) investigated the influence of coastline curvature on erosion and sedimentation patterns using lidar surveys of the coast near North Carolina (United States). The study found that there is a negative correlation between coastline position and coastline curvature when the wave angle of incidence is less than 45 degrees. A convex-shaped coast leads to erosion and a concave-shaped coast leads to sedimentation.

In addition to the two studies mentioned above, more studies (such as Ashton and Murray, 2006a; Lauzon et al., 2019; Valvo et al., 2006) are performed on the relationship between coastline development and coastline curvature. All these studies show that a larger gradient in coastline curvature leads to a larger gradient in coastline development as well as that a convex-shaped coast leads to erosion.

2.5. Concluding remarks

This chapter has evaluated the main processes that play a role in beach width development. The literature review revealed that infragravity waves have a major influence on beach development relative to short waves because infragravity waves are present in the surf zone and swash zone and almost all short waves are dissipated. In addition, the largest changes occur as a result of transport processes. These transport processes are influenced by factors such as wave height, wave period and wave direction.

The main parameters investigated in Chapter 4 are beach width, beach slope, MKL position, beach volume change, and dune foot orientation.

Furthermore, other studies on the influence of shoreline curvature have also been discussed in this chapter. It follows that stronger curvature leads to larger gradients in sediment transport. In addition, stronger curvature leads to larger variations in beach width in the alongshore direction. Erosion can be seen on convex-shaped coasts.

3

Methodology

This section begins with the data analysis performed looking at what information is available that is needed in the XBeach model. For example, this section discusses bathymetry and waves, which can be used as input parameters for both the schematic model and the complex model of the HD. In Section 3.2, the numerical model XBeach is discussed. Section 3.3 and Section 3.4 discuss the setup of the schematic model and the complex XBeach model of the HD respectively.

3.1. Data study

This section describes the data available at the HD site. This data is collected to answer the first sub question looking at the relationship between the processes present and the developments of the beach. In addition, this data is used later in the study as input values for the numerical models.

3.1.1. Bathymetry

This subsection shows the bathymetry of the coast around the HD. The bathymetry as shown in Figure 3.1 is a combination of the measured JARKUS data and Vaklodingen surveys. To obtain the Vaklodingen surveys, measurements are taken from the shoreline to NAP - 20.0 m. The JARKUS data is measured every year with the JARKUS data shown in the figure being from the year 2015. The Vaklodingen surveys are not conducted annually and therefore no data is available from 2015. Vaklodingen data from 2017 was chosen because it is closest to 2015. Furthermore, this data is applied further offshore because at these depths no JARKUS data is available. Therefore it has a small impact on the development of the beach width because the JARKUS data is available in the region where most changes which have an impact on the beach width occur, namely around the waterline. In the figure, the coordinates on the x- and y-axes correspond to the Universal Transverse Mercator (UTM) system.

The bathymetry data is used to determine at which locations erosion or sedimentation occurs. This can be done by calculating the difference between the bottom in 2015 and the bottom after at the end of the simulation, i.e. in 2020. By applying this method, the volume loss of the HD can be calculated.

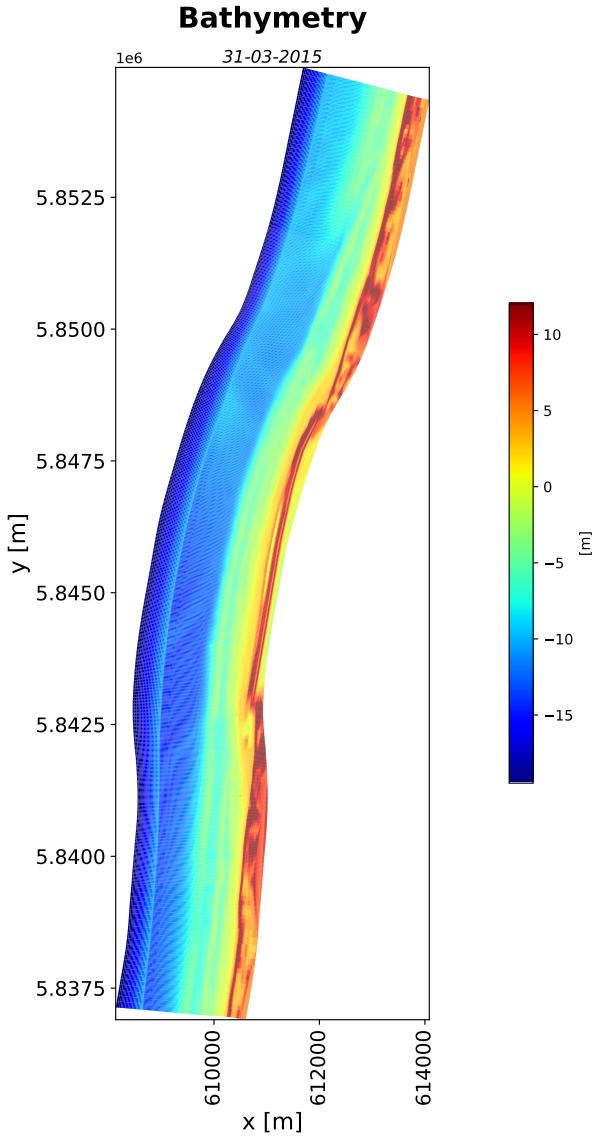

Figure 3.1: The bathymetry of 2015, indicated by the colour bar in [m], of the Hondsbossche Dunes. Combined JARKUS data and Vaklodingen surveys.

3.1.2. Wave climate

The wave characteristics which will be analysed are from April 2015 to March 2020 because the HD was implemented in 2015 and the objective of this research is to improve the predictions of the beach width on a scale of 5 years, so this means from 2015 to 2020.

The relevant wave characteristics are mainly obtained from the wave station IJmuiden munitiestortplaats which is located near IJmuiden. This wave station is the nearest station which is located south of the HD at a depth of 21 m. The missing data is supplemented with data obtained from the wave station K13 platform. This measuring station is located north of the HD at a depth of 25 m (De Jongh, 2018). For both wave stations, the interval between measurements is equal to 10 minutes, so 6 measurements were taken for each hour. The locations of the measurement stations used to obtain the hydrodynamic data are shown in Figure 3.2.

Figure 3.2: The locations of the measurement stations.

Wave height

The measured wave height is the significant wave height estimated from a wave spectrum (Holthuijsen, 2007). The wave height data shows that no very large variations occur over the years. For example, the average wave height for each year is approximately equal to 1.30 m and the maximum wave height is around 6 m. The wave data of 2015 and 2016, which can be seen in, respectively, Figure 3.3 and Figure 3.4, show that more high waves occur in the first year after the implementation of the nourishment. With that, it can be said that in the first year, 2015, there was a more energetic wave environment compared to 2016.

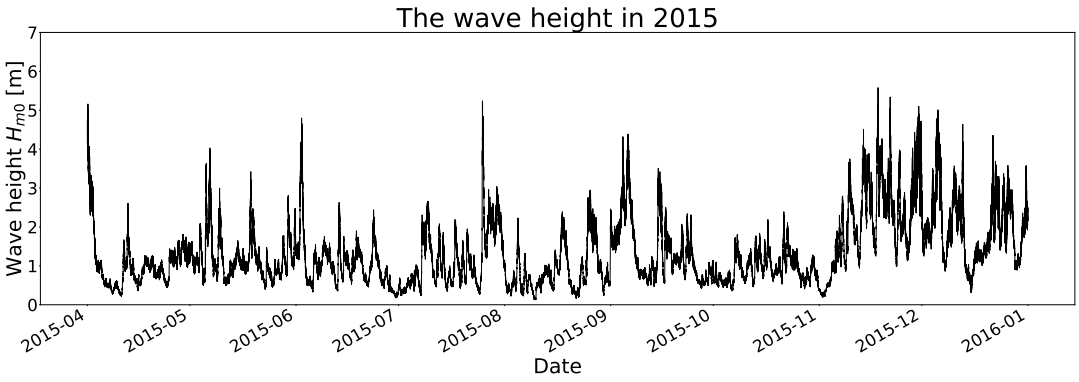

Figure 3.3: The wave height in 2015 obtained from wave stations IJmuiden munitiestortplaats and K13 platform. Modified from data of Rijkswaterstaat (Rijkswaterstaat, 2024).

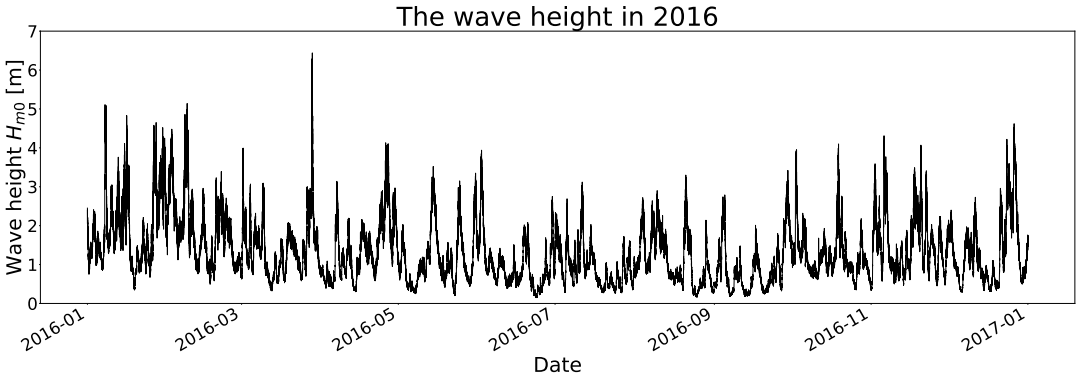

Figure 3.4: The wave height in 2016 obtained from wave stations IJmuiden munitiestortplaats and K13 platform. Modified from data of Rijkswaterstaat (Rijkswaterstaat, 2024).

In general, over the years, less and less energetic wave climate is present. The wave rose of 2020, from Figure 3.5, shows that this year also had an energetic wave climate. However, this year contains only the data from January to April. These are the winter months when generally the largest waves are present, so this picture is not representative of the full year. The wave roses of all years separately are shown in Appendix B.

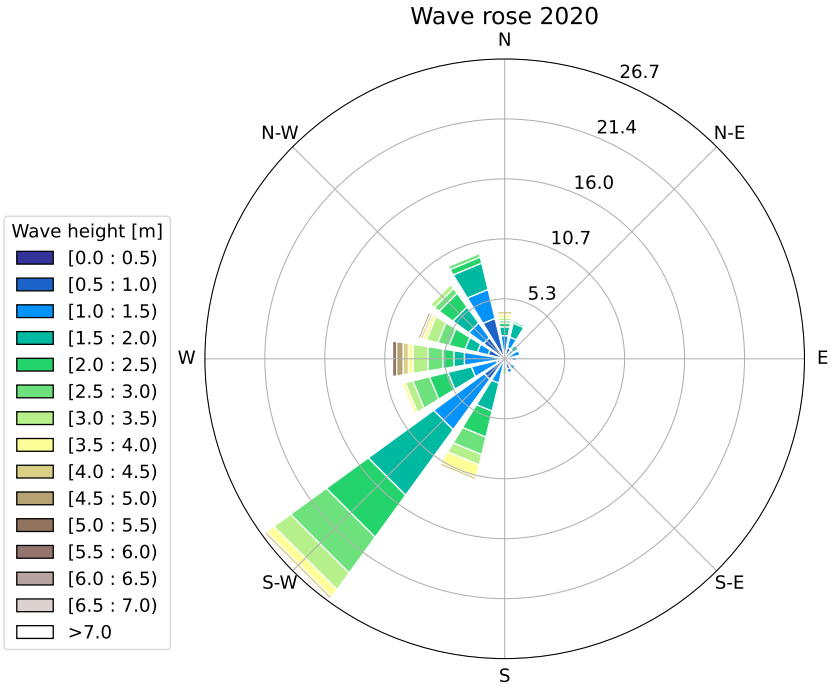

Figure 3.5: The wave rose from 2020. This wave rose included the wave height and the wave direction obtained from wave stations IJmuiden munitiestortplaats and K13 platform. The numbers on the radial axis represent the percentage of occurrence. Modified from data of Rijkswaterstaat (Rijkswaterstaat, 2024).

Figure 3.6 shows the wave rose for all years combined. This wave rose shows that in the five years focused on during this study, most of the waves range between a wave height of 1.0 m to a wave height of 3.0 m.

Appendix B shows the measured wave height during the year. These plots show that the largest waves occur at the beginning and at the end of the year. These are the winter months in the northern hemisphere and the largest waves occur during these times.

Wave period
The measured wave period obtained from data of Rijkswaterstaat (Rijkswaterstaat, 2024) is the T_{m02}. Throughout the year, variations in the wave period occur. In general, the higher wave periods correspond to the waves with higher wave height as was also found in the literature review of Chapter 2.

The average wave period for each year is approximately between 4.5 and 5.0 s. Here it is noticeable that the variation over the years is small. The minimum wave period also hardly varies over the different years and is around 2.5 seconds. However, a greater variation can be seen among the maximum wave periods. The maximum wave periods range from 7.5 s to 10.7 s.

The wave periods for all years individually can be found in Appendix B.

Wave direction
Based on the wave rose from Figure 3.6, it can be concluded that most of the waves in the Netherlands during the period from 2015 to 2020 come from the southwest direction. This implies that most waves have an angle of incidence of approximately 225 degrees with respect to the north. The wave rose also shows that some waves also come from the north. However, there are more waves from the southwest and the waves from the southwest are higher waves so the net sediment transport is from south to north. The coastline orientation ranges from about 270° to 310°. The coastline orientation on the north side of the HD is larger. To the south, the coastline orientation is approximately 270° to 280° (Kroon et al., 2022).

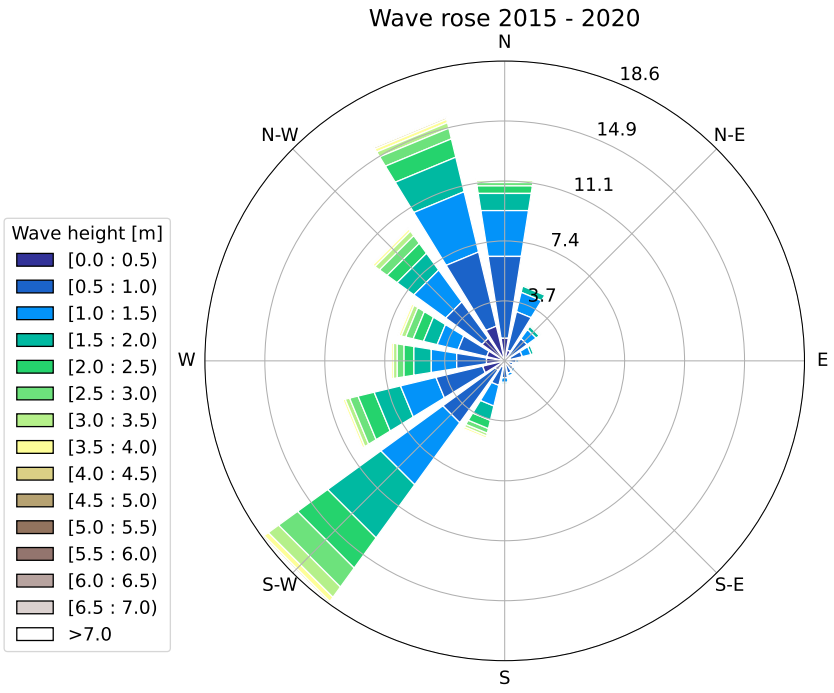

Figure 3.6: Wave rose of all waves in the years between 2015 and 2020. This wave rose included the wave height and the wave direction obtained from wave stations IJmuiden munitiestortplaats and K13 platform. Modified from data of Rijkswaterstaat (Rijkswaterstaat, 2024).

3.1.3. Water levels
One of the input parameters of XBeach is the water level, which can be measured by measurement stations located in the North Sea. This measured water level contains the astronomical tide and a surge contribution. The wave station IJmuiden Stroommeetpaal is used to obtain the data of the water level because this station is the nearest station where there is enough data available. The location of this station can be seen in Figure 3.2.

The measured range of water levels hardly varies over the five years considered in this study. In general, the maximum water level is approximately equal to 2.0 m and the minimum water level is approximately equal to - 1.0 m. In addition to the water level, the astronomical tide is also measured at the measurement station. The measurements show that the astronomical tide varies between - 1.0 m and 1.0 m for each year. Using the measured water level and the astronomical tide, the surge can be calculated. It follows that the surge varies between about 1.0 m and - 0.5 m.

Figure 3.7 shows the different water levels of 2015. The water levels of the other years can be seen in Appendix B.

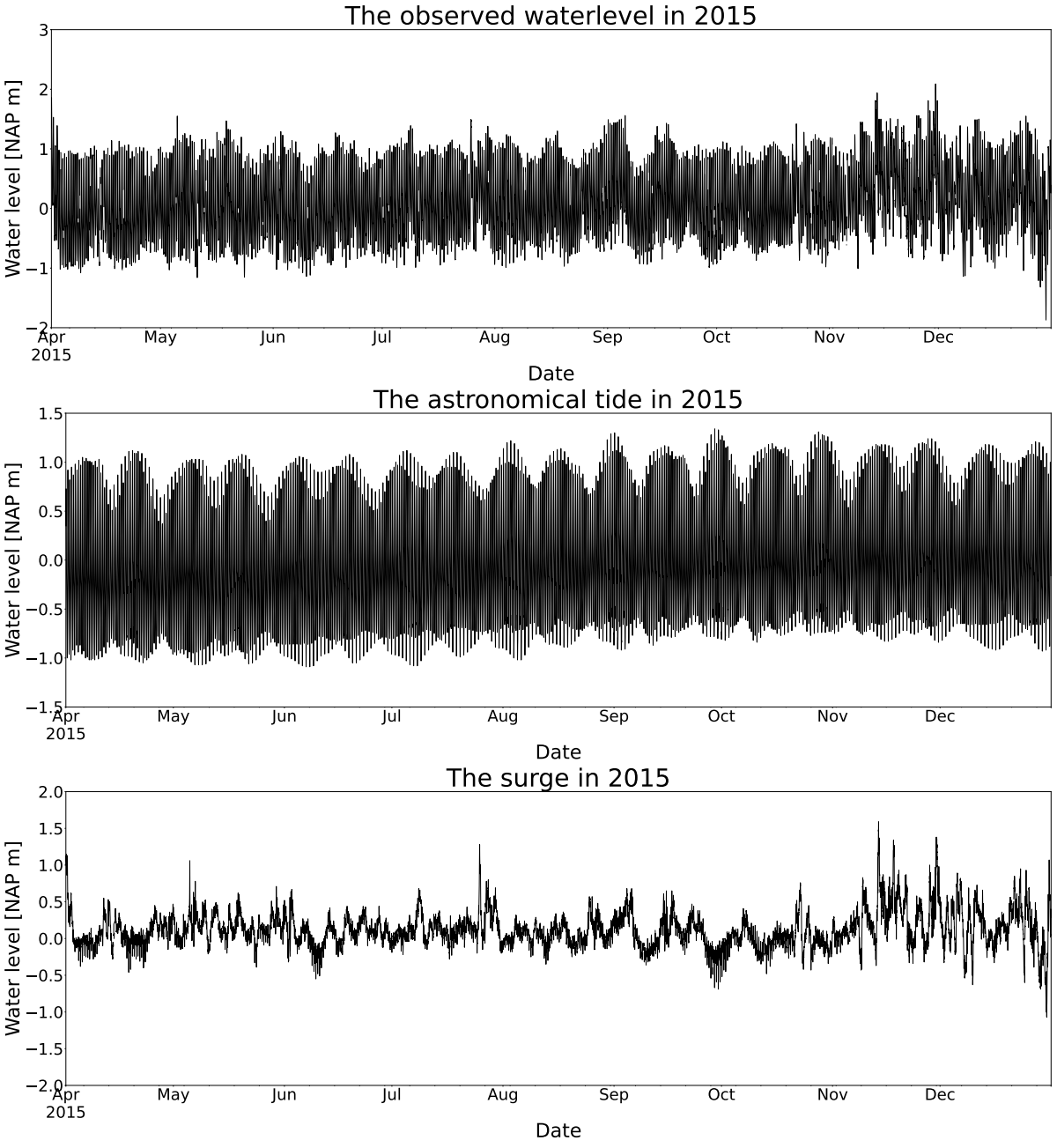

Figure 3.7: The water level and astronomical tide measured at water station IJmuiden Stroommeetpaal. The surge is calculated using these two water levels. Modified from data of Rijkswaterstaat (Rijkswaterstaat, 2024).

To determine the beach width, calculating the waterline position requires the MHW level and the MLW level. For the location of the HD, the MHW level is approximately equal to NAP + 0.8 m and the MLW level is approximately equal to NAP - 0.8 m (Kroon et al., 2022).

3.1.4. Sediment characteristics

The sand used to implement the HD was taken from two borrow pits in the North Sea. A hopper was used to transport the sand to the location of the HD. Sediment samples were taken from the sand in the hopper to determine the characteristics of the sand, such as the average median grain size. The grain size of the nourishment varies with the bed elevation with the grain size with the highest bed elevation being the largest. It is considered that the median grain size D_{50} is equal to 185 µm below NAP - 7.0 m, 255 µm between NAP - 7.0 m and NAP + 3.5 m and 280 µm above NAP + 3.5 m. The grain size in the northernmost part of the nourishment is equivalent to about 350 µm (Cleveringa, 2019; De Jongh, 2018).

The grain size applied in this study is equal to 250 µm, because this is the grain size that is present within the boundaries of the beach according to the definition in Subsection 2.1.2.

3.1.5. Coastal curvature

The curvature of the coastline is an important parameter in this study. As a result of a change in coastline orientation and thus curvature, a change in longshore transport occurs. Due to a change in the orientation of the coastline, the wave angle of incidence of the waves on the shore normal varies. A larger change in the orientation of the shore leads to a larger variation in the wave angle of incidence with the shore normal as a result of this assumption. It was investigated in Chapter 2 that the larger the differences in the wave angle of incidence the larger the differences in the amount of longshore sediment transport.

The amount of sediment transport and thus the changes in the amount of volume transported are not the same for every year. Immediately after the nourishment is implemented, it is most out of equilibrium so the largest changes and therefore the most sediment transport occurs in the first year. Another reason is that the waves do not have exactly the same angle of incidence, nor the wave period and wave height, every year, and as a result of these variations, variations also occur in the longshore sediment transport each year.

The curvature of the HD is stronger than the curvature of the shoreline prior to the placement of the nourishment. The orientation of the shoreline before the implementation of the nourishment varies about 0.5° per kilometre. For the HD, the curvature of the shoreline varies depending on the location considered. On the north side of the HD and on the south side of the HD, the curvature of the shoreline is approximately equal to 1.3° per kilometre while the curvature in the middle of the nourishment is equal to approximately 4° per kilometre (Kroon et al., 2022).

3.2. Motivation for using XBeach

3.2.1. Introduction of XBeach

XBeach is an open-source numerical model that can be used to simulate hydrodynamic and morphodynamic processes (Zhou et al., 2023). It is a two-dimensional process-based model on wave propagation, long waves and mean flow, sediment transport and changes in coastal areas during storms (Roelvink et al., 2009). The model is primarily applied when wave-driven coastal processes have a major impact (Van Rijn, 2007). The model can be used to determine beach width development because the model can calculate sediment transport and morphological changes.

XBeach has a 1D mode and a 2DH mode. In the 1D mode, the longshore gradients are ignored while in the 2DH mode, the gradients can be affected. Therefore, using the 2DH mode, an analysis of the influence of the longshore processes on erosion can be performed (Roelvink et al., 2015). In this study, the longshore sediment transport is considered and therefore the 2DH mode is applied for the different simulations.

For sediment transport, a distinction is made between bed load transport and suspended load transport. There are several formulas that can be applied for equilibrium sediment concentration. In XBeach, the transport formulae of Soulsby-van Rijn is used (Trouw et al., 2012). If there is bed load transport, the particles remain close to the bed (Stein, 1997). There is suspended load transport if the particles are lifted from the bed. In this transport type, the flow is above the critical flow rate so the particles are in suspension by moving water (Parsons et al., 2015). The transport calculated by this formula is the total amount of transport. In general, more sediment is transported when the concentration is higher because more sediment is available.

The equations for the equilibrium concentration for the bed load (subscript b) and suspended load (subscript s) are (De Ridder, 2023; Roelvink et al., 2010):

$$\begin{aligned} C_{eq,b} &= \frac{A_{sb}}{h}\left(\sqrt{v_{mg}^2 + 0.018\frac{u_{rms,2}^2}{C_d}} - U_{cr}\right)^{2.4} \\ C_{eq,s} &= \frac{A_{ss}}{h}\left(\sqrt{v_{mg}^2 + 0.018\frac{u_{rms,2}^2}{C_d}} - U_{cr}\right)^{2.4} \end{aligned} \tag{3.1}$$

where:

$C_{eq,b}$	equilibrium sediment concentration of the bed load	[kg/m^3]
$C_{eq,s}$	equilibrium sediment concentration of the suspended load	[kg/m^3]
A_{sb}	bed load coefficient	[-]
A_{ss}	suspended load coefficient	[-]
h	water depth	[m]
v_{mg}	velocity magnitude	[m/s]
u_{rms}	root-mean-square wave orbital velocity	[m/s]
U_{cr}	critical flow velocity	[m/s]
C_d	drag coefficient due to current	[-]

3.2.2. Surfbeat and stationary mode in XBeach

The model considers both the transformation of long waves (such as dissipation) and the transformation of short waves (such as refraction). The long, infragravity waves are important during storm conditions. The long wave motions can be modelled using the so-called surf beat. The processes modelled in XBeach are shown in Figure 3.8. In the stationary mode, there are no variations in a wave group and thus infragravity waves are neglected. This mode is mainly used for moderate wave conditions while the surfbeat mode is used for larger waves and when the focus is on the processes taking place in the swash zone (Clare et al., 2022).

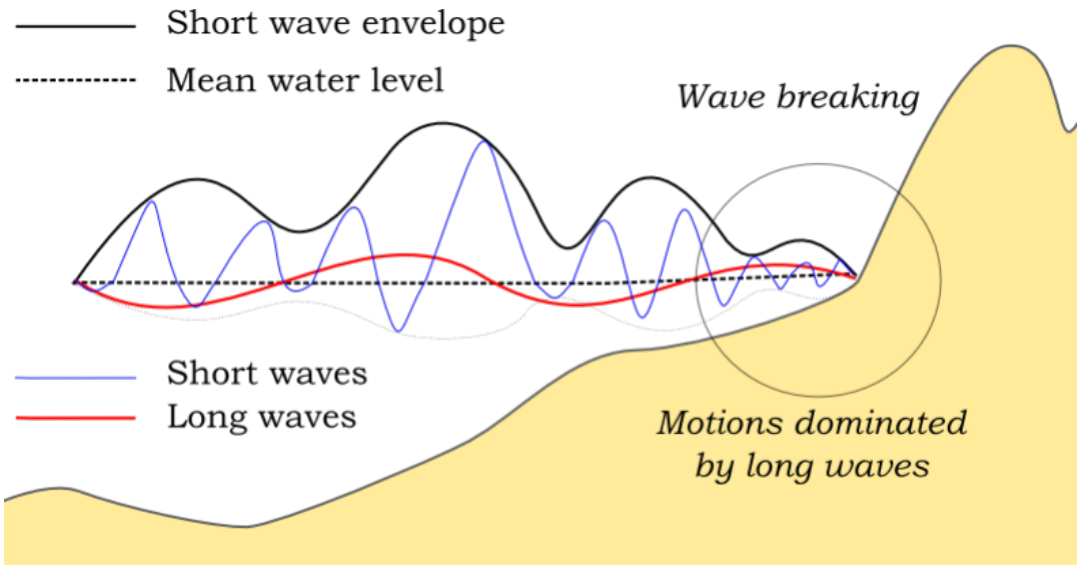

Figure 3.8: The relevant processes in XBeach (Roelvink et al., 2015).

In both stationary mode and surfbeat mode, the following wave action equation for short wave energy is solved (Clare et al., 2022):

$$\frac{\partial A}{\partial t} + \frac{\partial c_x A}{\partial x} + \frac{\partial c_y A}{\partial y} + \frac{\partial c_\theta A}{\partial \theta} = -\frac{D_w + D_f + D_v}{\sigma} \tag{3.2}$$

where:

c_x	group velocity in the x-direction	[m/s]
c_y	group velocity in the y-direction	[m/s]
c_ϑ	refraction speed	[m/s]
D_w	dissipation by wave energy	[W/m^2]
D_f	dissipation by bottom friction	[W/m^2]
D_v	dissipation by vegetation	[W/m^2]
A	wave energy	[m^2/s]
σ	intrinsic wave frequency	[1/s]

In the stationary mode, the first term of Equation 3.2 equals zero, indicating that the wave energy remains constant over time. The waves, which are applied as boundary conditions, are constant in height, period, and direction for a specified duration, for example, one hour. Since wave groups form in surfbeat mode, a gradient in the momentum stress develops, leading to variations in the water level (Bart, 2017).

XBeach takes into account the variation of the wave height that can take place over time and thus models long waves that can hit the dune front and thus cause erosion of the dune. This allows the model to predict when a dune will flood or even break through (Roelvink et al., 2009).

3.3. Setting-up the schematic XBeach model

In this section, the schematic model performed in XBeach is discussed. This is part of stage three in which the second sub-question is answered. It starts by describing the purpose of the schematic model. Next, the hypotheses are discussed, because based on the hypotheses the input parameters can be determined. Based on these hypotheses, the parameters to be varied can be determined in order to make a comparison between the results and see the influence of the different parameters on the results. The results of the schematic model will be discussed in Chapter 5.

3.3.1. Objective of the schematic model

Before starting to create a full XBeach model of the HD, a schematic model is first used. The purpose of the schematic model is to gain insight into the influences of the various parameters and to isolate the combined effect of coastal curvature and long waves. The parameters considered are wave height (including the associated wave period and surge level), wave direction and coastal curvature. The literature review in Chapter 2 showed that these parameters can have a major influence on the amount of sediment transport that occurs. As a result of the sediment transport present, there may be a change in the beach width present.

3.3.2. Hypotheses of the schematic model

In this section, hypotheses are given about the influence of the different parameters. These hypotheses are related to the objective as mentioned in the previous section. It is examined in this section which parameters have the greatest influence on the transport process and the associated erosion or sedimentation that occurs.

Based on the literature review of Chapter 2, it can be assumed that wave height has the greatest influence on the amount of sediment transport that will occur because wave height is multiplied by a power of 2 in the formulas for both cross-shore transport and longshore transport. Therefore, in the schematic model, multiple wave conditions will be applied where the wave height varies. In this way, we will see what happens to the beach width in the case of higher waves and what happens to the beach when relatively low waves are applied. The higher waves correspond to waves that have a larger wave period and a higher water level due to a higher surge, which also leads to more sediment transport.

The model applies waves that have different angles of incidence, namely a normal incident wave and an oblique incident wave of 45 degrees and thus maximum sediment transport. Due to the curvature in the coastline, the angle of incidence on the shore normal will vary in the longitudinal direction. For the wave angle of 0 degrees, hardly any longshore sediment transport will occur at the beginning of the curvature, while it will increase toward the end of the curvature until the angle exceeds 45 degrees and sediment transport decreases. For the 45-degree angle, the opposite will happen. Here the longshore sediment transport is maximum at the beginning of the curvature and as the curvature progresses the amount of longshore sediment transport will decrease as the angle of incidence of the wave increases.

In the variation of the strength of the curvature, the gradient in the amount of sediment transport is expected to be larger for a strong curvature relative to a straight line or barely present curvature.

To investigate the effect of long waves compared to short waves, the model will be run in stationary mode and in surfbeat mode. Then a comparison can be made between the decrease in beach width that occurs and the erosion and sedimentation patterns that occur. The expectation here is that more erosion occurs and there is a greater decrease in beach width when the surfbeat mode is applied compared to the simulation in stationary mode.

3.3.3. Model input of the schematic model

This subsection discusses the input parameters and lists the model settings for each run. The input parameters are based on the data study from Section 3.1.

General

To run XBeach, it requires a directory that must contain a number of specific files. First, this directory contains what is called a *params.txt* file. This file defines the parameters as they apply to the HD. An example of a *params.txt* file is shown in Section C.1 or Section C.2. In addition to the parameters, the grid is also an input parameter of the model. In addition to the aforementioned input parameters, wave conditions and tide conditions can also be specified. This indicates when and for how long a particular wave or water level occurs.

Bathymetry

For the schematic model, an alongshore uniform coast is assumed where there are no changes in the coastal profile, in the initial situation, in the coastal longitudinal direction. By applying an alongshore uniform coast, any influences due to variations in bathymetry are not included in the simulation. As a result, the differences that occur can only occur due to the parameters being varied.

The bathymetry applied in the schematic model is based on a transect of the HD taken from the JARKUS data. The chosen transect does not contain many bars, as these bars may have an impact on the result after the simulation. XBeach is a numerical model where simulating sand bars is not always representative of reality, as XBeach flattens out many sand bars. The flattening or sometimes disappearance of sand bars can cause a large difference in beach width between the initial situation and the end of the simulation. As a result, a transect from 2016 and not 2015 was chosen because, after the implementation of the nourishment, large irregularities are present which take some time to disappear. Figure 3.9 shows the profile that has been applied. This profile is applied along the entire coast and creates a longshore uniform coast.

Figure 3.9: The beach profile of the transect which is used for the schematic model.

In Figure 3.9 it can be seen that the profile slopes linearly from about NAP - 10.0 m until it reaches NAP - 20.0 m. This increase in water depth has been applied artificially because otherwise, the edge of the model is too shallow relative to the waves that will be applied (see Figure 3.3.3). If the edge of the model is at NAP - 10.0 m, this means that most waves will break immediately upon entering the model. Figure 3.10 shows the top view of the bathymetry.

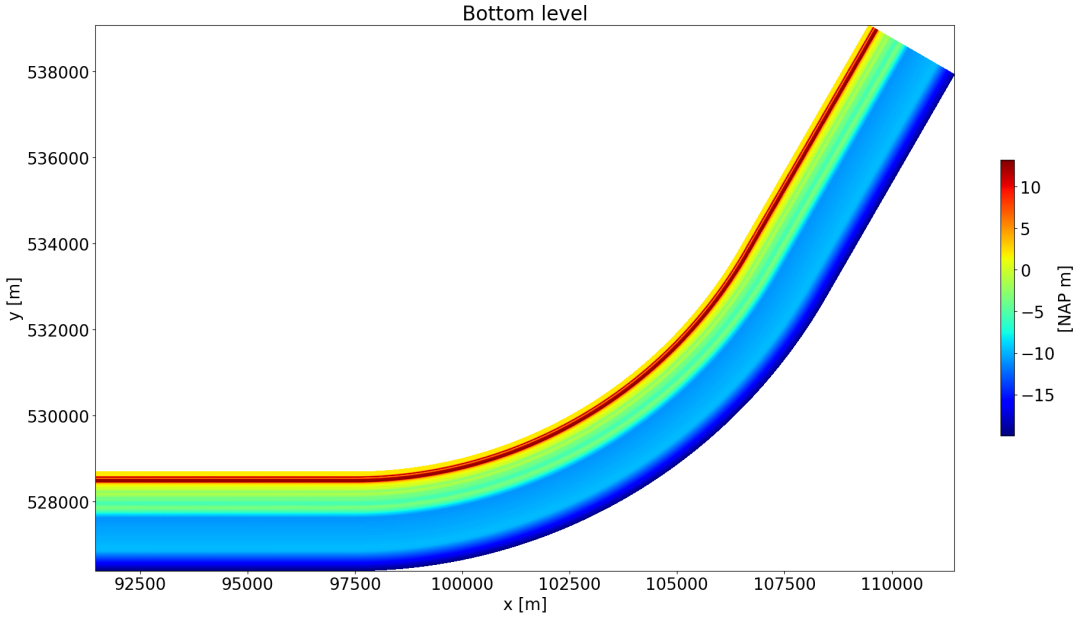

Figure 3.10: A top view of the bathymetry showing the curvature and the straight sections at the beginning and end of the curvature. The coordinate system of this figure is random and is not based on the coordinate system used for the HD.

Grid

In the schematic model, a curvilinear grid was applied to add curvature to the model. The sizes of the grid cells are not uniform throughout the grid. This is because the grid is coarser at the offshore boundary of the model because the changes that occur here do not affect the change in beach width. Therefore by making the grid coarser here, the simulation time can be reduced. In the cross-shore direction, the grid varies from a grid size of 1 m onshore to a grid size of 5 m offshore. In the longshore direction, there is also a variation in the size of the grid cells due to the curvature. The size of the onshore side of the grid is smaller than the size of the offshore side of the grid. The grid cells are 25 meters wide in the longshore direction on the straight section of the grid.

In the longshore direction, a straight section is applied on both sides of the curvature, as can be seen in Figure 3.10. For the waves coming in at a 45-degree angle, these straight sections have been applied so that boundary effects are no longer present as the waves approach the curvature. Thus, these effects are disregarded and do not affect the results of beach profile development due to the curvature present.

Coastal curvature

Multiple simulations are run varying the amount of curvature applied. The curvature that is currently present at the HD is about 4 degrees per kilometre (Kroon et al., 2022). To investigate the effect of curvature, models were set up where there is twice the amount of curvature present (approximately 8 degrees per kilometre) and a model where there is twice less the amount of curvature present (approximately 2 degrees per kilometre).

Wave input

This subsection discusses the wave conditions applied in the simulations. A variation in the wave conditions to be applied takes place to see the influence of each parameter.

Wave height and wave period

For this study, we assume a time-varying wave height. The wave heights applied were based on data obtained from the wave stations in the North Sea. Sensitivity simulations were performed to test the model's sensitivity to the wave height and corresponding period. Initially, three wave heights were applied, namely average conditions, moderate storm conditions and maximum conditions. After an initial simulation, it was found that the effect of the average conditions with a wave height of 1.31 m and a wave period of 4.5 s was minimal. The results of this simulation are shown in Section D.4. Therefore,

it was chosen to disregard these conditions in further simulations and focus only on the remaining conditions. The duration of the simulations varies for the type of conditions because the maximum conditions take place for a shorter period of time than the average conditions.

The moderate storm conditions have a wave height of 2.50 m and a wave period of 5.7 s. These moderate storm conditions have a duration of about 3 days in a row. Therefore, the duration of this simulation is equal to 3 days and 9 hours. For the maximum conditions, the duration of the simulation is only 24 hours because these conditions generally occur 1 day in a row and then it gradually decreases. The wave height is equal to 5.88 m and the wave period is equal to 7.6 s.

The applied wave height for both conditions has a natural progression. This means that the wave height slowly increases to its maximum wave height and then decreases again. Thus, there is not a constant wave of 5.88 m, but a wave that builds up to this height. The same also applies to the wave period. The figures in Figure 3.11 show the progress of the wave height, wave period and water level.

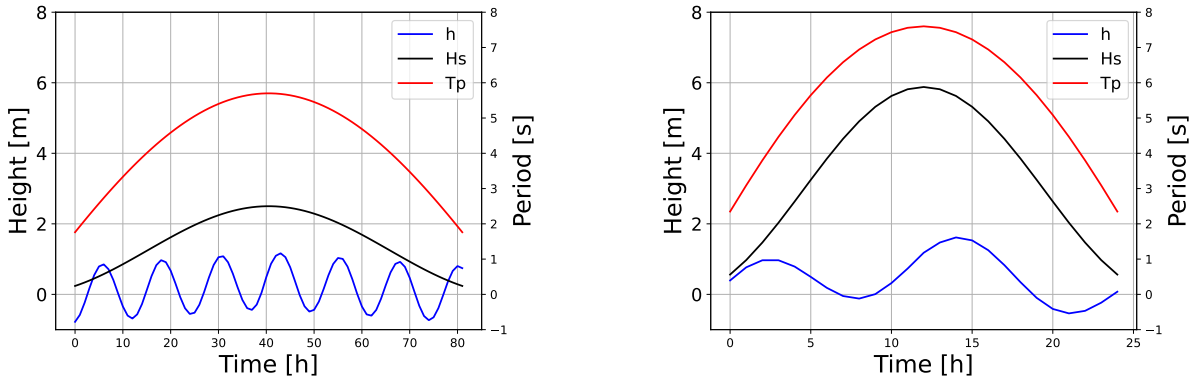

(a) The wave conditions of a moderate storm.

(b) The wave conditions of the maximum wave.

Figure 3.11: Wave type conditions applied in the model.

Wave direction
Simulations are performed with two different wave directions. The wave directions applied are an angle of incidence of 0 degrees and an angle of incidence of 45 degrees. An angle of incidence of 0 degrees corresponds to waves coming from the South. Thereby, for the model, the angle of incidence is perpendicular to the straight, horizontal part of the grid.

The angle of incidence of 45 degrees maximises longshore sediment transport. In addition, this angle corresponds to a wave direction from the southwest, which is the most frequent wave direction in the Netherlands as can also be seen in Figure 3.6.

Short and long waves
In order to investigate the effect of the long waves on the reduction of the beach width, a simulation is also run where no long waves are applied so that it can be used as a reference case. In this case, the model is run in the stationary mode where the infragravity waves are not considered. These runs are performed only for the maximum conditions because the simulation time of these runs is shorter and thus time can be saved.

Water level
The water level, like the wave height and wave period, is also represented in Figure 3.11. Due to a surge occurring, the water level at some times is higher than a normal sine wave where the amplitude is the same everywhere. The water level is equal to the sum of the tide and the surge present. The surge is different for each wave condition, a larger surge occurs when there are larger waves.

The water level in Figure 3.11 consists of the astronomical tide and the surge. The astronomical tide has an amplitude of 0.8 m. The surge occurs about halfway through the time period, there is a small delay, of the astronomical tide (Chbab, 2015). Therefore, there is a higher peak in the water level almost halfway along the x-axis compared to at the beginning.

3.3.4. Overview runs

The table below shows a summary of the different runs that were performed. For each run, the parameters applied in the run are indicated. All runs were performed for the three different curves being tested. The simulations were run with a morfac of 10 so that even in the case of storm conditions, where the simulation time is only 1 day, results can be seen and comparisons can be made.

Table 3.1: An overview of the runs which are performed for the schematic model.

	Wave height [m]	Wave period [s]	Surge [m]	Wave direction [deg]	Wave model	Simulation time
Run 1	2.50	5.7	0.47	0	Surf beat	3 days 9 hours
Run 2	5.88	7.6	0.94	0	Surf beat	1 day
Run 3	5.88	7.6	0.94	0	Stationary	1 day
Run 4	2.50	5.7	0.47	45	Surf beat	3 days 9 hours
Run 5	5.88	7.6	0.94	45	Surf beat	1 day
Run 6	5.88	7.6	0.94	45	Stationary	1 day

3.4. Setting-up the XBeach model of the Hondsbossche Dunes

This section discusses the complex XBeach model modelling of the HD. This model is used to answer sub-question 3 and constitutes stage 4 of the study. Bathymetry based on measured JARKUS data and Vaklodingen are applied with which the simulation resembles reality. In addition, a representative wave climate is used as an input parameter for the waves with which the waves almost resemble how they occur in reality.

The section begins by discussing the objective. Next, it discusses the hypotheses and finally, the model input parameters are discussed in this section.

3.4.1. Objective

The purpose of this model is to investigate whether the change in beach width can be modelled with long waves using XBeach. Based on the results from this simulation, the research question of this report can be answered. The research question is formulated in Section 1.3.

3.4.2. Hypotheses

Varying wave conditions will be applied in this model. The wave conditions have been adjusted so that they form a representative wave climate that matches reality as closely as possible. Based on the wave rose in Figure 3.6, it can be concluded that most of the waves are from the southwestern direction. It is thus expected that most erosion occurs at the edge to the south, as the waves will approach this edge first. Furthermore, based on previous studies discussed in Chapter 2, erosion can be expected to occur on the convex-shaped coast. The results of the schematic model also showed that the high waves with a larger surge elevation and higher wave period lead to more sediment transport than the small waves.

3.4.3. Model input

This subsection discusses the input parameters which are mainly based on the data study from Section 3.1.

Bathymetry

For the model of the HD, bathymetry is applied based on the 2016 JARKUS measurements. The measurements from 2016 are chosen because this is the second year after the implementation of the nourishment so there are no initial effects present anymore.

Data was not measured for all transects on the HD, creating some gaps in the bathymetry. By interpolating between the transects where data is known, the unknown data can be determined to create a continuous bathymetry. Furthermore, the JARKUS data cannot be measured far enough offshore. This data cannot be interpolated with known JARKUS data and therefore, data obtained from the Vaklodingen surveys are used. The Vaklodingen surveys are measured more offshore and by combining

the JARKUS data and the Vaklodingen data, the complete grid can be determined. The Vaklodingen data was not measured in 2016 but in 2017. This is the year closest to 2016 and therefore this data is used. The data from the Vaklodingen surveys is only applied at the offshore boundary for bathymetry and therefore does not affect the beach width.

The bathymetry which is used in the model can be seen in Figure 3.12

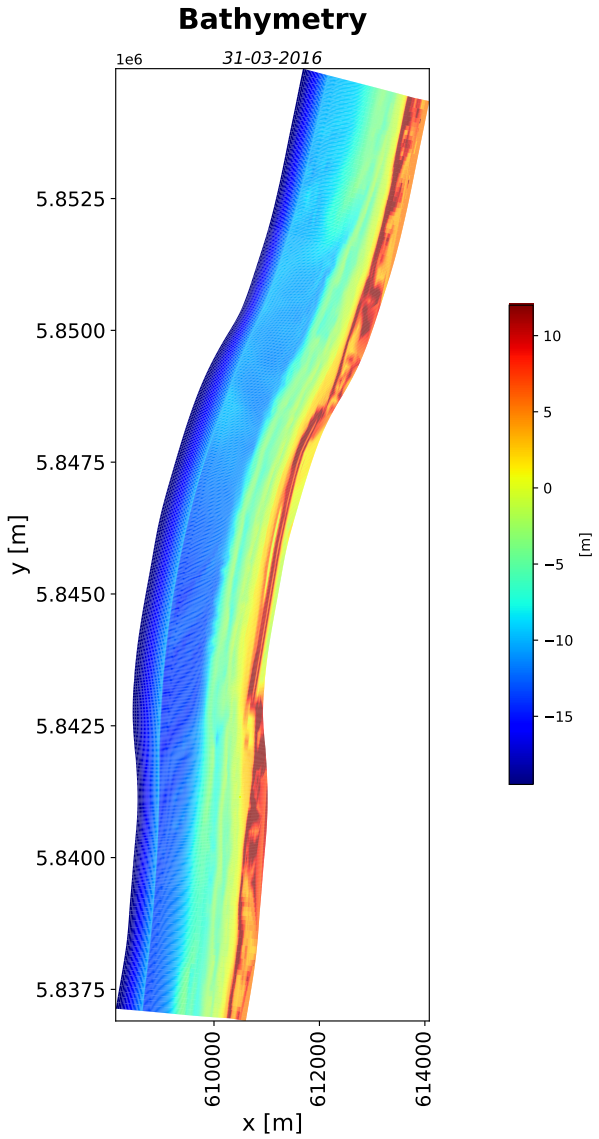

Figure 3.12: The bathymetry, indicated by the colour bar in [m], applied in the model runs for XBeach. Combined JARKUS data and Vaklodingen surveys.

Grid

The total size of the grid corresponds to the size for which bathymetry data is known. Here the grid size differs for the locations in the grid. At the locations where many changes are expected and which are important for the study, there is a higher resolution than at the locations where the changes hardly affect the beach change. The length of the entire grid in the longshore direction equals about 18 km. Of this, about 12 km is the HD with associated curvature and the remaining 6 km is an almost straight coast without curvature (3 km on both sides of the HD). In the offshore direction, the length of the grid equals about 2.1 km. Of this 2.1 km, 200 m of the grid is on the onshore side, in this part of the grid the dune can be found because the bottom is here higher than the waterline.

The grid size is the finest around the waterline because, in the neighbourhood of the waterline, the largest changes are expected to affect the bottom width. Both the grid onshore of the waterline and offshore of the waterline have a grid size in the cross-shore direction of 2.5 m. The size of the grid in cross-shore direction increases to 25 m offshore, i.e. towards the sea. Towards the dune, the grid size will increase to 6.5 m. Furthermore, there is also a variation in the grid size in the longshore direction. At the location of the HD, the grid size in the longshore direction is equal to 25 m, while the 6 km of straight coast has a grid size in the longshore direction of 100 m. In total, the grid consists of 305 grid points in cross-shore direction (nx) and 553 grid points in longshore direction (ny).

Wave input
A representative wave climate is used in the model. Each wave condition from this wave climate is run as an individual simulation in XBeach using the final bottom of the previous simulation. In this way, the parameters for each wave condition can be varied making the computation time faster. The wave climate contains several different wave conditions that provide about as much sediment transport as the waves actually cause. The actual wave conditions are the wave conditions that occur from 01-04-2016 to 31-03-2020.

First, a pivot table was created for each year in which the wave height and the wave direction were shown. For each direction, the sediment transport was then determined using Kamphuis' formula (Equation 2.2). If it turns out that there is a directional bin where a lot of sediment transport takes place, then this directional bin is divided into several directional bins. The aim is to ensure that each condition provides approximately the same amount of sediment transport. The sediment transport per directional bin is approximately equal to 5 % of the total sediment transport per year. This means that there are about 20 different conditions per year. If the bins are too large then more waves will fall within a certain bin. Because the wave direction, wave period and wave height are based on the waves within a bin, the wave climate becomes less representative. However, if the bins become too small then more conditions are created which causes the computation time to increase.

The results described in Section D.4 showed that the change in bed level for the average conditions was very low. In the average conditions, the wave height was equal to 1.33 m. An XBeach simulation involving calculation in the surf beat mode takes longer than an XBeach simulation in the stationary mode. Because the surf beat mode has little impact on beach changes for waves in the order size of 1.33 m, it was decided to use these results in the XBeach model of the HD. All waves that have a wave height smaller than 1.50 m are run in stationary mode to speed up the calculation time. However, the wave conditions where the wave height is greater than 1.50 m are run in the surf beat mode. Previous studies have shown that the stationary conditions can be applied for waves smaller than 1.50 m without having much impact on the developments taking place (Van Leeuwen & Attema, 2019).

The order in which the different wave climates are applied is arbitrary. This means that it is not the case that all large waves are applied first and then all small waves. By applying a random order, the reality can best be simulated because in reality the wave conditions also occur randomly and not in order.

Water level
The model includes the variation in the water level as there is a tide present that causes these variations. The waves arrive at the shore at a different location each time. For each XBeach simulation for the wave condition, precise one high water and one low water takes place. The minimum water level of the tide is equal to NAP - 0.8 m and the maximum water level is equal to NAP + 0.8 m. A water level set-up due to, for example, waves also takes place for each condition.

Morphological acceleration factor
A morphological acceleration factor (from hereafter referred to as morfac) is applied in the model to speed up the computation time. The morfac is not the same for all simulations because each wave condition from the wave climate is run as an individual XBeach simulation. If there are lower wave conditions fewer changes in the bed level are expected and thus a higher morfac is applied. A lower morfac is applied for the higher wave conditions. The total duration of the simulation for the large waves is larger than for the high waves and therefore the computation time can be accelerated using a high morfac.

The morfac is calculated for each model such that the hydrodynamic time is the same for all conditions. The hydrodynamic time is equal to the morphological time divided by the morfac.

3.5. Validation of XBeach

The previous sections described how the models were set up in XBeach and the data used as input parameters. To evaluate the performance of the XBeach model, the outcomes of the simulation are compared with the outcomes of the measurements. For this purpose, only the outcomes of the complex HD model are considered because reference material is available for these outcomes in the form of measurements. For the measurements, the JARKUS data is used in combination with the Vaklodingen surveys. The results, and hence the validation of the XBeach model, are shown in Chapter 6.

4

Analysis of the effects of the mega nourishment based on data

This chapter analyses the development of the HD based on the main parameters defined in Chapter 2. The analysis is based on the yearly coastal measurements carried out along the Dutch coast. After the simulation of the HD was carried out, a comparison was made between the results of the model and the results based on the reality discussed in this chapter. By performing this comparison, it was examined whether the model is a good representation of the reality. The results of this validation are shown in Chapter 6.

4.1. Trends Hondsbossche Dunes

4.1.1. Introduction

In this section, the trends of the HD are analysed to find out what happens in the years after the implementation of the nourishment. The trends investigated come from the JARKUS data. This dataset consists of coastal profiles of the entire Dutch coast where the alongshore intervals are equal to 250 m. The coastal profiles have been measured annually since 1965 (Van Koningsveld & Mulder, 2004).

In the plots of the trends shown in this section, the x-axis runs from north to south showing the entire North-Holland coast. Two black vertical lines are shown in each plot indicating the location of the HD where the HD lies within these two black vertical lines. On the x-axis, the alongshore distance is expressed in RSP. In the Netherlands, so-called Rijksstrandpalen were placed on the beach every 200 meters. These Rijksstrandpalen are used to measure the width of the beach and were part of a reference system. Nowadays this reference system does not happen very often anymore. The origin of the Rijksstrandpalen is in Den Helder and thereon this place, located in the northernmost point of North-Holland, belongs to number 1 on the x-axis (Op het strand, 2024; R & M, 2021).

The plots show the development of the coast near the HD from 2015 to 2020. These years are focused on because these are the first five years after the HD was implemented. Based on the theory from Subsection 2.1.4, it is expected that the largest changes occur in the first year after the implementation so between 2015 and 2016. By analysing the different trends, a prediction can be made to the behaviour of beach width and perhaps find a cause for why there is a rapid reduction in beach width.

4.1.2. Beach width development 2015 - 2020

In Figure 4.1 the beach width for all transects on the North-Holland coast is shown. The definition of beach width is given in Subsection 2.1.2. In the figure, the recreation zones are shown in the grey-shaded areas.

The figure shows that the beach width decreases over the years in almost the entire area of the HD. It also shows that the largest decrease in beach width occurred between March 2015 and March 2016. In the southern recreational zone, that is, the right grey area, it can be seen that there was an increase in beach width in 2017 and 2018. This is the result of an additional nourishment that was implemented in March 2018 (Leenders et al., 2018; Pak, 2019).

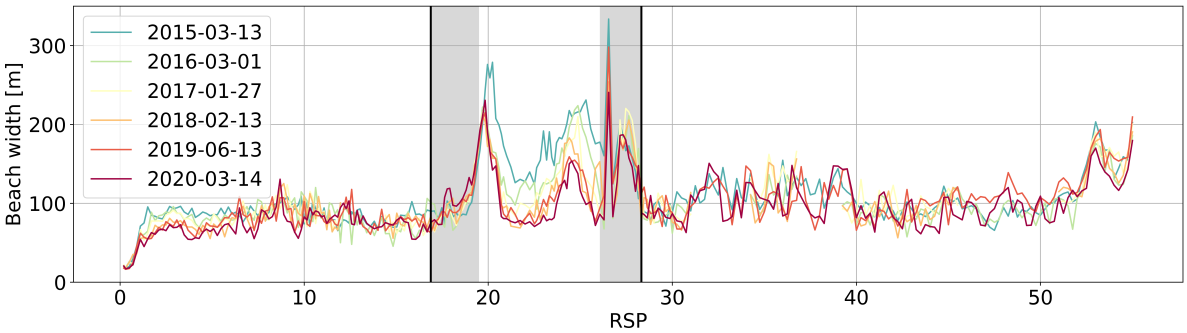

Figure 4.1: Beach width between March 2015 and March 2020, data obtained from JARKUS data. The vertical black lines indicate the HD and the grey areas are the recreational zones of the HD.

Figure 4.2 shows the difference in beach width for different years between 2015 and 2020, where a negative value means a decrease in beach width and a positive value means an increase in beach width. The figure shows that the beach width for the HD decreases more than the beach width for the rest of the North-Holland coast, so outside of the black vertical lines, where hardly any difference can be seen. Particularly in the first year immediately after the nourishment was implemented, a large decrease in beach width can be seen. This may be caused by the fact that the beach profile wants to be in equilibrium condition, and this is not the case immediately after the nourishment is placed, as discussed in Subsection 2.1.4. It is notable that an increase in beach width can be seen around 2018. This increase can be the consequence of the additional nourishment that was implemented in 2018.

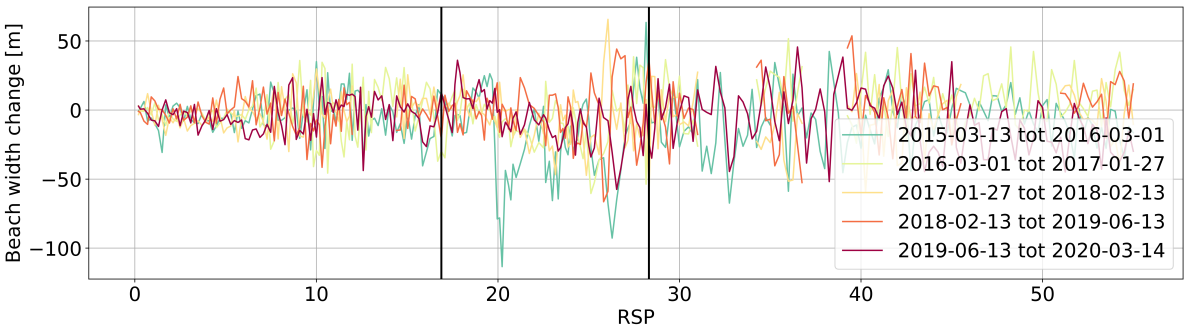

Figure 4.2: Beach width difference between March 2015 and March 2020, data obtained from JARKUS data. The vertical black lines indicate the HD. A negative value means a decrease in beach width and a positive value a increase in beach width.

4.1.3. Beach slope development 2015 - 2020

In Figure 4.3 the beach slope is shown. It was explained in Subsection 2.2.2 that there is a positive correlation between slope and wave run-up and, therefore, with erosion and beach width changes. If a steeper slope is present, then beach width is expected to change more rapidly.

The beach slope is defined as the slope of the beach between NAP + 0.0 m and NAP + 3.0 m (De Vries et al., 2012). The figure shows that the beach slope increased (in absolute terms) between 2015 and 2018. This implies that a milder slope was present when the nourishment was implemented. After the nourishment was implemented, the slope increased which may be due to erosion and the decrease in beach width. In March 2020, it appears that the slope is smaller in a number of locations than the slope in February 2018 which may be due to the additional nourishment implemented in March 2018. Due to the additional nourishment, the width of the beach has increased and therefore the beach slope

is decreasing. This does not correspond to the theory from Subsection 2.2.2. The beach slope is considered in these figures, i.e., the slope above NAP + 0.0 m and not the slope of the lower shoreface which can be different.

From this, it can be concluded that the beach width and beach slope are inversely proportional (Seddon & Fitton, 2011).

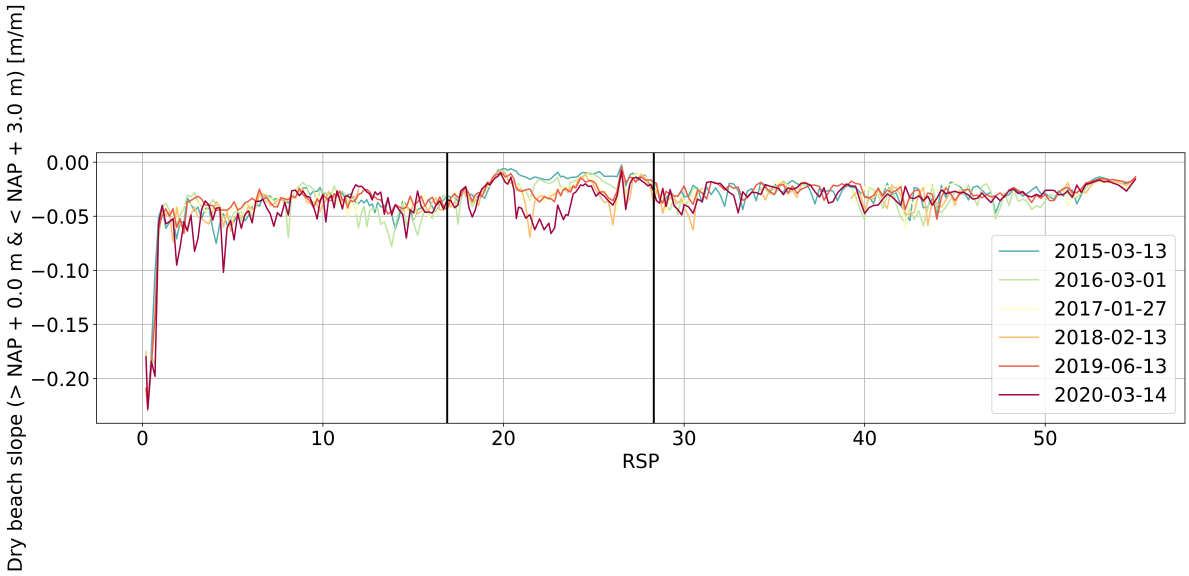

Figure 4.3: Beach slope between March 2015 and March 2020, data obtained from JARKUS data. The vertical black lines indicate the HD.

4.1.4. MKL position change 2015 - 2020

In Figure 4.4 the MKL position is shown between March 2015 and February 2019. The definition of the MKL position is given in Subsection 2.1.3 and in Equation 2.1. The change in MKL position is considered because it has an influence on the beach width change.

The figure shows that the position of the MKL line has decreased over the years. A decrease in the MKL position indicates a shift in the landward direction. The largest shift in the MKL position occurred between March 2015 and March 2016, i.e., in the first year after the nourishment was implemented. Furthermore, the graph also shows that there are few changes in the MKL position after the additional nourishment was implemented.

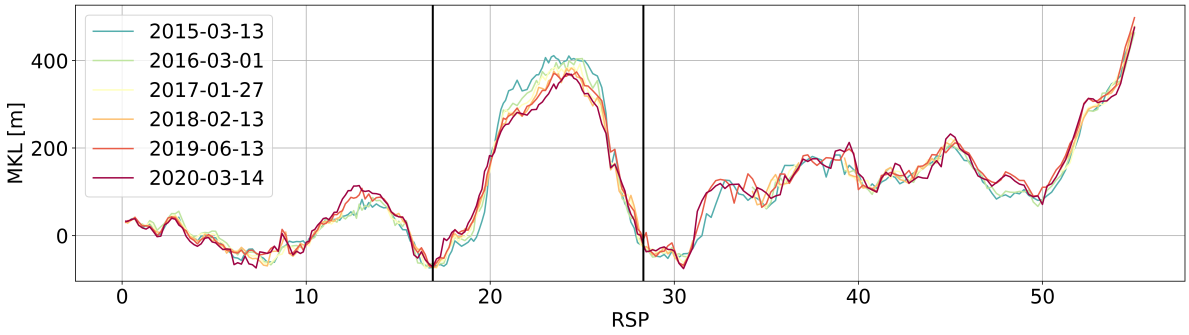

Figure 4.4: MKL position between March 2015 and March 2020, data obtained from JARKUS data. The vertical black lines indicate the HD.

The figure below, Figure 4.5, shows the difference of the MKL position between years. This figure shows that the largest decrease occurred between March 2015 and March 2016, almost immediately after the nourishment was implemented. It also appears from the figure that an increase, or seaward shift, occurred between March 2018 and March 2019 which may be due to the additional nourishment in March 2018.

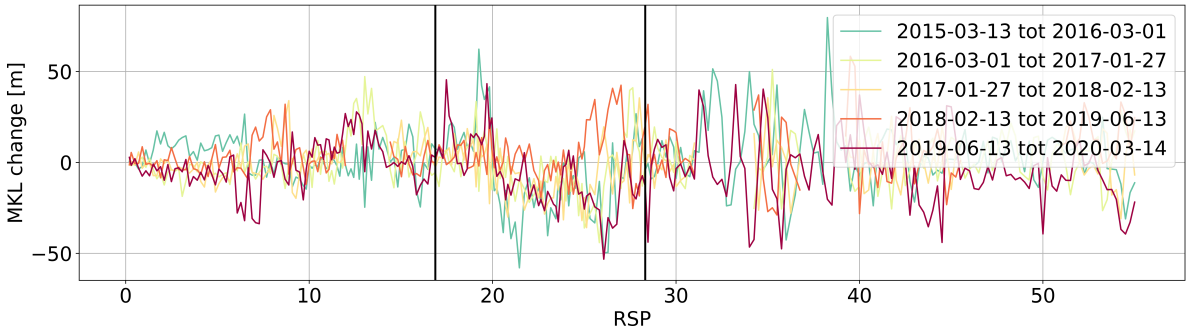

Figure 4.5: Difference in MKL position between March 2015 and March 2020, data obtained from JARKUS data. The vertical black lines indicate the HD.

4.1.5. Dune volume change 2015 - 2020

The dune volume is shown in Figure 4.6. It is defined as the volume of sand located above NAP + 3.0 m (Kroon et al., 2022; Leenders et al., 2018). This is also shown in Figure 2.2 in Subsection 2.1.2. Dune volume is studied to investigate whether there is a relationship between dune volume and beach volume. A decrease in beach volume and an increase in dune volume can be explained by the presence of the cross-shore sediment transport processes.

This figure shows that there is only a small difference in dune volume over the first five years. There is a small increase in dune volume the longer the nourishment is in place. Where the beach width decreases over the years, the dune volume shows a slight increase over the years. The largest increase in dune volume is at the locations where the dune volume is lower, i.e., in the troughs of the graph from the figure, for example around RSP 25.

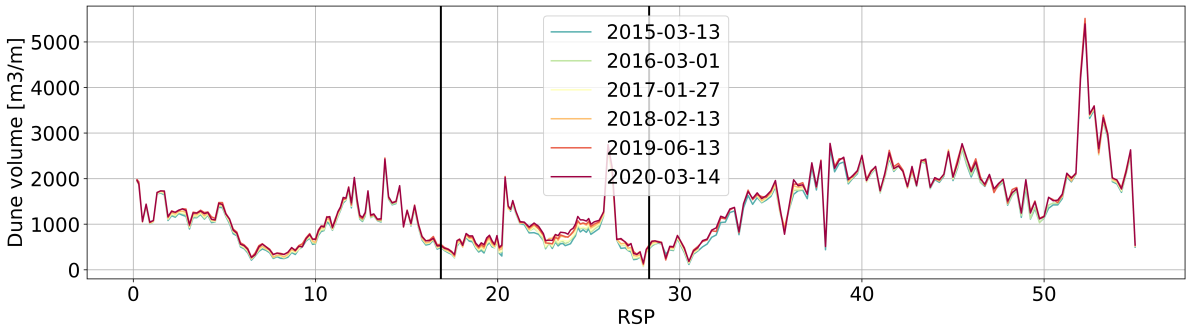

Figure 4.6: Dune volume between March 2015 and March 2020, data obtained from JARKUS data. The vertical black lines indicate the HD.

Figure 4.7 shows the difference in dune volume between years. It shows that the dune volume generally continues to increase after several years and thus there is no stagnation. There is a sharp decrease in dune volume between February 2018 and February 2019. This is the period immediately after the additional nourishment is implemented. There is a strong increase in the change of dune volume in the period immediately before the nourishment is implemented.

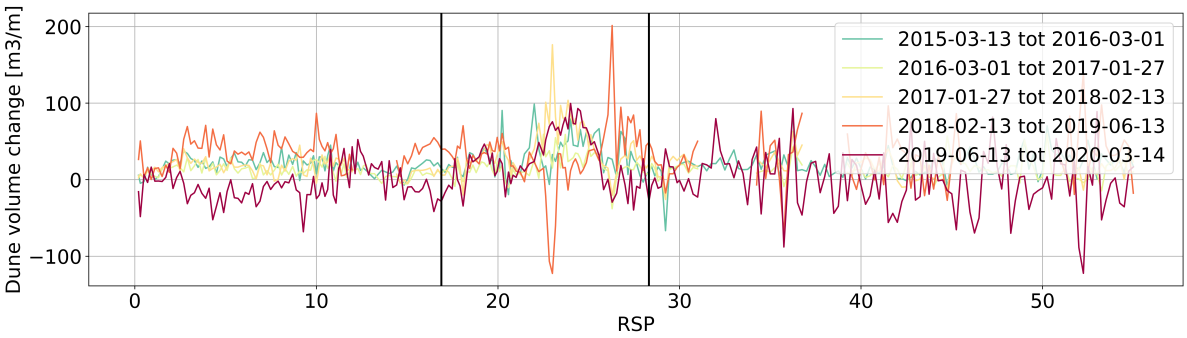

Figure 4.7: Difference in the dune volume between March 2015 and March 2020, data obtained from JARKUS data. The vertical black lines indicate the HD.

4.1.6. Dune foot orientation development 2015 - 2020

The figure below shows the dune foot orientation. The dune foot orientation can be obtained from the transects of the JARKUS data. These transects have an orientation which is perpendicular to the coast, with this the orientation of the dune foot can be determined (Kroon et al., 2022).

As shown in the figure, the orientation ranges from about 285 degrees north to 275 degrees north. Around RSP 20 there is a large peak and the orientation equals 310 degrees north. The figure shows that there are hardly any variations in orientation over the years.

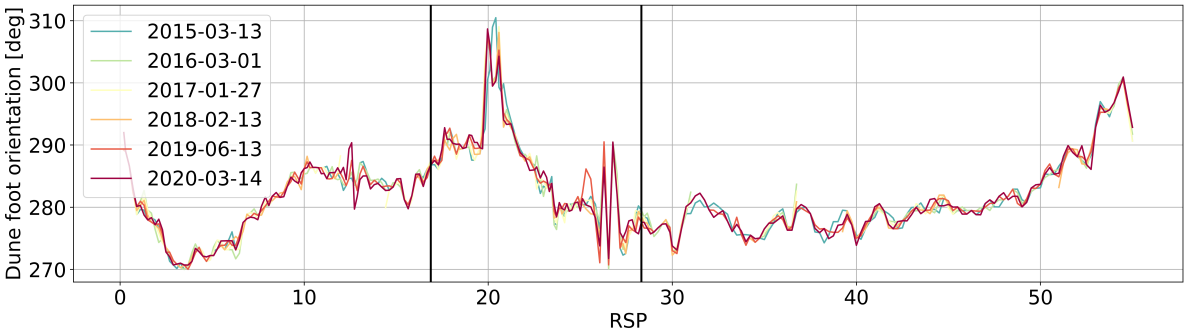

Figure 4.8: Dune foot orientation between March 2015 and March 2020, data obtained from JARKUS data. The vertical black lines indicate the HD.

4.2. Finding correlations between parameters

This section shows the correlations based on the JARKUS data. The focus here is only on the HD and therefore not on the other parts of the North-Holland coast. The correlations shown are the correlations for the five years between 2015 and 2019. As in Section 4.1, these correlations are also based on the available JARKUS measurements. The purpose of the correlations is to find a relationship between different parameters or trends.

4.2.1. Change in beach width vs. change in MKL position

A strong correlation can be seen (r^2 = 0.66) between the change in MKL position and the change in beach width. This correlation indicates that the MKL position moved in a landward direction at the locations where there is a decrease in beach width. This is equivalent to there being erosion above water and erosion below water where the amount of erosion is approximately equal. If there is a conservation of volume, this may mean that there will also be a conservation of beach width.

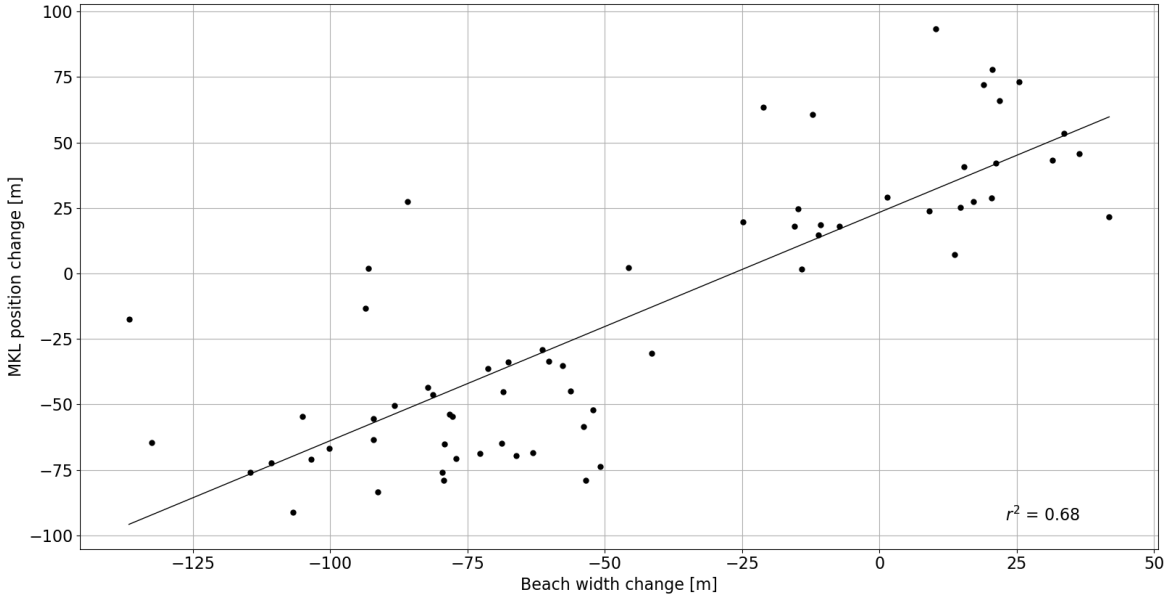

Figure 4.9: Correlation between the change in beach width and the change in MKL position between March 2015 and March 2020, data obtained from JARKUS data.

The figure below shows the correlation from 2015 to when the additional nourishment was implemented. The implementation of the nourishment increases the beach width. This human action may affect the correlation between the beach width and the MKL position. The influence mentioned above appears to be minimal because in the period from 2015 until the implementation of the additional nourishment in 2018, the correlation is about the same (r^2 = 0.68).

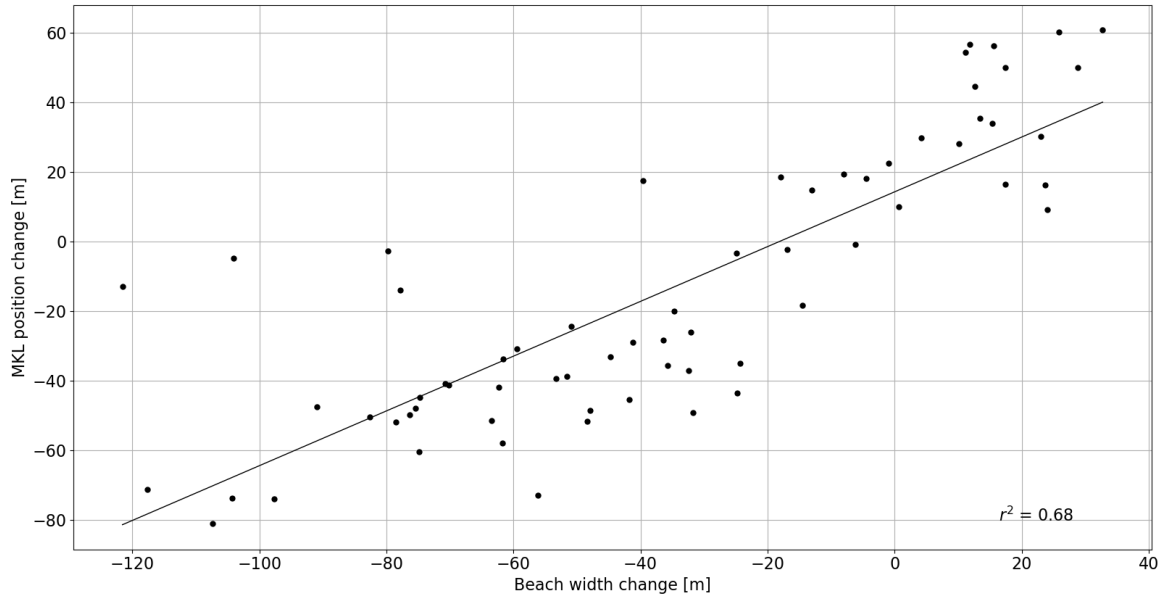

Figure 4.10: Correlation between the change in beach width and the change in MKL position between March 2015 and February 2018, data obtained from JARKUS data.

4.2.2. Change in beach volume vs. change in dune volume

It can be seen in Figure 4.11 that there is no correlation between the change in beach volume and the change in dune volume because there is a low correlation coefficient (r^2 = 0.08). The definitions of the two volumes are discussed in Subsection 2.1.2.

The low correlation between these two factors means that sediment is not only transported in the cross-shore direction but that sediment is also transported in the longshore direction. The sediment that has entered the dune, after all, there is a growth in dune volume, is not entirely originating from the beach. This involves the sand on the same transect. As a result of sediment transport in the longshore direction, sediment from one transect may be transported to sediment in the other transect.

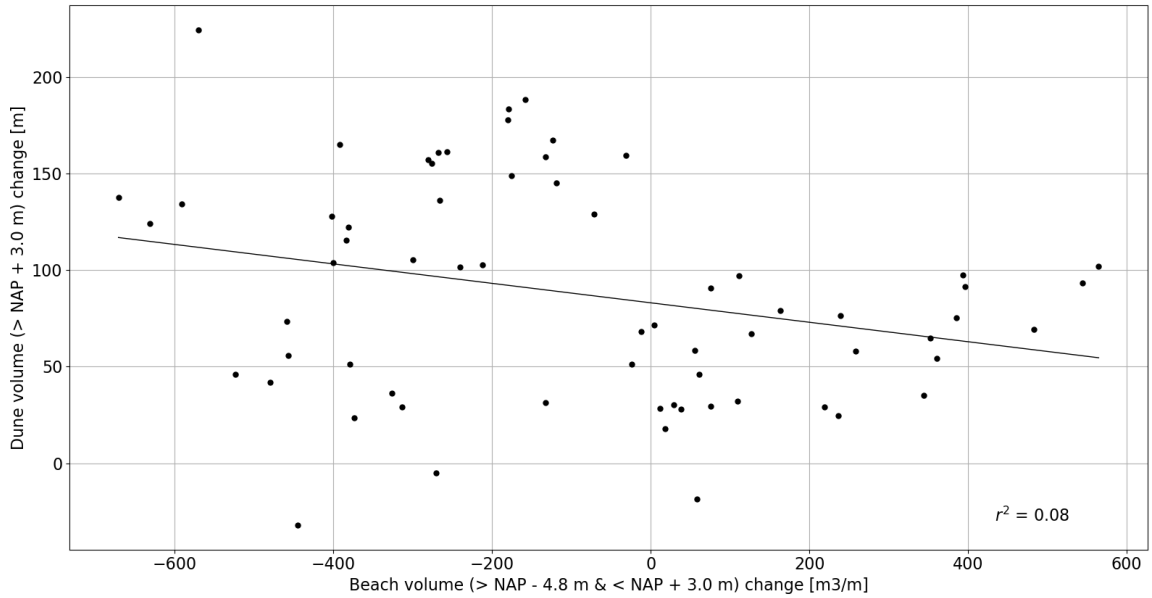

Figure 4.11: Correlation between the change in beach volume and the change in dune volume between March 2015 and February 2018, data obtained from JARKUS data.

4.3. Erosion and sedimentation patterns

This section compares the 2020 JARKUS data with the 2015 JARKUS data. By comparing these data, an initial prediction can be made of the patterns that should develop on the HD for the simulations to be run. In addition, the results of the simulations can be compared with the JARKUS data to investigate whether the simulations give a representative result of reality.

Figure 4.12 plots the bed level change between the 2015 measurement and the 2020 measurement. The blue colour in the figure indicates erosion and the red colour indicates sedimentation/accretion. The figure shows that erosion occurs at the convex coastline and sedimentation occurs at the concave coastline. Most of the changes occur in the area more onshore because in this area the waves start to feel the bottom and thus sediment is transported. In particular, an erosion hotspot can be seen on the curvature, while a sedimentation hotspot can be seen north of the curvature at y = 5.85e6 m. Most of the waves from the Netherlands come from the southwest (see Figure 3.6) with the result that the sediment that has eroded in the curvature is transported to the north. This created the pattern shown in the figure.

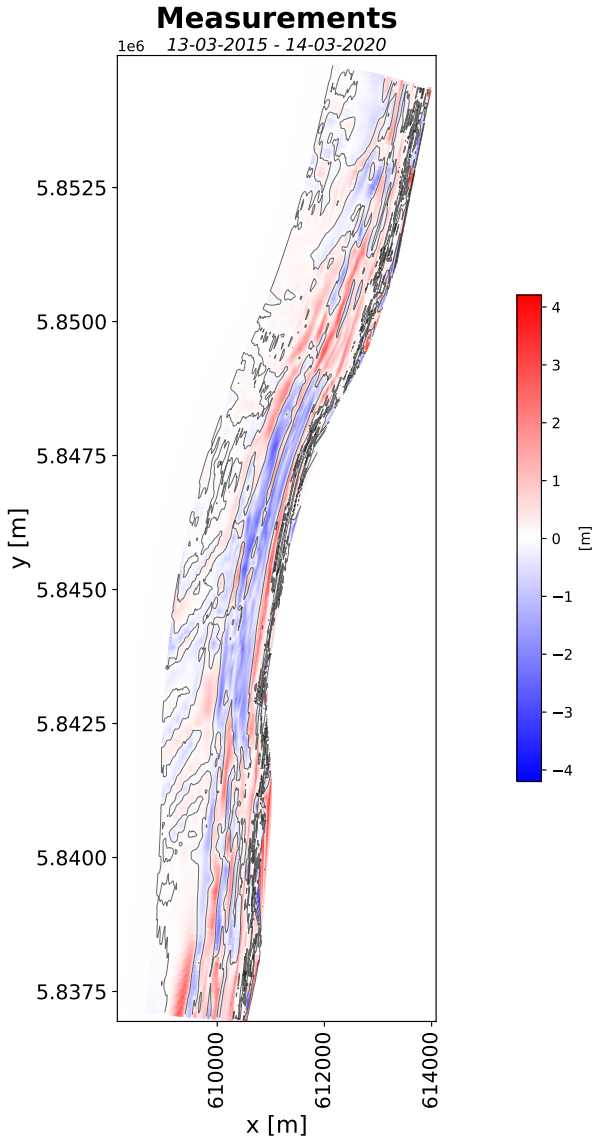

Figure 4.12: The bed level changes occurred during the first five years after implementation of the HD, so from 2015 to 2020. The blue colours indicate erosion and the red colours indicate sedimentation. The black contour lines indicate a bed level difference of zero.

To examine the response time of nourishment, the erosion and sedimentation patterns of the first year and the last year are shown below in, Figure 4.13a and Figure 4.13b, respectively. The figure shows that the bed level changes occurring in the first year after the implementation of the nourishment are larger than in the last year. There are more erosion hotspots in the first year, for example at y = 5.8425e6 m or at y = 5.8560e6 m. Thus, the response time in the first year is larger than in the last year which is consistent with the theory from Subsection 2.1.4. A similarity between the two years is that erosion occurs on a convex-shaped coast while sedimentation occurs on a concave-shaped coast.

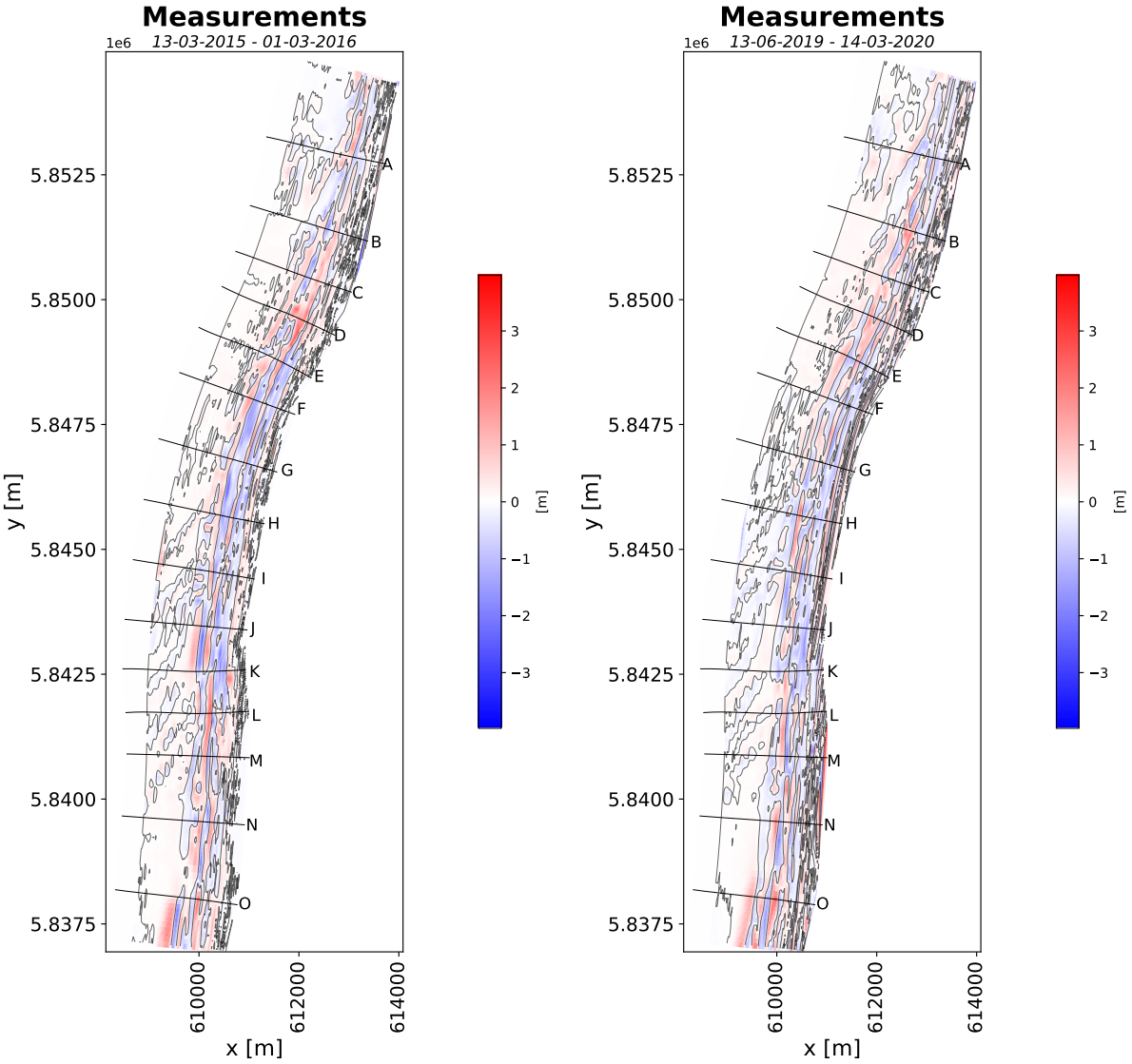

(a) The bed level difference based on JARKUS data of 2015 and 2016. (b) The bed level difference based on JARKUS data of 2019 and 2020.

Figure 4.13: The bed level difference based on JARKUS data. The blue colours indicate erosion and the red colours indicate sedimentation. The black contour lines indicate a bed level difference of zero.

4.4. Concluding remarks

In this chapter, the HD developments have been analysed based on measured data. This section draws conclusions as a result of the analysis carried out.

The largest changes occurred mainly in the period of 2015 and 2016, so the period immediately after the nourishment was implemented for the HD. In general, the greatest change occurs in the first year and decreases as the years progress. This is also consistent with the theory discussed in the Literature Review in Subsection 2.1.4. The profile aims to reach equilibrium as quickly as possible after an abrupt change, with the changes occurring faster at the beginning than when the profile has nearly reached equilibrium. Besides the changes that occur in the first year after the implementation of the nourishment, relatively large changes can also be seen in 2018 after the additional nourishment is applied. Again, the system has been brought out of balance by the nourishment of additional sediment.

5

Results schematic XBeach model

This research focuses on the impact of long waves and coastal curvature on the change in beach width. The research question to be answered in this chapter is *"What is the impact of long waves and coastal curvature on the reduction in beach width when tested in an idealised coastal setting?"*. This research question is divided in this chapter into two questions that will be answered through multiple simulations. The two sub-questions are:

- What is the effect of the strength of coastal curvature on the change in beach width?
- What is the difference between the change in beach width when the simulation is run in stationary mode and in surfbeat mode?

The model input is discussed in Subsection 3.3.3 and in Table 3.1 a summary is provided of the different runs performed to find answers to the above sub-questions.

5.1. Effect of the degree of coastal curvature

5.1.1. Degree of curvatures applied in the schematic model

This section answers the first sub-question. For this, several of the results of the different curvatures are compared for different parameters such as sediment transport and beach width difference. The length of the grids for the different curves is unequal because the grid with the largest curvature consists of more grid points. To compare the results with each other, the results of the smaller grids are ”stretched” so that the curvature starts and ends at the same places. In Table 5.1 below, the strength of the curvatures is shown.

Table 5.1: Coastal curvatures applied in the different runs

Two times less curvature [° per kilometre]	2
Original case [° per kilometre]	4
Two times more curvature [° per kilometre]	8

The conditions in surfbeat mode are all applied for all three curvatures. For the conditions in stationary mode, they are only applied for twice the curvature strength and therefore the answer to this sub-question is answered by comparing the results of the surfbeat mode runs.

5.1.2. Longshore sediment transport

In Figure 5.1 the longshore sediment transport is shown for the conditions from Run 2. The longshore sediment transport is calculated by integrating over the cross-section. Here the coastline curvature was taken into account because the coordinate system of the longshore sediment transport output does not rotate when the coast rotates. The longshore sediment transport is constant up to an alongshore distance of about 95,000 m. To the left of the first vertical black line in the plot is the straight part of the grid. Here almost no variations in the angle of incidence of the wave relative to the shore normal

take place yet. Once these variations increase a gradient can also be seen in the longshore sediment transport where in this case it increases due to an increasing wave angle of incidence.

The gradient of the longshore sediment transport for the stronger curvature is larger than the gradient for the other two curvatures. Stronger curvature causes a larger gradient to be present in the change of shore normal. The angle of incidence of the waves on the offshore boundary does not change, but a change in the shore normal changes the angle of incidence of the waves on the shore normal. A larger change in the gradient in the shore normal leads to a larger change in the angle of incidence of the waves. The longshore sediment transport depends on the angle of incidence, Subsection 2.3.2, where a larger gradient in the angle of incidence leads to a larger gradient in the longshore sediment transport.

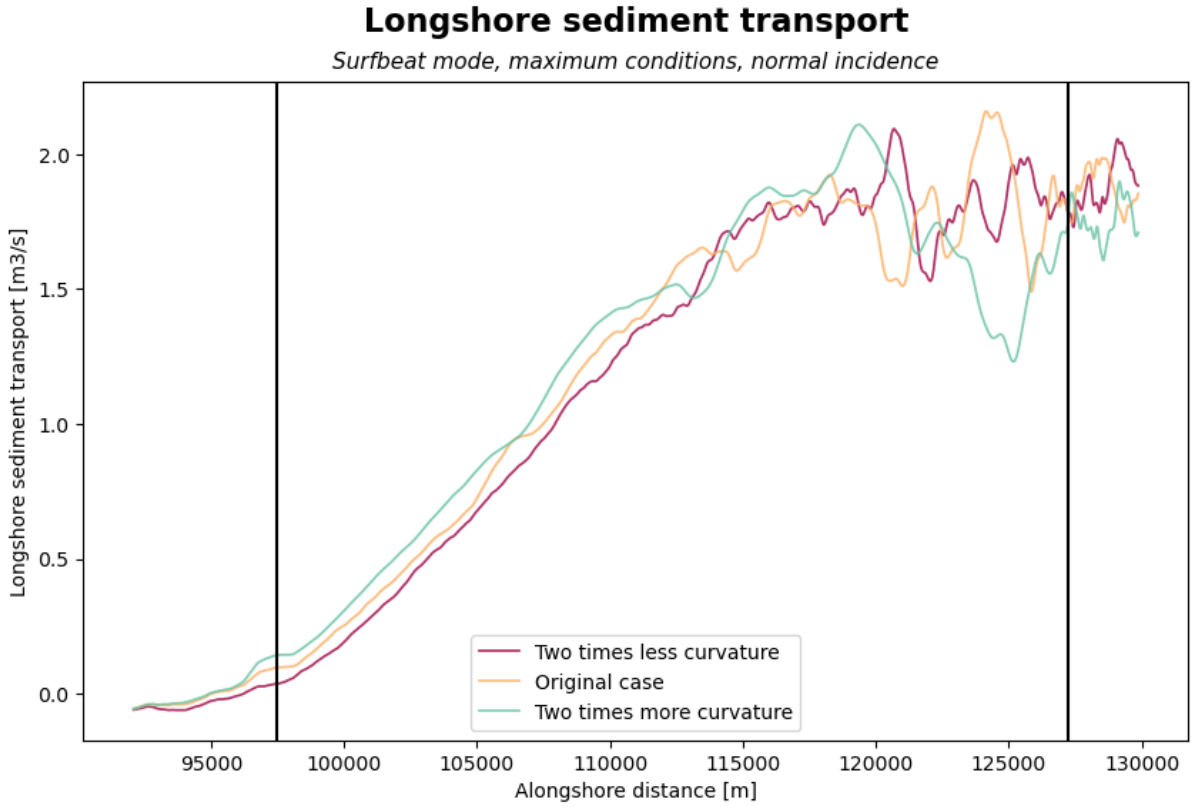

Figure 5.1: Comparison of the longshore sediment transport between the different coastal curvatures. Results of the maximum wave conditions with a wave angle of incidence of 0 degrees. The black vertical lines indicate the start and end of the curvature. Modified from XBeach output.

5.1.3. Beach width difference

Figure 5.2 shows the beach width difference at the end of the simulation with the conditions of Run 2. This figure shows that the differences in the curvature are small for the different types of curvatures. As the beginning of the curvature is reached, however, differences can be seen. The variations for the beach width difference are larger for the stronger curvature. As larger variations occur in the longshore sediment transport, larger variations also occur in the beach width differences, these are correlated with each other.

The gradient in the beach width difference is larger for the stronger curvature. This is due to the larger gradient that the longshore sediment transport has.

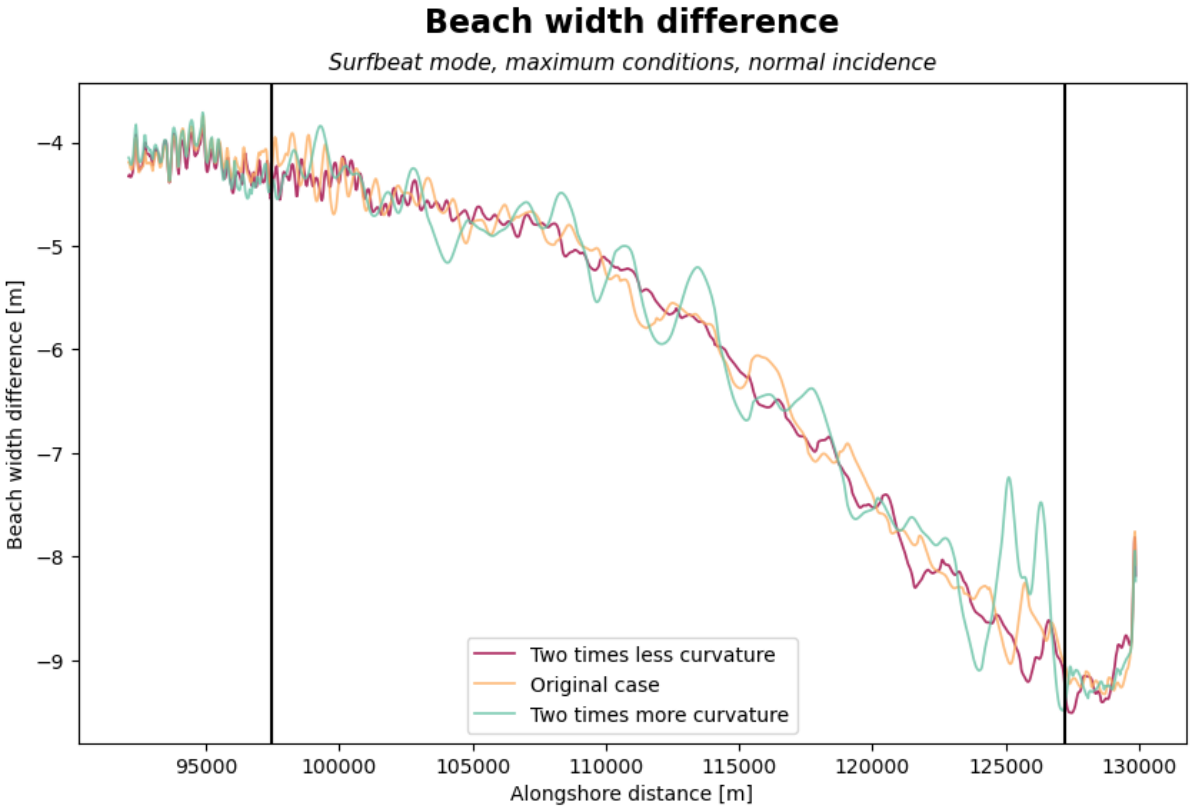

Figure 5.2: Comparison of the beach width difference between the different coastal curvatures. Results of the maximum wave conditions with a wave angle of incidence of 0 degrees. The black vertical lines indicate the start and end of the curvature. Modified from XBeach output.

5.1.4. Beach volume difference

In Figure 5.3 the difference in beach volume is plotted for the different curvatures. This figure shows that for all transects, there is a decrease in beach volume when there is an increase in alongshore distance. Before and after the curvature, on the straight sections, almost no differences can be seen between the different curvatures. In the figure, it can be seen that the variations for two times more curvature are bigger than the variations for two times less curvature. Based on the figures of the longshore sediment transport (Figure 5.1) and the volume difference (Figure 5.3), it can be concluded that an increase in the longshore sediment transport leads to a decrease in the beach volume. A comparison between the figures of the beach width difference and the beach volume difference, Figure 5.2 and Figure 5.3 respectively, indicates that a decrease in beach width leads to a decrease in beach volume. For the beach volume, depths between NAP - 4.8 m and NAP + 3.0 m are considered while for the beach widths, depths between approximately NAP - 0.8 m and NAP + 3.0 m are considered. It follows that a decrease in beach width does not have to directly lead to a decrease in beach volume because the volume can be deposited further offshore. These figures show that this is not the case for the simulation.

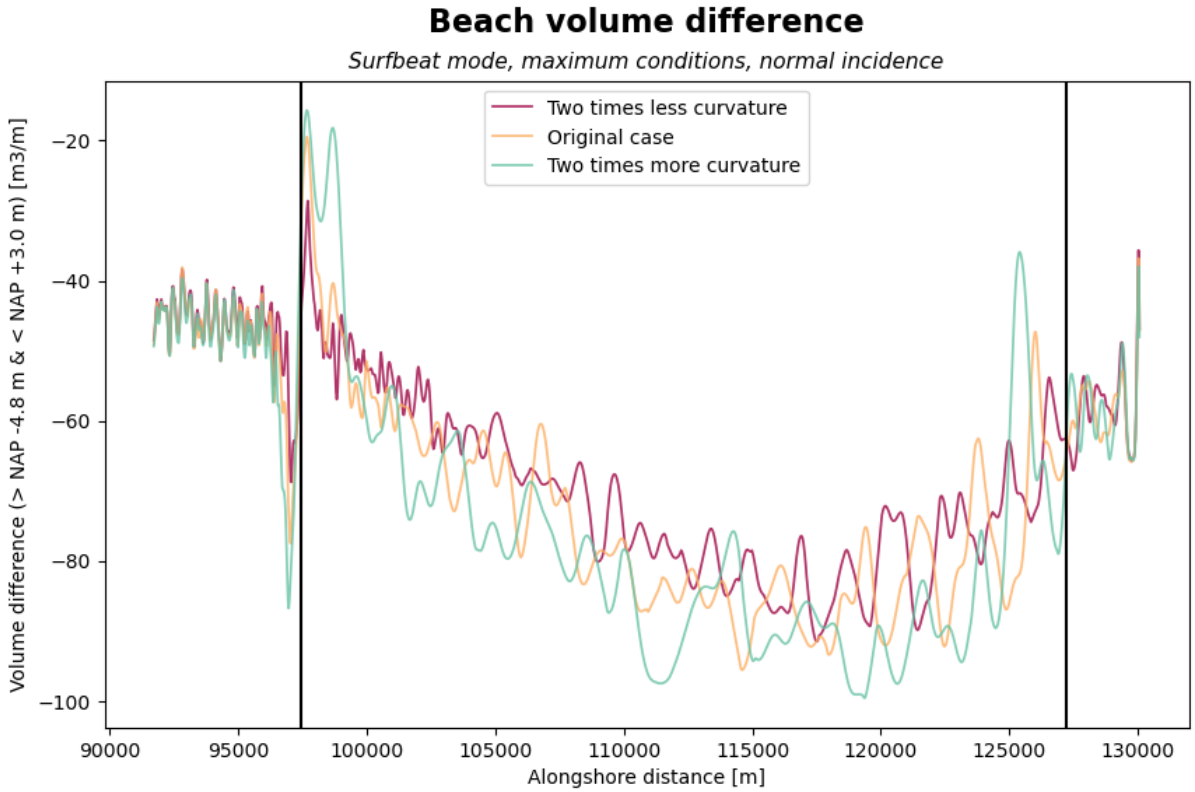

Figure 5.3: Comparison of the beach volume difference between the different coastal curvatures. Results of the maximum wave conditions with a wave angle of incidence of 0 degrees. The black vertical lines indicate the start and end of the curvature. Modified from XBeach output.

5.2. Difference between stationary mode and surfbeat mode

The wave conditions applied when comparing the differences between the stationary mode and the surfbeat mode are the maximum wave conditions where the wave height is equal to 5.88 m. The figures below show the same type of figures as above with the difference being that these simulations were performed in the stationary mode. In this section, the results of the surfbeat mode and stationary mode are compared so that an answer can be found to the second sub-question established in this chapter.

5.2.1. Longshore sediment transport

Figure 5.4 shows the longshore sediment transport for the stationary mode. There is almost no longshore sediment transport present in the straight part of the grid where there are normal incident waves (to the left of the first vertical black line). As soon as the curvature increases, the amount of longshore sediment transport also increases. Moreover, this figure shows that the variations for the strongest curvature are the largest and the variations for the smallest curvature are the smallest.

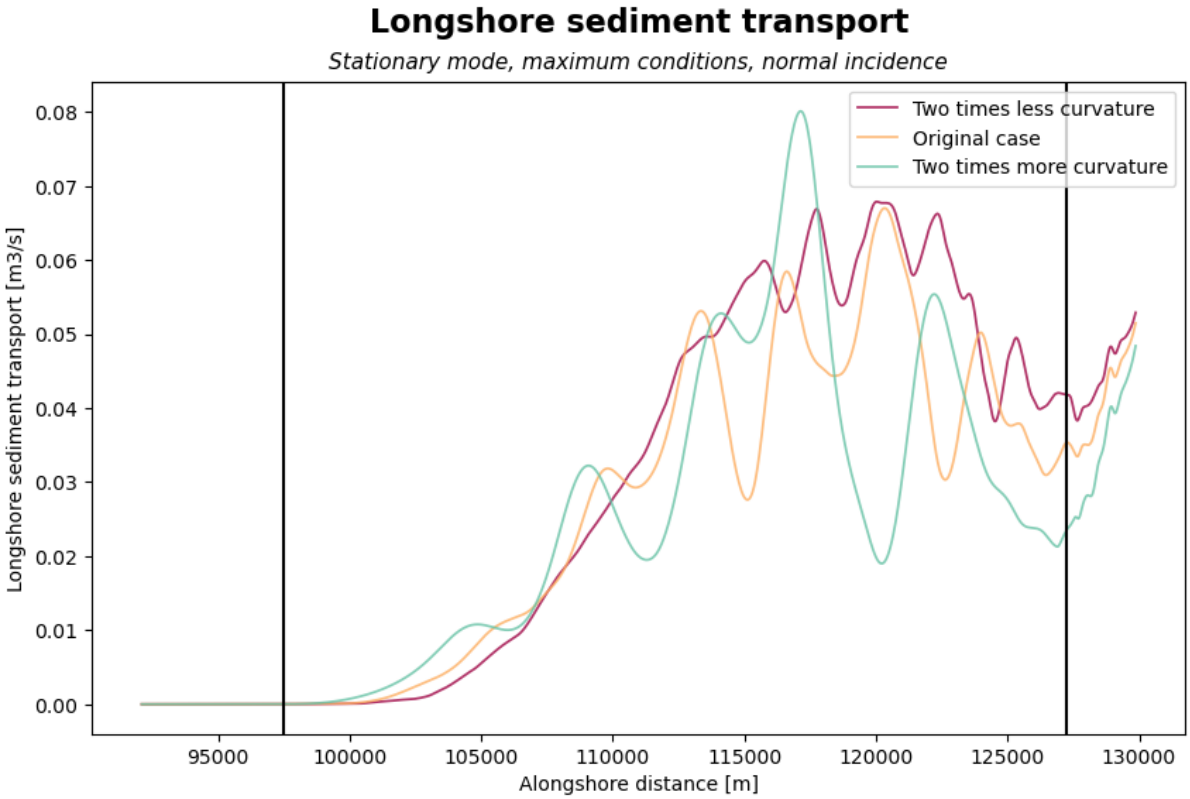

Figure 5.4: Comparison of the longshore sediment transport between the different coastal curvatures. The simulation is performed in stationary mode. Results of the maximum wave conditions with a wave angle of incidence of 0 degrees. The black vertical lines indicate the start and end of the curvature. Modified from XBeach output.

5.2.2. Beach width difference

In Figure 5.2 the beach width difference is shown for the stationary mode. The result of this figure is compared with the result from Figure 5.2. It follows from this comparison that the differences in the beach width for the surfbeat mode are larger than for the stationary mode. For the stationary mode, the beach width changes are approximately equal to a decrease of O(0.5) m while the beach width differences in the surfbeat mode are equal to a decrease of O(5) m.

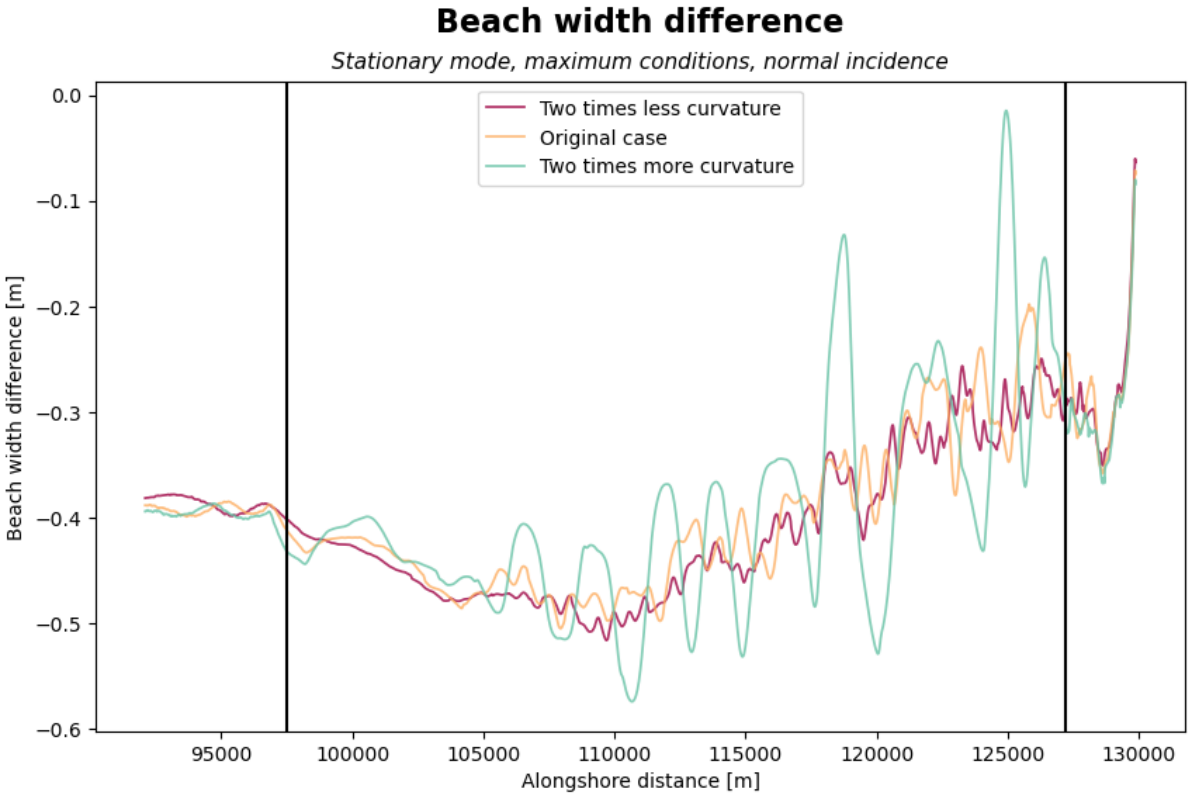

Figure 5.5: Comparison of the beach width difference between the different coastal curvatures. The simulation is performed in stationary mode. Results of the maximum wave conditions with a wave angle of incidence of 0 degrees. The black vertical lines indicate the start and end of the curvature. Modified from XBeach output.

5.2.3. Beach volume difference

In Figure 5.6 the change in beach volume is shown. It follows from this figure that there is little change in beach volume. The change in beach volume for the surfbeat case was almost 10 times larger. This order of magnitude corresponds to the difference in change in beach width.

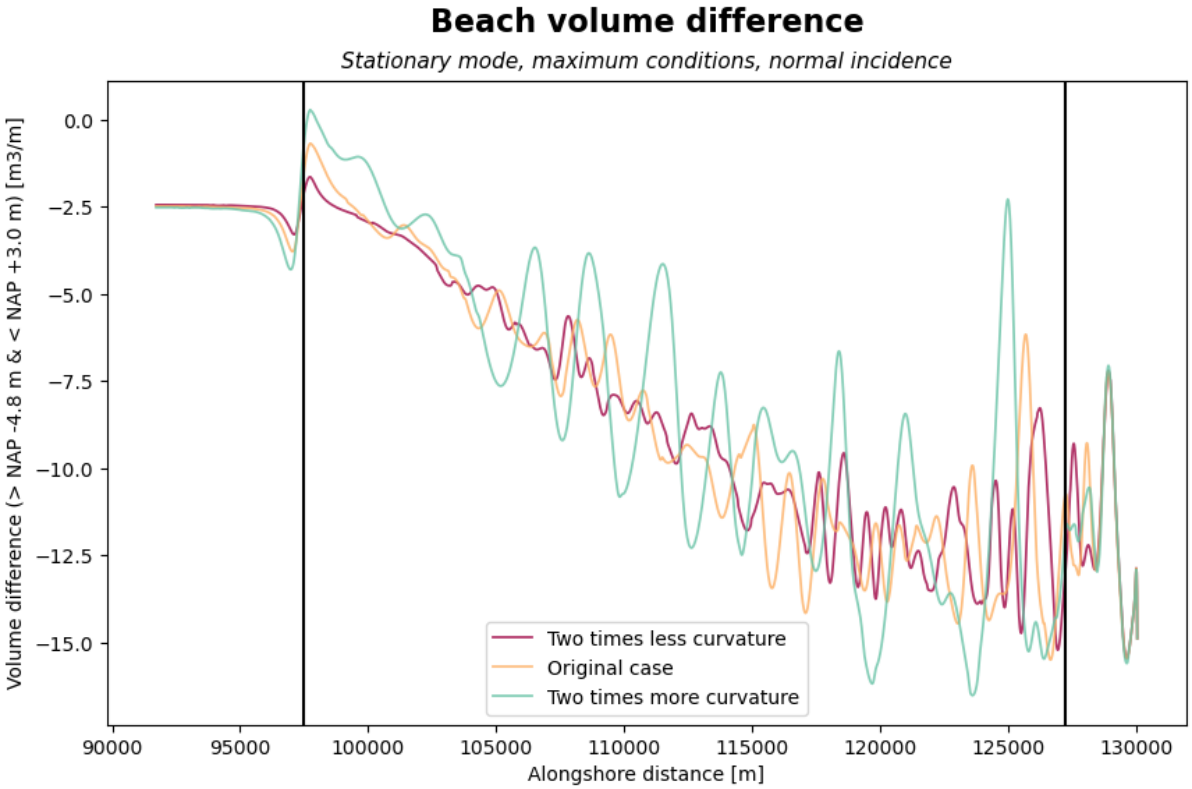

Figure 5.6: Comparison of the beach volume difference between the different coastal curvatures. The simulation is performed in stationary mode. Results of the maximum wave conditions with a wave angle of incidence of 0 degrees. The black vertical lines indicate the start and end of the curvature. Modified from XBeach output.

5.3. Sensitivity analysis wave conditions

The sections above, Section 5.1 and Section 5.2, discussed the conditions of one run. Multiple runs were performed with multiple conditions. This section briefly discusses the influence of these conditions and whether adjusting the conditions leads to major changes in the results.

The wave height applied in the runs is equal to 2.50 m for the moderate storm conditions or 5.88 m for the maximum conditions. An increase in wave height also leads to an increase in wave period and surge. The wave height applied affects the results because the simulations showed that a higher wave height leads to more longshore sediment transport. As a result, the beach width decreases faster and a larger decrease in beach volume is seen.

In addition to the wave height, the wave direction was also varied. The wave directions used were 0° and 45°. A change in wave direction affects the location where the largest decrease in beach width occurs. For an angle of incidence of 0 degrees, the largest decrease in beach width occurs around halfway through the curve while the largest decrease in beach width for an angle of incidence of 45 degrees occurs at the beginning of the curve.

Wave height, wave period, surge elevation and wave period do not affect the differences found between the strengths of the curvature and the differences between simulations in stationary mode and surfbeat mode. A more comprehensive analysis can be found in Section D.3.

5.4. Concluding remarks

In this chapter, the research question *"What is the impact of long waves and coastal curvature on the reduction in beach width when tested in an idealised coastal setting?"* was answered by dividing this sub-question into two sub-questions addressing both aspects.

An alongshore uniform grid has been used in the schematic model of this chapter which is seen as an idealised coastal setting. It follows from the figures shown in this chapter (Figure 5.1 to Figure 5.3) and in Appendix D that the strength of the coastline curvature affects the gradient of the longshore sediment transport. A stronger coastline curvature causes a larger gradient of the wave angle of incidence relative to the shore normal resulting in a larger gradient in transport. As more sediment is transported, larger variations in beach width change occur. Besides a decrease in beach width, variations in the decrease in beach volume also occur.

The effect of infragravity waves in the surfbeat mode is also clearly visible in the above figures (the results of the surfbeat mode are shown in Figure 5.1 to Figure 5.3 and the figures of the stationary mode are shown in Figure 5.4 to Figure 5.6). Comparing the figures shows that the magnitudes of the results are larger in the surfbeat mode. The longshore sediment transport in the surfbeat mode is about a factor of 25 larger compared to the longshore sediment transport in the stationary mode. Few differences can be seen in the variations and gradients, for both modes the variations and gradients are largest for the strongest curvature. For the beach width variations, the difference in beach width in the surfbeat mode is about 15 times larger.

6

Results XBeach model of the Hondsbossche Dunes

This section presents the results of the XBeach model simulation of the HD. The purpose of this section is to answer the question *"To what extent is the 2DH model, XBeach, able to predict the reduction in beach width of the Hondsbossche Dunes?"*. To answer this question, the validation of the XBeach model is performed by comparing the results of the model simulation with those derived from the JARKUS data and Vaklodingen surveys. More detailed results can be found in Appendix E.

The erosion and sedimentation patterns in the plots in the following sections show transects whose cross-section is plotted. These transects are also shown in Figure 6.1 so that it can be seen at which locations these transects were taken. For example, the location of transect K is at the location where a lagoon is present which affects the change in beach width.

Figure 6.1: Google Earth image with the boundaries of the grid applied in the XBeach model and the location of the different transects. Modified from Google Earth.

To find the best possible answer to the sub-question described above, several simulations were performed. Based on the correlation coefficients that follow from the comparison between the measured and modelled beach width differences, it was decided to take the year 2016 as the first year of the simulation. The correlations are shown in Appendix E. The initial effects that occur immediately after mooring are excluded if 2016 is taken as the first year of the simulation.

6.1. Bed level changes

The results from April 2016 to March 2017 are the results of the second year after the nourishment was implemented. The bed level change is determined by subtracting the bed profile at the end of the simulation from the initial bed profile.

The three figures below, Figure 6.2 to Figure 6.4, show the bed level change for the second year after the nourishment was implemented, the bed level change in the third year after the nourishment was implemented and the bed level change in the final year. In Appendix E, the figures are shown for all years.

When the results of the model and the 2016 - 2017 measurements are compared, it becomes clear that the amount of erosion taking place is slightly larger according to the predictions of the numerical model than what is actually measured. In addition, sedimentation takes place on the south side at y = 5.800e6 m of the curvature according to the measurements, this is not reproduced in the numerical model.

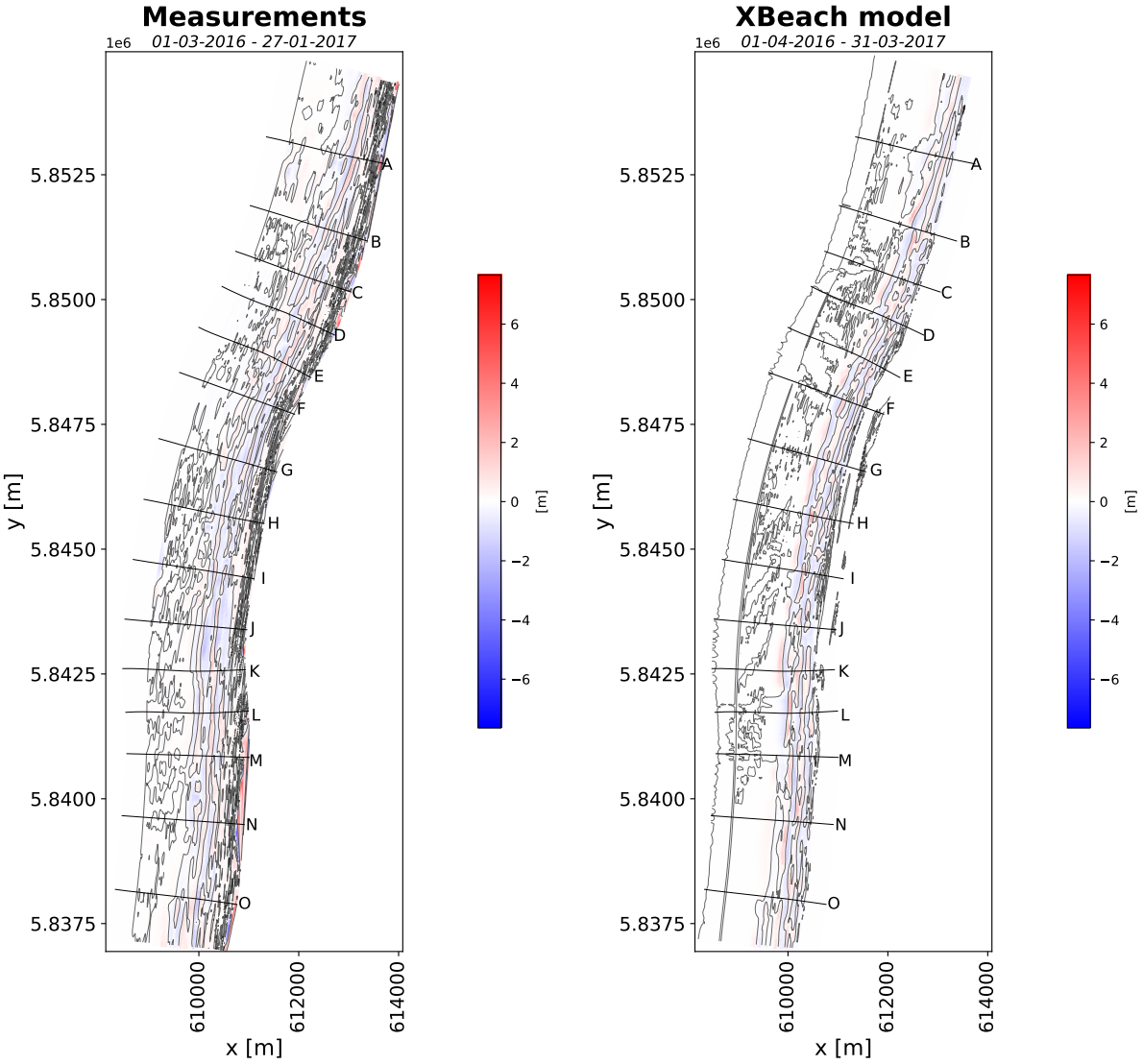

(a) Measurements (b) Output model

Figure 6.2: The results from 2016 to 2017. The blue colours indicate erosion and the red colours indicate sedimentation. The black contour lines indicate a bed level difference of zero. Modified from JARKUS data and XBeach output.

It can be seen in Figure 6.3 that there is a sedimentation hotspot south of the curvature between transects M and N. This sedimentation hotspot is observed in the measurements of the JARKUS data, but not in the results of the model. In addition, it follows from the figure that there is more erosion on the curvature based on the measurements than based on the XBeach model results.

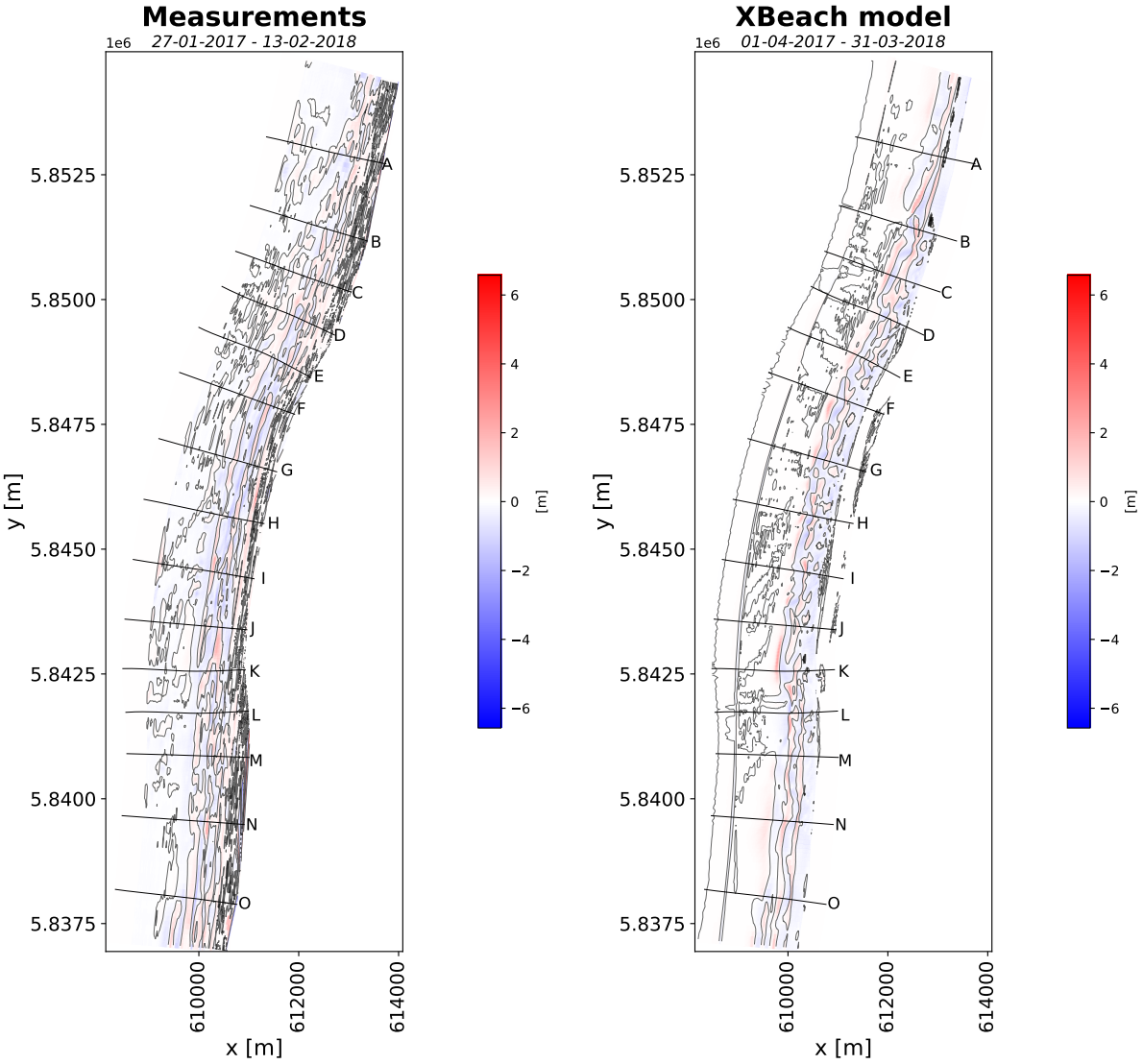

(a) Measurements

(b) Output model

Figure 6.3: The results from 2017 to 2018. The blue colours indicate erosion and the red colours indicate sedimentation. The black contour lines indicate a bed level difference of zero. Modified from JARKUS data and XBeach output.

The results for the last year show the least changes in bed level compared to the other years. The comparison of the results for the measurements and the simulation shows that there is a larger decrease in bed level for the measurements than what is predicted by the numerical model in XBeach.

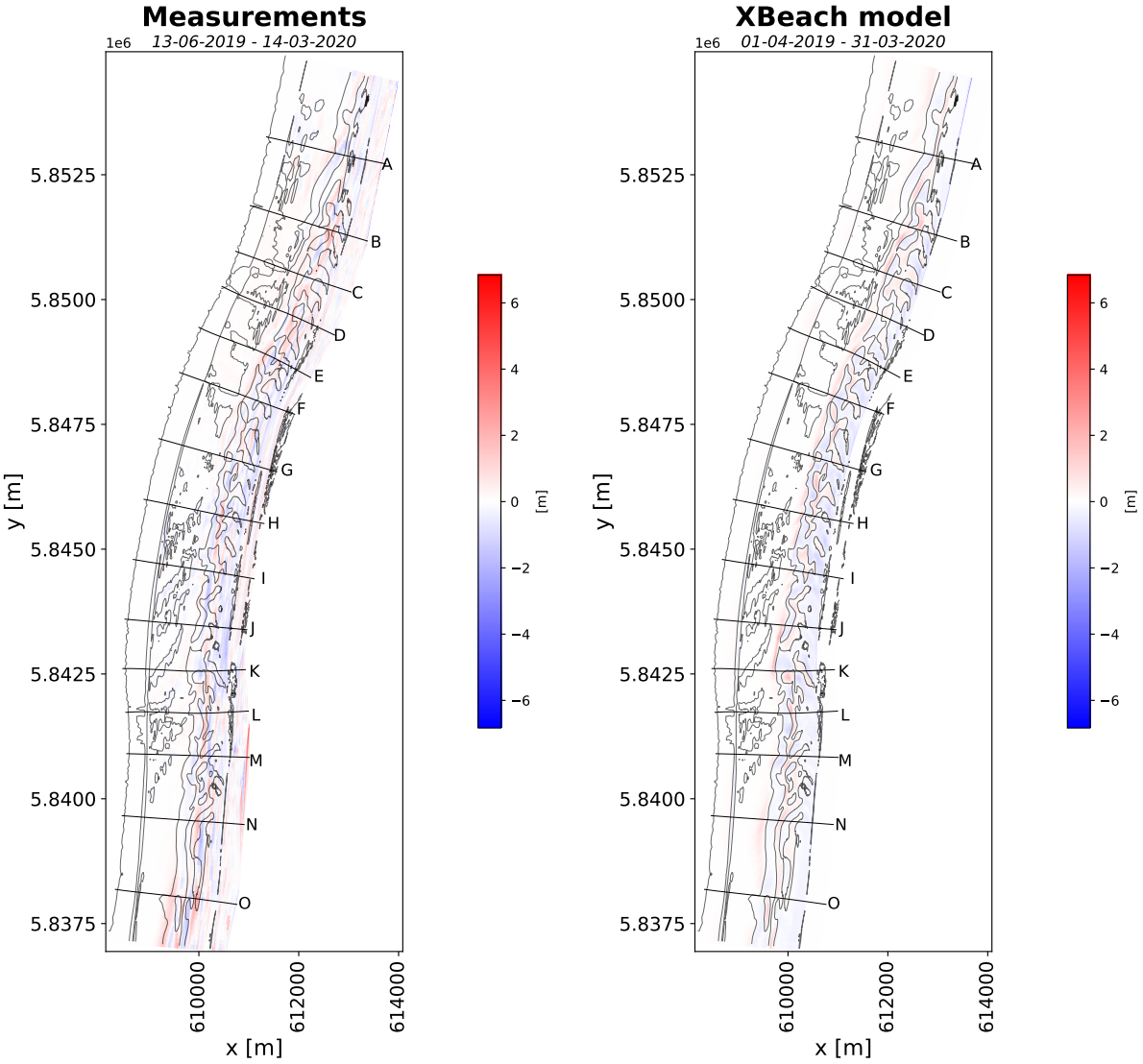

(a) Measurements

(b) Output model

Figure 6.4: The results from 2019 to 2020. The blue colours indicate erosion and the red colours indicate sedimentation. The black contour lines indicate a bed level difference of zero. Modified from JARKUS data and XBeach output.

6.2. Beach width differences

In this section, the change in beach width is shown. Here, a comparison is made between the results of the measurements of the JARKUS data and the results of the simulations of the XBeach model. The beach width is calculated using the definition given in Subsection 2.1.2 where a negative beach width difference leads to a decrease in beach width. In the plots, the x-axis runs from south to north.

In the second year after the nourishment is implemented, it can be seen that the variations in beach width change between the transects are approximately the same for the JARKUS data and the XBeach model. In general, XBeach does have a decrease in beach width as a result of the locations where the measurements also show this.

The large peak seen in the results is found at transect K. It follows from Figure 6.1 that this transect is located where a lagoon is present. As a result of this lagoon, the beach profile of this transect is different from the other beach profiles in that a profile is present on the seaward side of the lagoon so it is higher than NAP + 3.0 m. In the calculations, this is seen as an extra dike, but the profile is not as high everywhere after one year, resulting in large differences due to the definition of the beach width.

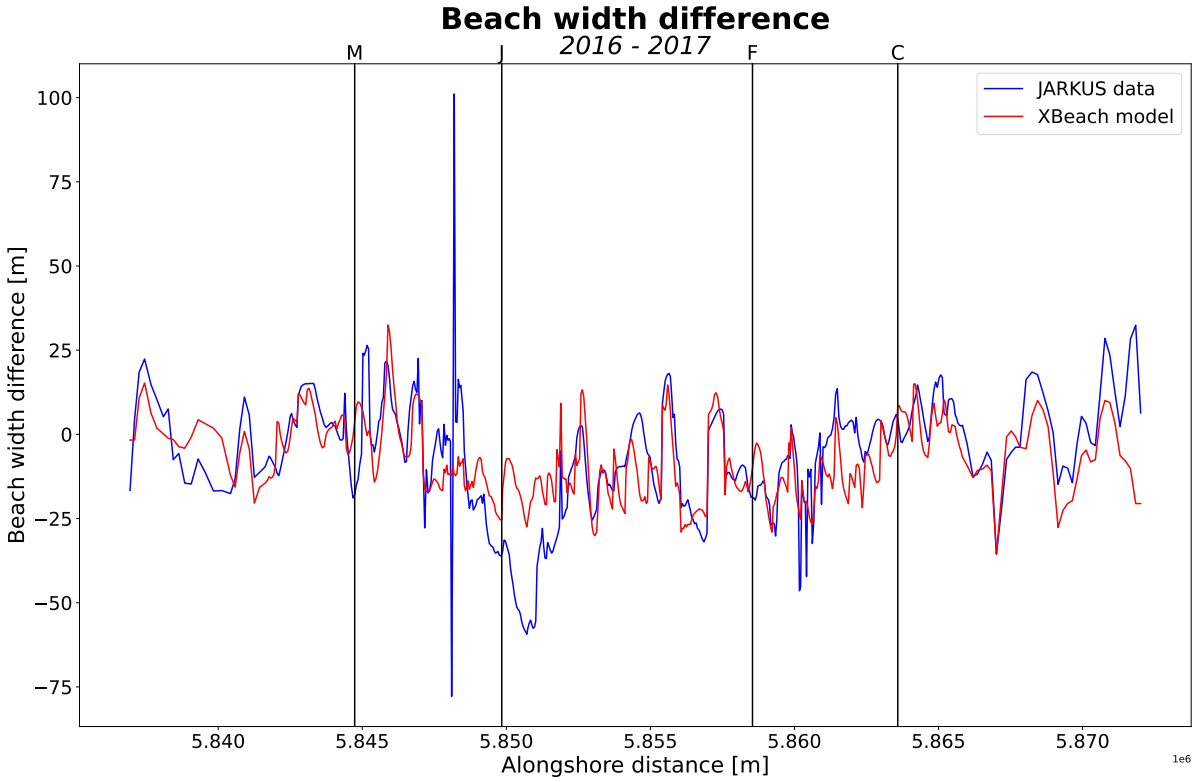

Figure 6.5: Comparison between the results of the XBeach model and the measurements. These figures are the results of 2016 - 2017. The black vertical lines indicate the transects as indicated in the figures for the bed level change. A negative beach width difference means a reduction in the beach width.

It follows from Figure 6.6 that the differences between the measured beach width difference and the modelled beach width difference are small between transects C and M, but are larger outside these transects. However, a large increase in beach width based on the JARKUS data can be seen around an alongshore distance of 5.849e6 m. This, like transect K, is a transect through the lagoon. It follows from this figure that the predictions agree almost well for the curvature, but the predictions on the straight parts of the coast do not.

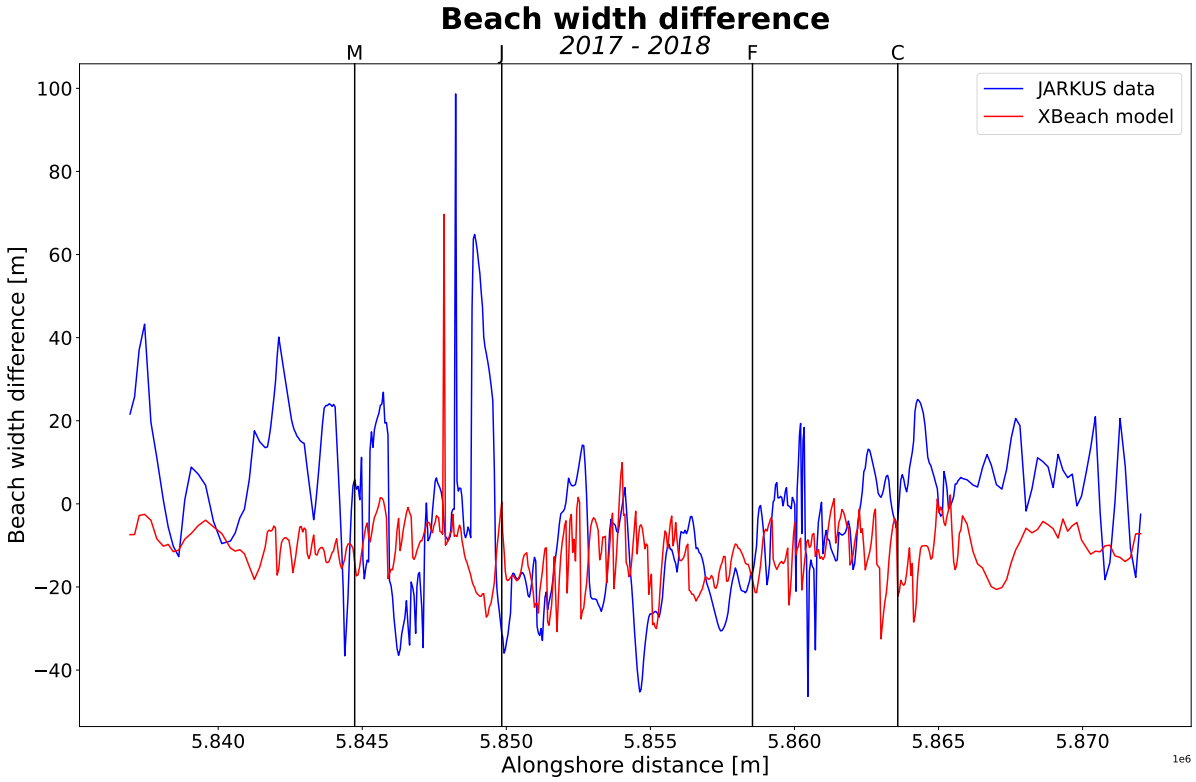

Figure 6.6: Comparison between the results of the XBeach model and the measurements. These figures are the results of 2017 - 2018. The black vertical lines indicate the transects as indicated in the figures for the bed level change. A negative beach width difference means a reduction in the beach width.

It can be seen in Figure 6.7 that there are few changes in the development of beach width in the last year of this study. In general, trends in measured and modelled beach width do not match. An increase in beach width based on the measured data often corresponds to a decrease in beach width based on the modelled data.

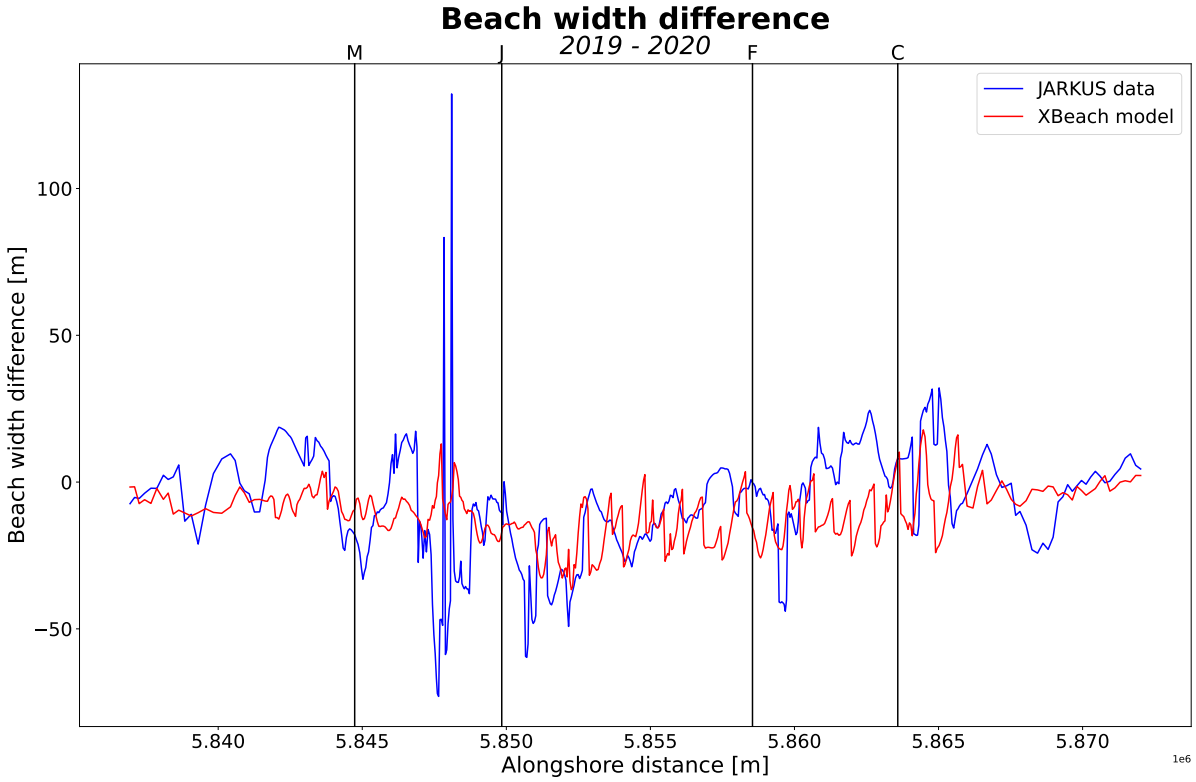

Figure 6.7: Comparison between the results of the XBeach model and the measurements. These figures are the results of 2019 - 2020. The black vertical lines indicate the transects as indicated in the figures for the bed level change. A negative beach width difference means a reduction in the beach width.

6.3. Volume differences

This section discusses the volume differences of the beach. The volume differences are based on the bed level changes. It is calculated by integrating the bed level changes at the locations where the initial bed is between NAP - 4.8 m and NAP + 3.0 m in the cross-shore direction.

Figure 6.8 shows the change in beach volume for the second year after implementation. The differences between the volume change of the beach based on the measured data and the modelled data match each other from an alongshore distance of about 5.850e6 m. The differences between the measured and modelled data are larger on the south side of the curvature. According to the XBeach model, more erosion occurs on the south side than according to the JARKUS data.

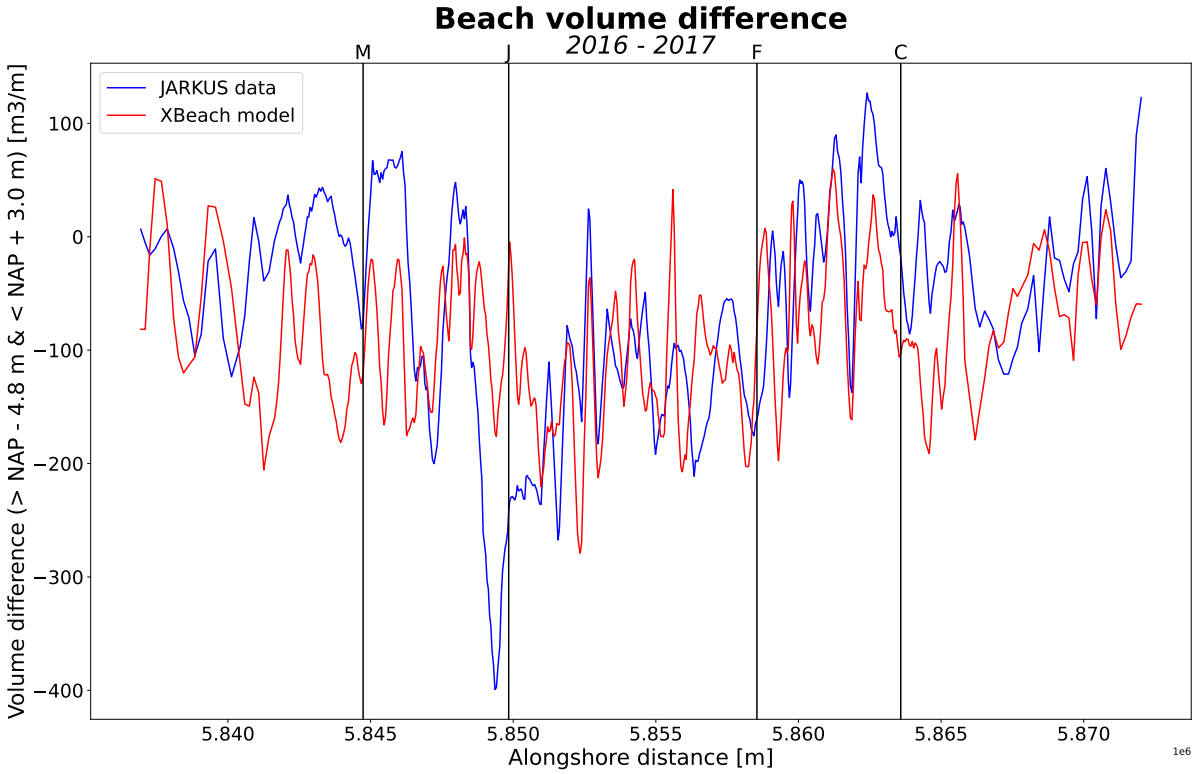

Figure 6.8: Comparison between the results of the XBeach model and the measurements. These figures are the results of 2016 - 2017. The black vertical lines indicate the transects as indicated in the figures for the bed level change. A negative volume difference means a reduction in the volume.

The volume changes for the third year after nourishment implementation do not match as closely, see Figure 6.9. In general, according to the JARKUS data, there is an increase in beach volume while there is a decrease in beach volume based on the simulations in XBeach.

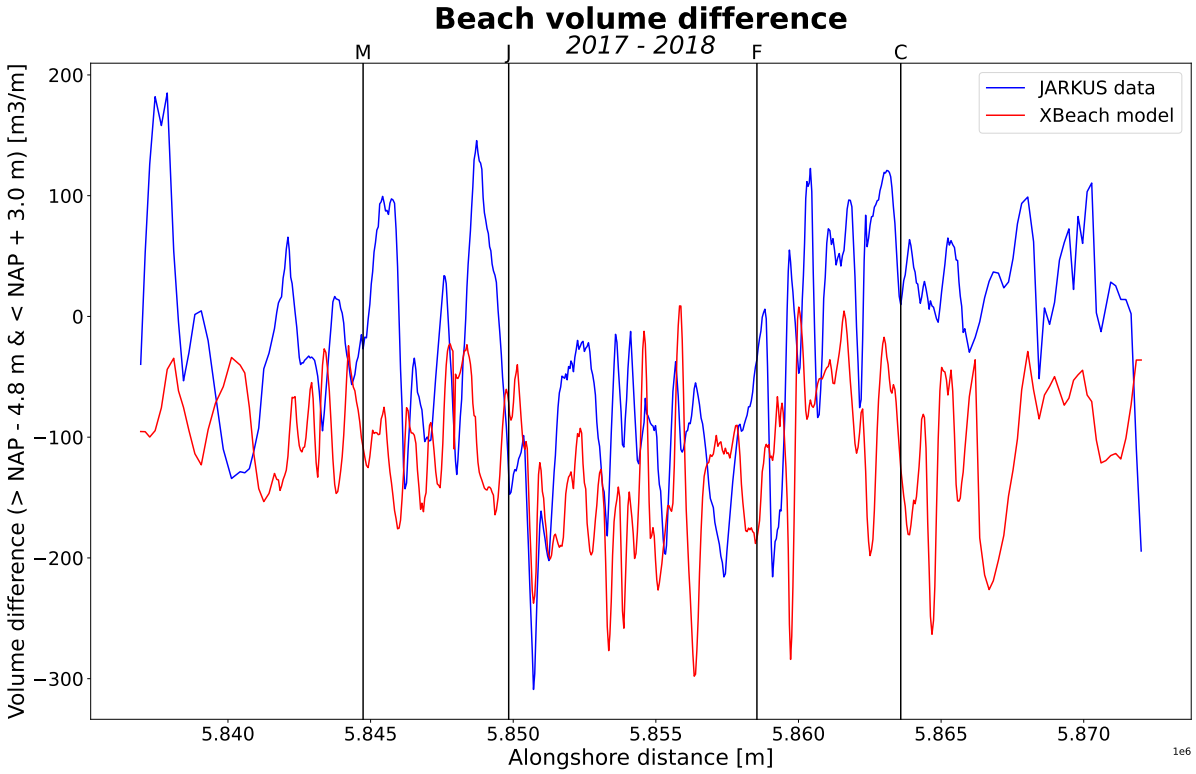

Figure 6.9: Comparison between the results of the XBeach model and the measurements. These figures are the results of 2017 - 2018. The black vertical lines indicate the transects as indicated in the figures for the bed level change. A negative volume difference means a reduction in the volume.

Figure 6.10 shows the volume difference of the last year. The figure shows that the differences between the measured data and the model do not match for all transects. The peaks of the measured differences are much larger than those of the model over almost the entire longshore direction. Only in the middle of the grid can it be seen that the results of the measurements and the results of the simulation have some similarities.

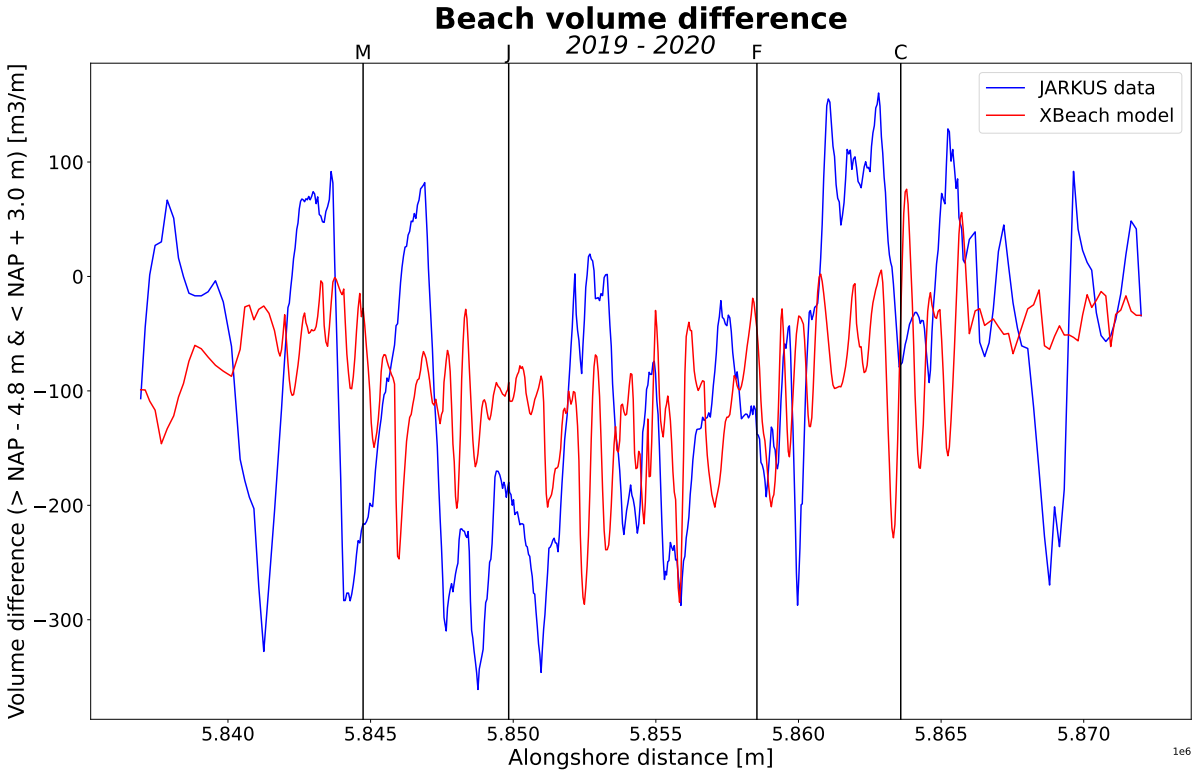

Figure 6.10: Comparison between the results of the XBeach model and the measurements. These figures are the results of 2019 - 2020. The black vertical lines indicate the transects as indicated in the figures for the bed level change. A negative volume difference means a reduction in the volume.

6.4. Validation

In this section, the performance of the XBeach model is validated by finding the correlation between the measured beach width difference and the modelled beach width difference. The figure below, Figure 6.11, shows that the correlation for the second year after nourishment is averaged with r^2 = 0.40. This implies that similarities can be seen between the model and the measurements and thus the model partially represents reality.

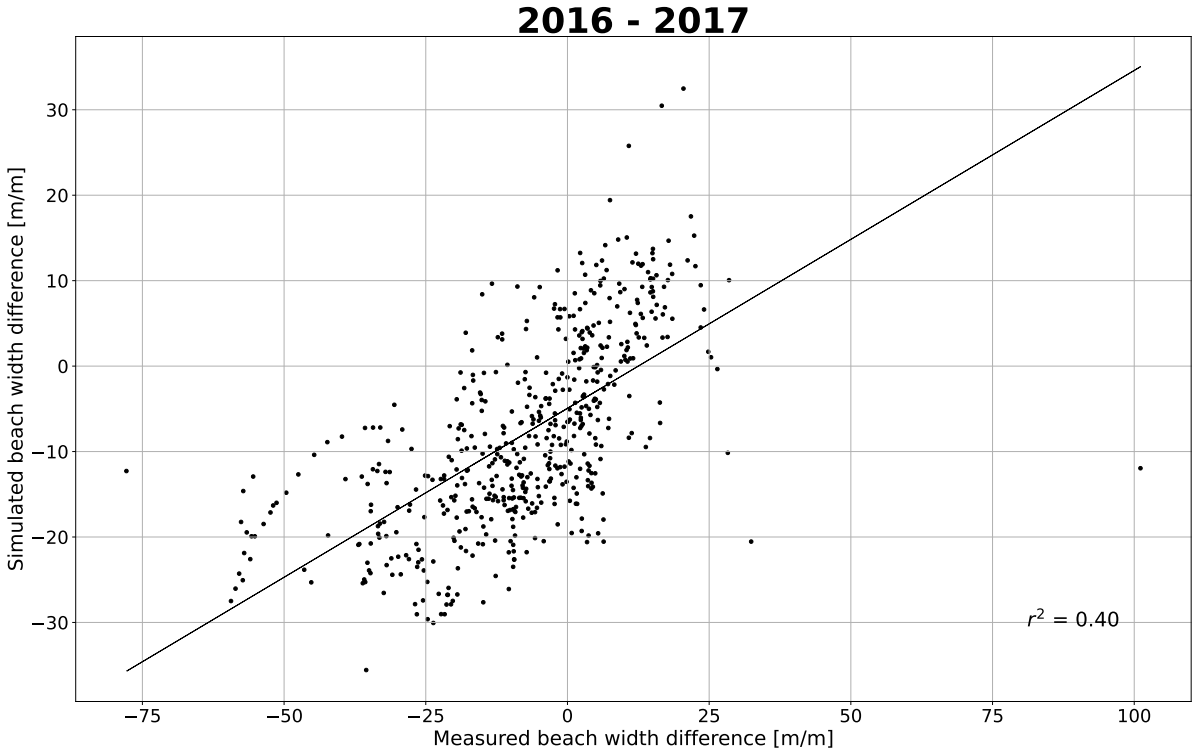

Figure 6.11: The correlation between the beach width difference obtained from the simulations from XBeach and the measurements in 2016 - 2017.

The correlation for the last year considered in this study, which is 2019 - 2020, can be seen in Figure 6.12. In this year, r^2 = 0.04, meaning that hardly any correlation can be found between the measured and modelled outcomes. This conclusion was also drawn in Section 6.2.

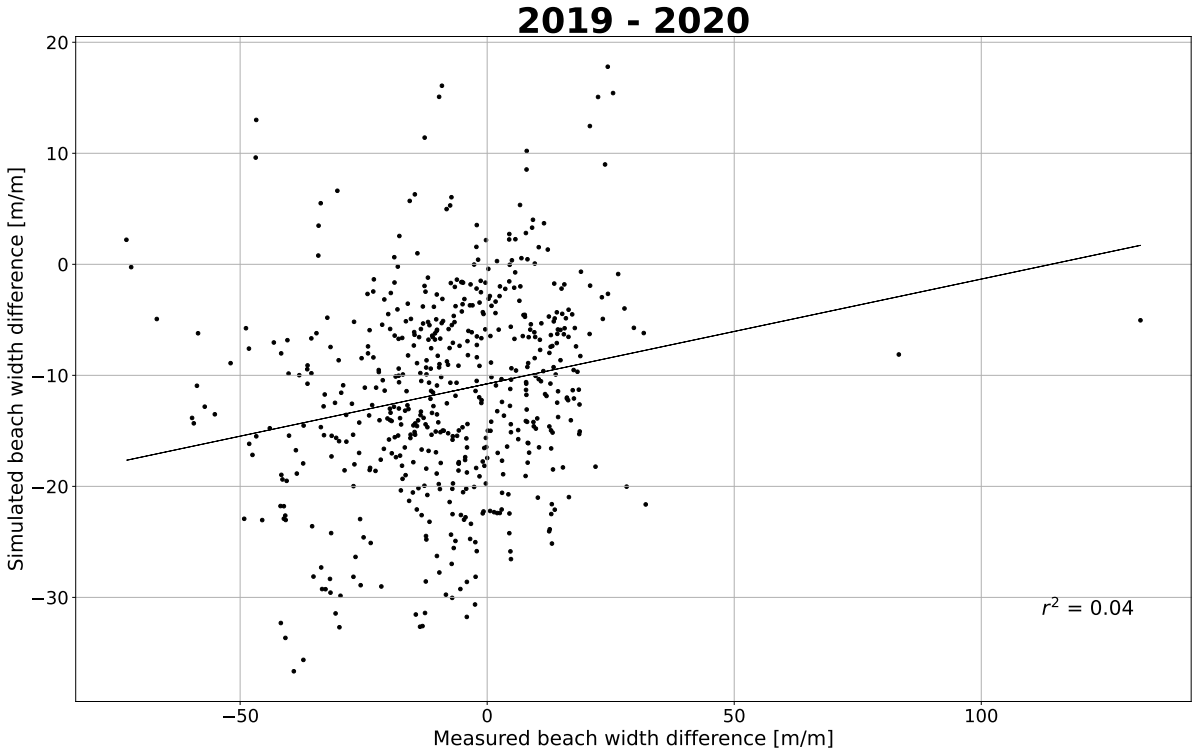

Figure 6.12: The correlation between the beach width difference obtained from the simulations from XBeach and the measurements in 2019 - 2020.

Based on the correlations of the different years, it can be concluded that the similarity between the measured beach width difference and the modelled beach width difference for the first year is the best. The correlations in the subsequent years are close to zero which means that the XBeach model does not predict well. In Section 6.2, it was found that in, for example, the third year, 2017 - 2018, the predictions for the curvature match the measurements well but this is not the case outside the curvature. This may lead to the correlation being higher if only the curvature is considered and not also the transects outside the curvature. The correlations of all years can be found in Section E.1.

An explanation for the decreasing correlation is that the final profiles after the simulation are used for the following year's simulation. This means that any deviations in year one are also applied in subsequent years resulting in increasing deviations. In addition, an additional nourishment was implemented south of the HD in 2018. The implementation of this nourishment is included in the measurement results, but not in the model results.

6.5. Concluding remarks

In this chapter, the results of the JARKUS data were compared with the results of the model simulation in XBeach to answer the question *"To what extent is the 2DH model, XBeach, able to predict the reduction in beach width of the Hondsbossche Dunes?"*. The results of the comparisons between the measurements and the model are variable for the different years.

From the analysis in this chapter, it can be concluded that there are also differences between the parameters being tested. The differences between the measurements and the model are smaller when looking at the beach width change than when looking at the difference in beach volume.

Based on the difference in the beach width, it can be concluded that the variations are larger for the measured data. The measured data shows larger peaks than the simulation results from XBeach which is relatively constant. The differences for the second year after nourishment implementation between the measured data and the model result are larger than from the first year at a number of locations. Around an alongshore distance of 617,500 m, the measurements show a larger decrease in beach

width than the XBeach model results for the second year. Differences were also seen in the first year, but they were smaller. For the second year, the model continued to calculate the final bed level change from the first year. Inequalities from the JARKUS data that arose in the first year are thus used for the calculation in the second year. As a result, the difference between the measurements and the model may increase even more.

7

Discussion

This chapter discusses the effects that affect the conclusion of the study. It first starts with the data analysis telling what was not included in the data analysis. It then discusses the model settings after which it concludes with the simulation results.

7.1. Data analysis

The literature review in this study was performed to gain insights into the processes involved in nourishment development. These processes can be used in the creation of the numerical model in XBeach to investigate the development of the coast, including the development of the beach width, by examining the relevant parameters for these processes. These relevant parameters, such as the wave angle of incidence, were used in the study as the input values of both models.

The literature study showed that sediment transports affect the development of the beach. A larger amount of sediment transport leads to larger changes. It depends on the conditions, such as bathymetry, wave height and wave direction, whether these changes lead to a widening or narrowing of the beach.

From the data analysis of coastal development at the HD, it follows that the largest changes occur in the first year after the nourishment is implemented. Based on theory from the Literature Review, (Eichentopf et al., 2019), it appears that the profile is furthest from its equilibrium profile immediately after the nourishment. The profile wants to search for a new equilibrium and the further the profile is from the equilibrium the faster the changes take place as is also the case for the HD.

7.2. Interpretation of the results of the models

This section discusses the results of the simulations of the two models that were performed. Here, these results are compared with previously conducted studies.

7.2.1. Schematic XBeach model

As in Chapter 5, the discussion of the schematic XBeach model is divided into two parts. The first part focuses on the influence of shoreline strength and the second part focuses on the influence of infragravity waves on beach width development.

The influence of coastal curvature was investigated by running simulations with different strengths of curvature. A total of three simulations were run, one with a curvature twice as small (2° per kilometre), one with the curvature as present at the HD (4° per kilometre) and the last simulation has a curvature twice as large (8° per kilometre). The figure below, Figure 7.1, shows one of the results where the wave conditions are maximum and there are normal incident waves. In this figure, it can be seen that for stronger curvature, larger variations occur between transects. This is in agreement with the research conducted by Radermacher (2018) who concluded that excessive curvature results in a decrease in swimmer safety due to the large variations and changes that then occur. In addition to the large variations, it can also be seen in Figure 7.1 that the gradient in beach width changes is larger for stronger

curvature. In his study, Den Heijer (2013) found that stronger curvature leads to larger gradients in longshore sediment transport. The wave angle of incidence on the local shore normal has a larger gradient with stronger curvature, and thus a larger gradient also takes place in the longshore sediment transport (Equation 2.2). This larger gradient in the longshore sediment transport leads to a larger gradient in the beach width changes that occur.

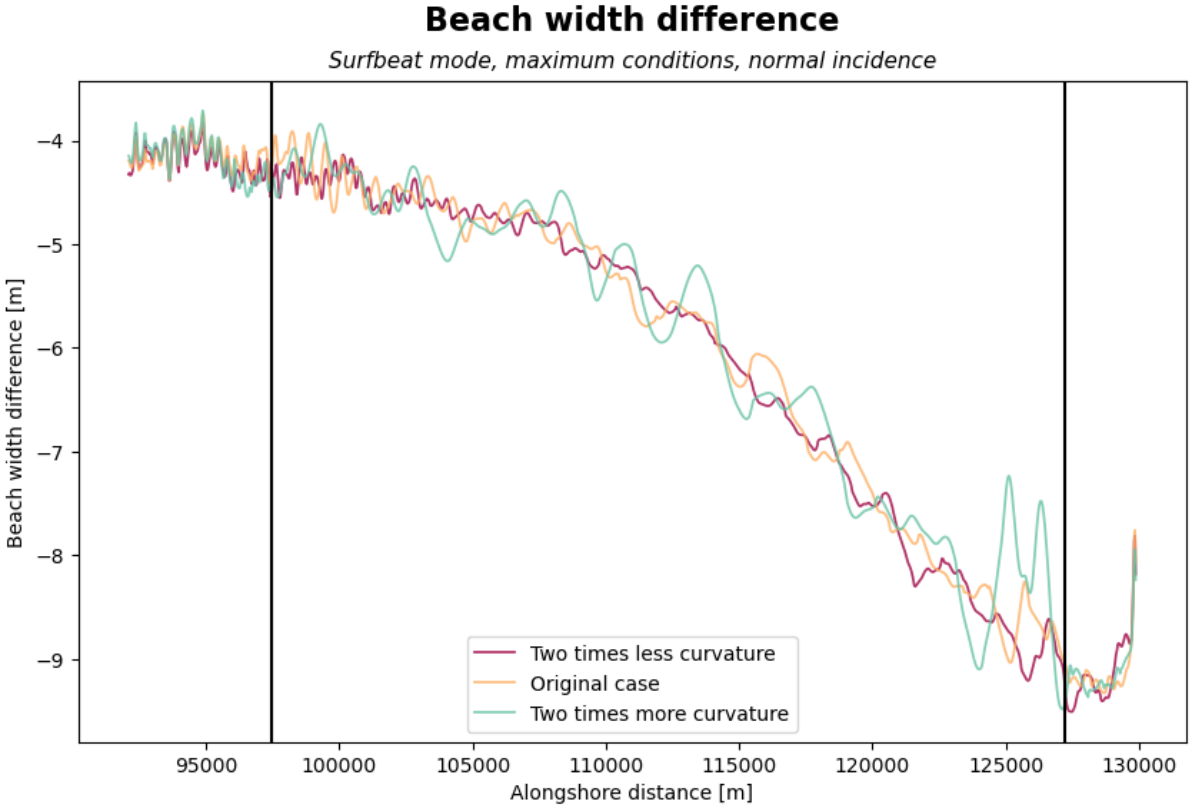

Figure 7.1: Comparison of the beach width difference between the different coastal curvatures. Results of the maximum wave conditions with a wave angle of incidence of 0 degrees. The black vertical lines indicate the start and end of the curvature. Modified from XBeach output.

To investigate the influence of infragravity waves, the same simulation as above was run again but in the stationary mode. In the stationary mode, only short waves are present and no wave groups. The results of the simulations performed in the stationary mode showed that the beach width changes are minimal. This result can also be seen in Figure 7.2. In the cross-sections of several transects, it can be seen that in the surf zone and in the swash zone hardly any changes occur. Outside these zones, more offshore, larger changes occur, but even these changes are not as large as the changes in the surfbeat mode.

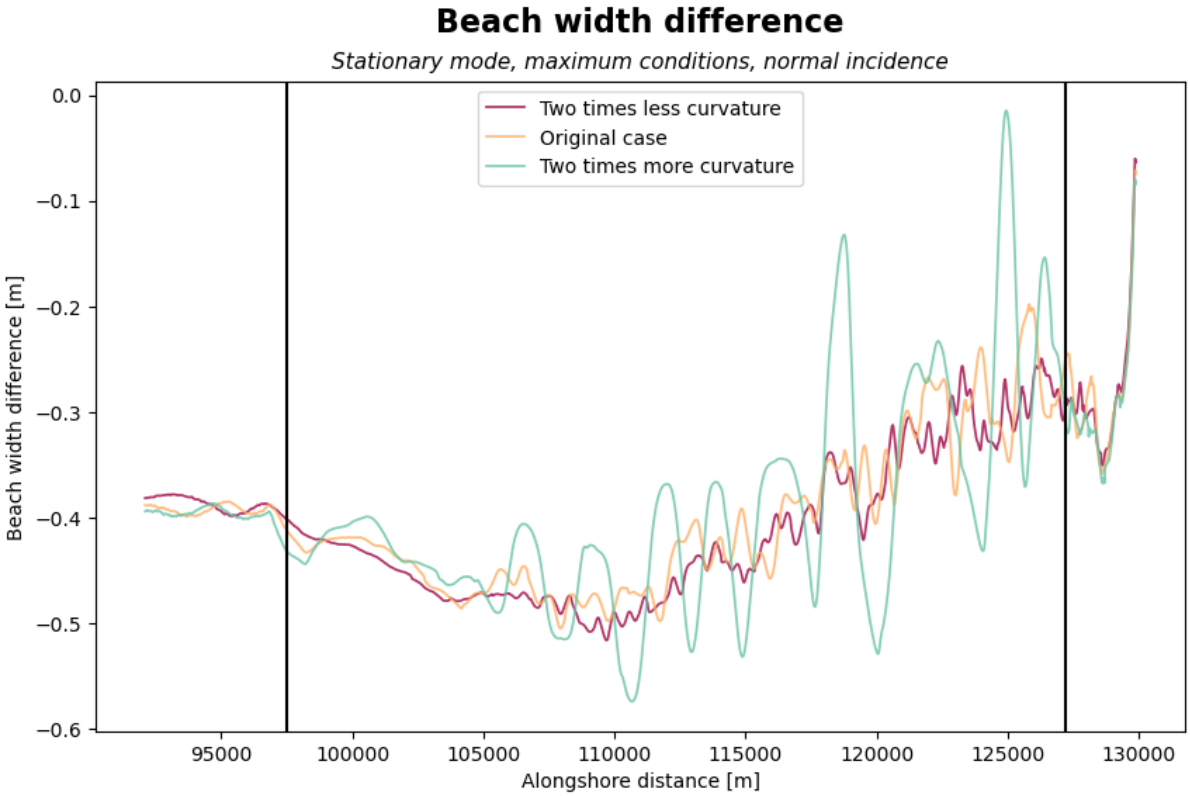

Figure 7.2: Comparison of the beach width difference between the different coastal curvatures. The simulation is performed in stationary mode. Results of the maximum wave conditions with a wave angle of incidence of 0 degrees. The black vertical lines indicate the start and end of the curvature. Modified from XBeach output.

7.2.2. XBeach model of the Hondsbossche Dunes

Based on the complex XBeach model, it can be concluded that the results from the schematic model are reflected in this complex model. In addition, the results based on the XBeach model are consistent with the results from previous studies. In the XBeach model, the convex-shaped coast is found to have the most erosion, as shown in Figure 7.3. The amount of bed level changes is not constant in the alongshore direction. It holds that the stronger the curvature is the more erosion or sedimentation takes place which results from the larger gradients in wave angle of incidence. These findings are consistent with the study by Den Heijer (2013), as well as with the findings from the schematic model performed in this study.

Radermacher (2018) examined the relationship between the strength of curvature and swimmer safety from which it followed that stronger curvature leads to more variations seen on the beach. The results of Figure 7.3 also show that at some locations in the alongshore direction, fewer bed level changes occur than at other locations.

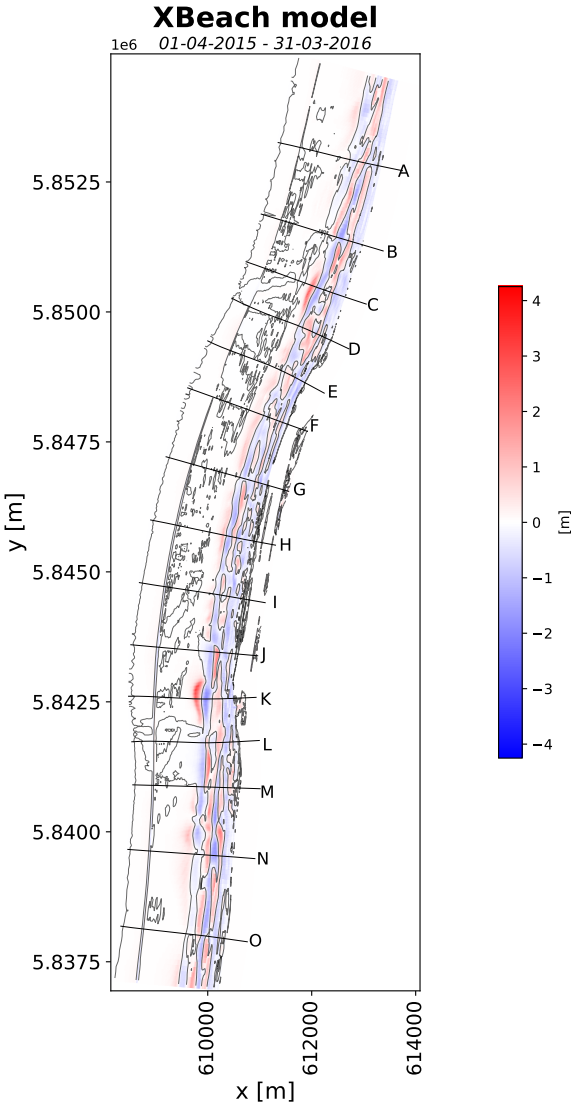

Figure 7.3: The results from 2015 to 2016. The blue colours indicate erosion and the red colours indicate sedimentation. The black contour lines indicate a bed level difference of zero. Modified from XBeach output.

One difference between my research and the previously conducted studies is that Den Heijer (2013) used a simplified model where there is an alongshore uniform coast. The results of this study did not take into account factors such as variation in bathymetry which can affect the waves approaching the coast and thus the sediment transport that takes place. Lazarus and Murray, 2007 performed a study of the influence of coastline curvature on the development of beach width in the United States. The study did not specifically address the influence of long waves on beach width differences in conjunction with shoreline curvature. This makes my conducted research apart from the previously mentioned studies.

7.3. Limitations of this research

In the model simulation, a number of natural processes that do occur in reality have been excluded. One example is wind. Any sediment transport due to the wind, aeolian sediment transport, is not included in the model simulation. However, the results based on the measured JARKUS data do take into account the effects of sediment transport due to wind. With that, it is more difficult to find out the influence of XBeach on the cause of the difference between the simulation and the measured data, because the JARKUS data is measured and thus aeolian sediment transport is included.

Another limitation of this study is the fact that it is not possible to attribute the difference in results between the stationary mode and the surfbeat to infragravity waves. No infragravity waves are present in the stationary mode, but no wave groups are present anymore either. Thus, there are two possible reasons why the surfbeat results are different from the stationary mode results. The consequence of this is that no clear answer can be given to the research question because, in addition to the long waves, the groupiness of the waves also influences the results.

Another limitation of this study has to do with the calculation of the beach width differences. At some locations, an additional dune is present as a result of the lagoon. As a result of this dune, the x-location of the dunefoot is further offshore than in the situation where no additional dune is present. This causes the beach width at the lagoon locations to differ from the other transects.

8

Conclusion and recommendations

This chapter discusses the conclusions of the study. The chapter then concludes with the recommendations for further research on the effect of long waves on the decrease in beach width.

8.1. Conclusion

The main objective of this study was to evaluate whether the reduction in beach width at the HD can be predicted using XBeach in surfbeat mode.

To investigate this objective, the study was divided into three sub-questions.

"What is the development of the mega nourishment of the Hondsbossche Dunes in the first years after the nourishment was implemented? Can differences be seen between development over years and processes?"

The first sub-question looks at the development of the HD from the first five years, till 2020, after the HD was implemented in 2015. This study showed that the largest changes in beach width and volume occurred in the first year after the nourishment was implemented, so from 2015 to 2016. After the nourishment is implemented, the system is thrown out of equilibrium and the system wants to return to a new equilibrium as soon as possible. Immediately after a nourishment in the system, the greatest changes take place and as time progresses, the rate of adjustment decreases.

Furthermore, this sub-question examined the full erosion and sedimentation pattern of the HD. It follows that much erosion occurs on the HD and that along the rest of the coast most sedimentation occurs. In the erosion and sedimentation patterns from the first year and the last year, differences can be seen in the development over the years. The bed level changes in the first year are higher than the bed level changes in the last year.

The wave conditions in the first year were more energetic than the wave conditions in 2016. A more energetic wave environment means that higher waves are present and these higher waves lead to more sediment transport. The wave conditions for the last year are the most energetic, this is because here the conditions from January through March were considered. Waves are generally higher during winter. Nevertheless, the changes in bed level in the first year are greater than in the last year which indicates that the profile is already close to its equilibrium.

"What is the impact of long waves and coastal curvature on the reduction in beach width when tested in an idealised coastal setting?"

This sub-question is divided into two sub-questions with the first sub-question focusing on the strength of the curvature and the second sub-question focusing on the differences between surfbeat mode and stationary mode.

It follows from the analysis of the strength in curvature that stronger curvature affects the magnitude of the beach width change and its gradient. Stronger curvature leads to larger variations in the beach width change in the longshore direction of the coast. In addition, the gradient of beach width change is larger for stronger curvature. The beach width differences at the beginning of the curvature and at the end of the curvature are about the same size, but stronger curvature reduces the distance resulting in a larger gradient.

The other part of the analysis was investigated by running the same runs again only this time in the stationary mode where only short waves are applied and there is no more groupiness. The results of this simulation (see the result for the beach width change in Figure 5.5) showed that the beach width changes for the stationary mode are much smaller than the changes in the surfbeat mode. Based on this, it can be concluded that the wave groups and infragravity waves have a large influence on the changes that occur.

"To what extent is the 2DH model, XBeach, able to predict the reduction in beach width of the Hondsbossche Dunes?"

To find an answer to the third and final sub-question, a complex XBeach model of the HD was run. For this purpose, a representative wave climate was applied and the bathymetry as present at the HD. The waves smaller than 1.50 m were run in stationary mode while higher waves were applied in surfbeat mode because surfbeat mode has little influence on low waves. The results of the simulation were compared with the results of the JARKUS data so that it can be verified that the results match reality. The results of this validation showed that hardly any correlation is present between the measurements and the outcomes of the model if 2015 is taken as the first year for the simulation (r^2 = 0.18). The correlation is greater, r^2 = 0.40, if the second year is used as the initial year of the simulation. By taking the second year, the initial effects disappear in the outcome of the measurements. However, the correlation decreases significantly when looking at the remaining years after the nourishment was constructed. It should be noted that in the third year, large similarities can be seen between the outcomes of the measurements and the simulation on the convex-shaped coast. However, large differences can be seen between the outcomes on the straight-shaped coast. The low correlation several years after the nourishment is implemented has several factors, namely the fact that an additional nourishment was implemented in 2018 which was not included in the model's simulation. In addition, the profile at the end of the simulation was used as the starting profile for the following year so any deviations are applied in subsequent years.

In addition, larger differences are seen between the outcomes of the beach volume differences compared to the beach width differences.

By answering the three sub-questions formulated above, the research question can be answered.

"To what extent can the interaction between the curved coastline and the beach width of a mega nourishment, with a focus on the Hondsbossche Dunes, be predicted using a numerical model including long waves?"

The results of this study have shown that the interaction between a curved coastline and the width of the beach means that stronger curvature causes larger variations in beach width differences. The simulation results show that erosion occurs on the convex-shaped shoreline, that is, at the location where the HD is implemented. This erosion is not equal on the entire convex-shaped shoreline, but here differences can be seen in the direction along the shoreline resulting in variations in the beach width changes.

Similarities can be seen in the beach width change in the alongshore direction. If the second year, i.e. 2016-2017, is applied as the starting year of the simulation so that the initial effects are excluded it follows that the correlation is equal to r^2 = 0.40. As the years progress, it is found that the predictions of the model deviate further from the results of the measurements and thus the correlation decreases.

The predictions using the simulations in XBeach for beach volume differ more from the measurements. Indeed, it can be seen here that the peaks and troughs in the volume changes are much larger for the measurements than for the model. In addition, at some locations, an increase in beach volume occurs according to the model while a decrease occurs according to the measurements.

This study concludes that the numerical model XBeach makes a reasonable initial prediction by applying infragravity waves in the numerical model. However, it should be taken into account that the prediction after the first year differs from the measurements and hardly any correlation can be found. Furthermore, it must be taken into account that the beach width changes in reality are somewhat more extreme than the model simulations suggest. In addition, while the beach width changes can be predicted well, the predictions of beach volume changes are much less accurate.

8.2. Recommendations

This section discusses the recommendations. The recommendations discuss what can be done differently in the future so that the result of the study will improve.

Many different processes come into play in the development of the HD making it a complicated issue. In this research, a number of factors and processes were not considered that may also affect nourishment development. For further research on the development of HD using long waves, other processes can also be added to the model to get even better results. The wind was not taken into account in this study. Wind can cause aeolian sediment transport and wind, especially for dry sand, can cause sand to be transported. The sand that is above water and thus dry can be transported to other locations as a result of aeolian transport. A combination of a 2DH model such as XBeach and a model that predicts aeolian transport, such as Aeolis, can provide an even more accurate prediction.

In this study, a representative wave climate was used. Although this wave climate is almost the same as the real wave climate and can therefore be applied, it does simplify the model. Fewer waves are applied, which improves the calculation time but makes it look less like reality. In the real wave climate, there are sometimes waves over 5 meters, which are not reflected in the representative wave climate. The maximum waves can cause high differences in the beach width (see Chapter 5) and by not including these maximum differences in the simulation, such large differences are not calculated.

In this model, a constant grain size diameter has been used, whereas it has been shown from Subsection 3.1.4 that there are differences in the grain size diameter along the alongshore direction of the HD. A smaller grain size reduces the weight of the sediment particles making them more easily transported. Thereby, the grain size diameter affects the amount of sediment transported causing larger bed level changes in reality than in the model where there is a constant grain size diameter.

The computation time of the HD's model was long. By investigating in the future what causes the long computation time, adjustments can be made in the simulation so that the model finishes computation faster. If it turns out that the grid size is causing a long computation time, then the grid size can be increased so that fewer grid cells are present. This should take into account what locations the grid should be finer because more changes are expected there. In the model, there are currently about 20 conditions per year which amounts to more than 100 conditions for the entire 5-year calculation period.

In further research, the different model parameters can be investigated. One example is the sediment transport formulae, as there are two options. One of the two sediment transport equations was used in this model. It has not been checked what the difference is between the two equations while the different equations each come up with its own different outcome.

In the beach width calculation, the horizontal distance between the dune foot and the waterline is assumed as the beach width. An additional dune is present at some locations, namely offshore of the lagoon. Because the dune at this location is higher than NAP + 3.0 m, the x-location of the dune foot is assumed further offshore than at the other transects. Once erosion occurs and the dune reaches an elevation less than NAP + 3.0 m then the position of the dune foot is further onshore causing a large difference in the beach width change. The beach width calculations do not take into account the possible presence of additional dunes or bars which can have a large impact on the difference in beach width between the beginning and the end of the simulation.

To make the results of the simulation more realistic, adjustments can be made to the parameters that are currently applied. For example, sediment transport parameters such as the facua can be varied to influence sediment transport and thus the amount of erosion and sedimentation that takes place. If by adjusting the parameters it turns out that a better prediction can be made of the first year then any deviations will have less impact in subsequent years.

References

Anthony, E. J., & Aagaard, T. (2020). The lower shoreface: Morphodynamics and sediment connectivity with the upper shoreface and beach. *Earth-Science Reviews*, *210*, 103334. https://doi.org/https://doi.org/10.1016/j.earscirev.2020.103334

Arends, I. (2018). *Evaluating the applicability of 2dh models for the prediciton of mega nourishments* [Master's thesis, Delft University of Technology]. https://repository.tudelft.nl/record/uuid:75ba269a-a890-4cb9-b6c9-86701d06f312

Ashton, A., & Murray, A. B. (2006a). High-angle wave instability and emergent shoreline shapes: 1. modeling of sand waves, flying spits, and capes. *Journal of Geophysical Research: Earth Surface*, *111*(F4). https://doi.org/https://doi-org.tudelft.idm.oclc.org/10.1029/2005JF000422

Ashton, A., & Murray, A. B. (2006b). High-angle wave instability and emergent shoreline shapes: 2. wave climate analysis and comparisons to nature. *Journal of Geophysical Research*, *111*. https://doi.org/10.1029/2005JF000423

Bart, L. J. C. (2017). *Long-term modelling with XBeach: Combining stationary and surfbeat mode in an integrated approach* [Master's thesis, Delft University of Technology]. https://repository.tudelft.nl/file/File_c522e539-de39-4063-a51a-fd8681616367?preview=1

Bechauf, R., Cutler, E., Gouett, M., & Guzzetti, M. (2021). *Sustainable Asset Valuation SAVi of Nature-Based Coastal Protection in the Netherlands* (tech. rep.). International Institute for Sustainable Development and United Nations Industrial Development Organization. https://nbi.iisd.org/wp-content/uploads/2021/12/savi-nature-based-coastal-protection-netherlands.pdf

Bertin, X., De Bakker, A., Van Dongeren, A., Coco, G., André, G., Ardhuin, F., Bonneton, P., Bouchette, F., Castelle, B., Crawford, W. C., Davidson, M., Deen, M., Dodet, G., Guérin, T., Inch, K., Leckler, F., McCall, R., Muller, H., Olabarrieta, M., … Tissier, M. (2018). Infragravity waves: From driving mechanisms to impacts. *Earth-Science Reviews*, *177*, 774–799. https://doi.org/https://doi.org/10.1016/j.earscirev.2018.01.002

Bosboom, J., & Stive, M. (2023). *Coastal dynamics*. TU Delft Open. https://doi.org/10.5074/T.2021.001

Brand, E., Ramaekers, G., & Lodder, Q. (2022). Dutch experience with sand nourishments for dynamic coastline conservation – An operational overview. *Ocean & Coastal Management*, *217*, 106008. https://doi.org/https://doi.org/10.1016/j.ocecoaman.2021.106008

Broer, J., De Pater, M., Blikman, D., Ouwerkerk, S., & Van Wijk, E. (2011). *Ruimte voor recreatie op het strand; onderzoek naar een recreatiebasiskustlijn* (Report). Decisio.

Chbab, H. (2015). *Waterstandsverlopen kust* (Report). Deltares.

Chen, W., Van der Werf, J., & Hulscher, S. (2023). A review of practical models of sand transport in the swash zone. *Earth-Science Reviews*, *238*, 104355. https://doi.org/https://doi.org/10.1016/j.earscirev.2023.104355

Clare, M. C., Piggott, M. D., & Cotter, C. J. (2022). Assessing erosion and flood risk in the coastal zone through the application of multilevel monte carlo methods. *Coastal Engineering*, *174*, 104118. https://doi.org/https://doi.org/10.1016/j.coastaleng.2022.104118

Cleveringa, J. (2019). Korrelgrootte van zandwindgebied tot strand. https://open.rijkswaterstaat.nl/publish/pages/76730/korrelgrootte_van_zandwingebied_tot_strand_anlayse_van_gegevens_1.pdf

Damsma, T. (2009). *Dune growth on natural and nourished beaches: 'A new perspective'* [Master's thesis, Delft University of Technology]. https://repository.tudelft.nl/record/uuid:96c401cb-fa67-407b-ab0d-8429452ba50b

de Bakker, A. T. M., Brinkkemper, J. A., van der Steen, F., Tissier, M. F. S., & Ruessink, B. G. (2016). Cross-shore sand transport by infragravity waves as a function of beach steepness. *Journal of Geophysical Research: Earth Surface*, *121*(10), 1786–1799. https://doi.org/https://doi.org/10.1002/2016JF003878

De Jongh, L. (2018). *Initial morphological evolution of a mega nourishment* [Master's thesis, Delft University of Technology]. http://resolver.tudelft.nl/uuid:56b2a490-e4ac-4a98-a4e5-06b6bd3b91c4

De Ridder, M. (2023). Xbeach manual. https://xbeach.readthedocs.io/en/latest/xbeach_manual.html

De Ruig, J. H., & Hillen, R. (1997). Developments in Dutch coastline management: Conclusions from the second governmental coastal report. *Journal of Coastal Conservation*, *3*, 203–210.

De Vries, S., Southgate, H., Kanning, W., & Ranasinghe, R. (2012). Dune behavior and aeolian transport on decadal timescales. *Coastal Engineering*, *67*, 41–53. https://doi.org/https://doi.org/10.1016/j.coastaleng.2012.04.002

De Wit, F. P. (2022, December). *Wave shape prediction in complex coastal systems* [PhD thesis]. Delft University of Technology. https://pure.tudelft.nl/ws/portalfiles/portal/141236966/PhDThesisFlorisDeWit.pdf

Dean, R. G. (1995). Cross-shore sediment transport processes. *Advances in Coastal and Ocean Engineering*, 159–220. https://doi.org/10.1142/9789812797582_0004

Den Heijer, C. (2013). *The role of bathymetry, wave obliquity and coastal curvature in dune erosion prediction*.

Eichentopf, S., Van der Zanden, J., Caceres, I., & Alsina, J. (2019). Beach Profile Evolution towards Equilibrium from Varying Initial Morphologies. *ournal of Marine Science and Engineering*, *7*. https://doi.org/10.3390/jmse7110406

Elgar, S., & Guza, R. T. (1985). Observations of bispectra of shoaling surface gravity waves. *Journal of Fluid Mechanics*, *161*, 425–448. https://doi.org/10.1017/S0022112085003007

Grasso, F., Michallet, H., & Barthélemy, E. (2011). Sediment transport associated with morphological beach changes forced by irregular asymmetric, skewed waves. *Journal of Geophysical Research: Oceans*, *116*(C3). https://doi.org/https://doi.org/10.1029/2010JC006550

Hillen, R., De Ruig, J. H. M., Roelse, P., & Hallie, F. P. (1991). De Basiskustlijn: Een techisch/morfologische uitwerking. *nota GWWS-91.006 (RKB 91-19)*. https://doi.org/10.1038/s1598-018-24630-6

Hillen, R., & Roelse, P. (1995). Dynamic preservation of the coastline in the Netherlands. *Journal of Coastal Conservation*, *1*, 17–28.

Hinton, C., & Nicholls, R. J. (2015). Spatial and Temporal Behaviour of Depth of Closure along the Holland Coast. *Coastal Engineering 1998*, 2913–2925. https://doi.org/10.1061/9780784404119.221

Holthuijsen, L. H. (2007). *Waves in Oceanic and Coastal Waters*. Cambridge University Press.

Jara, M., González, M., & Medina, R. (2015). Shoreline evolution model from a dynamic equilibrium beach profile. *Coastal Engineering*, *99*, 1–14. https://doi.org/https://doi.org/10.1016/j.coastaleng.2015.02.006

Johnson, M., Goodliffe, R., Doygun, G., & Flikweert, J. (2020). The UK's First Sandscaping Project (Bacton, Norfolk) from Idea to Reality. In *Coastal management 2019* (pp. 333–345). Thomas Telford Limited. https://doi.org/10.1680/cm.65147.333

Kraus, N. C., Larson, M., & Wise, R. A. (1998). Depth of Closure in Beach-fill Design. *Coastal Engineering Technical Note CETN II-40*, *3/98*.

Kroon, A., De Schipper, M., De Vries, S., & Aarninkhof, S. (2022). Subaqueous and subaerial beach changes after implementation of a mega nourishment in front of a sea dike. *Journal of Marine Science and Engineering*, *10*, 1152. https://doi.org/10.3390/jmse10081152

Kroon, A., Spaans, L., & Pak, T. (2020). *Update onderhoudsprognose Hondsbossche Duinen Zwakke Schakels Noord-Hsolland* (Report). Svašek Hydraulics.

Lauzon, R., Murray, A. B., Cheng, S., Liu, J., Ells, K. D., & Lazarus, E. D. (2019). Correlation Between Shoreline Change and Planform Curvature on Wave-Dominated, Sandy Coasts. *Journal of Geophysical Research: Earth Surface*, *124*(12), 3090–3106. https://doi.org/https://doi-org.tudelft.idm.oclc.org/10.1029/2019JF005043

Lazarus, E. D., & Murray, A. B. (2007). Process signatures in regional patterns of shoreline change on annual to decadal time scales. *GEOPHYSICAL RESEARCH LETTERS*, *34*(19). https://doi.org/10.1029/2007GL031047

Leenders, J., Wegman, C., Bodde, W., & Verheijen, A. (2018). Optimalisatie veiligheidsontwerp Hondsbossche Duinen.

Luijendijk, A. P., Ranasinghe, R., De Schipper, M. A., Huisman, B. A., Swinkels, C. M., Walstra, D. J., & Stive, M. J. (2017). The initial morphological response of the sand engine: A process-based modelling study. *Coastal Engineering*, *119*, 1–14. https://doi.org/https://doi.org/10.1016/j.coastaleng.2016.09.005

Marra, J., Ruggiero, P., Komar, P., McDougal, W., & Beach, R. (2001). Wave Runup, Extreme Water Levels, and the Erosion of Property Backing Beaches. *Journal of Coastal Research*, *17*, 407–419. https://doi.org/10.2307/4300192

Mather, A. A., Stretch, D., & Garland, G. (2010). Wave run up on natural beaches. *Proceedings of the International Conference on Coastal Engineering*, *1*. https://doi.org/10.9753/icce.v32.currents.45

Morang, A., & Birkemeier, W. A. (2019). Depth of closure on sandy coasts. In C. W. Finkl & C. Makowski (Eds.), *Encyclopedia of coastal science* (pp. 700–704). Springer International Publishing. https://doi.org/10.1007/978-3-319-93806-6_116

Muller, M., Roelvink, D. J., Luijendijk, A., Vries, S., & Vries, J. (2012). Process-based Modeling of Coastal Dune Development. *Coastal Engineering Proceedings*, *1*. https://doi.org/10.9753/icce.v33.sediment.33

Munk, W. H. (1949). Surf beats. *Eos, Transactions American Geophysical Union*, *30*(6), 849–854. https://doi.org/https://doi.org/10.1029/TR030i006p00849

Op het strand. (2024). Strandpalen langs de nederlandse kust. https://ophetstrand.com/strandpalen-langs-de-nederlandse-kust/

Pak, T. S. (2019). *Marine and aeolian sediment transport at the Hondsbossche Dunes* [Master's thesis, Delft University of Technology]. https://repository.tudelft.nl/record/uuid:55ab068a-aac8-44d4-94b7-b9e53cb5f3bd

Parsons, A., Cooper, J., & Wainwright, J. (2015). What is suspended sediment? *Earth Surface Processes and Landforms*, *40*. https://doi.org/10.1002/esp.3730

Power, H., & Hughes, M. (2008). Wave behaviour in the inner surf zone. *Proceedings of the International Conference on Civil and Environmental Engineering*.

R & M. (2021). Https://www.ruiterenenmennen.nl/n473-rijksstrandpalen-digitaal-op-de-routeplanner.html.

Radermacher, M. (2018, June). *Impact of sand nourishments on hydrodynamics and swimmer safety* [PhD thesis]. Delft University of Technology. https://repository.tudelft.nl/file/File_eb143583-ba62-4655-9077-9b2c66af7986?preview=1

Rijkswaterstaat. (1985). *Dww hondsbossche zeewering, luchtfoto.* https://proxy.archieven.nl/0/F2A79AA59B704D14A5577919C3300AC9

Rijkswaterstaat. (2024). *Waterinfo actuele waterdata*. https://www.rijkswaterstaat.nl/water/waterdata-en-waterberichtgeving/waterdata

Roelvink, D., Reniers, A., Van Dongeren, A., Van Thiel de Vries, J., Lescinski, J., & McCall, R. (2010). *Xbeach model description and manual*. Unesco-IHE Institute for Water Education, Deltares and Delft University of Technology.

Roelvink, D., Reniers, A., Van Dongeren, A., Van Thiel de Vries, J., McCall, R., & Lescinski, J. (2009). Modelling storm impacts on beaches, dunes and barrier islands. *Coastal Engineering*, *56*(11), 1133–1152. https://doi.org/https://doi.org/10.1016/j.coastaleng.2009.08.006

Roelvink, D., Van Dongeren, A., McCall, R., Hoonhout, B., Arnold, A. V., Van Geer, P., De Vet, L., Nederhoff, K., & Quataert, E. (2015). Xbeach technical reference: Kingsday release. https://doi.org/10.13140/RG.2.1.4025.6244

Roelvink, D. J., & Stive, M. (1989). Bar-generating cross-shore flow mechanisms on a beach. *Journal of Geophysical Research*, *94*, 4785–4800. https://doi.org/10.1029/JC094iC04p04785

Rossouw, M., Terblanche, L., & Moes, J. (2013). General characteristics of long waves around the South African Coast. *Coasts and Ports 2013*, 653–658.

Ruessink, B. G. (1998). Bound and free infragravity waves in the nearshore zone under breaking and nonbreaking conditions. *Journal of Geophysical Research: Oceans*, *103*, 12795–12805. https://doi.org/10.1029/98jc00893

Sánchez-Arcilla, A., Sierra, J., Brown, S., Casas-Prat, M., Nicholls, R., Lionello, P., & Conte, D. (2016). A review of potential physical impacts on harbours in the mediterranean sea under climate change. *Regional Environmental Change*, *16*. https://doi.org/10.1007/s10113-016-0972-9

Seddon, K. D., & Fitton, T. G. (2011). Realistic beach slope prediction and design (R. Jewell & A. B. Fourie, Eds.), 281–293. https://doi.org/10.36487/ACG_rep/1104_26_Seddon

Seymour, R. J. (2005a). Cross-shore sediment transport. *Encyclopedia of Coastal Science*, 352–353. https://doi.org/10.1007/1-4020-3880-1_104

Seymour, R. J. (2005b). Longshore Sediment Transport. *Encyclopedia of Coastal Science*, 600–600. https://doi.org/10.1007/1-4020-3880-1_199

Stein, R. A. (1997). Bed load. In *Geomorphology* (pp. 73–74). Springer Berlin Heidelberg. https://doi.org/10.1007/3-540-31060-6_32

Taal, M., Mulder, J., & Cleveringa, J. (2006). 15 year of coastal management in the Netherlands; Policy, implementation and knowledge framework.

Teixeira, M., Horstman, E. M., & Wijnberg, K. M. (2024). Exploring the bio-geomorphological evolution of mega nourishments with a cellular automata model. *Geomorphology*, *463*, 109371. https://doi.org/https://doi.org/10.1016/j.geomorph.2024.109371

Trouw, K., Zimmermann, N., Mathys, M., Delgado, R., & Roelvink, D. (2012). Numerical Modelling of Hydrodynamics and Sediment Transport in the surf zone: A sensitivity study with different types of numerical models. *Coastal Engineering Proceedings*, *1*(33). https://doi.org/10.9753/icce.v33.sediment.23

Valvo, L. M., Murray, A. B., & Ashton, A. (2006). How does underlying geology affect coastline change? an initial modeling investigation. *Journal of Geophysical Research: Earth Surface*, *111*(F2). https://doi.org/https://doi-org.tudelft.idm.oclc.org/10.1029/2005JF000340

Van der Zanden, J. (2016, December). *Sand transport processes in the surf and swash zone* [PhD thesis]. University of Twente. https://www.utwente.nl/en/et/cem/research/wem/research/phd-thesis/vdzanden.pdf

Van Dongeren, A., Battjes, J., Janssen, T., Van Noorloos, J., Steenhauer, K., Steenbergen, G., & Reniers, A. (2007). Shoaling and shoreline dissipation of low-frequency waves. *Journal of Geophysical Research: Oceans*, *112*(C2). https://doi.org/https://doi.org/10.1029/2006JC003701

Van IJzendoorn, C., De Vries, S., Hallin, C., & Hesp, P. (2021). Sea level rise outpaced by vertical dune toe translation on prograding coasts. *Scientific Reports*, *11*. https://doi.org/10.1038/s41598-021-92150-x

Van Koningsveld, M., & Mulder, J. P. M. (2004). Sustainable coastal policy developments in the netherlands. a systematic approach revealed. *Journal of Coastal Research*, *20*, 375–385. https://doi.org/10.2112/1551-5036(2004)020[0375:SCPDIT]2.0.CO;2

Van Leeuwen, B., & Attema, Y. (2019). *Achtergrondrapport: XBeach modellering windturbines op de Tweede Maasvlakte* (Report). Svašek Hydraulics.

Van Rijn, L. (2007). Unified View of Sediment Transport by Currents and Waves. II: Suspended Transport. *Journal of Hydraulic Engineering*, *133*. https://doi.org/10.1061/(ASCE)0733-9429(2007)133:6(668)

Van Rijn, L. C. (2014). A simple general expression for longshore transport of sand, gravel and shingle. *Coastal Engineering*, *90*, 23–39. https://doi.org/https://doi.org/10.1016/j.coastaleng.2014.04.008

Zhou, Y., Feng, X., Liu, M., & Wang, W. (2023). Influence of Beach Erosion during Wave Action in Designed Artificial Sandy Beach Using XBeach Model: Profiles and Shoreline. *Journal of Marine Science and Engineering*, *11*, 984. https://doi.org/10.3390/jmse11050984

A

Extended analysis of the effects of the mega nourishment

This appendix takes a closer look at the erosion and sedimentation patterns taking place around HD. The figures shown are made from the measured JARKUS data. The JARKUS data is measured each year around the months of February and March so the results are the effect of a full year.

A.1. Erosion and sedimentation 2015 - 2020

The JARKUS data show that most erosion occurs at the curvature of the HD, which is shown in the plot below by the colour blue. North of the curvature most sedimentation takes place, as a so-called sedimentation hotspot can also be seen here. The waves in the Netherlands come mainly from the Southwest which may explain the locations of the erosion hotspot and the sedimentation hotspot. The sediment that has eroded near the HD is carried with the waves northward where it will settle and form a sedimentation hotspot. In most places, the decrease in bed level is about 2 to 3 meters, meaning the bottom will be lower than in the initial situation in 2015. In the figure below, the contour lines indicate where no bed level changes occur. Erosion may result in a decrease in beach width. South of the curvature relatively few changes occur in the bed level, while north of the curvature mostly sedimentation occurs.

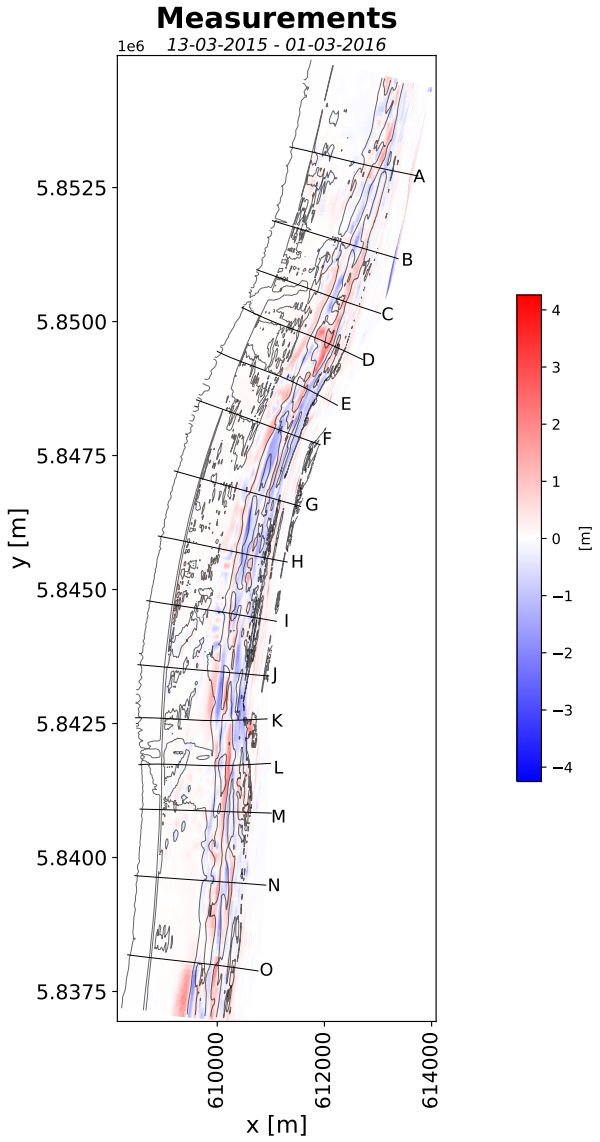

Figure A.1: The bed level changes occurred during the first five years after implementation of the HD, so from 2015 to 2020. The blue colours indicate erosion and the red colours indicate sedimentation. The black contour lines indicate a bed level difference of zero. Combined JARKUS data and Vaklodingen surveys.

A.2. Erosion and sedimentation per year

This section discusses the erosion and sedimentation patterns that occur for each year separately. By analysing each year, it shows which years have relatively high erosion rates and which have relatively low rates. This can then be compared to the conditions present to examine in this way which conditions have the most influence on the development of the HD.

A.2.1. Erosion and sedimentation 2015 - 2016

In the first year after the nourishment implementation, many changes take place. The order of magnitude of the changes taking place (the scale is from about 3.5 m to -3 m) corresponds to the order of magnitude of the changes over 5 years. Implementing a nourishment puts the system out of equilibrium with respect to forcing. As mentioned in Subsection 2.1.4, a profile wants to return to the equilibrium state as quickly as possible when it is brought out of equilibrium. The changes toward the new equilibrium profile are always faster in the first few years than when the profile is near the equilibrium state.

From the figure below, it appears that, even as after 5 years, erosion occurs mainly in the curvature of the HD. The sedimentation hotspots are at a large depth and thus it will have minimal influence on the change in beach width.

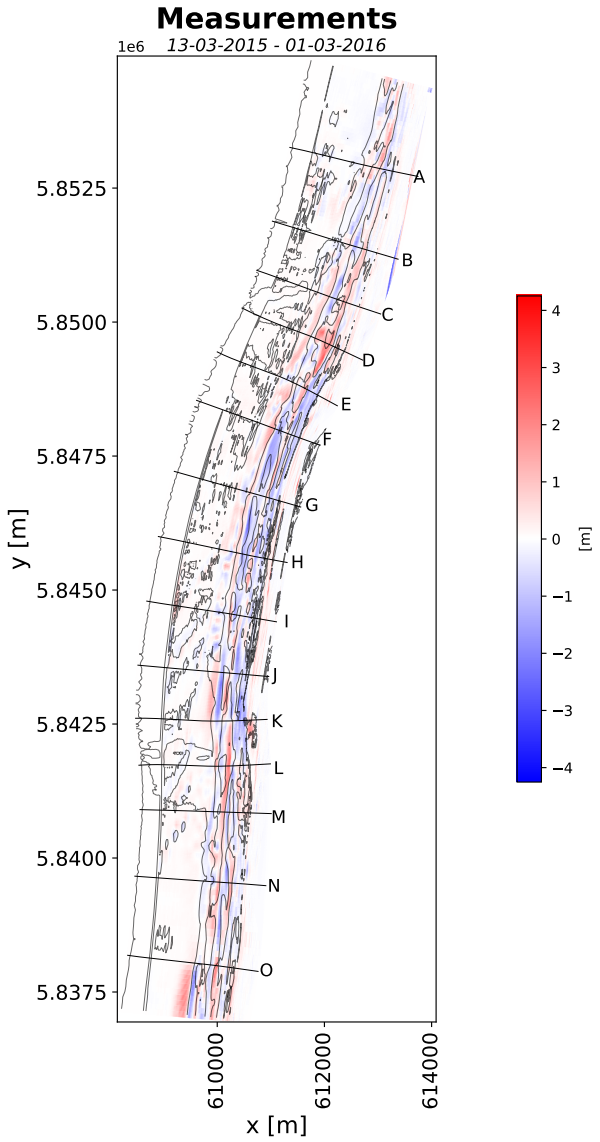

Figure A.2: The bed level changes occurred during the first five years after the implementation of the HD, so from 2015 to 2016. The blue colours indicate erosion and the red colours indicate sedimentation. The black contour lines indicate a bed level difference of zero. Combined JARKUS data and Vaklodingen surveys.

A.2.2. Erosion and sedimentation 2016 - 2017

The changes in bed level in the second year after nourishment implementation are much less than in the first year as can also be expected due to the adjustment to the equilibrium profile. In the second year, hardly any erosion can be seen on the curvature of the HD, as well as the amount of sedimentation taking place. Because there is little change in the bed level, it is expected that there will also be little change in the beach profile and beach width. Sedimentation can be seen to the south, at y = 5.8400e6 m, of the curve along the coast.

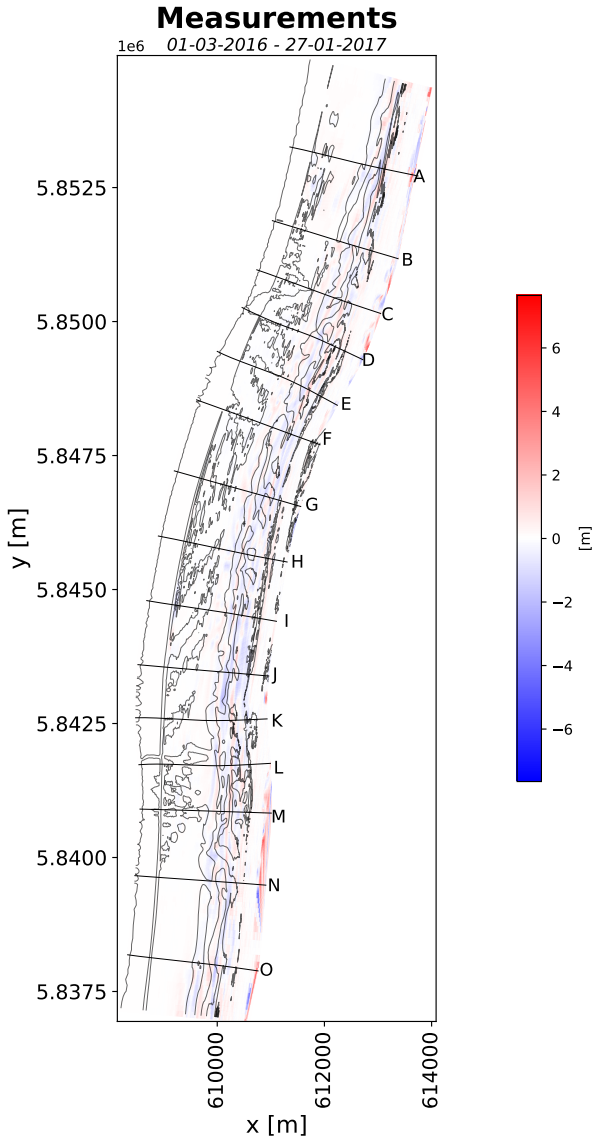

Figure A.3: The bed level changes occurred during the first five years after the implementation of the HD, so from 2016 to 2017. The blue colours indicate erosion and the red colours indicate sedimentation. The black contour lines indicate a bed level difference of zero. Combined JARKUS data and Vaklodingen surveys.

A.2.3. Erosion and sedimentation 2017 - 2018

The figure below shows that the amount of erosion and sedimentation has decreased compared to previous years. The maximum amount of erosion taking place is about 1 m, but in most places no bed level change takes place. As a result, the change in beach width is also expected to be minimal.

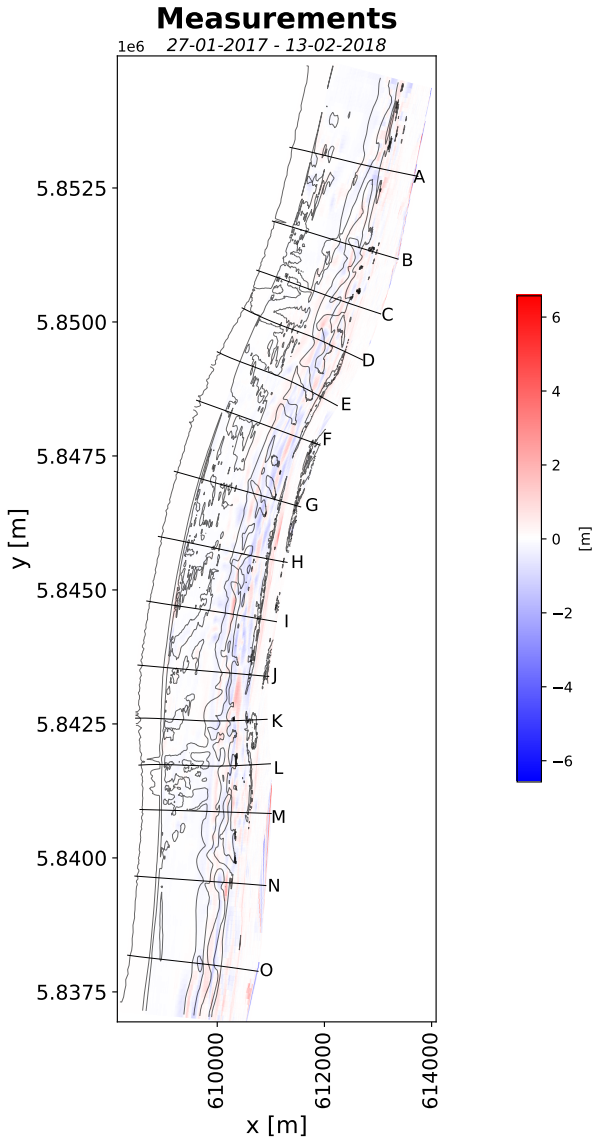

Figure A.4: The bed level changes occurred during the first five years after the implementation of the HD, so from 2017 to 2018. The blue colours indicate erosion and the red colours indicate sedimentation. The black contour lines indicate a bed level difference of zero. Combined JARKUS data and Vaklodingen surveys.

A.2.4. Erosion and sedimentation 2018 - 2019

A sedimentation hotspot can be seen on the south side of the HD at y = 5.8425e6 m, in 2018. The reason the bed level change is positive in the south of the HD is because an additional nourishment was implemented at this location in February 2018. This nourishment has been implemented on the beach which can also be seen in the plot. The location of the additional nourishment and thus where a sedimentation hotspot can now be seen corresponds to the location where an erosion hotspot can be seen in 2015 (see Figure A.2). At this location, it was found that the beach width had decreased to the extent that additional nourishment was necessary.

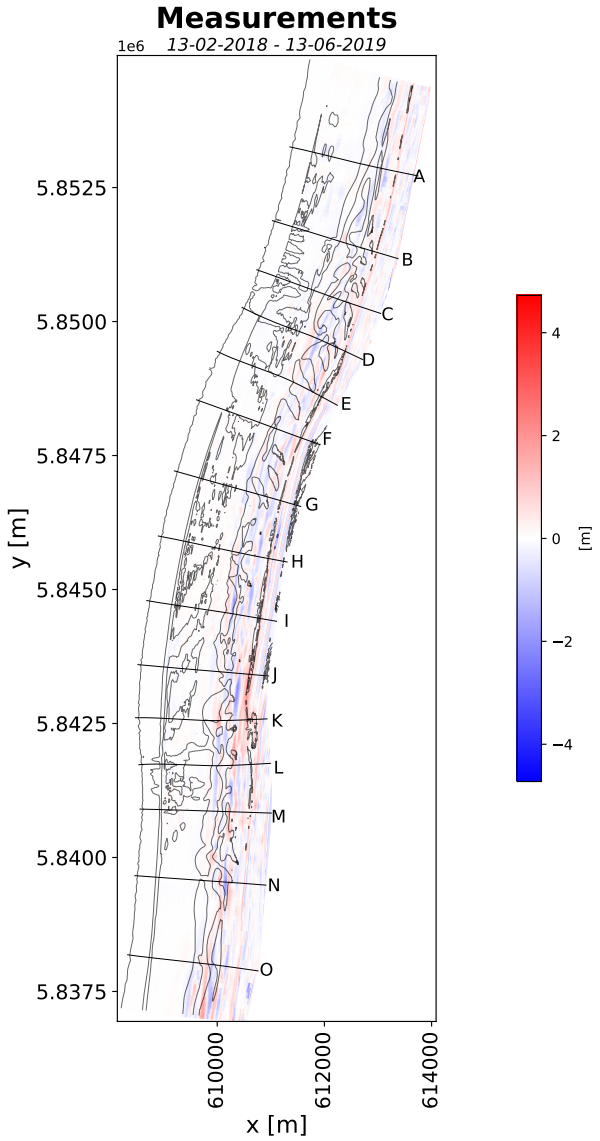

Figure A.5: The bed level changes occurred during the first five years after the implementation of the HD, so from 2018 to 2019. The blue colours indicate erosion and the red colours indicate sedimentation. The black contour lines indicate a bed level difference of zero. Combined JARKUS data and Vaklodingen surveys.

A.2.5. Erosion and sedimentation 2019 - 2020

At the location where the additional nourishment was implemented in 2018, more erosion can be seen in 2019. As was also the case in 2015, the system wants to return to equilibrium as soon as possible and with the implementation of a nourishment, the system is brought out of equilibrium.The erosion does not only occur at the nourishment location, but erosion occurs all over the HD. The waves that occur in the years 2019 and 2020 are relatively high which leads to more sediment transport. The figure also shows that more sedimentation takes place north of the HD. From this, it can be concluded that the sediment that is eroded away ends up north of the HD between approximately y = 5.8500e6 m and y = 5.8525e6 m.

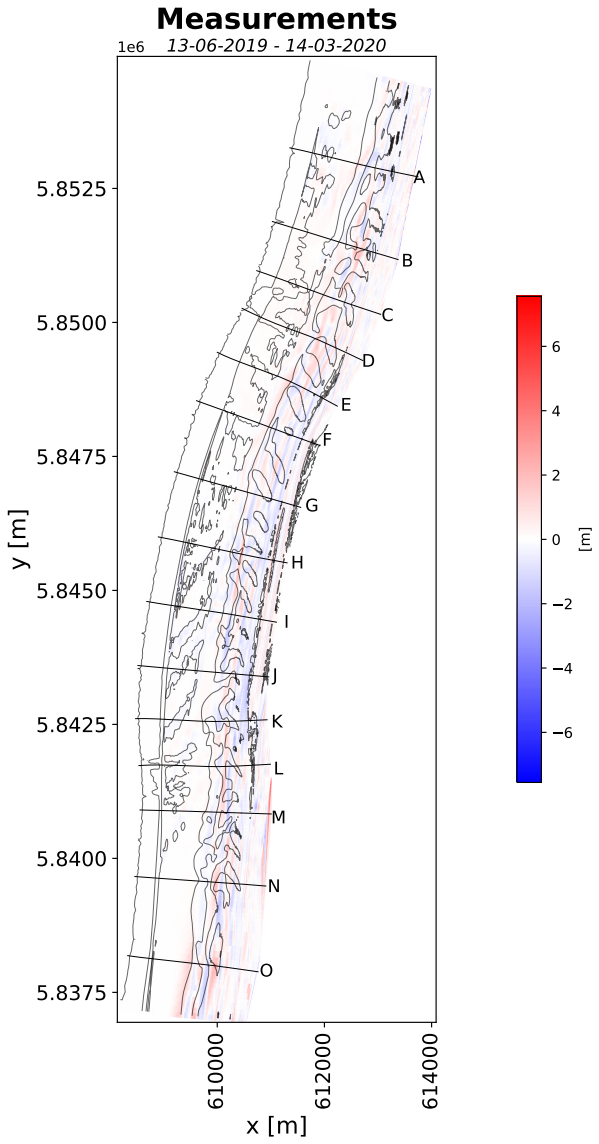

Figure A.6: The bed level changes occurred during the first five years after the implementation of the HD, so from 2019 to 2020. The blue colours indicate erosion and the red colours indicate sedimentation. The black contour lines indicate a bed level difference of zero. Combined JARKUS data and Vaklodingen surveys.

A.3. Concluding remarkt

In the figures above and the accompanying analysis, it was found that most erosion occurs in the years immediately after the nourishment is implemented. The largest nourishment was implemented in 2015 and the largest differences were observed in the following year. Also in 2018 after the additional nourishment of south of the HD, more changes were observed in the bed level.

The plots also showed that the largest changes occur around the waterline where the beach is, so between NAP - 0.8 m and NAP + 3.0 m. At this location, the bottom affects the waves, and as a result of wave breaking and associated undertow, the sand comes into suspension and can be more easily transported.

Based on the erosion and sedimentation patterns from this chapter, a prediction of the development of beach width over the years can be made. At the locations where there is a decrease in bed level, it can be expected that there will also be a decrease in beach width. This is because sediment will be transported to a different location and since the areas where this takes place are mainly the beaches (according to the definition from Subsection 2.1.2) the change in bed level will affect the change in beach width.

B

Extended data study of morphological and hydrodynamic data

This appendix provides a detailed analysis of the morphological and hydrodynamic data. It will show all the figures for the different conditions present over the different years and it will also include an explanation of how some of the data were obtained.

B.1. Wave climate

This section shows the wave data measured at wave station IJmuiden munitiestortplaats. There were some measurements where the wave height was not realistic, i.e. more than 100 metres. These are points where either no data is present and therefore automatically filled with an unrealistic value or there is a measurement error. The measurements are replaced by the wave data measured at wave station K13a platform because this station is the nearest wave station compared to IJmuiden munitiestortplaats with realistic wave data available. This measuring station is located more to the north of the measuring station IJmuiden munitiestortplaats as also indicated in Figure 3.2.

B.1.1. Wave height

The wave height which will be shown in the plots below is the significant wave height H_{m0} (Holthuijsen, 2007). In general, the wave heights of different years are approximately equal to each other, so there is little variation over the years. The average wave height for each year is approximately equal to 1.30 m, while the maximum wave heights vary between 5 and 6 m.

In the figures below, Figure B.1 to Figure B.6, the wave height is plotted for each year separately. In general, the wave height is greater the months that there is a Northern Hemisphere winter, i.e. from about November to April. Based on the graphs shown below, it can be concluded that mild conditions were present in the Netherlands in 2019 because the wave height is lower compared to previous years. The wave height in 2020 seems relatively high, but in this year only the winter months are plotted and because the waves are higher in the winter months, it is logical that larger wave heights are shown here.

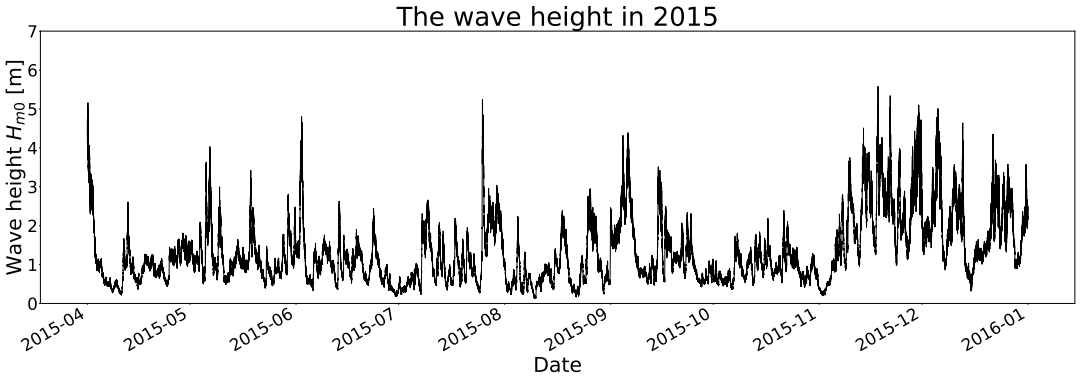

Figure B.1: The wave height in 2015. Modified from data of Rijkswaterstaat (Rijkswaterstaat, 2024).

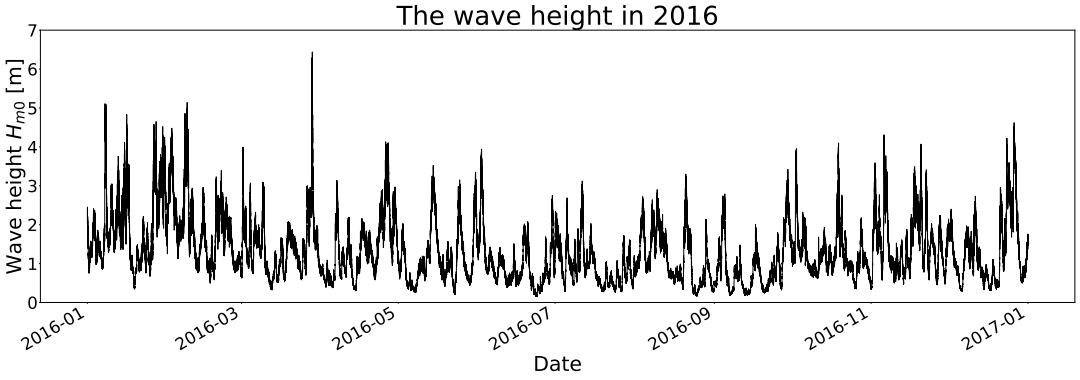

Figure B.2: The wave height in 2016. Modified from data of Rijkswaterstaat (Rijkswaterstaat, 2024).

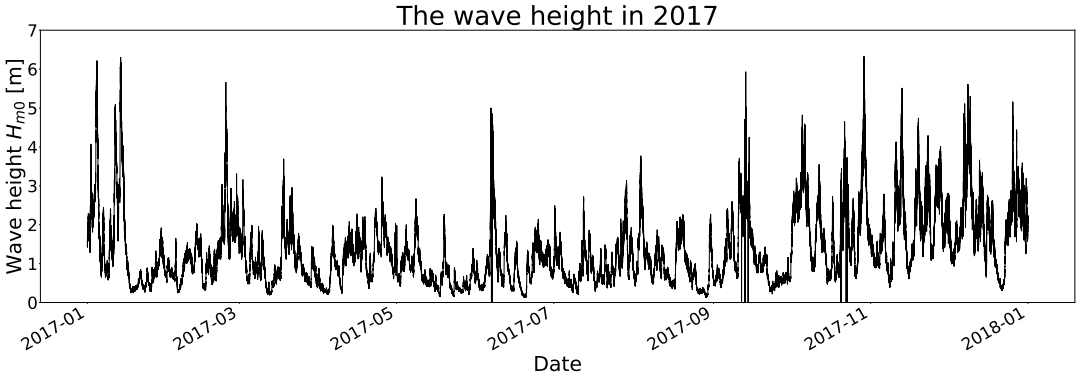

Figure B.3: The wave height in 2017. Modified from data of Rijkswaterstaat (Rijkswaterstaat, 2024).

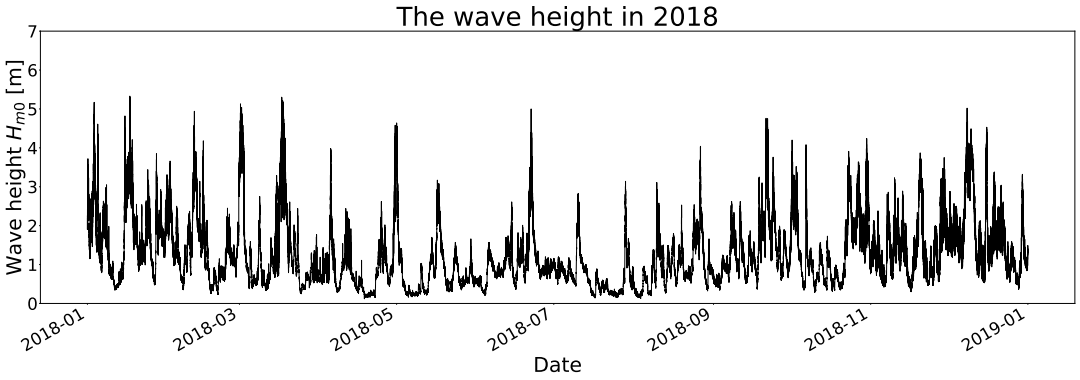

Figure B.4: The wave height in 2018. Modified from data of Rijkswaterstaat (Rijkswaterstaat, 2024).

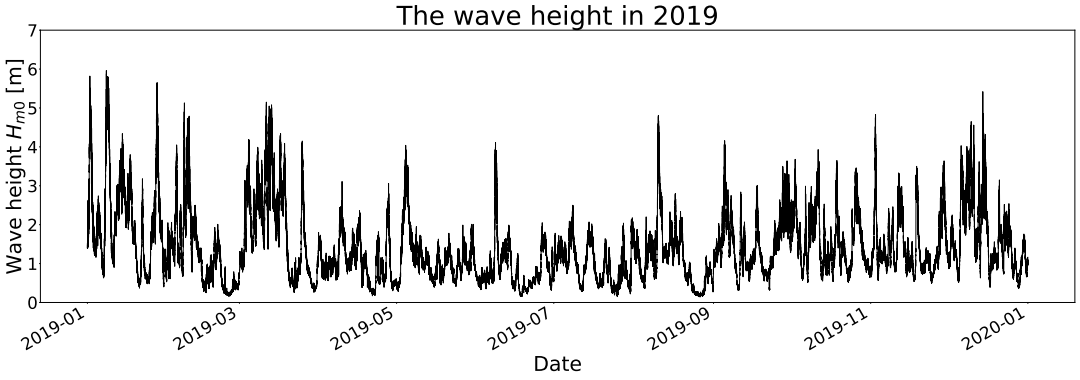

Figure B.5: The wave height in 2019. Modified from data of Rijkswaterstaat (Rijkswaterstaat, 2024).

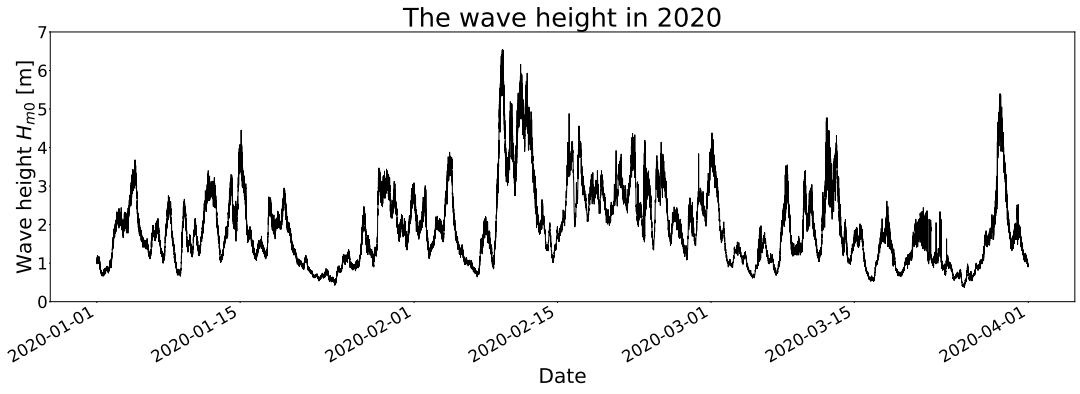

Figure B.6: The wave height in 2020. Modified from data of Rijkswaterstaat (Rijkswaterstaat, 2024).

B.1.2. Wave period

The wave period as plotted in the following figures is the wave period from the wave spectrum, namely T_{m02}. In Figure B.7 to Figure B.12, the wave period for each year can be seen separately. Here it can be seen that the maximum wave period occur in the period of the maximum wave height, which corresponds to the theory from the Literature Review of Chapter 2.

The average wave period varies over the years, but is generally equal to 4.5 to 5 s. In doing so, there is a small variation over the years. The variations in the wave period for the minimum wave value is small compared to the variation of the maximum wave period. The maximum wave period varies from 7.5 s to 10.7 s, while the minimum wave period for the years is approximately equal to 2.5 s. In the year 2020, the wave period is slightly higher than the other years, which is 2.8 s. This concerns only the waves that occur in winter and thus may lead to a higher wave peak because the wave heights are also higher in winter.

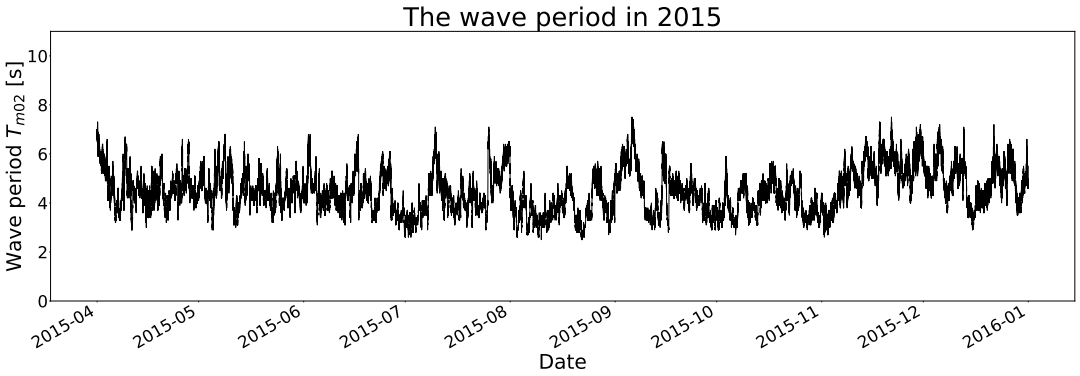

Figure B.7: The wave period in 2015. Modified from data of Rijkswaterstaat (Rijkswaterstaat, 2024).

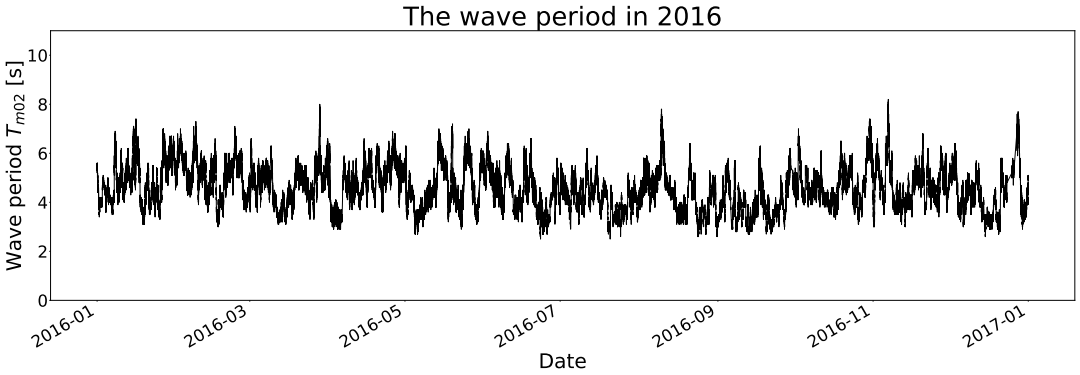

Figure B.8: The wave period in 2016. Modified from data of Rijkswaterstaat (Rijkswaterstaat, 2024).

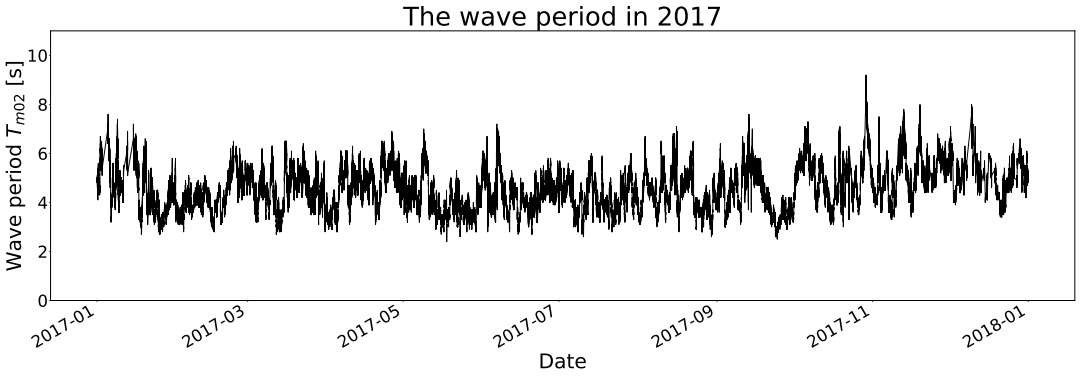

Figure B.9: The wave period in 2017. Modified from data of Rijkswaterstaat (Rijkswaterstaat, 2024).

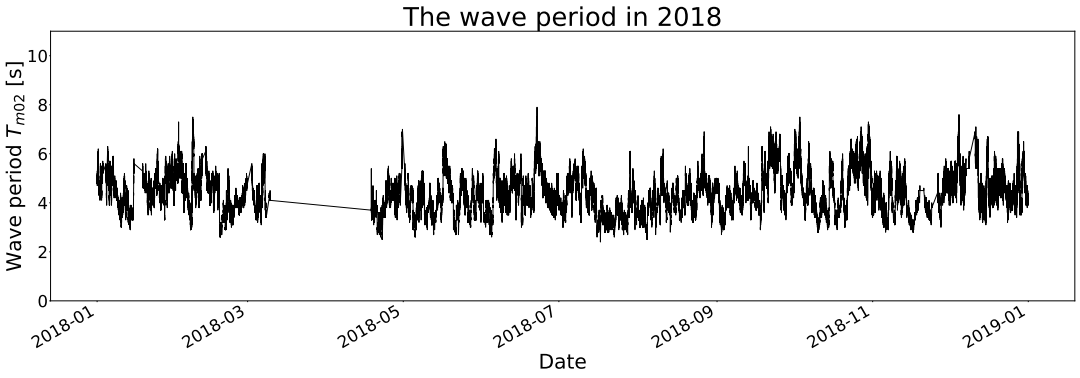

Figure B.10: The wave period in 2018. Modified from data of Rijkswaterstaat (Rijkswaterstaat, 2024).

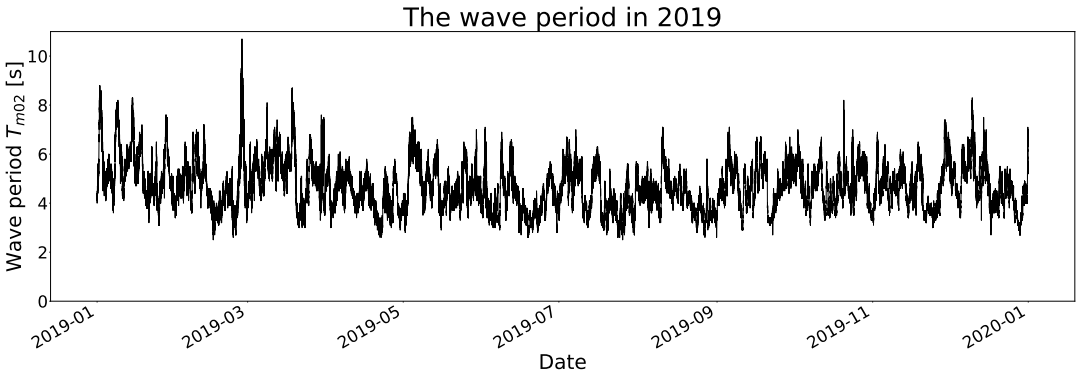

Figure B.11: The wave period in 2019. Modified from data of Rijkswaterstaat (Rijkswaterstaat, 2024).

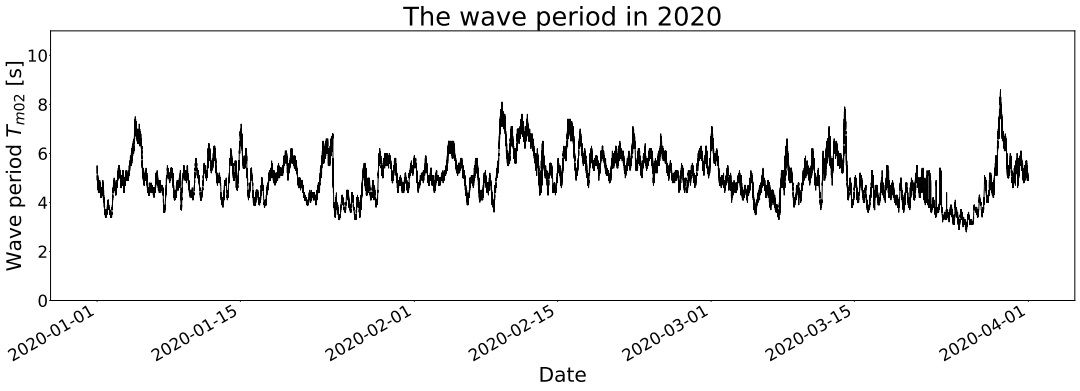

Figure B.12: The wave period in 2020. Modified from data of Rijkswaterstaat (Rijkswaterstaat, 2024).

B.1.3. Wave direction

The wave direction of waves per year are represented in a wave rose. Based on a wave rose, it is possible to examine how often a wave height occurs and from which direction most waves occur. In general, most waves occurring in the Netherlands come from the southwest. In 2017 and 2018, however, it was found that most waves come from the north northwest. Also in the other years, many waves come from this direction. Therefore, it can be concluded that the waves that will be applied in the modelling come from southwest or north-northwest. The reason why hardly any waves come from the east is because east of the coast is the hinterland of the Netherlands, so no waves are generated here.

The wind roses from Figure B.13 to Figure B.18 show that the most energetic environment took place in 2020. However, as mentioned earlier, this involves only the winter months so the wave heights are larger than in the years where the summer months are also included in the analysis. It further follows that the first year was also very energetic environment and gradually decreased in the following years.

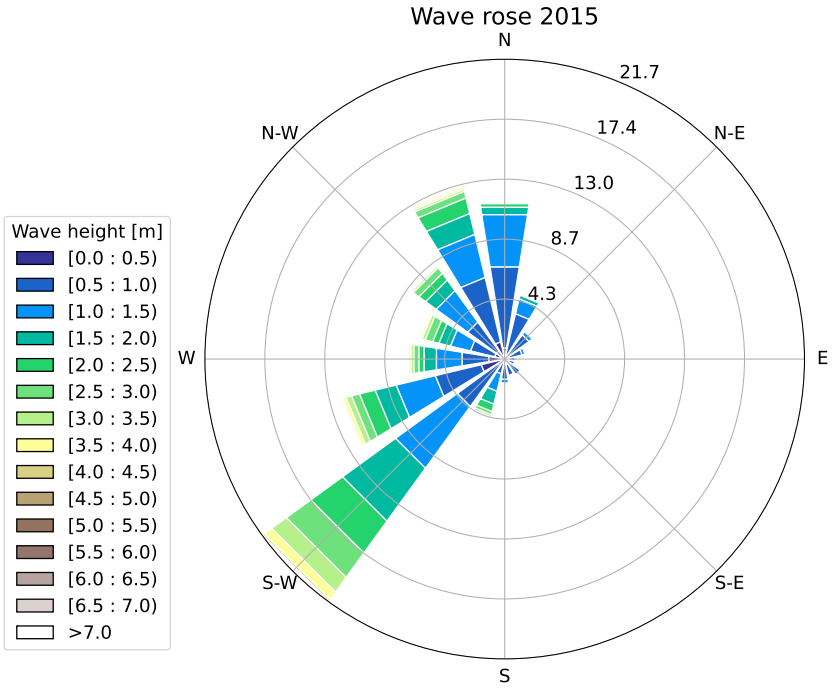

Figure B.13: The wave rose from 2015. Modified from data of Rijkswaterstaat (Rijkswaterstaat, 2024).

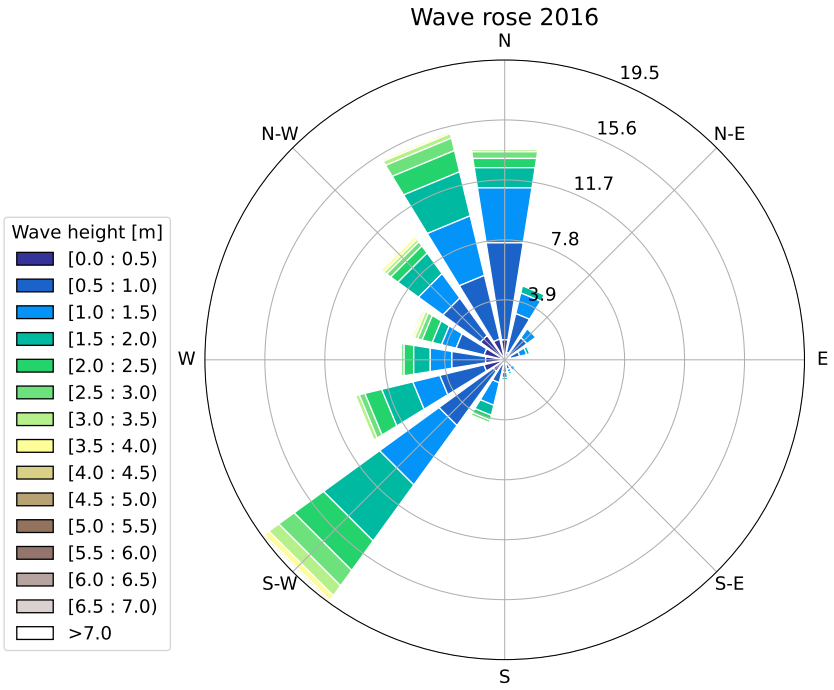

Figure B.14: The wave rose from 2016. Modified from data of Rijkswaterstaat (Rijkswaterstaat, 2024).

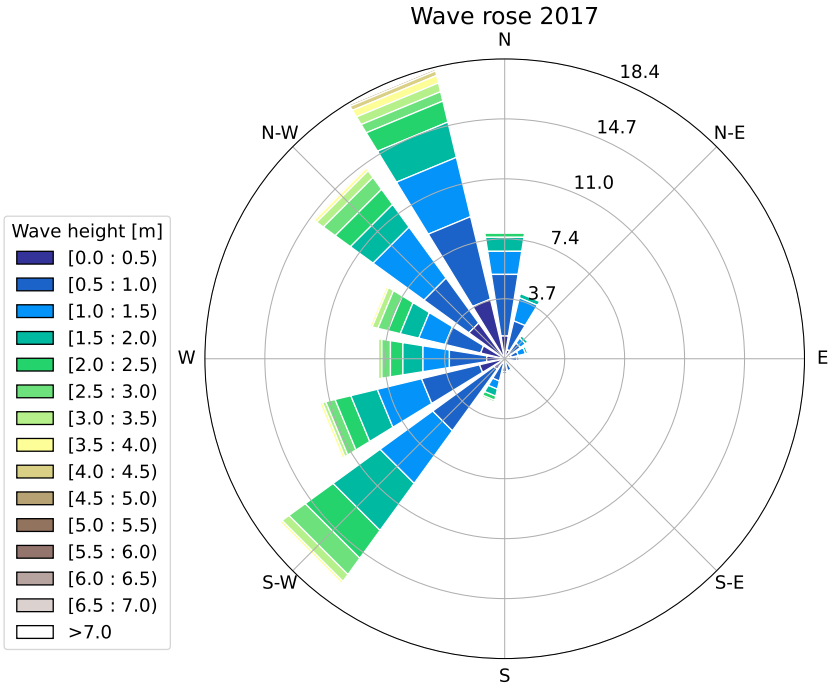

Figure B.15: The wave rose from 2017. Modified from data of Rijkswaterstaat (Rijkswaterstaat, 2024).

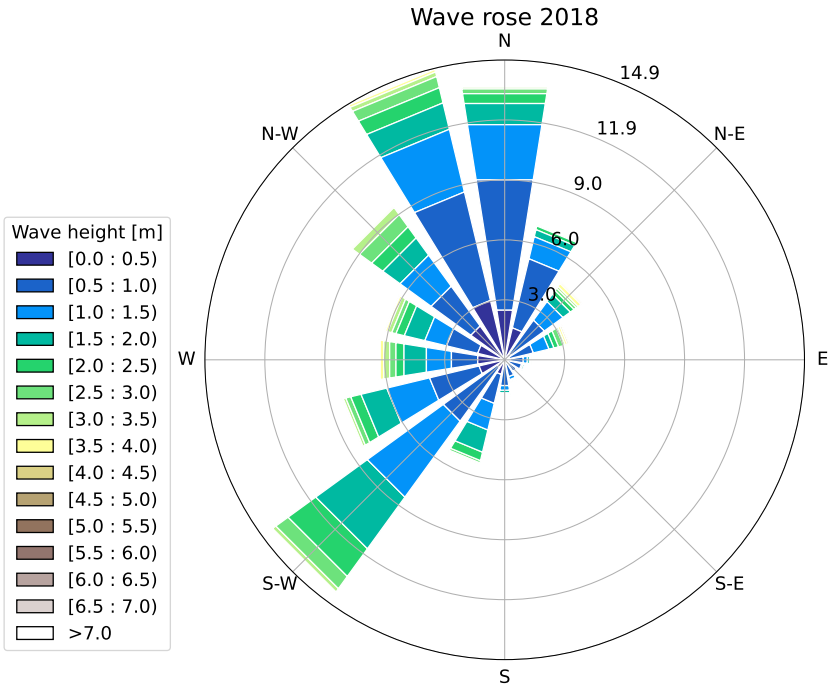

Figure B.16: The wave rose from 2018. Modified from data of Rijkswaterstaat (Rijkswaterstaat, 2024).

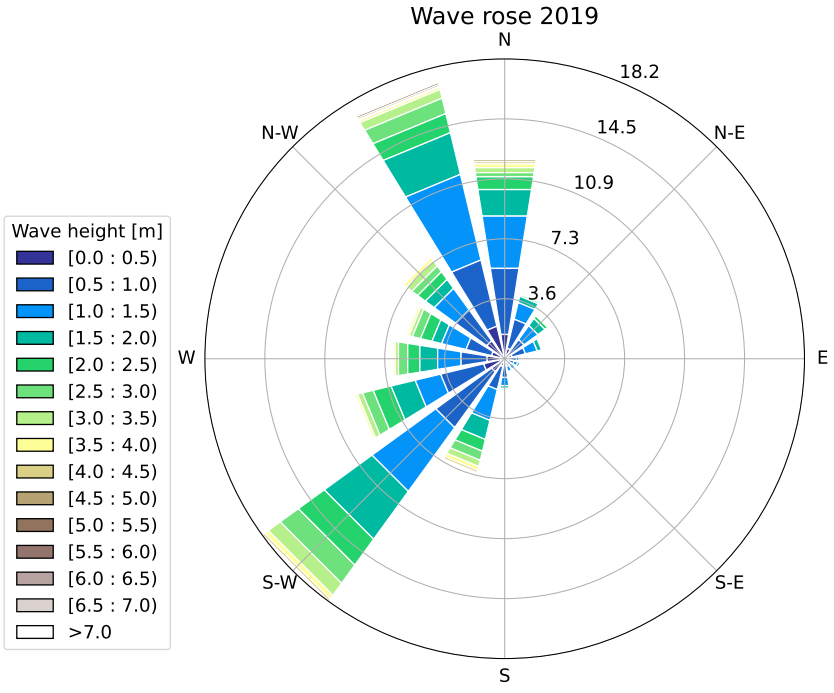

Figure B.17: The wave rose from 2019. Modified from data of Rijkswaterstaat (Rijkswaterstaat, 2024).

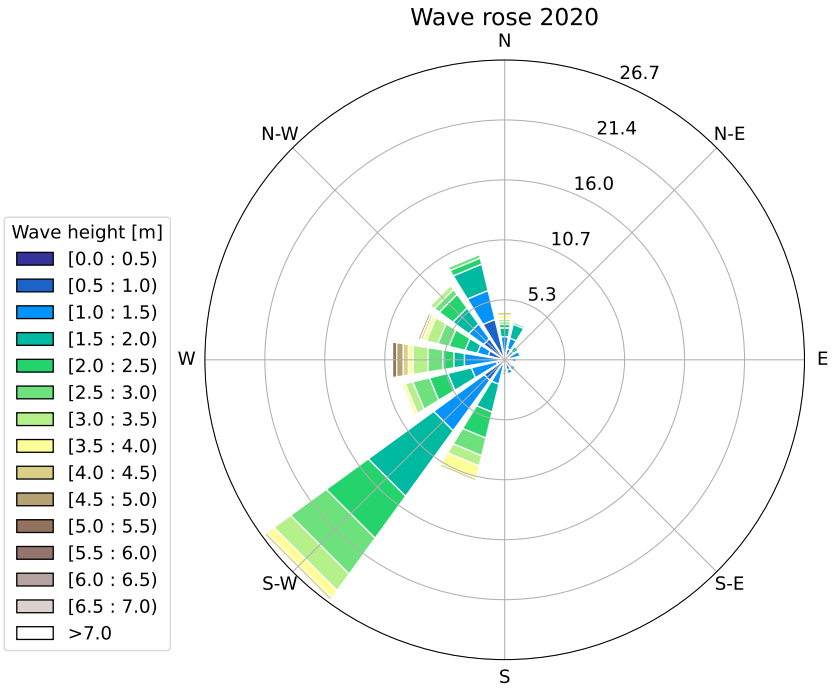

Figure B.18: The wave rose from 2020. Modified from data of Rijkswaterstaat (Rijkswaterstaat, 2024).

B.2. Water level

The water level consists of an astronomical tide and a surge contribution. The surge term is not measured using the measuring stations in the North Sea, but the water level and the astronomical tide are. By subtracting the astronomical tide from the total water level, the surge can be obtained.

The figures below, Figure B.19, show the total water level in the Netherlands at measuring station IJmuiden Stroommeetpaal (see Figure 3.2), so this means that this is the water level consisting of the surge and the astronomical tide. It can be seen from Figure B.19 that the water level generally varies between 2 m and -1 m.

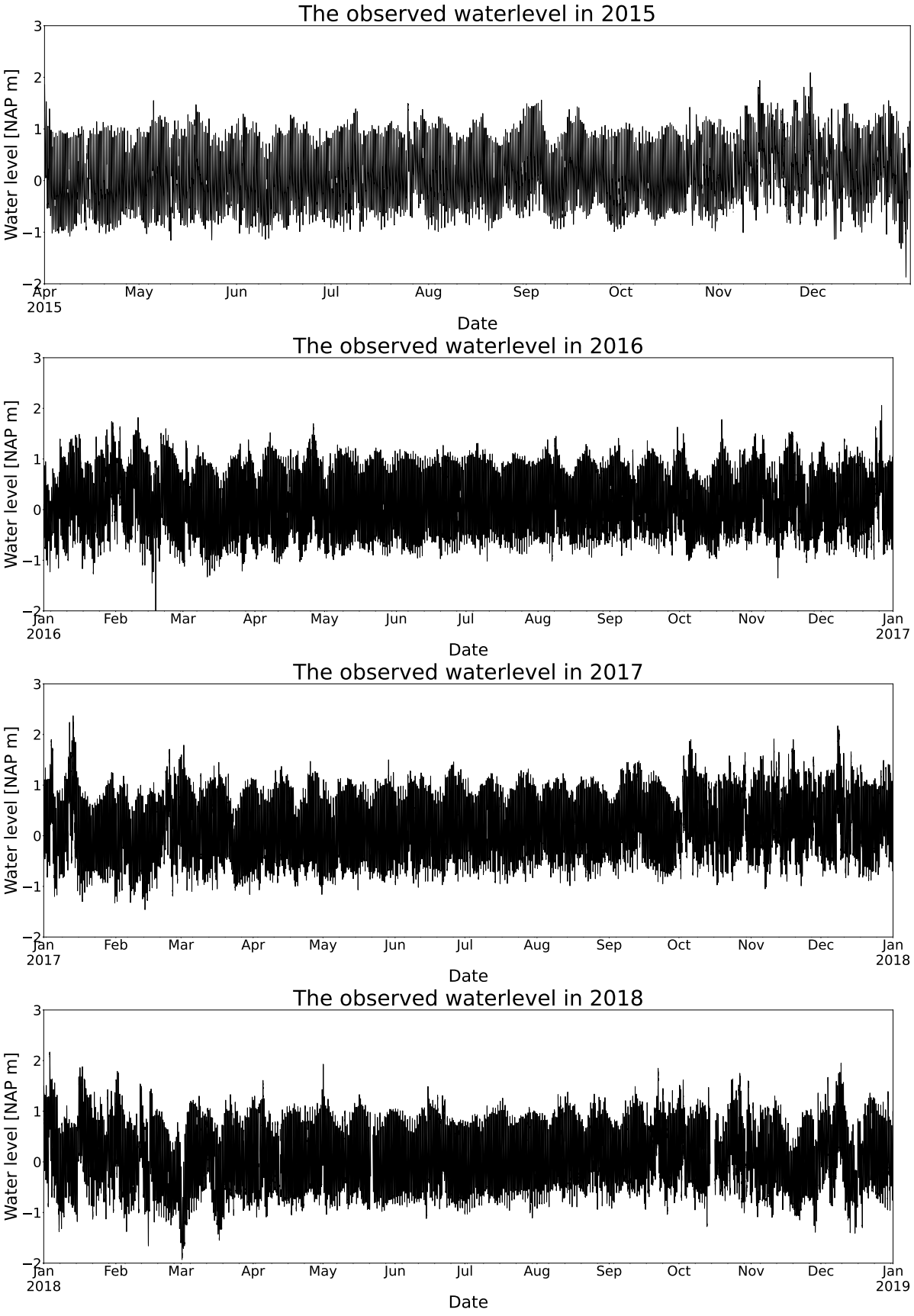
The observed waterlevel in 2015
Water level [NAP m]
3
2
1
0
−1
−2
Apr
2015
May
Jun
Jul
Aug
Sep
Oct
Nov
Dec
Date
The observed waterlevel in 2016
Water level [NAP m]
Jan
2016
Feb
Mar
Apr
May
Jun
Jul
Aug
Sep
Oct
Nov
Dec
Jan
2017
Date
The observed waterlevel in 2017
Water level [NAP m]
Jan
2017
Feb
Mar
Apr
May
Jun
Jul
Aug
Sep
Oct
Nov
Dec
Jan
2018
Date
The observed waterlevel in 2018
Water level [NAP m]
Jan
2018
Feb
Mar
Apr
May
Jun
Jul
Aug
Sep
Oct
Nov
Dec
Jan
2019
Date

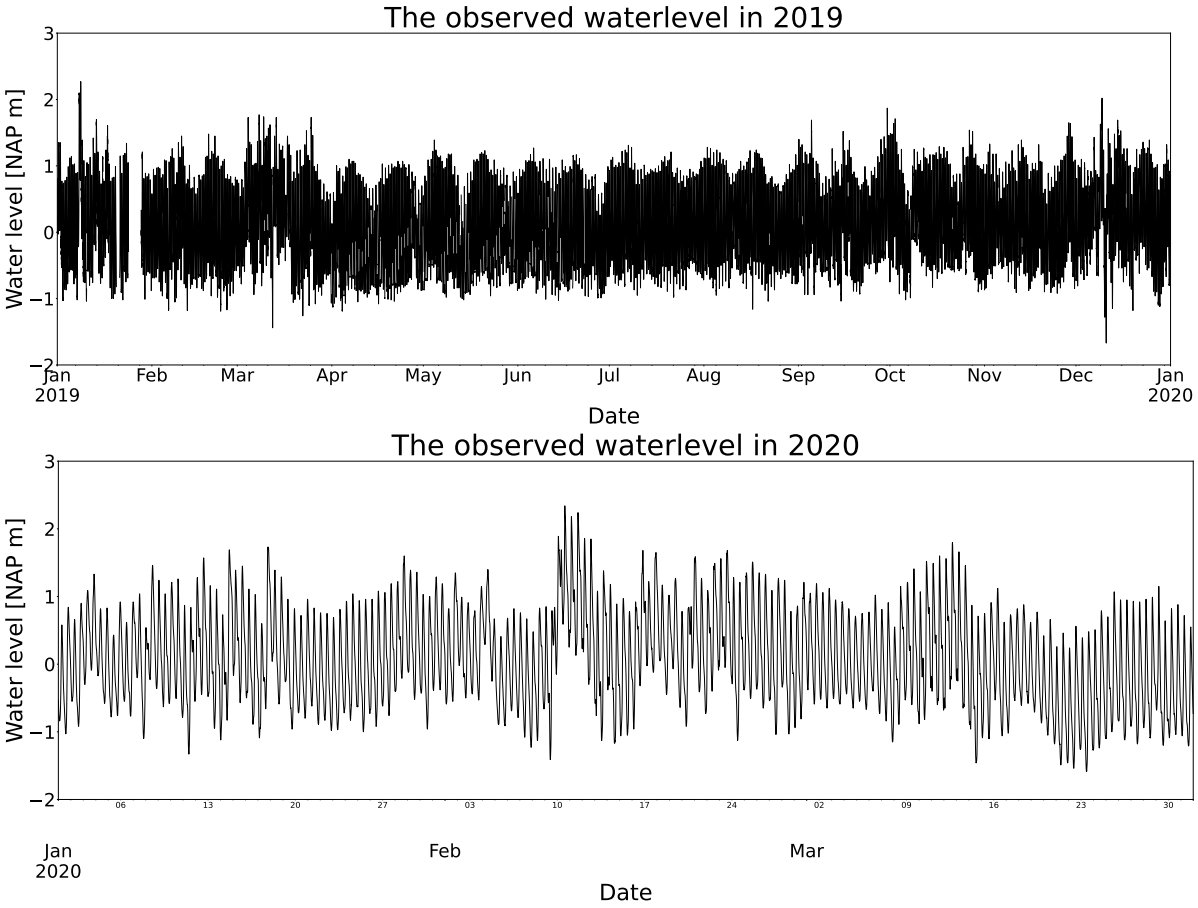

Figure B.19: The water level measured at water station IJmuiden Stroommeetpaal. Modified from data of Rijkswaterstaat (Rijkswaterstaat, 2024).

The astronomical water level is shown in the figure below, Figure B.20, where each year is shown separately.

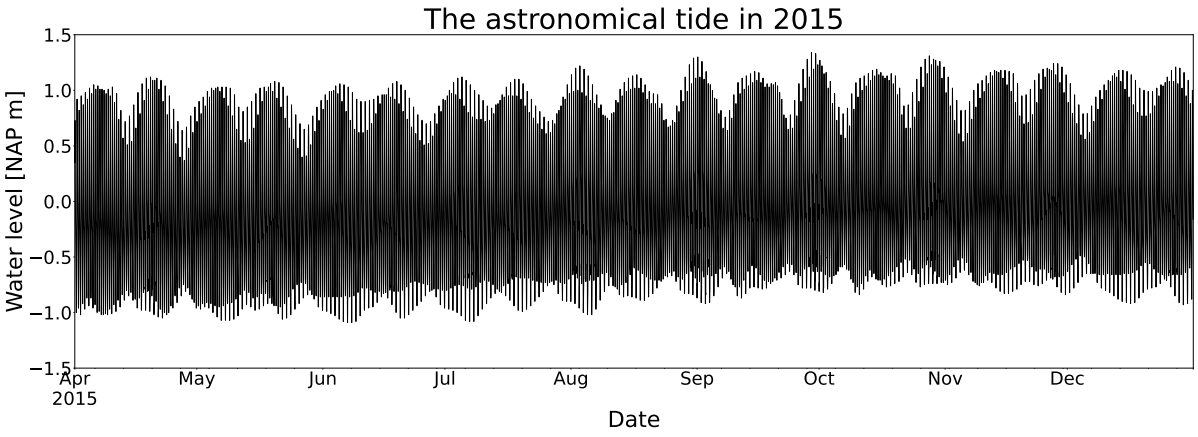

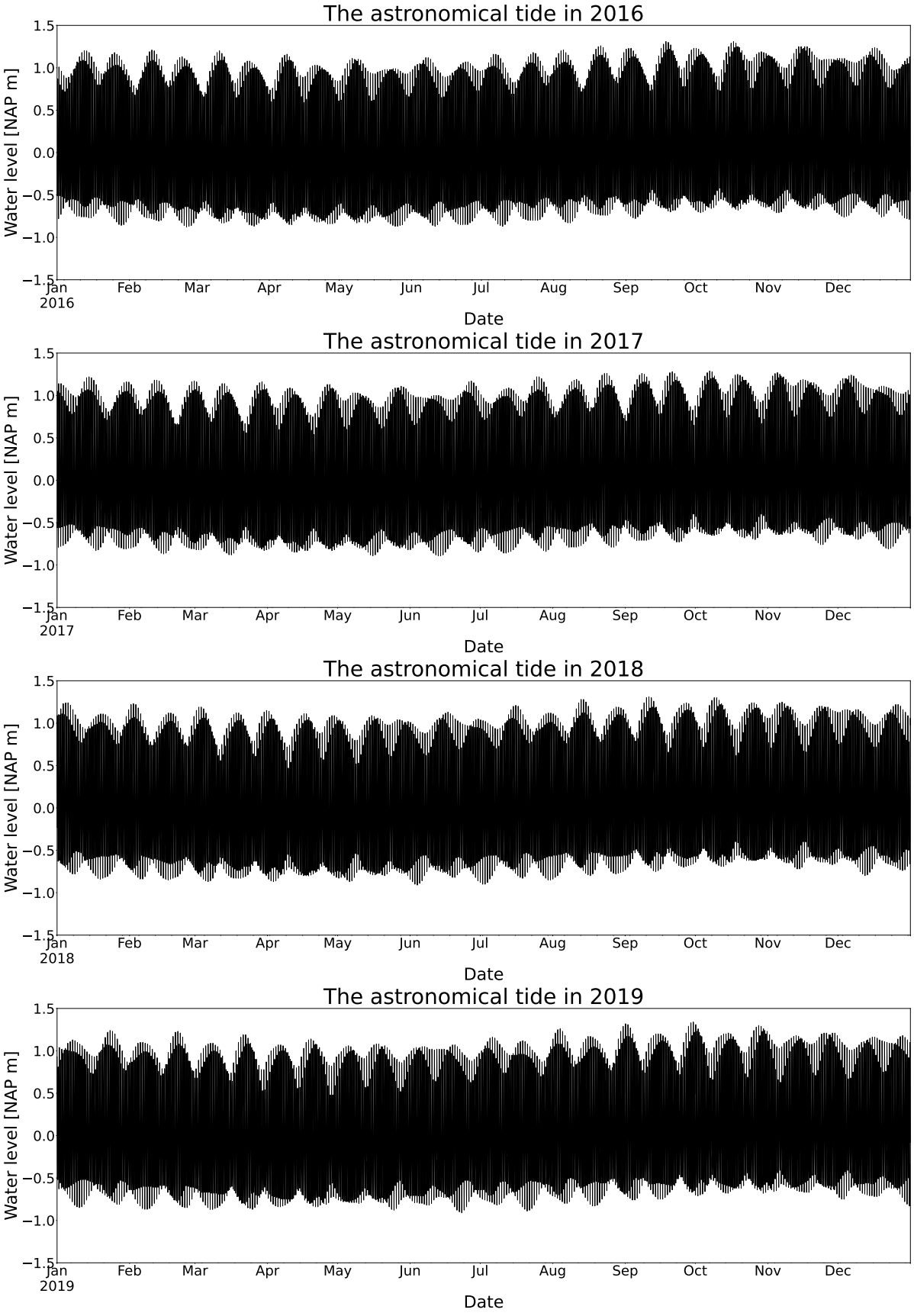
The astronomical tide in 2016
Water level [NAP m]
1.5
1.0
0.5
0.0
−0.5
−1.0
−1.5
Jan
2016
Feb
Mar
Apr
May
Jun
Jul
Aug
Sep
Oct
Nov
Dec
Date
The astronomical tide in 2017
Water level [NAP m]
Jan
2017
Date
The astronomical tide in 2018
Water level [NAP m]
Jan
2018
Date
The astronomical tide in 2019
Water level [NAP m]
Jan
2019
Date

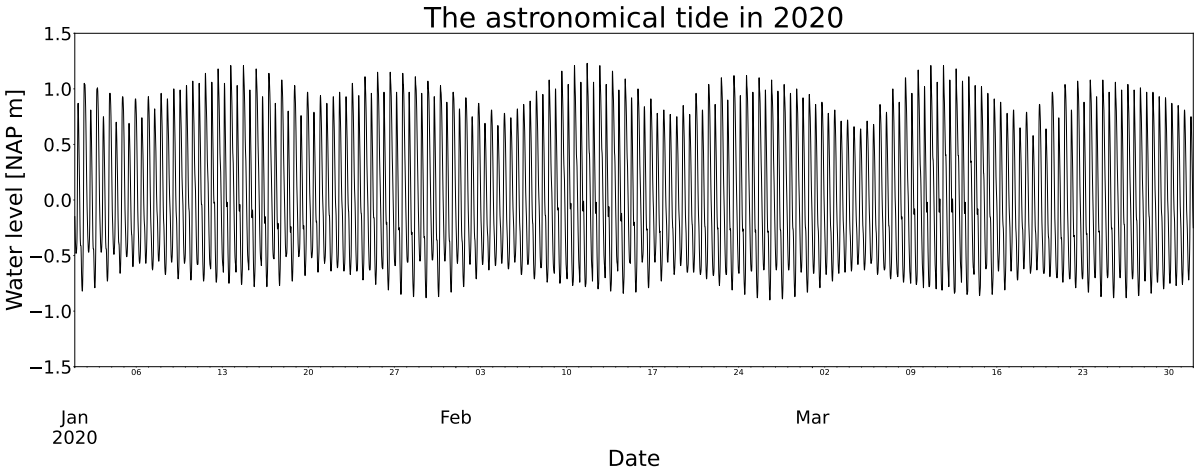

Figure B.20: The astronomical tide measured at water station IJmuiden Stroommeetpaal. Modified from data of Rijkswaterstaat (Rijkswaterstaat, 2024).

The difference in water level between Figure B.20 and the water level from Figure B.19 is called the surge. The surge is shown in Figure B.21.

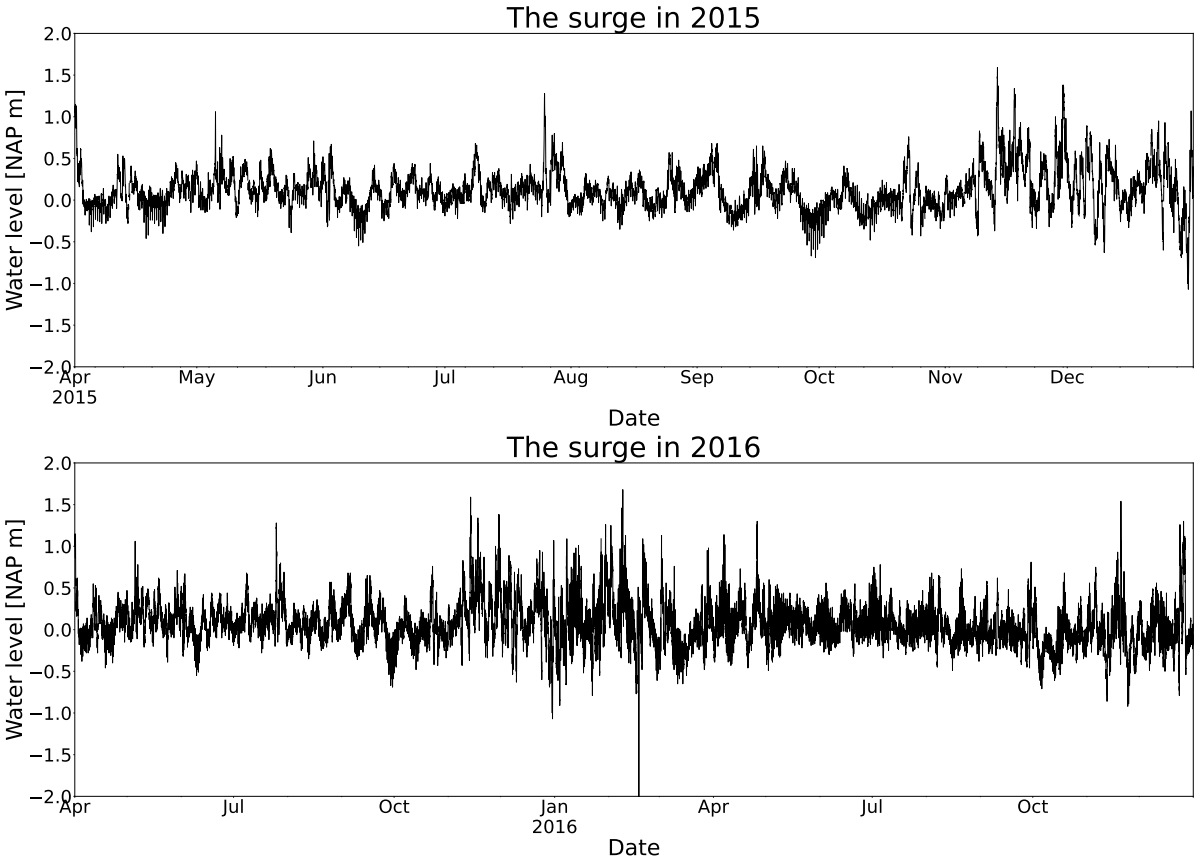

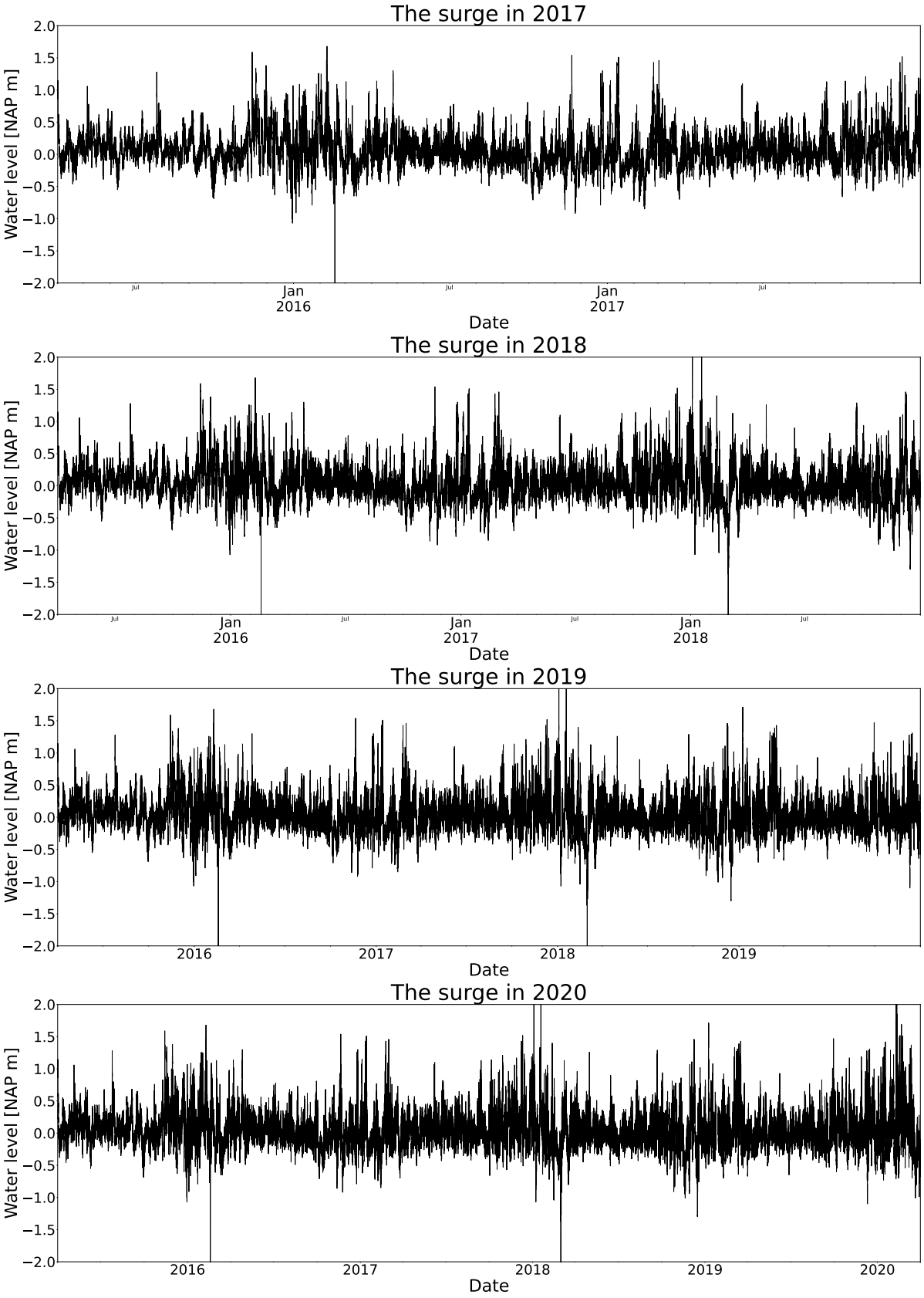

Figure B.21: The surge based on the water level and the astronomical tide measured at water station IJmuiden Stroommeetpaal. Modified from data of Rijkswaterstaat (Rijkswaterstaat, 2024).

C

Parameter settings of XBeach

C.1. Params.txt schematic model surf beat

```
%%%%%%%%%%%%%%%%%%%%%%%%%%%%%%%%%%%%%%%%%%%%%%%%%%%%%%%%%%%%%%%%%%%%%%%%%%%%%%%%
%%% XBeach parameter settings input file                                      %%%
%%%                                                                           %%%
%%% date:     02-Apr-2024 10:08:12                                            %%%
%%% function: xb_write_params                                                 %%%
%%%%%%%%%%%%%%%%%%%%%%%%%%%%%%%%%%%%%%%%%%%%%%%%%%%%%%%%%%%%%%%%%%%%%%%%%%%%%%%%

%%% Grid parameters %%%%%%%%%%%%%%%%%%%%%%%%%%%%%%%%%%%%%%%%%%%%%%%%%%%%%%%%%%%%

depfile    = bed.dep
posdwn     = -1
nx         = 1097
ny         = 782
alfa       = 0
vardx      = 1
xfile      = x.grd
yfile      = y.grd
xori       = 97470
yori       = 526850
thetamin   = 30
thetamax   = 270
dtheta     = 10
thetanaut  = 1
single_dir = 0

%%% Model time %%%%%%%%%%%%%%%%%%%%%%%%%%%%%%%%%%%%%%%%%%%%%%%%%%%%%%%%%%%%%%%%

tstop      = 291600
CFL        = 0.9

%%% Physical constants %%%%%%%%%%%%%%%%%%%%%%%%%%%%%%%%%%%%%%%%%%%%%%%%%%%%%%%%

g          = 9.810000
rho        = 1025

%%% Tide boundary conditions %%%%%%%%%%%%%%%%%%%%%%%%%%%%%%%%%%%%%%%%%%%%%%%%%%
```

```
tideloc    = 1
zs0file    = Tide.txt

%%% Wave boundary condition parameters %%%%%%%%%%%%%%%%%%%%%%%%%%%%%%%%%%%%%%%%

bcfile     = Waves.txt
wbctype    = jonstable
wavemodel  = surfbeat

%%% Bed composition parameters %%%%%%%%%%%%%%%%%%%%%%%%%%%%%%%%%%%%%%%%%%%%%%%

rhos       = 2650
por        = 0.400000
D50        = 0.000250
D90        = 0.000375
sedcal     = 1

%%% Flow boundary condition parameters %%%%%%%%%%%%%%%%%%%%%%%%%%%%%%%%%%%%%%%

left       = 0
right      = 0

%%% Flow parameters %%%%%%%%%%%%%%%%%%%%%%%%%%%%%%%%%%%%%%%%%%%%%%%%%%%%%%%%%%

C          = 60

%%% Physical processes %%%%%%%%%%%%%%%%%%%%%%%%%%%%%%%%%%%%%%%%%%%%%%%%%%%%%%

sedtrans   = 1
morphology = 1
swave      = 1
lwave      = 1

%%% Roller parameters %%%%%%%%%%%%%%%%%%%%%%%%%%%%%%%%%%%%%%%%%%%%%%%%%%%%%%%

roller     = 1
beta       = 0.100000

%%% Wave breaking parameters %%%%%%%%%%%%%%%%%%%%%%%%%%%%%%%%%%%%%%%%%%%%%%%%

break      = 3
gamma      = 0.55
alpha      = 1
n          = 10
gammax     = 2

%%% Sediment transport parameters %%%%%%%%%%%%%%%%%%%%%%%%%%%%%%%%%%%%%%%%%%%

waveform   = 1
form       = 1

%%% Morphology parameters %%%%%%%%%%%%%%%%%%%%%%%%%%%%%%%%%%%%%%%%%%%%%%%%%%%

morfac     = 10
morfacopt  = 1
```

```
%%% Output variables %%%%%%%%%%%%%%%%%%%%%%%%%%%%%%%%%%%%%%%%%%%%%%%%%%%%%%%%%%%%

tintm      = 3600
tintg      = 3600
tstart     = 0


nglobalvar = 13
zs
zb
zs0
H
R
ue
ve
u
v
ccg
E
Sutot
Svtot

nmeanvar   = 1
H
```

C.2. Params.txt schematic model stationary

```
%%%%%%%%%%%%%%%%%%%%%%%%%%%%%%%%%%%%%%%%%%%%%%%%%%%%%%%%%%%%%%%%%%%%%%%%%%%%%%%%
%%% XBeach parameter settings input file                                     %%%
%%%                                                                          %%%
%%% date:     02-Apr-2024 10:08:12                                           %%%
%%% function: xb_write_params                                                %%%
%%%%%%%%%%%%%%%%%%%%%%%%%%%%%%%%%%%%%%%%%%%%%%%%%%%%%%%%%%%%%%%%%%%%%%%%%%%%%%%%

%%% Grid parameters %%%%%%%%%%%%%%%%%%%%%%%%%%%%%%%%%%%%%%%%%%%%%%%%%%%%%%%%%%%%%

depfile    = bed.dep
posdwn     = -1
nx         = 1097
ny         = 782
alfa       = 0
vardx      = 1
xfile      = x.grd
yfile      = y.grd
xori       = 97470
yori       = 526850
thetamin   = 30
thetamax   = 270
dtheta     = 10
thetanaut  = 1
single_dir = 0

%%% Model time %%%%%%%%%%%%%%%%%%%%%%%%%%%%%%%%%%%%%%%%%%%%%%%%%%%%%%%%%%%%%%%%%%

tstop      = 291600
CFL        = 0.9

%%% Physical constants %%%%%%%%%%%%%%%%%%%%%%%%%%%%%%%%%%%%%%%%%%%%%%%%%%%%%%%%%%

g          = 9.810000
rho        = 1025

%%% Tide boundary conditions %%%%%%%%%%%%%%%%%%%%%%%%%%%%%%%%%%%%%%%%%%%%%%%%%%%%

tideloc    = 1
zs0file    = Tide.txt

%%% Wave boundary condition parameters %%%%%%%%%%%%%%%%%%%%%%%%%%%%%%%%%%%%%%%%%%

bcfile     = Waves.txt
wbctype    = jonstable
instat     = 0

%%% Bed composition parameters %%%%%%%%%%%%%%%%%%%%%%%%%%%%%%%%%%%%%%%%%%%%%%%%%%

rhos       = 2650
por        = 0.400000
D50        = 0.000250
D90        = 0.000375
sedcal     = 1

%%% Flow boundary condition parameters %%%%%%%%%%%%%%%%%%%%%%%%%%%%%%%%%%%%%%%%%%
```

```
left       = 0
right      = 0

%%% Flow parameters %%%%%%%%%%%%%%%%%%%%%%%%%%%%%%%%%%%%%%%%%%%%%%%%%%%%%%%%%%%%

C          = 60

%%% Physical processes %%%%%%%%%%%%%%%%%%%%%%%%%%%%%%%%%%%%%%%%%%%%%%%%%%%%%%%%

sedtrans   = 1
morphology = 1
swave      = 1
lwave      = 1

%%% Roller parameters %%%%%%%%%%%%%%%%%%%%%%%%%%%%%%%%%%%%%%%%%%%%%%%%%%%%%%%%%

roller     = 1
beta       = 0.100000

%%% Wave breaking parameters %%%%%%%%%%%%%%%%%%%%%%%%%%%%%%%%%%%%%%%%%%%%%%%%%%

break      = 3
gamma      = 0.55
alpha      = 1
n          = 10
gammax     = 2

%%% Sediment transport parameters %%%%%%%%%%%%%%%%%%%%%%%%%%%%%%%%%%%%%%%%%%%%%

waveform   = 2
form       = 2

%%% Morphology parameters %%%%%%%%%%%%%%%%%%%%%%%%%%%%%%%%%%%%%%%%%%%%%%%%%%%%%

morfac     = 10
morfacopt  = 1

%%% Output variables %%%%%%%%%%%%%%%%%%%%%%%%%%%%%%%%%%%%%%%%%%%%%%%%%%%%%%%%%

tintm      = 3600
tintg      = 3600
tstart     = 0


nglobalvar = 13
zs
zb
zs0
H
R
ue
ve
u
v
ccg
```

```
E
Sutot
Svtot

nmeanvar    = 1
H
```

C.3. Params.txt XBeach model HD surf beat

```
%%%%%%%%%%%%%%%%%%%%%%%%%%%%%%%%%%%%%%%%%%%%%%%%%%%%%%%%%%%%%%%%%%%%%%%%%%%%%%%%
%%% XBeach parameter settings input file                                     %%%
%%%                                                                          %%%
%%% date:     02-Apr-2024 10:08:12                                           %%%
%%% function: xb_write_params                                                %%%
%%%%%%%%%%%%%%%%%%%%%%%%%%%%%%%%%%%%%%%%%%%%%%%%%%%%%%%%%%%%%%%%%%%%%%%%%%%%%%%%

%%% Grid parameters %%%%%%%%%%%%%%%%%%%%%%%%%%%%%%%%%%%%%%%%%%%%%%%%%%%%%%%%%%%%

depfile    = bed.dep
posdwn     = -1
nx         = 305
ny         = 553
alfa       = 0
vardx      = 1
xfile      = x.grd
yfile      = y.grd
thetamin   = 145.9338
thetamax   = 325.9338
dtheta     = 20
thetanaut  = 1
single_dir = 0

%%% Model time %%%%%%%%%%%%%%%%%%%%%%%%%%%%%%%%%%%%%%%%%%%%%%%%%%%%%%%%%%%%%%%%%

tstop      = 315626
CFL        = 0.9

%%% Physical constants %%%%%%%%%%%%%%%%%%%%%%%%%%%%%%%%%%%%%%%%%%%%%%%%%%%%%%%%%

g          = 9.810000
rho        = 1025

%%% Tide boundary conditions %%%%%%%%%%%%%%%%%%%%%%%%%%%%%%%%%%%%%%%%%%%%%%%%%%%

tideloc    = 1
zs0file    = tide.txt

%%% Wave boundary condition parameters %%%%%%%%%%%%%%%%%%%%%%%%%%%%%%%%%%%%%%%%%

bcfile     = jons_table.txt
wbctype    = jonstable
wavemodel  = 1
wavint     = 185.5531
rt         = 3600
%%% Bed composition parameters %%%%%%%%%%%%%%%%%%%%%%%%%%%%%%%%%%%%%%%%%%%%%%%%%

rhos       = 2650
por        = 0.400000
D50        = 0.000250
D90        = 0.000375
sedcal     = 1

%%% Flow boundary condition parameters %%%%%%%%%%%%%%%%%%%%%%%%%%%%%%%%%%%%%%%%%
```

```
left       = neumann
right      = neumann

%%% Flow parameters %%%%%%%%%%%%%%%%%%%%%%%%%%%%%%%%%%%%%%%%%%%%%%%%%%%%%%%%%%%%

C          = 60
nuhfac     = 0

%%% Physical processes %%%%%%%%%%%%%%%%%%%%%%%%%%%%%%%%%%%%%%%%%%%%%%%%%%%%%%%%

sedtrans   = 1
morphology = 1
swave      = 1
lwave      = 1

%%% Roller parameters %%%%%%%%%%%%%%%%%%%%%%%%%%%%%%%%%%%%%%%%%%%%%%%%%%%%%%%%%

roller     = 1
beta       = 0.100000

%%% Wave breaking parameters %%%%%%%%%%%%%%%%%%%%%%%%%%%%%%%%%%%%%%%%%%%%%%%%%%

break      = roelvink2
gamma      = 0.45
alpha      = 1
n          = 10
gammax     = 2

%%% Sediment transport parameters %%%%%%%%%%%%%%%%%%%%%%%%%%%%%%%%%%%%%%%%%%%%%

waveform   = 1
form       = 1
facua    = 0.175
facAs      = 0.2
facSk      = 0.15

%%% Morphology parameters %%%%%%%%%%%%%%%%%%%%%%%%%%%%%%%%%%%%%%%%%%%%%%%%%%%%%

morfac     = 37.1106
morstart   = 66799

%%% Output variables %%%%%%%%%%%%%%%%%%%%%%%%%%%%%%%%%%%%%%%%%%%%%%%%%%%%%%%%%

tintm      = 4976
tintg      = 4976
tstart     = 66799
tintp    = 37


nglobalvar = 14
zs
zb
zs0
H
R
ue
```

```
ve
u
v
ccg
E
Sutot
Svtot
thetamean

nmeanvar    = 1
H
```

C.4. Params.txt XBeach model HD stationary

```
%%%%%%%%%%%%%%%%%%%%%%%%%%%%%%%%%%%%%%%%%%%%%%%%%%%%%%%%%%%%%%%%%%%%%%%%%%%%%%%%
%%% XBeach parameter settings input file                                       %%%
%%%                                                                           %%%
%%% date:     02-Apr-2024 10:08:12                                            %%%
%%% function: xb_write_params                                                 %%%
%%%%%%%%%%%%%%%%%%%%%%%%%%%%%%%%%%%%%%%%%%%%%%%%%%%%%%%%%%%%%%%%%%%%%%%%%%%%%%%%

%%% Grid parameters %%%%%%%%%%%%%%%%%%%%%%%%%%%%%%%%%%%%%%%%%%%%%%%%%%%%%%%%%%%%

depfile    = bed.dep
posdwn     = -1
nx         = 305
ny         = 553
alfa       = 0
vardx      = 1
xfile      = x.grd
yfile      = y.grd
thetamin   = 242.9055
thetamax   = 62.9055
dtheta     = 20
thetanaut  = 1
single_dir = 0

%%% Model time %%%%%%%%%%%%%%%%%%%%%%%%%%%%%%%%%%%%%%%%%%%%%%%%%%%%%%%%%%%%%%%%

tstop      = 1837735
CFL        = 0.9

%%% Physical constants %%%%%%%%%%%%%%%%%%%%%%%%%%%%%%%%%%%%%%%%%%%%%%%%%%%%%%%%

g          = 9.810000
rho        = 1025

%%% Tide boundary conditions %%%%%%%%%%%%%%%%%%%%%%%%%%%%%%%%%%%%%%%%%%%%%%%%%%

tideloc    = 1
zs0file    = tide.txt

%%% Wave boundary condition parameters %%%%%%%%%%%%%%%%%%%%%%%%%%%%%%%%%%%%%%%%%

bcfile     = jons_table.txt
wbctype    = jonstable
wavemodel  = 0
wavint     = 1080.3848
rt         = 3600
%%% Bed composition parameters %%%%%%%%%%%%%%%%%%%%%%%%%%%%%%%%%%%%%%%%%%%%%%%%

rhos       = 2650
por        = 0.400000
D50        = 0.000250
D90        = 0.000375
sedcal     = 1

%%% Flow boundary condition parameters %%%%%%%%%%%%%%%%%%%%%%%%%%%%%%%%%%%%%%%%%
```

```
left       = neumann
right      = neumann

%%% Flow parameters %%%%%%%%%%%%%%%%%%%%%%%%%%%%%%%%%%%%%%%%%%%%%%%%%%%%%%%%%%%%

C          = 60
nuhfac     = 0

%%% Physical processes %%%%%%%%%%%%%%%%%%%%%%%%%%%%%%%%%%%%%%%%%%%%%%%%%%%%%%%%

sedtrans   = 1
morphology = 1
swave      = 1
lwave      = 1

%%% Roller parameters %%%%%%%%%%%%%%%%%%%%%%%%%%%%%%%%%%%%%%%%%%%%%%%%%%%%%%%%%

roller     = 1
beta       = 0.100000

%%% Wave breaking parameters %%%%%%%%%%%%%%%%%%%%%%%%%%%%%%%%%%%%%%%%%%%%%%%%%%

break      = baldock
gamma      = 0.55
alpha      = 1
n          = 10
gammax     = 2

%%% Sediment transport parameters %%%%%%%%%%%%%%%%%%%%%%%%%%%%%%%%%%%%%%%%%%%%%

waveform   = 1
form       = 1
facua    = 0.175
facAs      = 0.2
facSk      = 0.15

%%% Morphology parameters %%%%%%%%%%%%%%%%%%%%%%%%%%%%%%%%%%%%%%%%%%%%%%%%%%%%%

morfac     = 216.077
morstart   = 388938

%%% Output variables %%%%%%%%%%%%%%%%%%%%%%%%%%%%%%%%%%%%%%%%%%%%%%%%%%%%%%%%%

tintm      = 28975
tintg      = 28975
tstart     = 388938
tintp    = 216


nglobalvar = 14
zs
zb
zs0
H
R
ue
```

```
ve
u
v
ccg
E
Sutot
Svtot
thetamean

nmeanvar   = 1
H
```

D

Schematic model

This appendix presents and discusses the results of the schematic model. Herein, a distinction is made between the different runs which are performed. The table below, Table D.1, gives an overview of the different runs.

Table D.1: An overview of the runs which are performed for the schematic model.

	Wave height [m]	Wave period [s]	Surge [m]	Wave direction [deg]	Wave model	Simulation time
Run 1	2.50	5.7	0.47	0	Surf beat	3 days 9 hours
Run 2	5.88	7.6	0.94	0	Surf beat	1 day
Run 3	5.88	7.6	0.94	0	Stationary	1 day
Run 4	2.50	5.7	0.47	45	Surf beat	3 days 9 hours
Run 5	5.88	7.6	0.94	45	Surf beat	1 day
Run 6	5.88	7.6	0.94	45	Stationary	1 day

D.1. Effect of the strength of coastal curvature

In this section, some additional aspects are analysed in addition to those mentioned in the report. Bed level difference figures are shown as well as three transects of each of the curvatures.

The erosion and sedimentation patterns from Figure D.1 show that most erosion occurs halfway through the curvature. This is true for all types of curvatures. Based on these erosion and sedimentation patterns, it appears that few differences occur between the different sizes of curvatures.

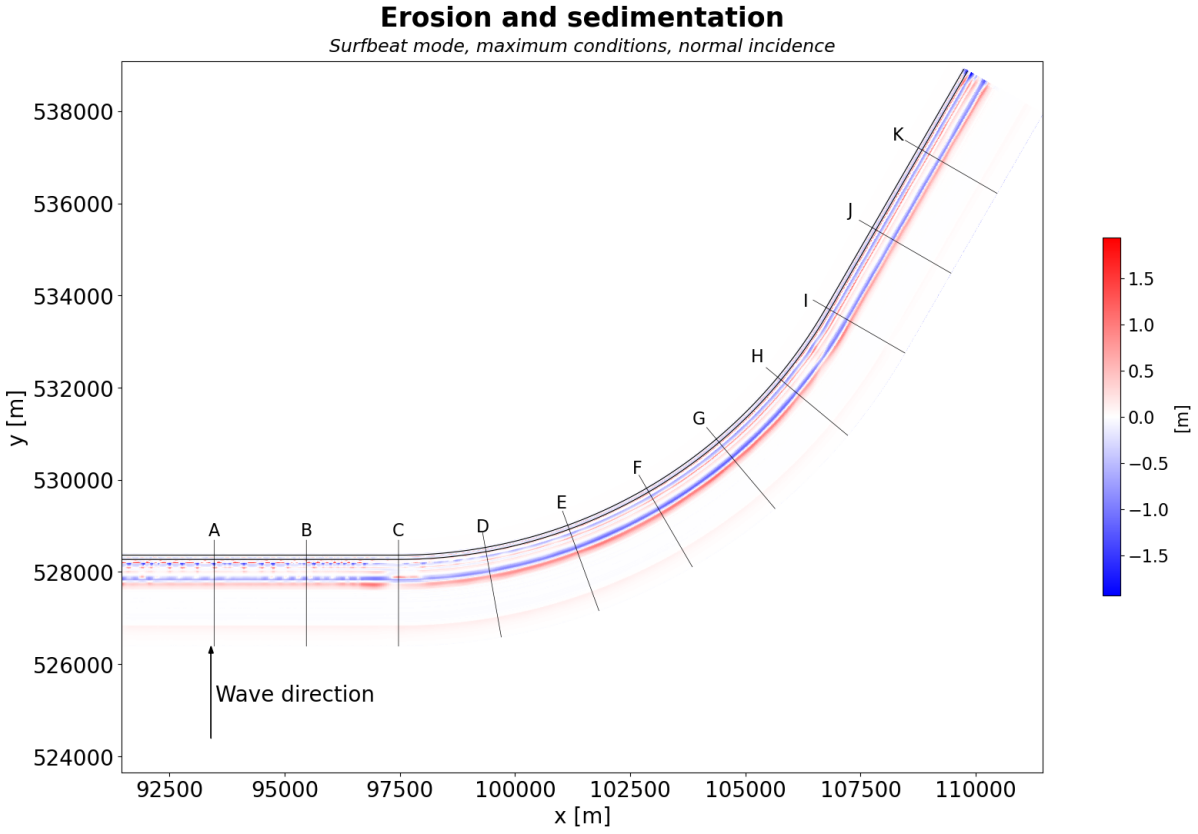

(a) Two times more curvature.

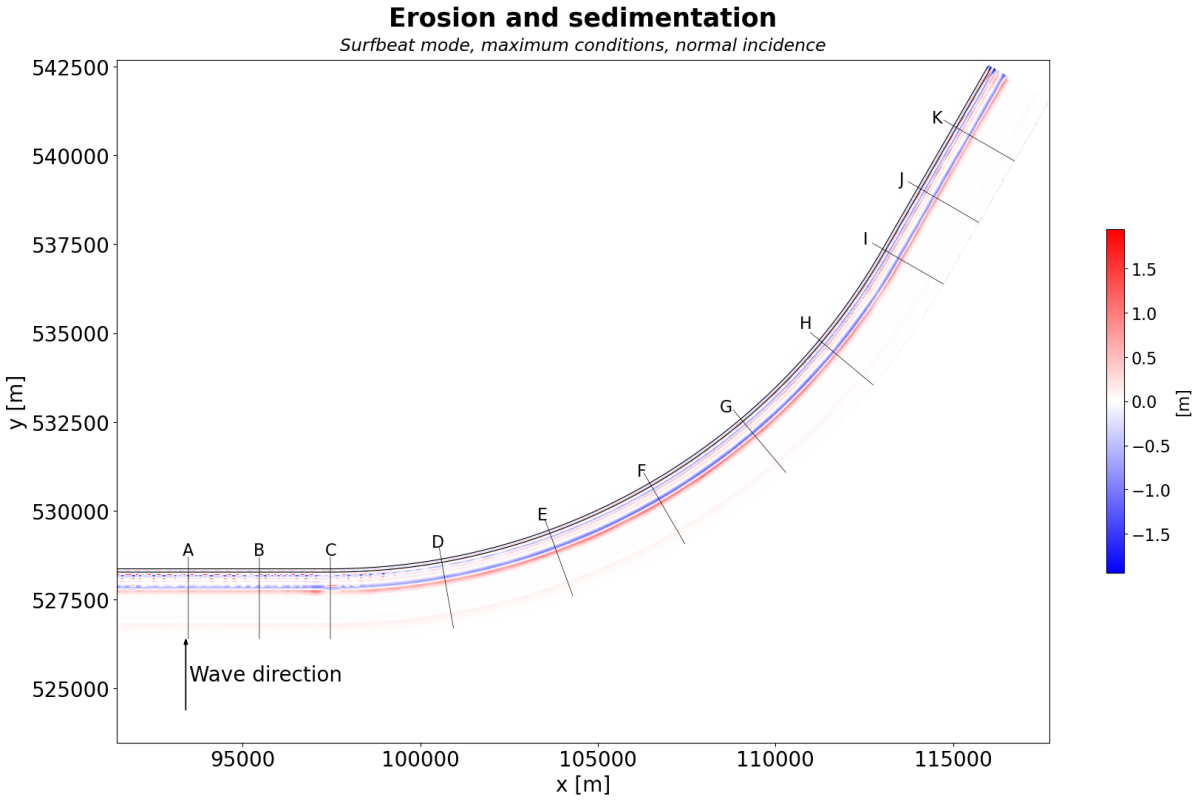

(b) The same curvature as present at the HD.

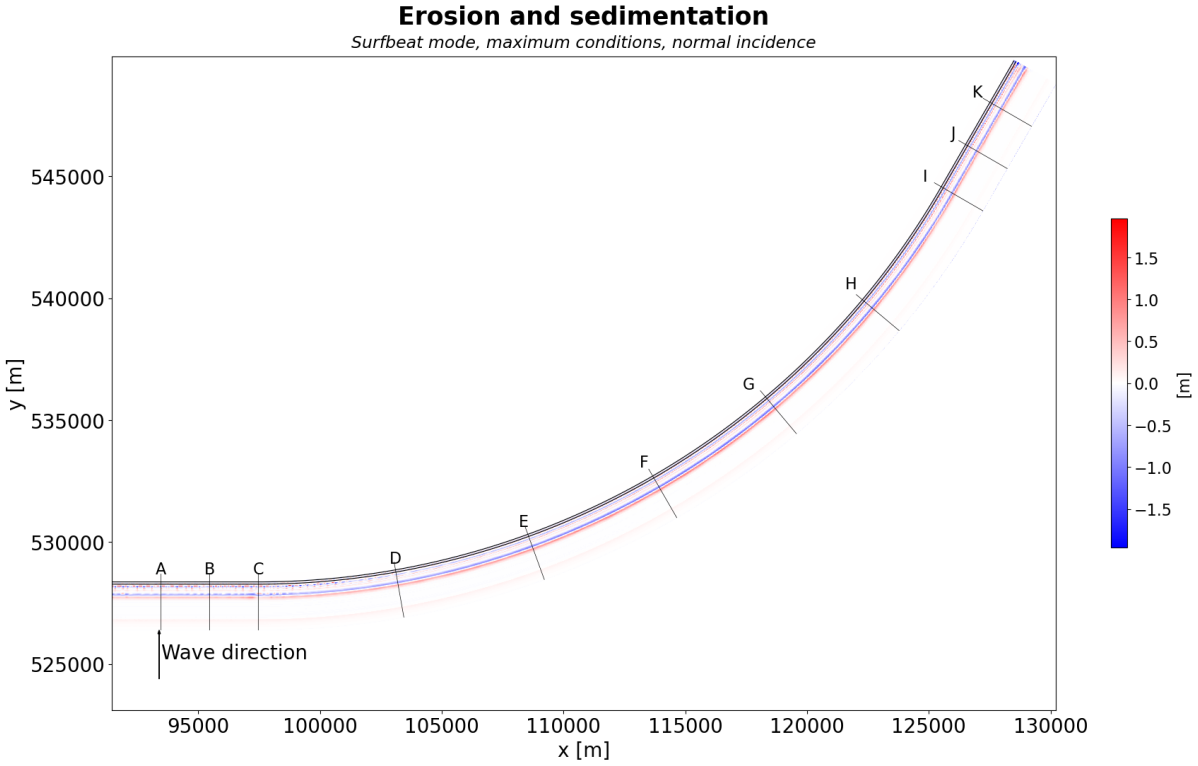

(c) Two times less curvature.

Figure D.1: The bed level difference for the conditions of Run 2. The blue colours indicate erosion and the red colours indicate sedimentation. Modified from XBeach output.

In the figures below, Figure D.2, Figure D.3 and Figure D.4 show three transects. The first and last transects are transects on the straight part before and after the curvature while the middle plot is the transect in the middle of the curvature. The beach width differences between the different strengths in curvatures do not differ much from each other. The purpose of the transects is to investigate where the erosion occurs and not to investigate the gradient of the differences in beach width as previously investigated in Chapter 5.

The largest change in beach width for all transects occurs at an alongshore distance of 1,460 m. At this location, there is a berm present in the initial situation which has flattened out as a result of erosion at the end of the simulation. It can also be seen that the profile becomes steeper with less unevenness in transect J compared to the other transects.

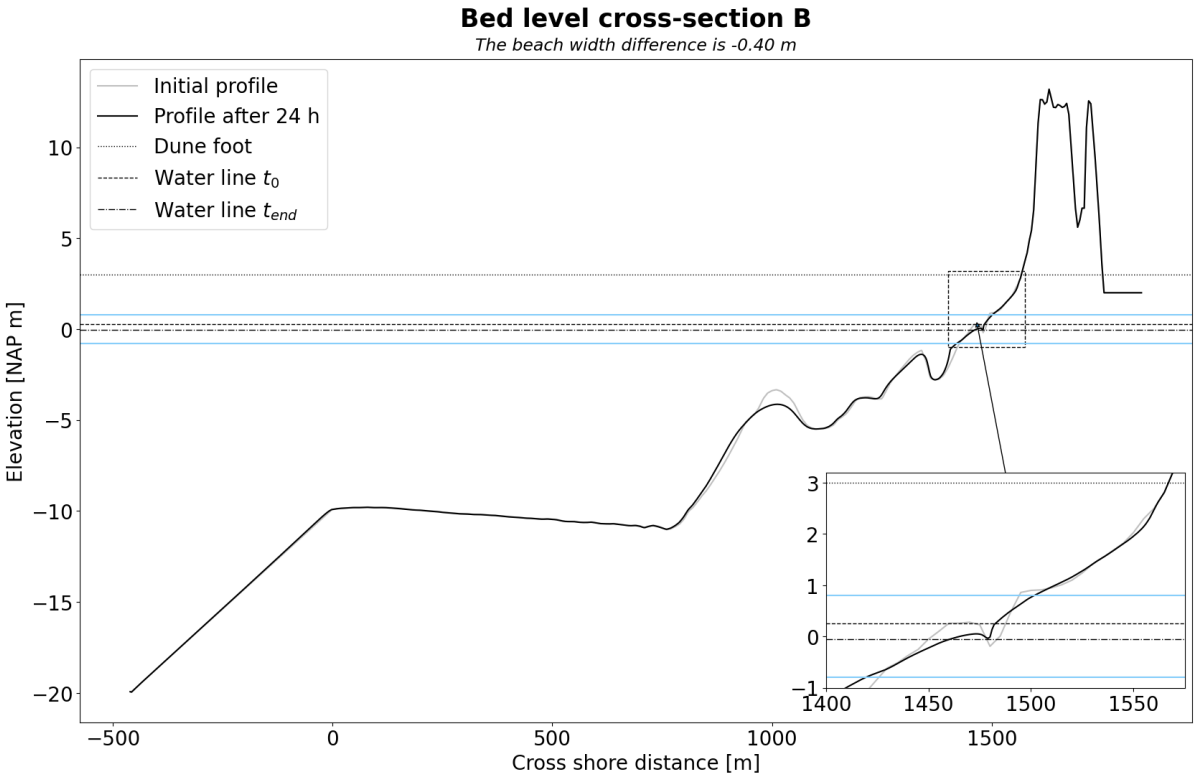

(a) Cross-section B.

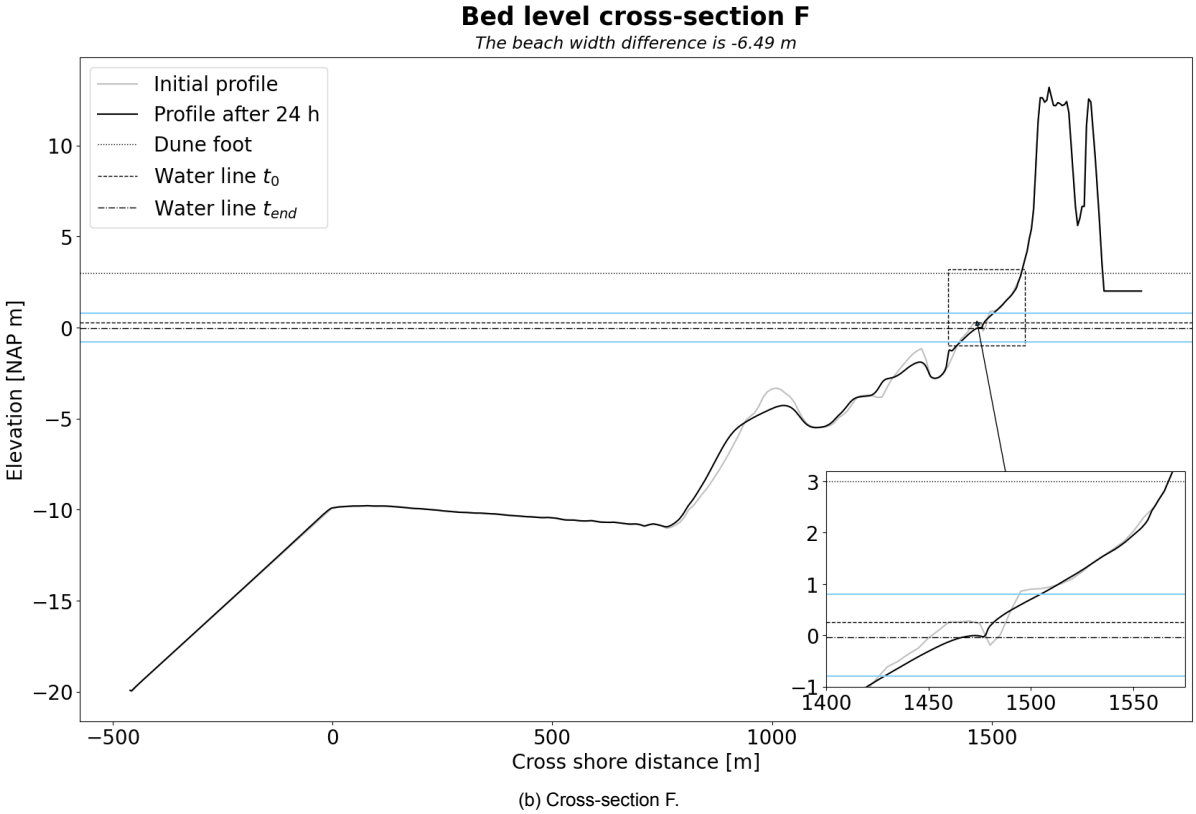

(b) Cross-section F.

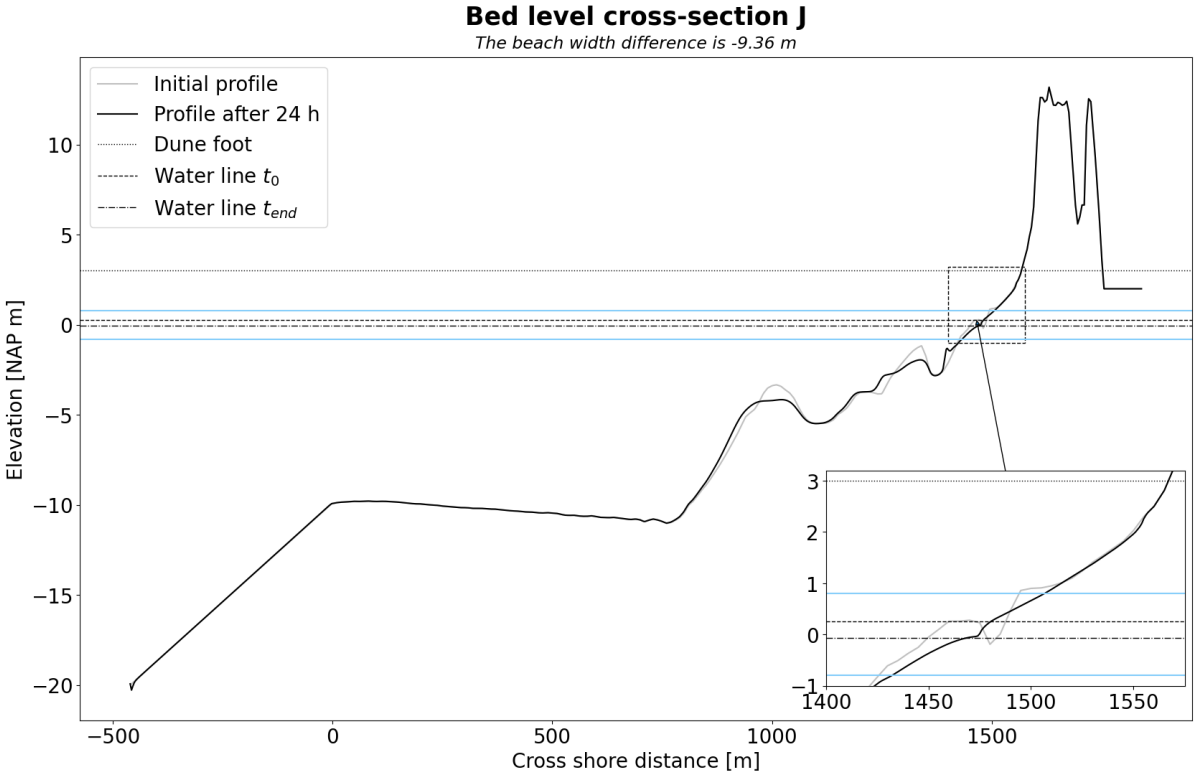

(c) Cross-section J.

Figure D.2: The cross-sections with the beach width differences for two times more curvature for the conditions of Run 2. Modified from XBeach output.

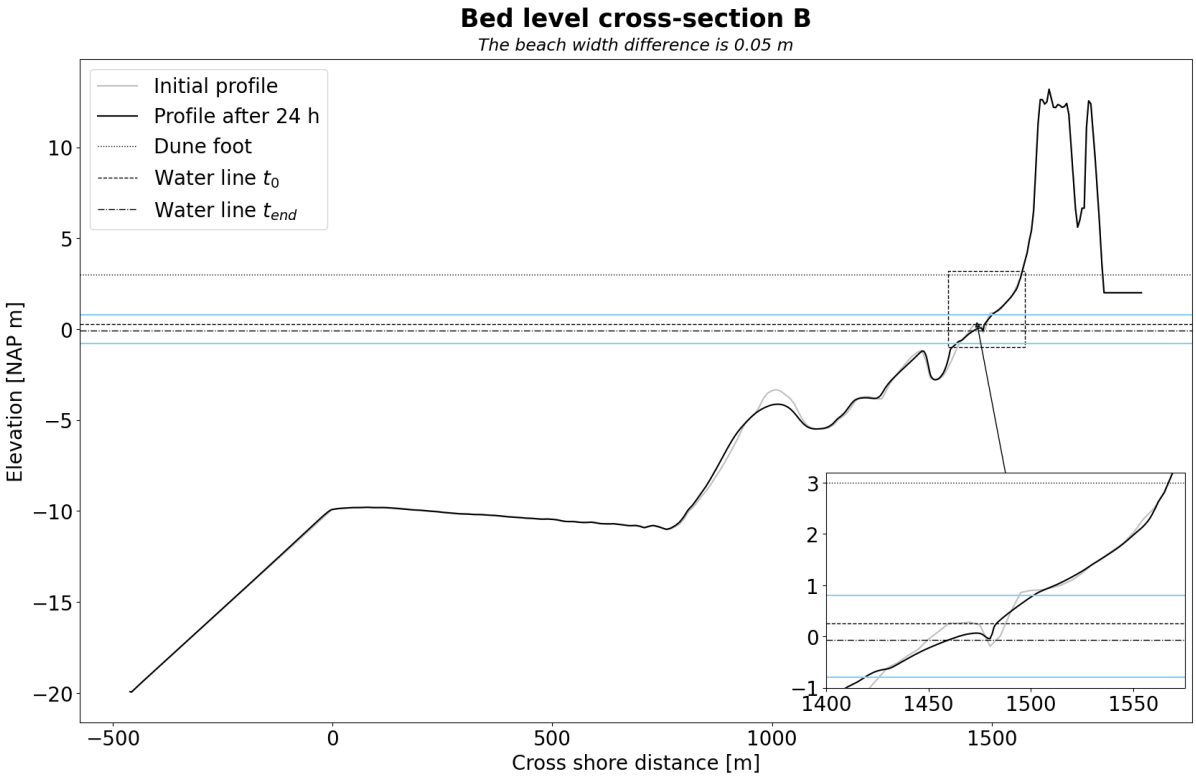

(a) Cross-section B.

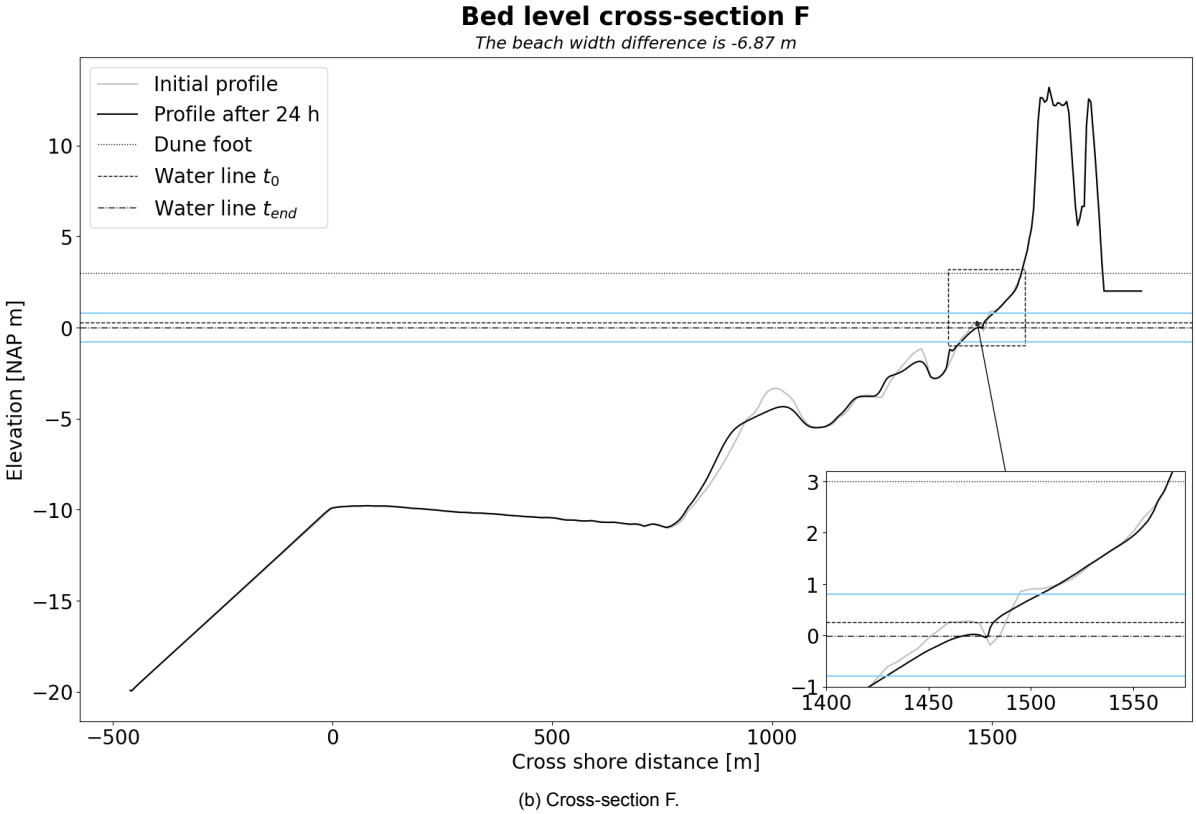

(b) Cross-section F.

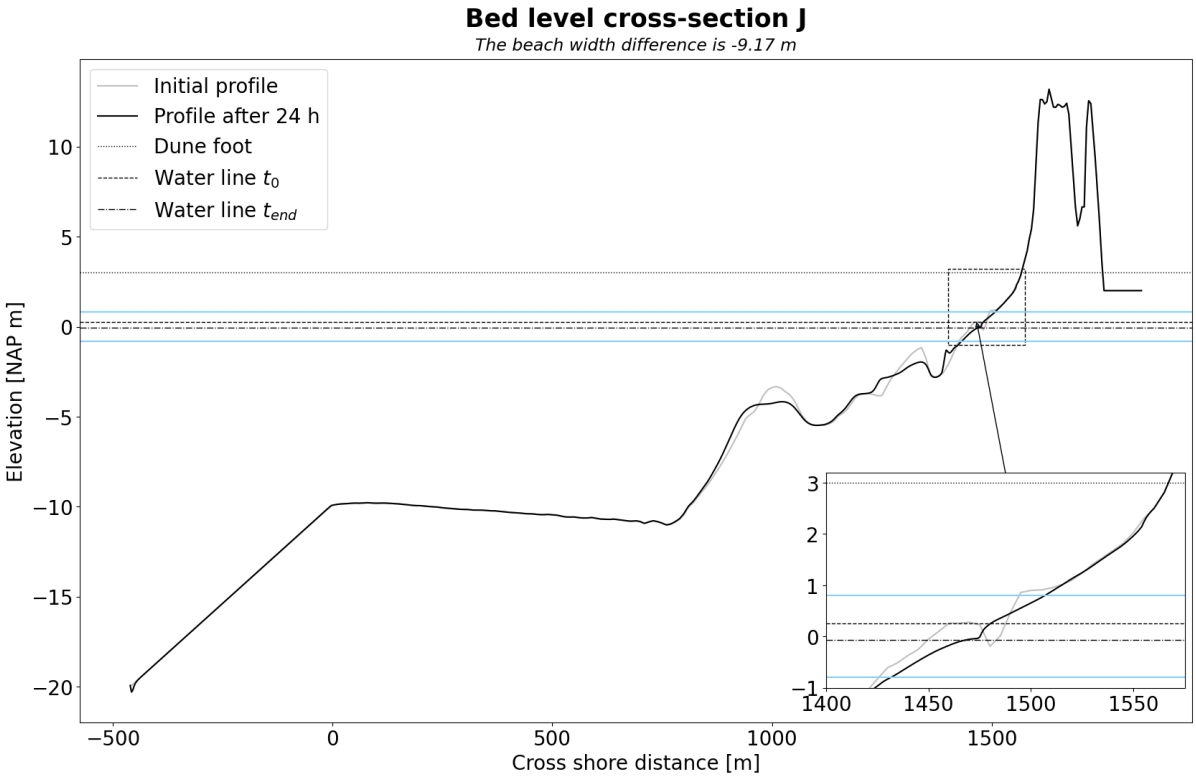

(c) Cross-section J.

Figure D.3: The cross-sections with the beach width differences for the normal curvature for the conditions of Run 2. Modified from XBeach output.

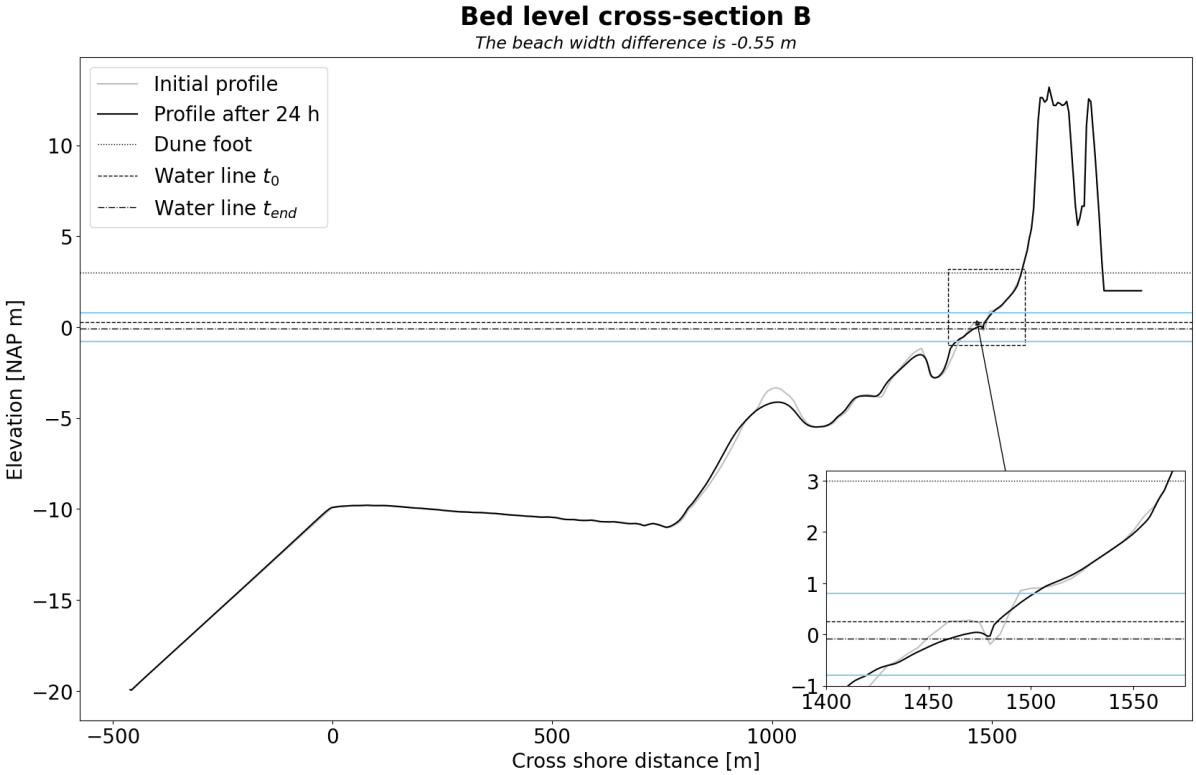

(a) Cross-section B.

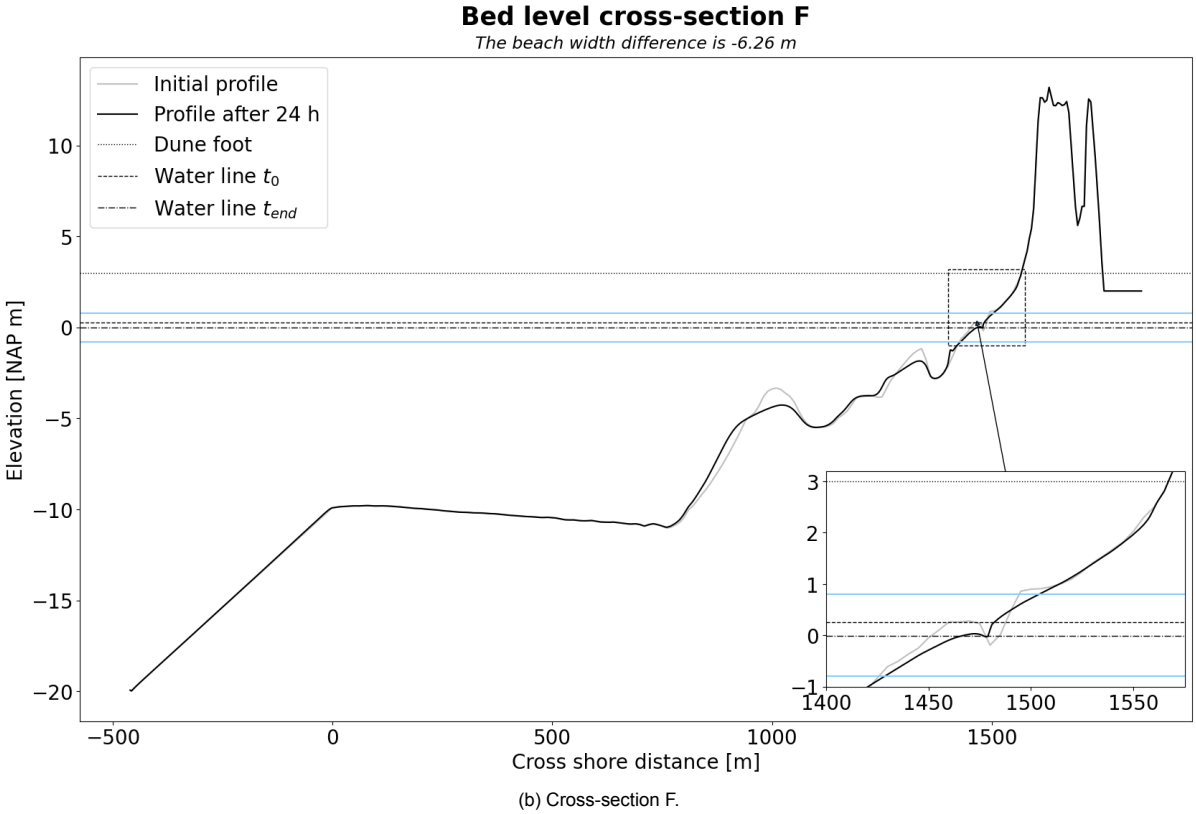

(b) Cross-section F.

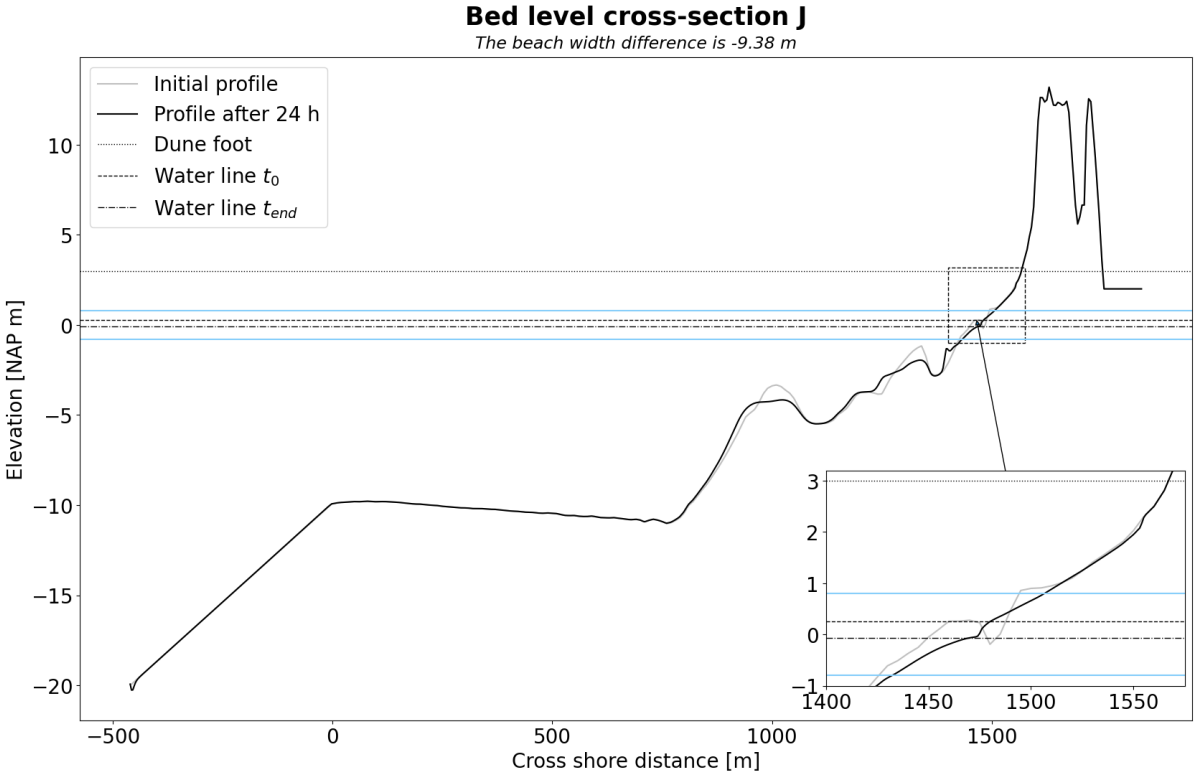

(c) Cross-section J.

Figure D.4: The cross-sections with the beach width differences for two times less curvature for the conditions of Run 2. Modified from XBeach output.

D.2. Difference between stationary mode and surfbeat mode

To investigate the differences between stationary mode and surfbeat mode, only the situation with twice the curvature is considered. This situation is compared with the results of twice the curvature from Section 5.2. To compare the results, the same transects are considered.

The erosion and sedimentation pattern from Figure D.5 shows that the maximum erosion and sedimentation in the stationary mode is much lower than in the surfbeat mode (Figure D.1. The location where most changes occur does not differ from each other, since in both cases most erosion occurs at the level of maximum curvature.

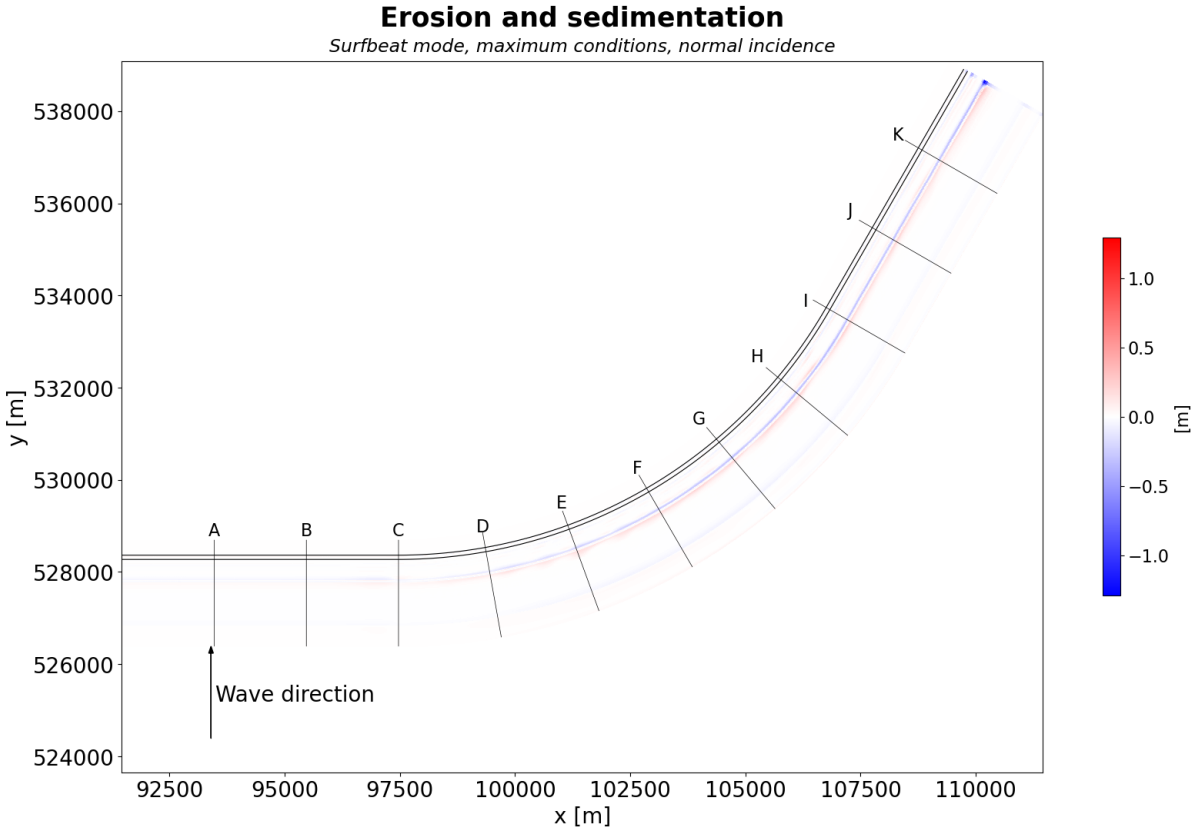

Figure D.5: The bed level difference for the conditions of Run 3. The blue colours indicate erosion and the red colours indicate sedimentation. Modified from XBeach output.

In the figures below in Figure D.6, the same three transects are shown as in Section D.1.

The first and last transects are transects on the straight part before and after the curvature while the middle plot is the transect in the middle of the curvature. The beach width differences between the different strengths in curvatures do not differ much from each other. The purpose of the transects is to examine where the erosion occurs and not to examine the gradient of the differences in beach width as previously examined in Chapter 5.

The largest change in beach width for all transects occurs at an alongshore distance of 1,460 m. At this location, there is a berm present in the initial situation which has flattened out as a result of erosion at the end of the simulation. It can also be seen that the profile becomes steeper with less unevenness in transect J compared to the other transects.

Based on the cross-sections from Figure D.6, it can be concluded that the beach width decrease in the stationary mode is significantly smaller than for the surfbeat mode. Hardly any differences can be seen between the initial profile (grey) and the profile after the simulation (black) in the swash zone. Around an alongshore distance of 1,000 m, a small amount of erosion can be seen at the level of NAP - 5.0 m. Based on these figures, it can be concluded that the short waves hardly affect the surf zone and swash zone.

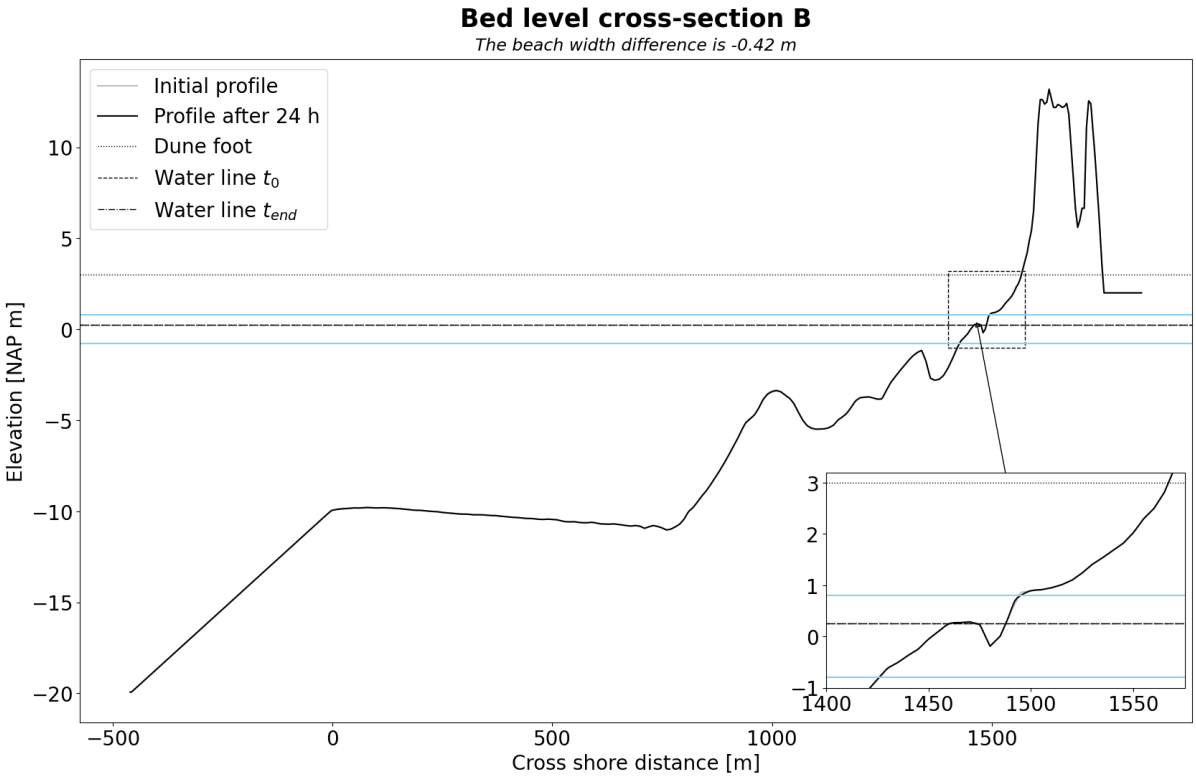

(a) Cross-section B.

(b) Cross-section F.

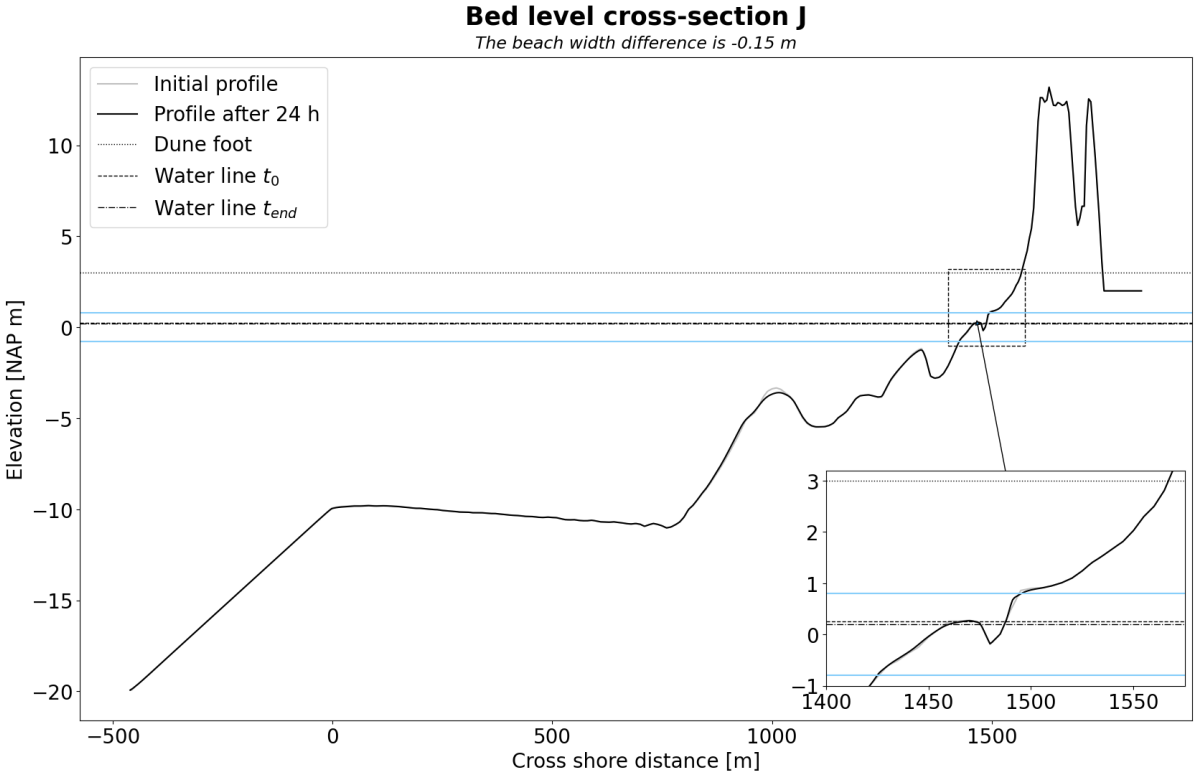

(c) Cross-section J.

Figure D.6: The cross-sections with the beach width differences for two times more curvature for the conditions of Run 3. Modified from XBeach output.

D.3. Sensitivity analysis wave conditions

In this section, the results are shown for different wave heights (and thus varying wave period and surge elevation) and wave angle of incidence.

In Figure D.7, Figure D.8 and Figure D.9 the results of the simulation in surfbeat mode with a wave angle of incidence equal to 0 degrees are shown. There is variation in wave height. The plot of Figure D.9 shows that there is almost no sediment transport for moderate storm conditions compared to the longshore sediment transport for maximum conditions. In addition, the figures show that wave height does not affect the patterns formed, that is, changes occur at the same location independently of wave height. Wave height does affect the magnitude of these changes or sediment transport because the higher the waves the more longshore sediment transport and changes in beach width and beach volume occur.

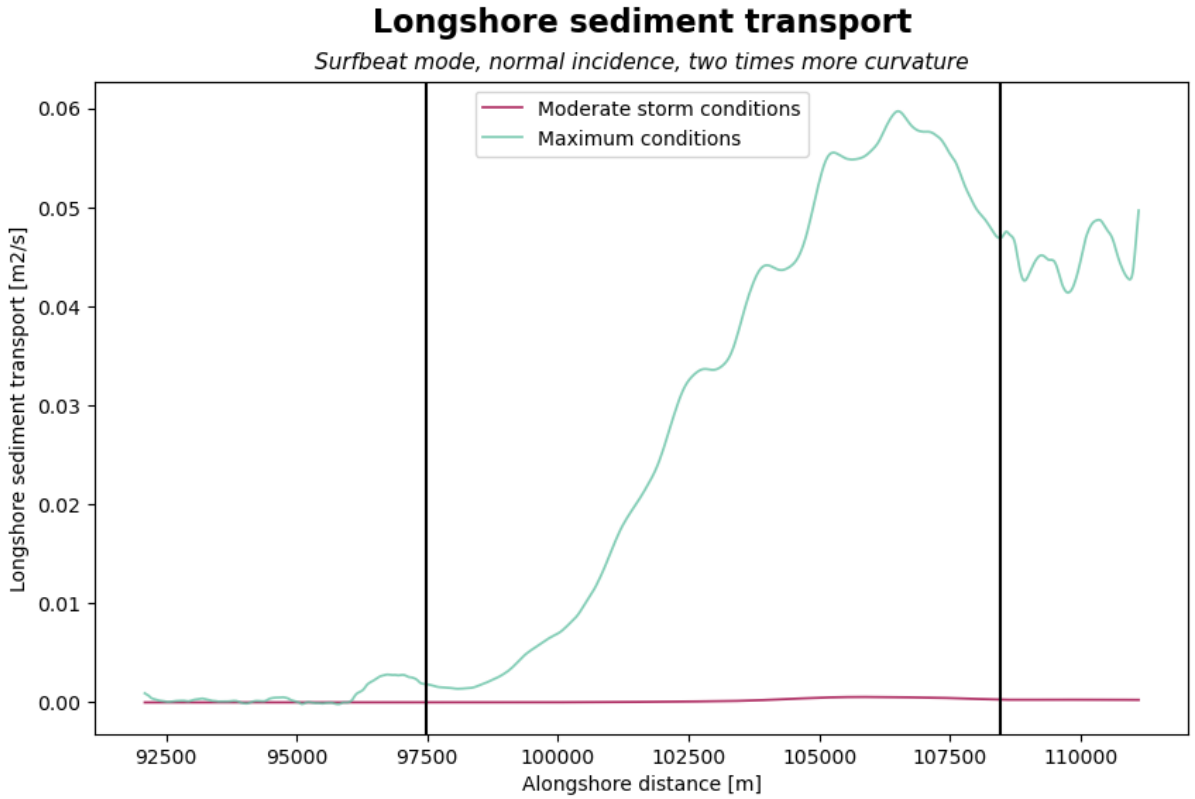

Figure D.7: Comparison of the longshore sediment transport between the different wave conditions. The simulation is performed in the surfbeat mode with a wave angle of incidence of 0 degrees. The black vertical lines indicate the start and end of the curvature. Modified from XBeach output.

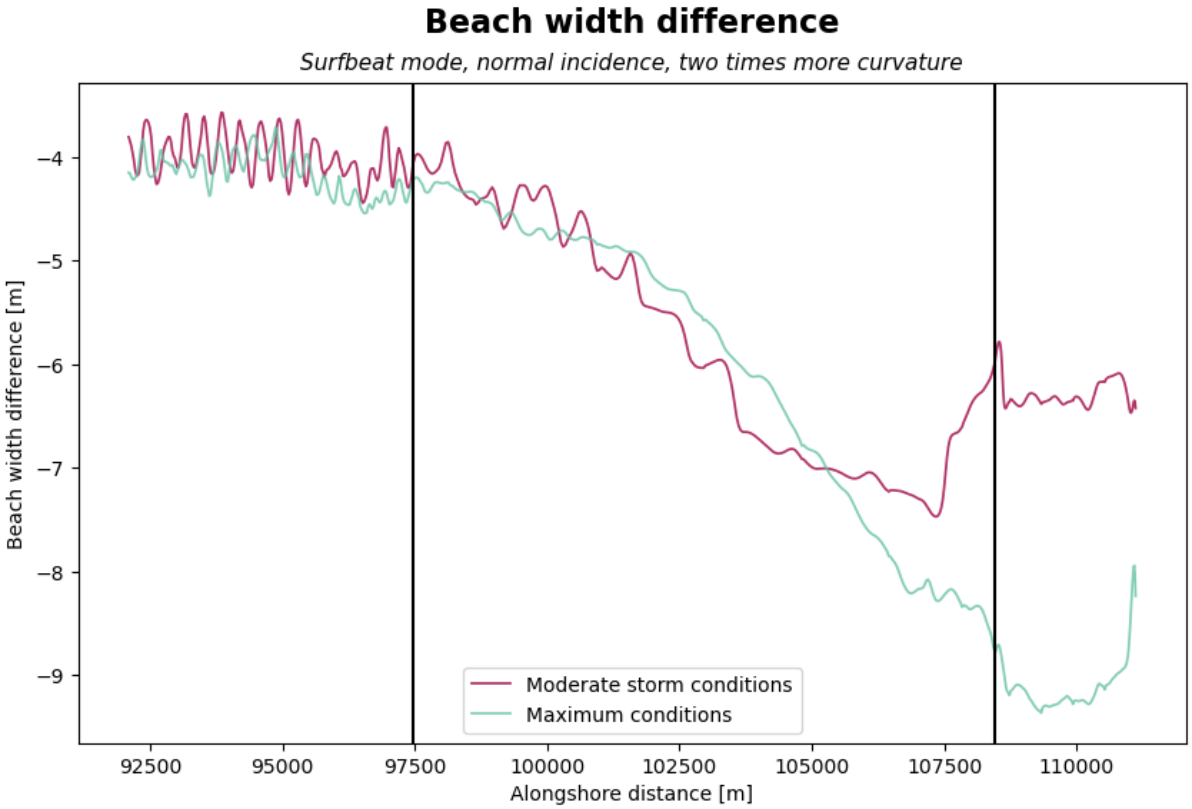

Figure D.8: Comparison of the beach width difference between the different wave conditions. The simulation is performed in the surfbeat mode with a wave angle of incidence of 0 degrees. The black vertical lines indicate the start and end of the curvature. Modified from XBeach output.

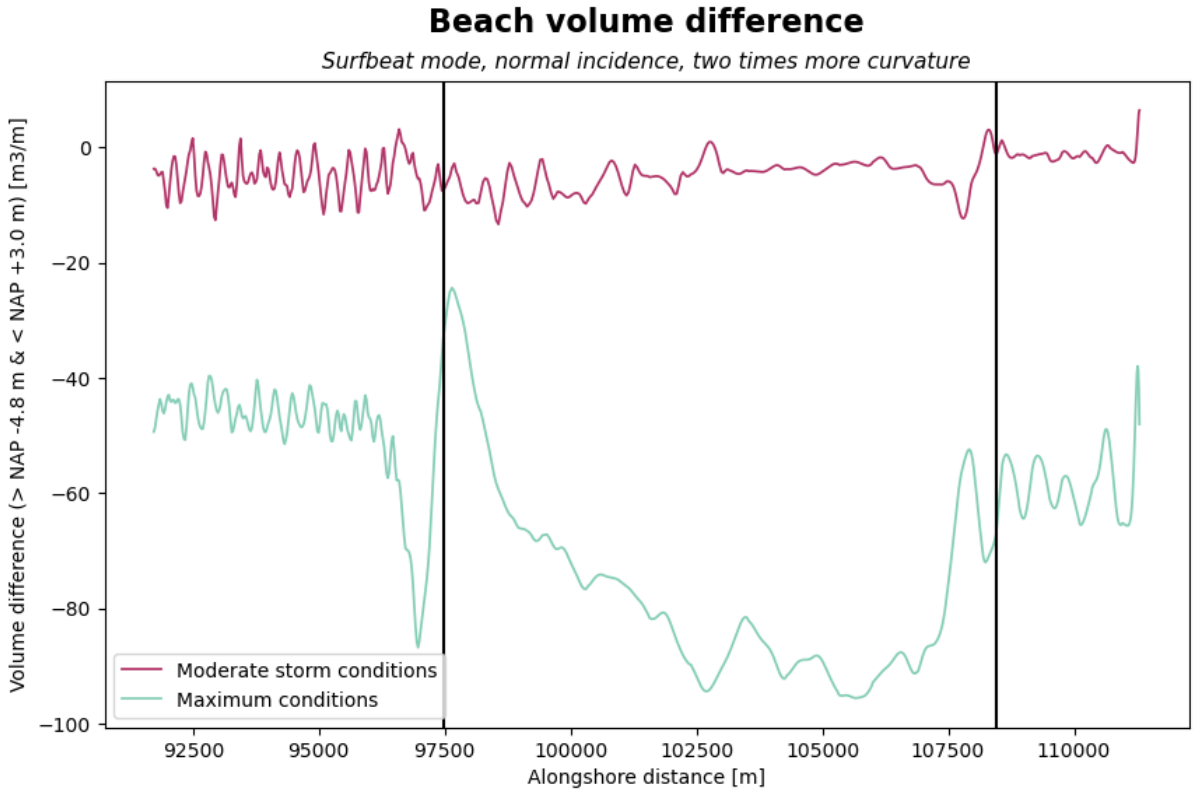

Figure D.9: Comparison of the beach volume difference between the different wave conditions. The simulation is performed in the surfbeat mode with a wave angle of incidence of 0 degrees. The black vertical lines indicate the start and end of the curvature. Modified from XBeach output.

In the three figures below, Figure D.10 to Figure D.12, the influence of the wave angle of incidence is shown for the maximum conditions with the strongest curvature.

The wave angle of incidence affects which location of the alongshore distance the largest changes occur. The figures show that no sediment transport occurs on the straight part before the curvature at an angle of incidence of 0 degrees while it occurs when the angle of incidence is equal to 45 degrees. It also follows that few changes occur for coastal curvature at a wave angle of incidence of 0 degrees while these changes in beach width and beach volume do occur at a wave angle of incidence of 45 degrees.

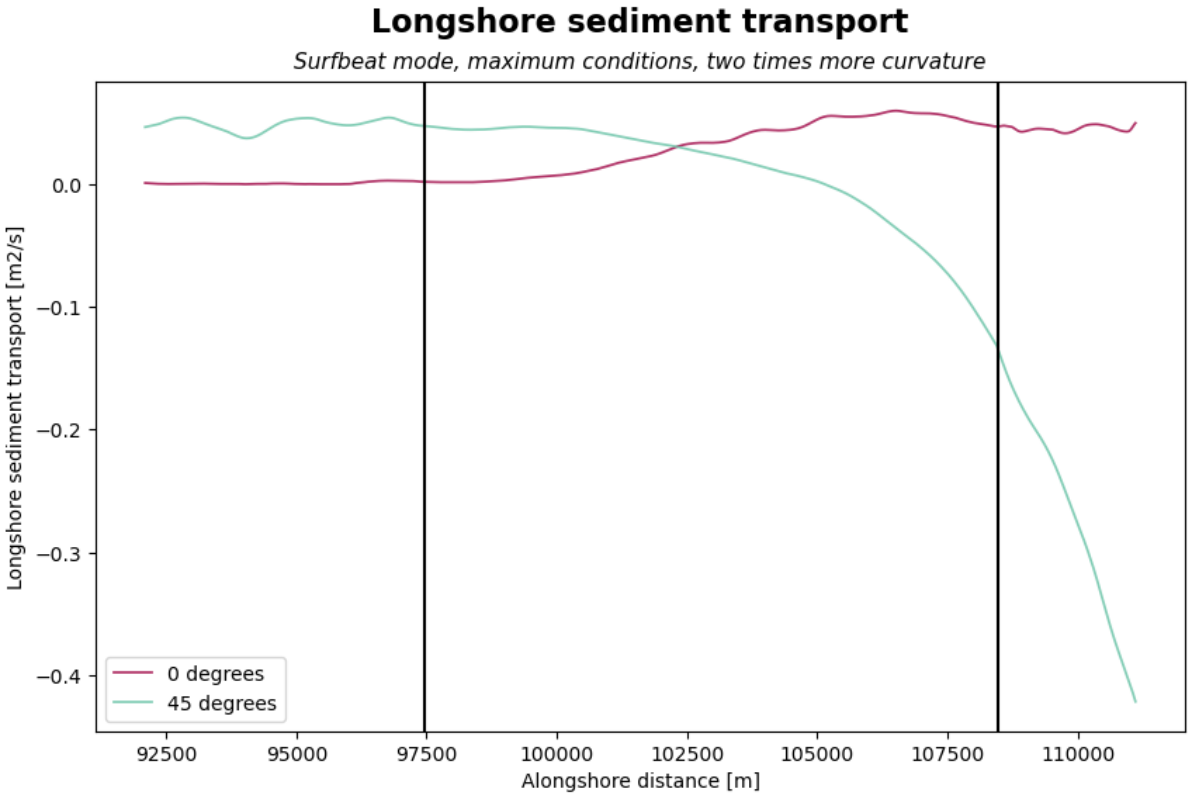

Figure D.10: Comparison of the longshore sediment transport between the different wave angles of incidence. The simulation is performed in the surfbeat mode with the maximum wave conditions. The black vertical lines indicate the start and end of the curvature. Modified from XBeach output.

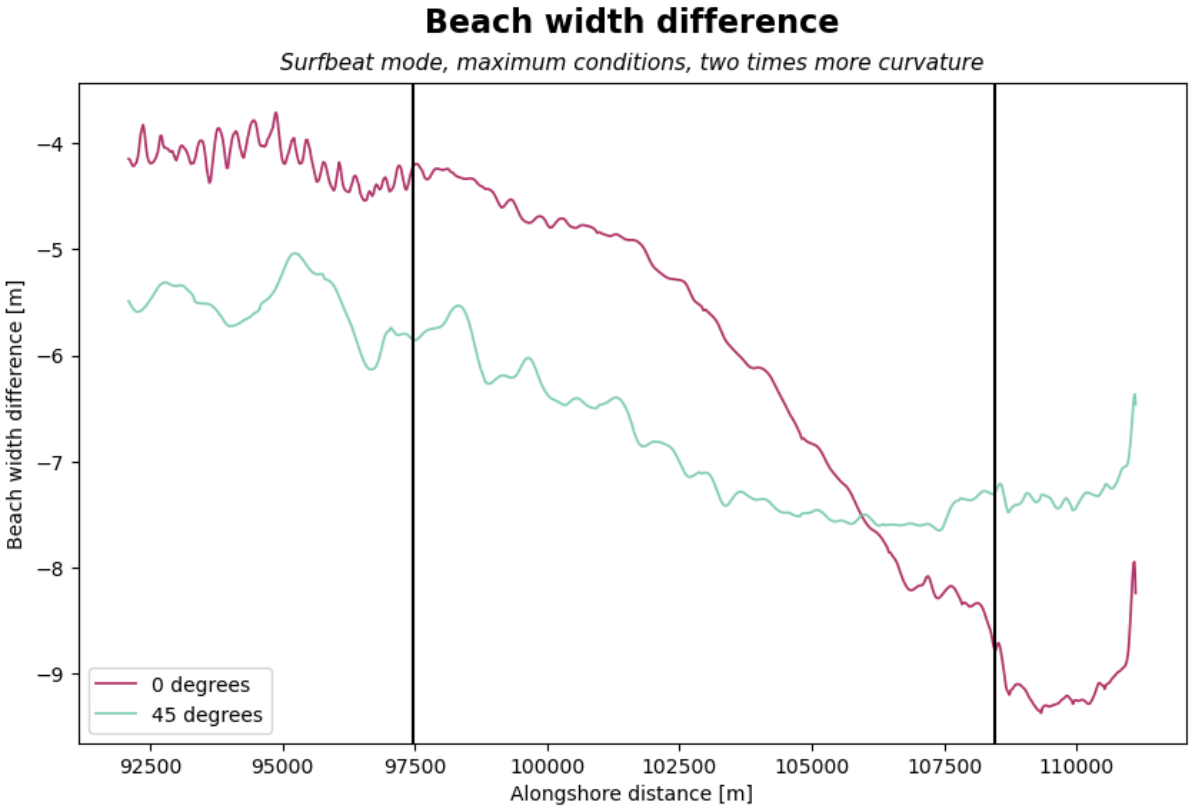

Figure D.11: Comparison of the beach width difference between the different wave angles of incidence. The simulation is performed in the surfbeat mode with the maximum wave conditions. The black vertical lines indicate the start and end of the curvature. Modified from XBeach output.

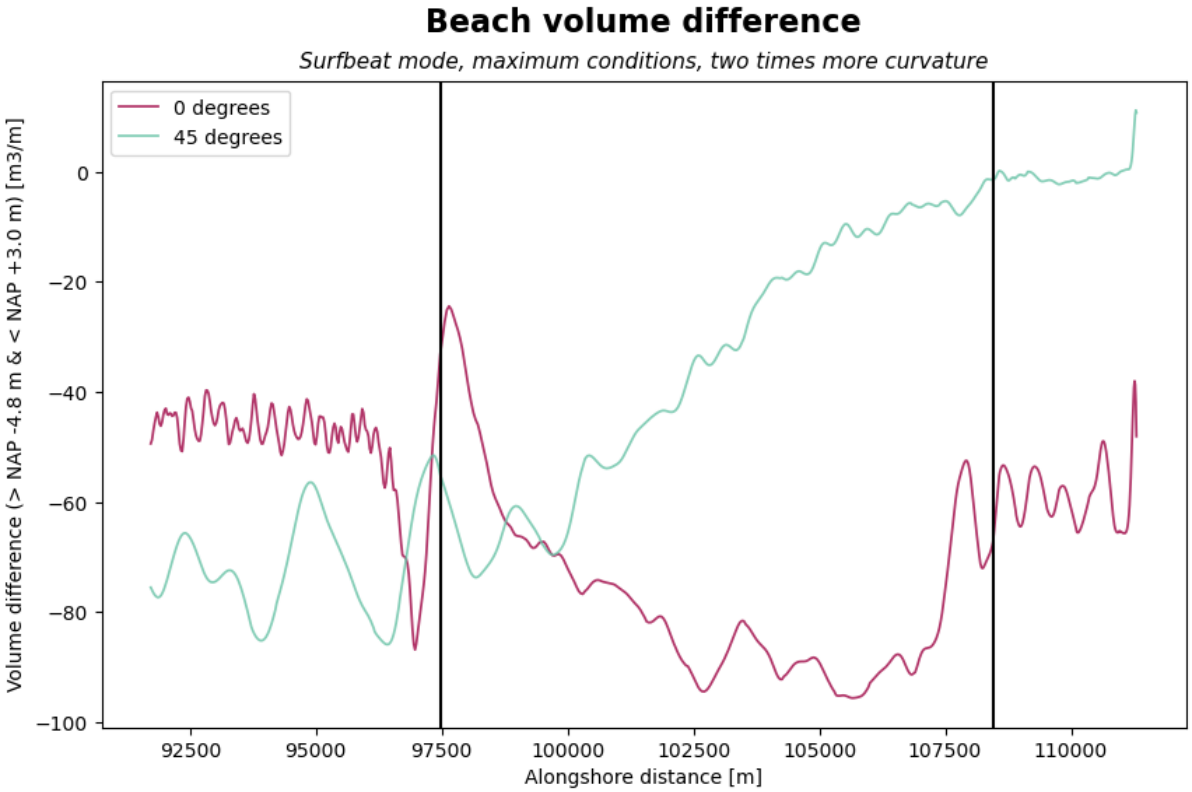

Figure D.12: Comparison of the beach volume difference between the different wave angles of incidence. The simulation is performed in the surfbeat mode with the maximum wave conditions. The black vertical lines indicate the start and end of the curvature. Modified from XBeach output.

D.4. Mean conditions, surf beat and obliquely incident waves

In addition to the runs mentioned above, a run was also performed with the average conditions. Initially, three wave conditions were simulated, namely average conditions, common conditions and maximum conditions. Using these three conditions, it was then possible to see how wave height affects the change in beach width. The input values for this simulation are shown in Table D.2.

Table D.2: Input parameters extra run.

Wave height [m]	1.31
Wave period [s]	4.5
Surge [m]	0.03
Wave direction [deg]	45
Wave model	Surf beat
Simulation time	8 days

In the figure below, Figure D.13, the decrease in beach width for all three wave conditions is plotted. The y-axis shows the decrease in beach width in the number of metres per hour in order to make a good comparison. This is because the simulation time for the average conditions is eight times longer than the simulation time for the maximum conditions. Based on this, the beach width decrease for the average conditions may be larger than that for the maximum conditions, while per hour the maximum conditions may have more influence.

The figure shows that the beach width change for the average conditions is almost zero compared to the other wave conditions. It was therefore chosen in the sequel to look only at these two conditions and disregard the average wave conditions.

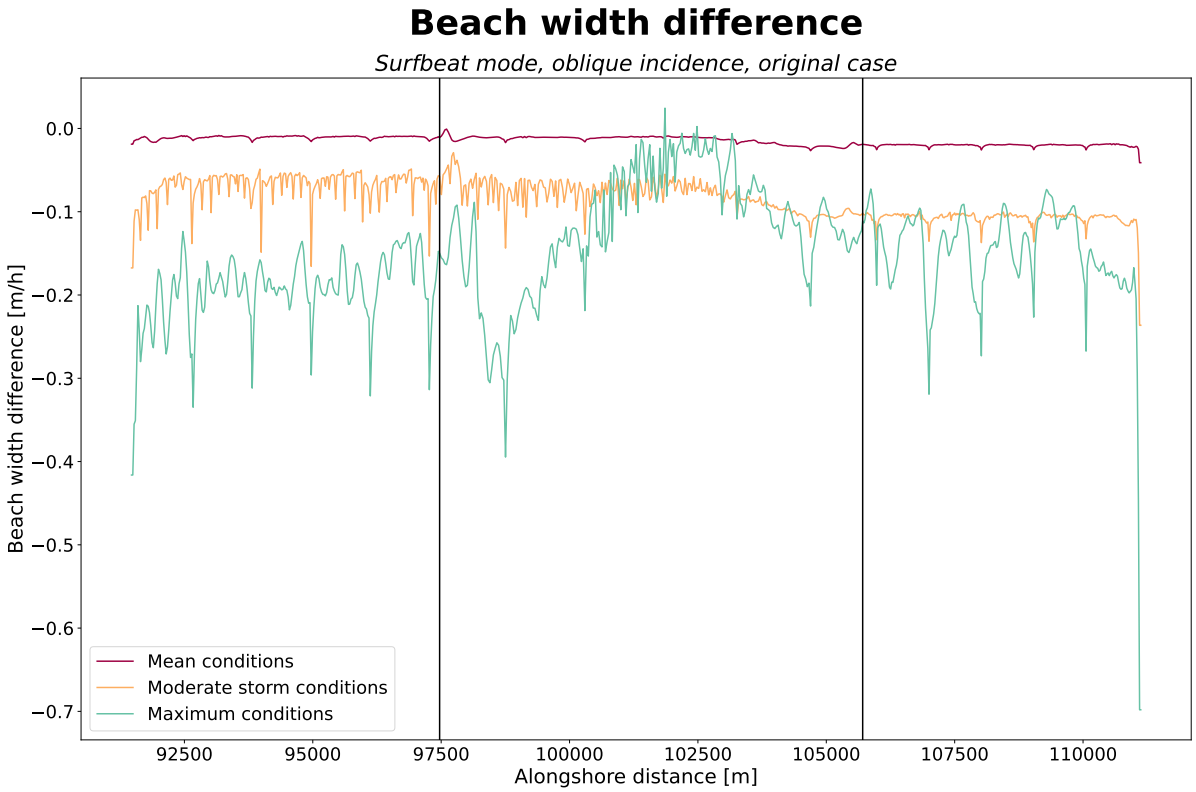

Figure D.13: The beach width difference for all three conditions. Modified from XBeach output.

E

Results XBeach model of the Hondsbossche Dunes

This appendix provides the extended results of the model of the HD. In this appendix, for each result, the comparison is made with the measurements of the JARKUS data to see how the XBeach model performs compared to the measured data, so a validation of the model is performed. If it is found that hardly any differences arise in the results of the simulation and the measured data then it can be concluded that the model performs well.

Multiple simulations were run, namely a simulation taking 2015 as the first year and a simulation taking 2016 as the first year. By taking 2016 as the first year, the initial effects that arise after the nourishment is implemented have disappeared. If it turns out that there are large differences in the results of the simulation and the measurements in 2015 then this may affect the results of the simulation in subsequent years. The resulting profile at the end of 2015 is used as the starting profile in 2016.

E.1. Correlation between the model and the measurements

This section discusses the correlation between beach width change based on the JARKUS measurements and the beach width change based on the outcome of the XBeach model. Herein, a distinction is made between the results with 2015 as the first year and the results with 2016 as the first year.

E.1.1. First year: 2015

The figures below show the correlation in the case where the 2015 JARKUS data was taken as the first year of the simulation. Thus, this simulation takes into account the initial effects that take place as a result of nourishment implementation.

The figures below, Figure E.1, show that the correlation between the measured beach width change and the modelled beach width change is low (r^2 = 0.19) for the first year after the nourishment is implemented. This implies that the results from XBeach hardly match reality.

It is also noticeable that the correlation coefficient is the largest in the first year and then it decreases until r^2 = 0.00 in the year 2018-2019. In the last year, the correlation coefficient has increased, making the simulation predictions more consistent with reality. The final bathymetry in the first year after the simulation deviates a lot from the final bathymetry based on the measurements. As this deviation occurs and the final bathymetry is used for the following year, the differences between the measured values and the modelled beach width change become larger causing the correlation coefficient to decrease.

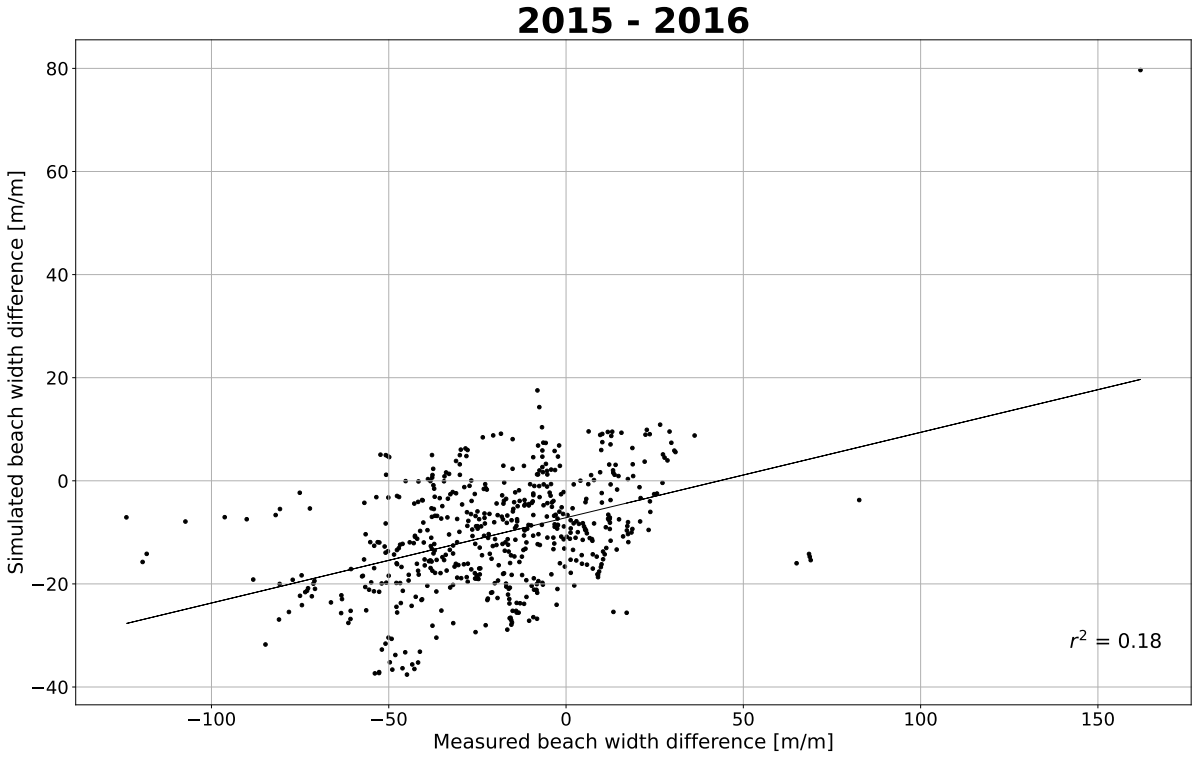
2015 - 2016
Simulated beach width difference [m/m]
Measured beach width difference [m/m]
r^2 = 0.18

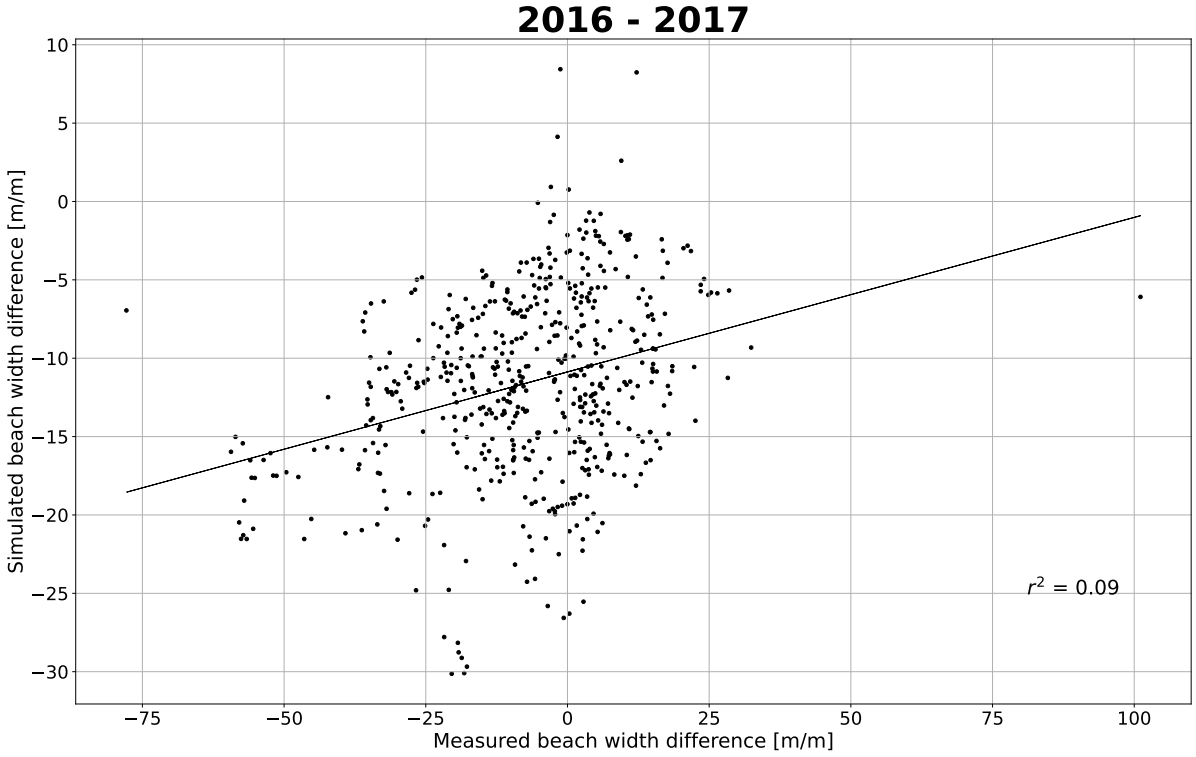
2016 - 2017
Simulated beach width difference [m/m]
Measured beach width difference [m/m]
r^2 = 0.09

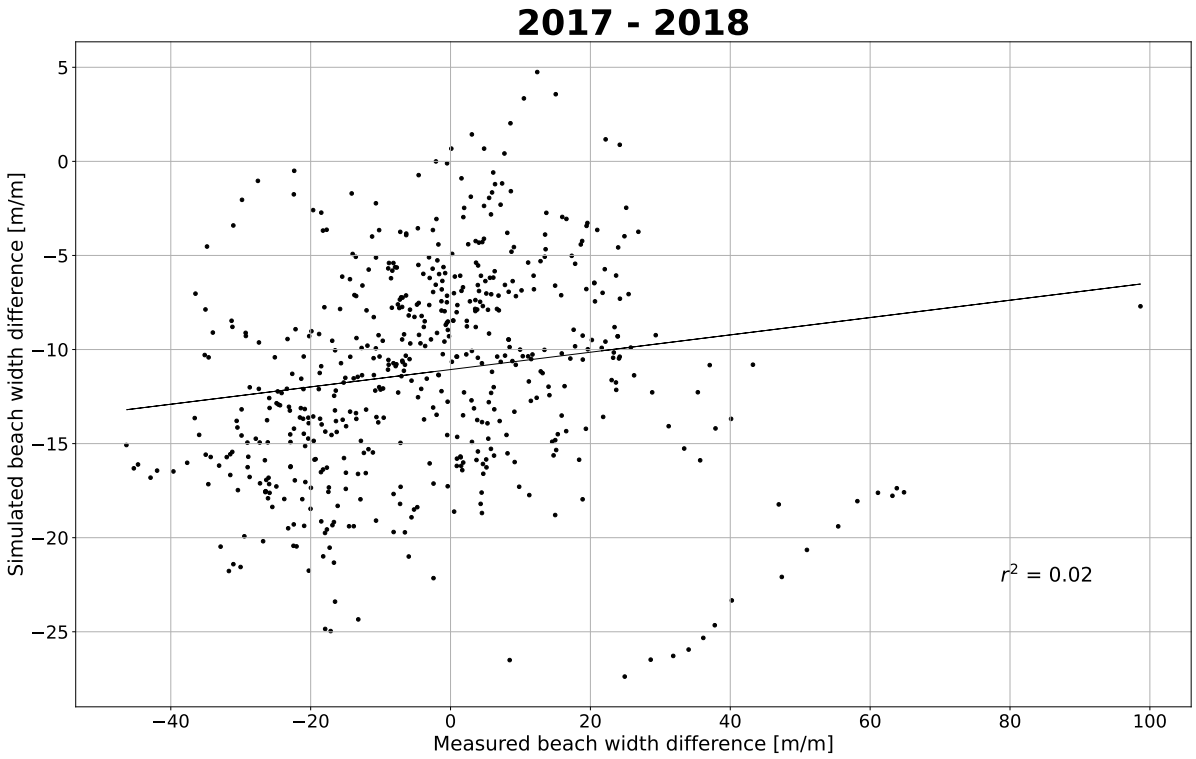

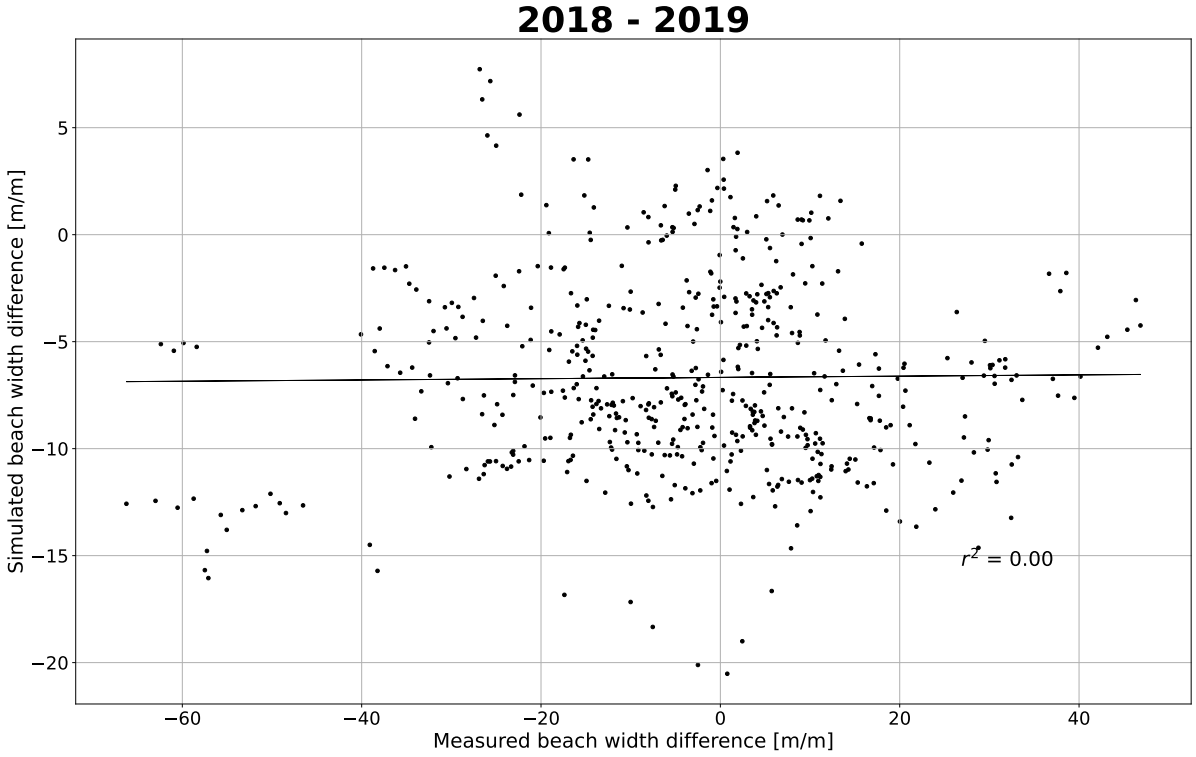

E.1.2. First year: 2016

In these simulations, not 2015 but 2016 was applied as the first year in the XBeach simulation. This shows that in the first year, the correlation coefficient is higher (r^2 = 0.40) than when 2015 is used as the first year. However, the correlation coefficients for subsequent years have the same order of magnitude as when 2015 is used. The measured beach width changes are higher than the modelled beach widths where there is a large increase in beach width based on the measurements.

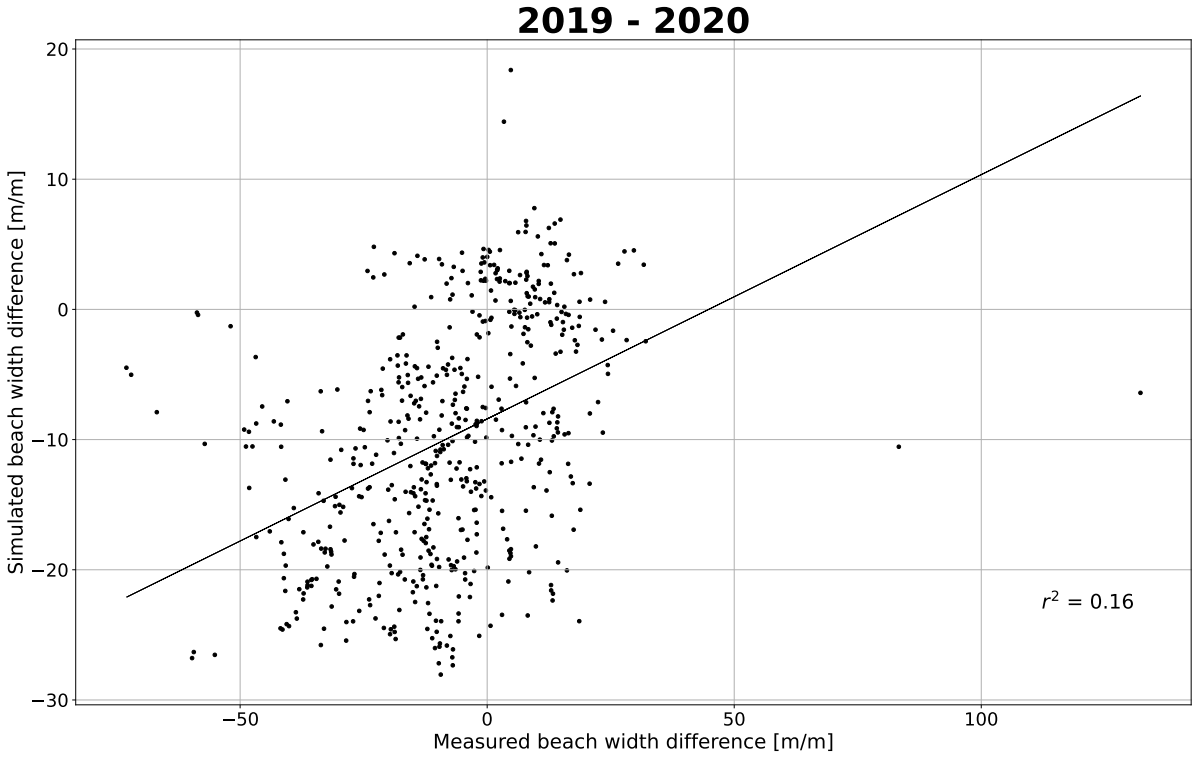

Figure E.1: The correlation between the beach width difference obtained from the simulations from XBeach and the measurements.

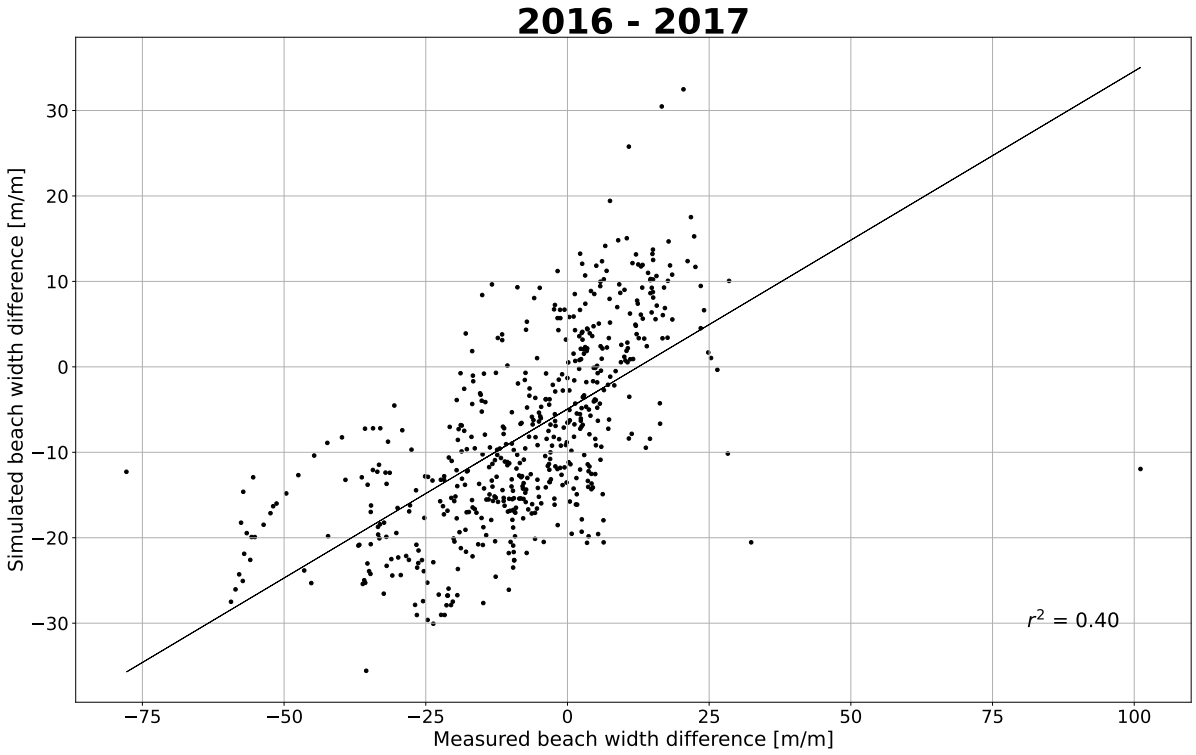

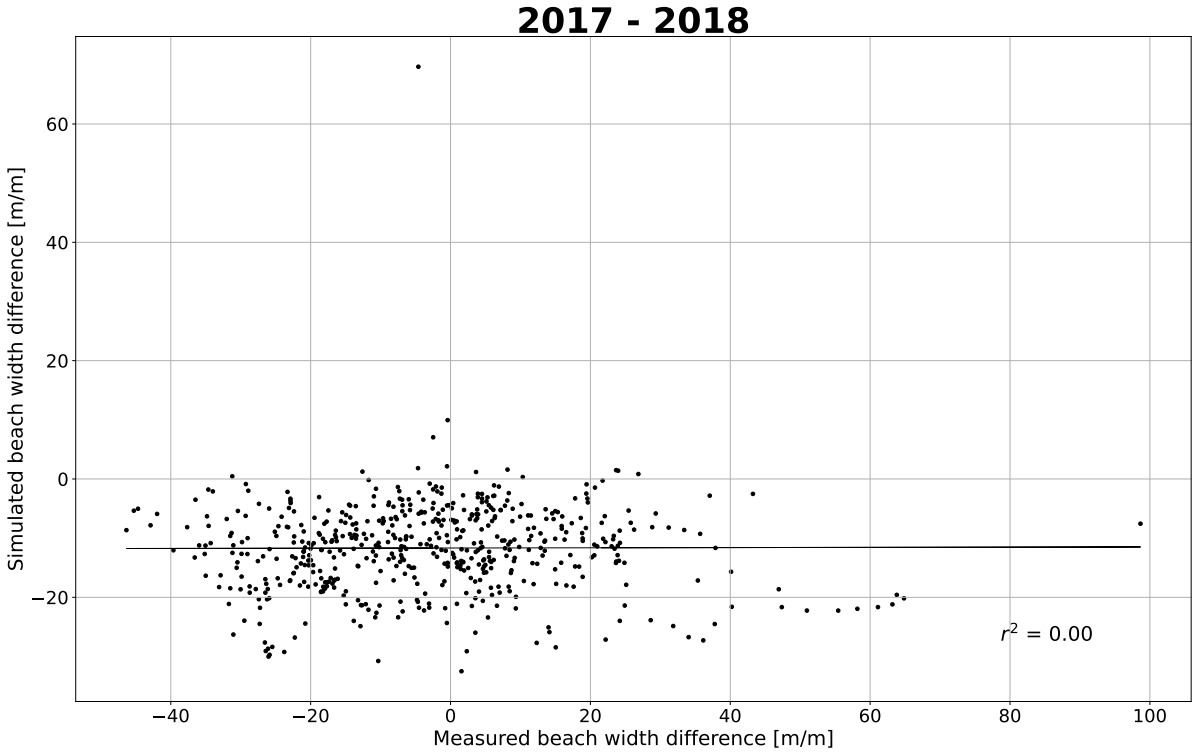
2017 - 2018
Simulated beach width difference [m/m]
Measured beach width difference [m/m]
r^2 = 0.00

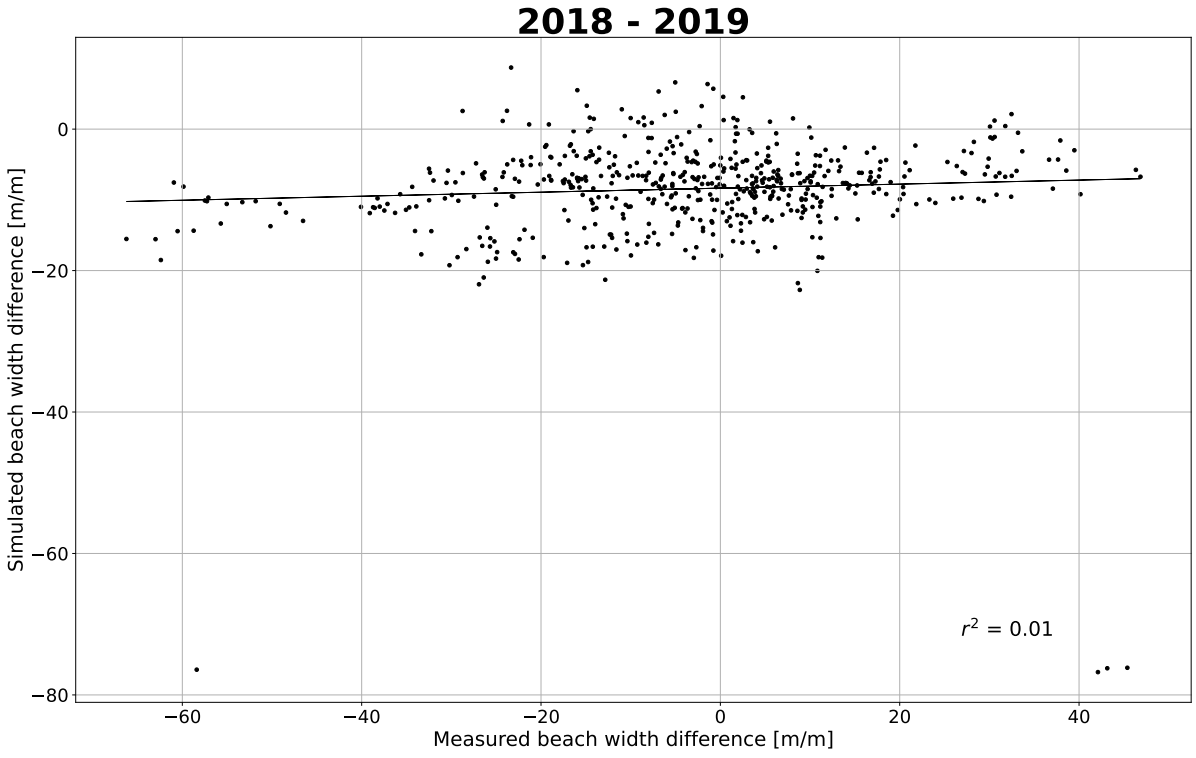
2018 - 2019
Simulated beach width difference [m/m]
Measured beach width difference [m/m]
r^2 = 0.01

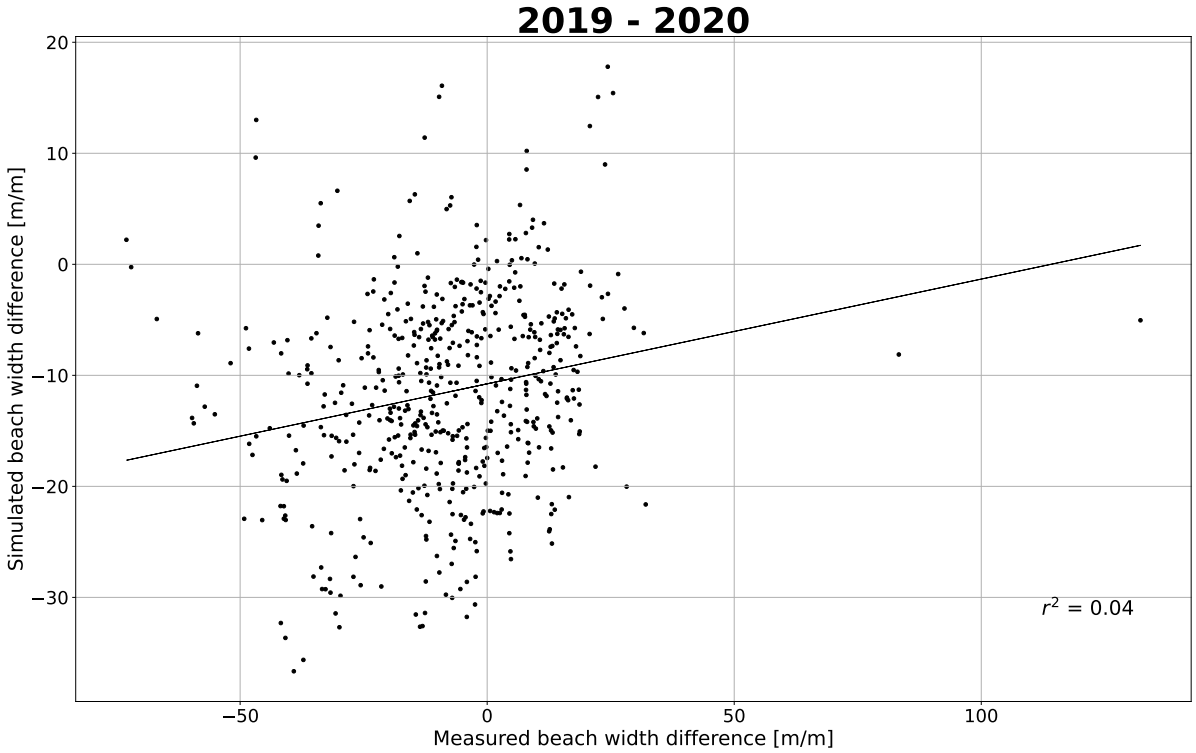

Figure E.2: The correlation between the beach width difference obtained from the simulations from XBeach and the measurements.

E.2. Bed level changes

This section shows the bed level changes of both the measured data, left and the modelled data, right.

The figure below, Figure E.3 shows that based on the predictions using the XBeach model, there is more erosion than what has been observed based on the measurements. Furthermore, according to the measurements, sedimentation occurs south of the HD around y = 5.800e6 m.

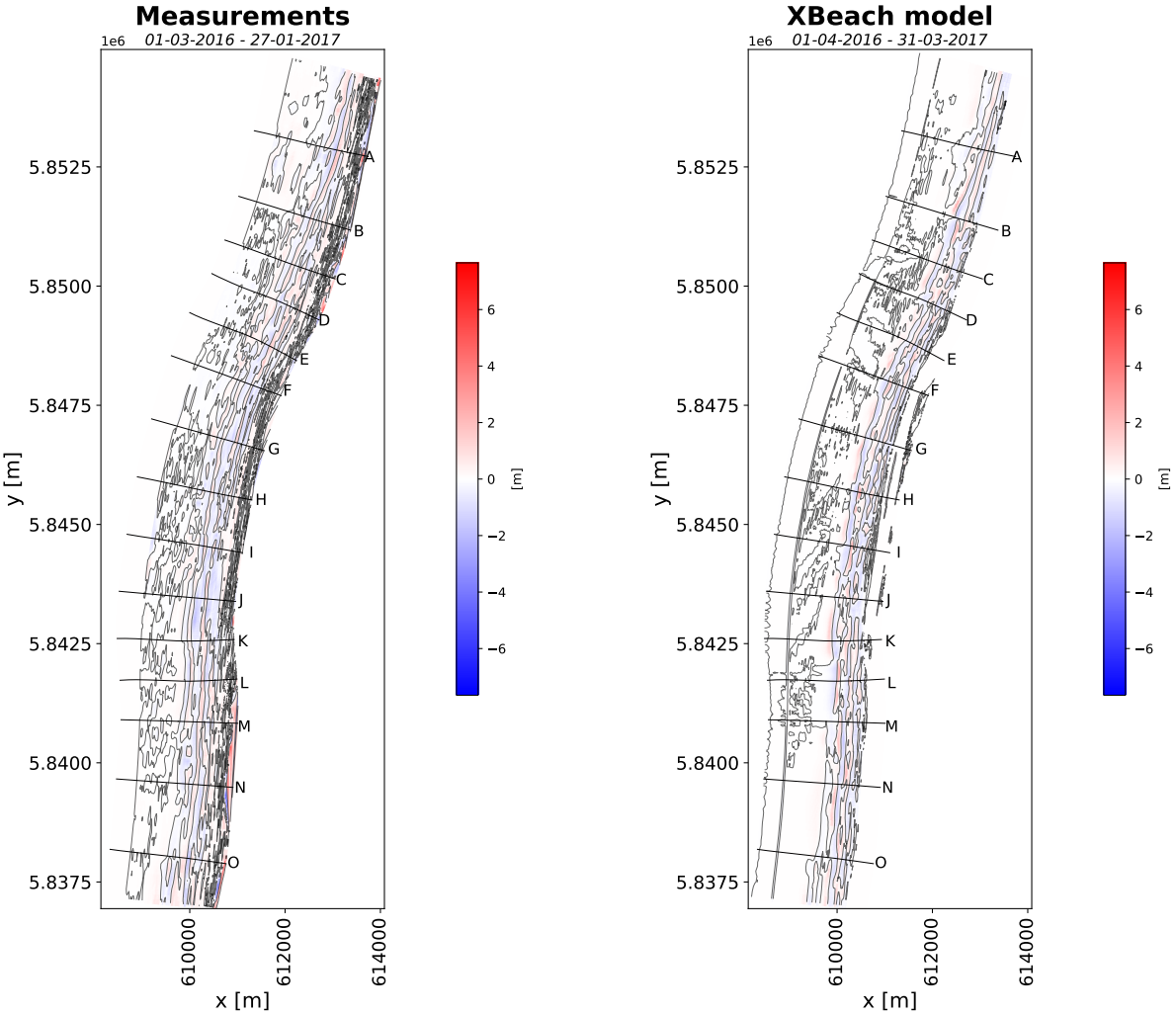

(a) Measurements

(b) Output model

Figure E.3: The results from 2016 to 2017. Modified from JARKUS data and XBeach output.

In the second year of the simulation, the measurements show a sedimentation hotspot south of the HD. This is the result of an additional nourishment that was implemented south of the HD. The extra nourishment that has been implemented has not been implemented in the model and therefore no sedimentation hotspot can be seen in the model result.

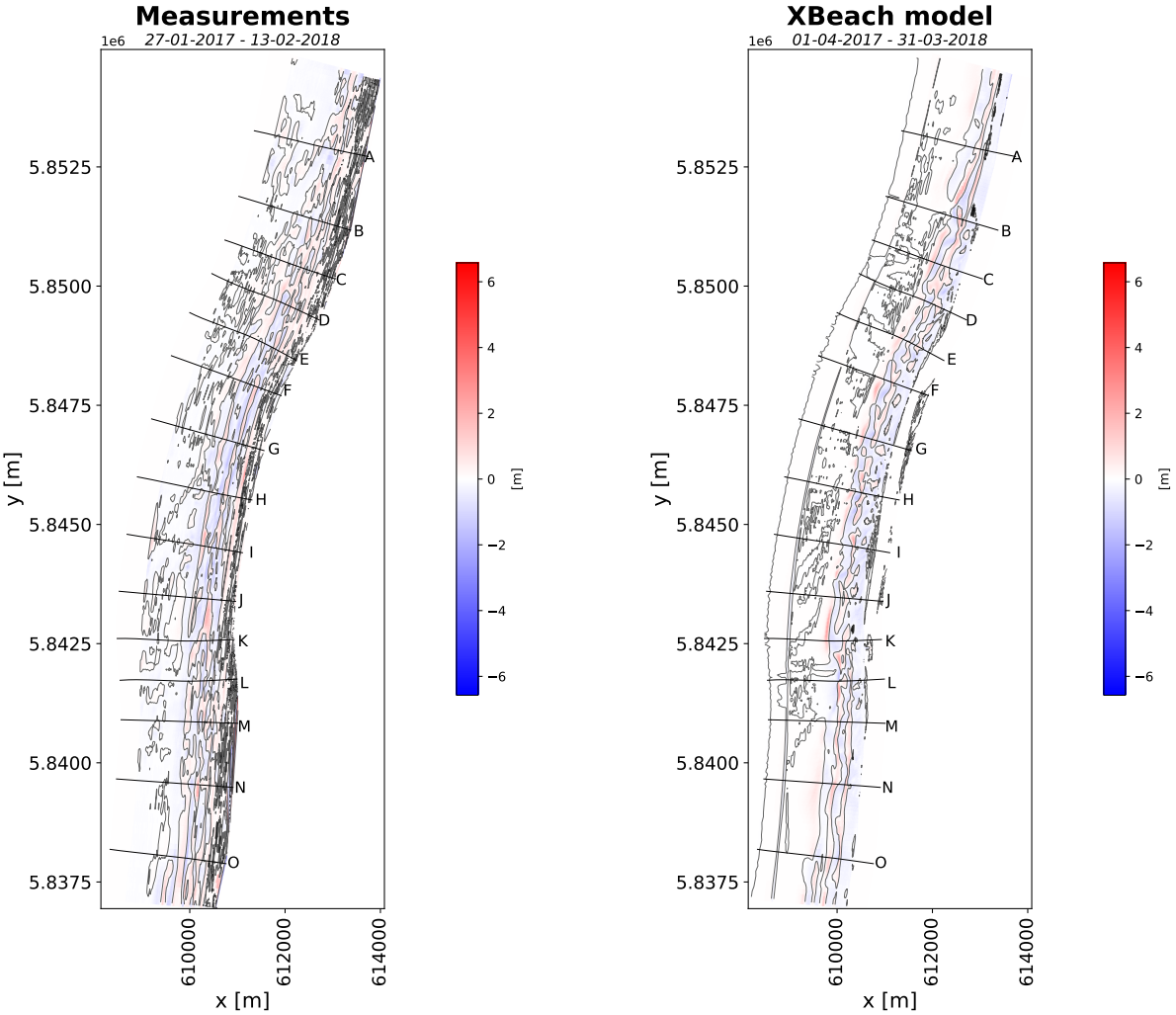

(a) Measurements (b) Output model

Figure E.4: The results from 2017 to 2018. Modified from JARKUS data and XBeach output.

In the fourth year after nourishment and the third year of simulation, the variations in the bed level for the measurements is larger than the variations in the bed level based on the XBeach model. Based on the measurements, there is some erosion at the south of the curvature between transects J and K.

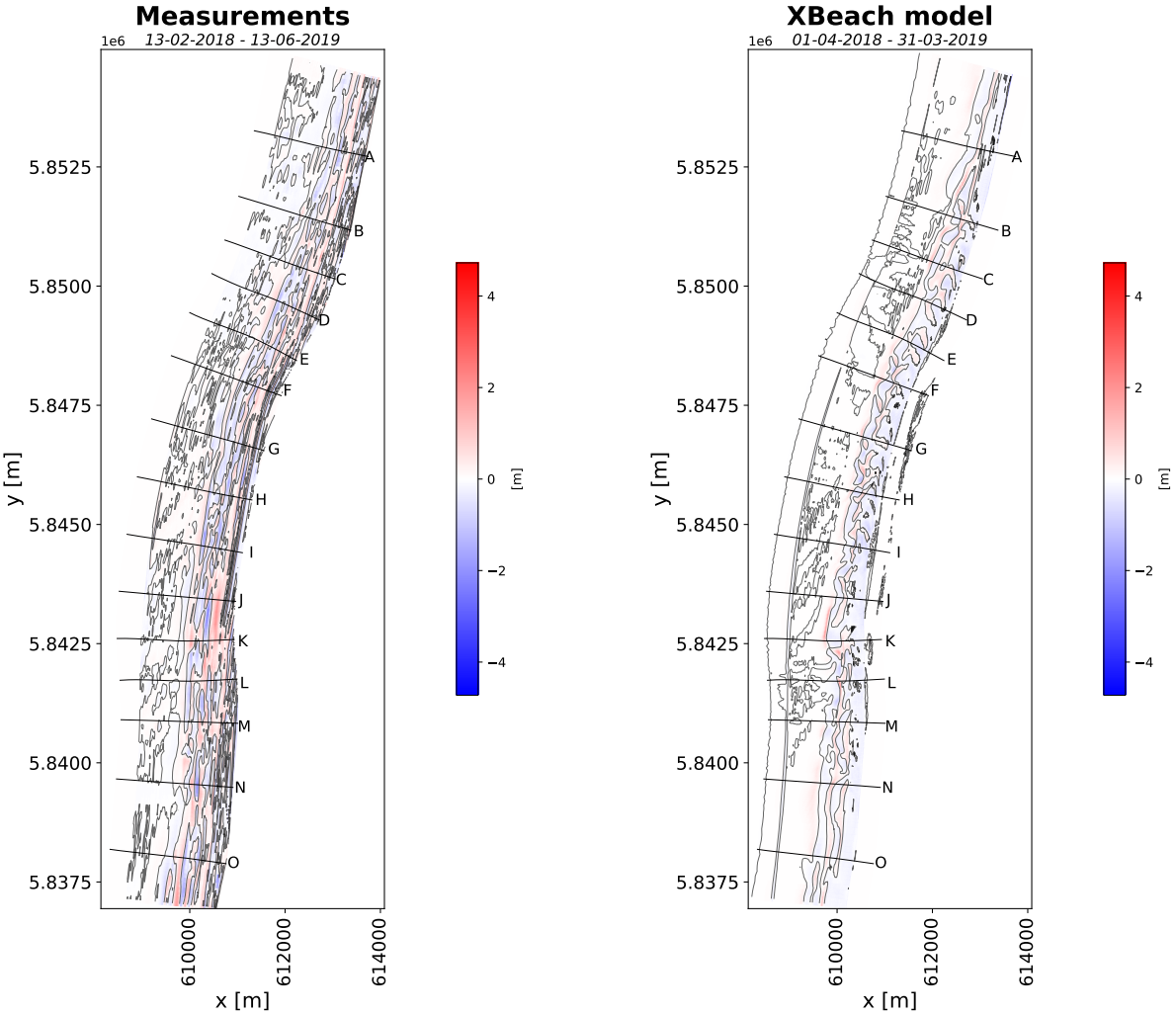

(a) Measurements

(b) Output model

Figure E.5: The results from 2018 to 2019. Modified from JARKUS data and XBeach output.

In the last year, the least changes occurred compared to the previous years. Based on the XBeach model, a larger decrease in bed level is expected than what was measured using the JARKUS data.

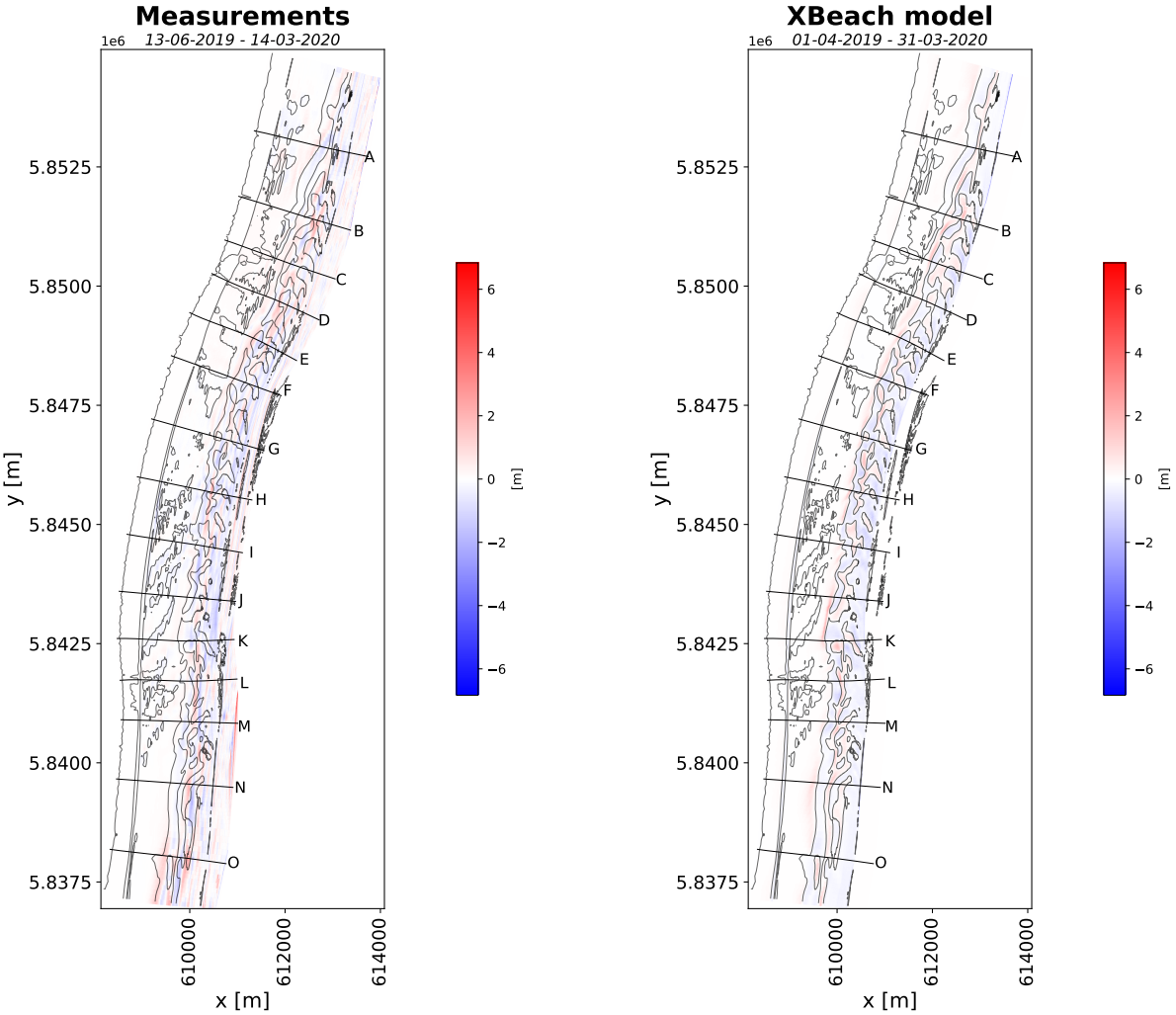

(a) Measurements

(b) Output model

Figure E.6: The results from 2019 to 2020. Modified from JARKUS data and XBeach output.

E.3. Beach width difference

This subsection shows the beach width differences in the alongshore direction. In these figures, the beginning and end of the curvature are indicated using black horizontal lines. In all the plots of the beach width difference large peaks can be seen around transect K. Transect K is a transect through a lagoon which has a major influence on the development of the beach width.

In the first year of the simulation, large similarities can be seen between the beach width change based on the measurements and based on the XBeach model. The locations where there is a decrease in beach width according to the measurements also show a decrease in beach width according to the predictions with XBeach.

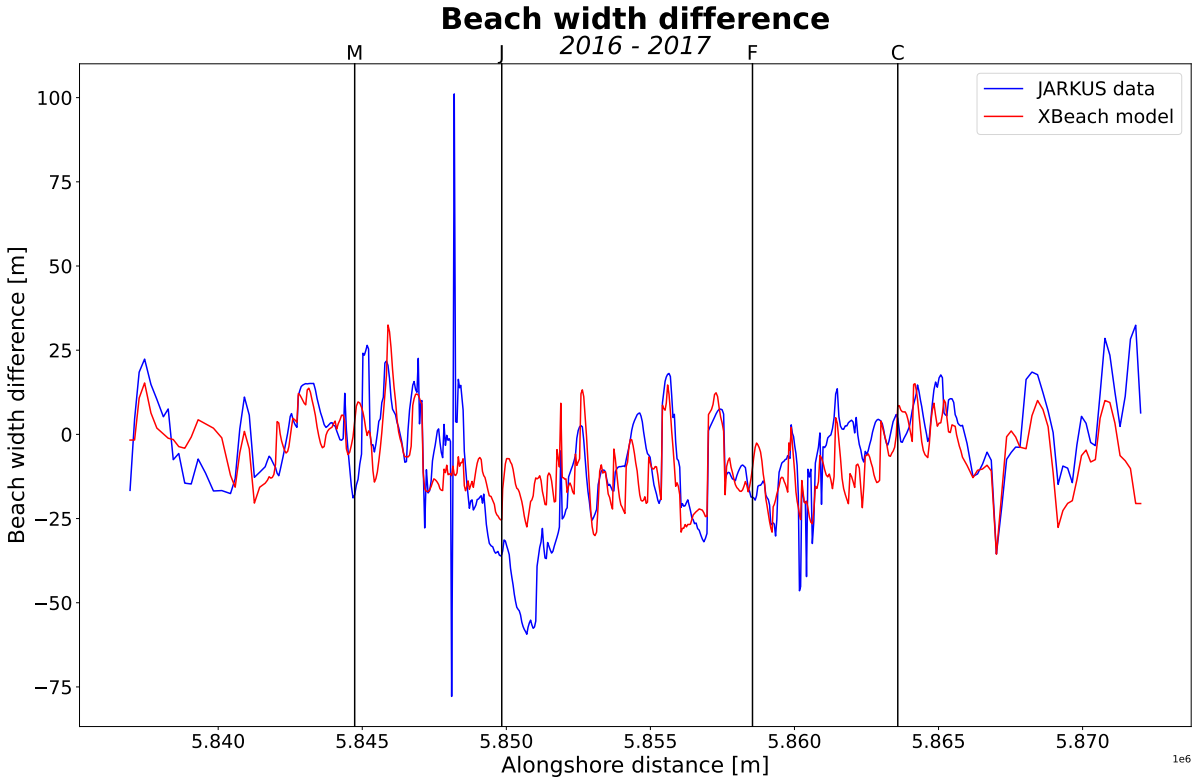

Figure E.7: Comparison between the results of the XBeach model and the measurements. These figures are the results of 2016 - 2017. The black vertical lines indicate the transects as indicated in the figures for the bed level change. A negative beach width difference means a reduction.

The difference between predictions and measurements increases in the second year of the simulation. Especially in the transects outside the curvature, i.e. outside transects C and M, large differences can be seen. Here, in general, according to the measurements, there is an increase in beach width while the beach width decreases according to the predictions of the XBeach model. In contrast, the predictions on the convex-shaped coast do agree well with the measurements.

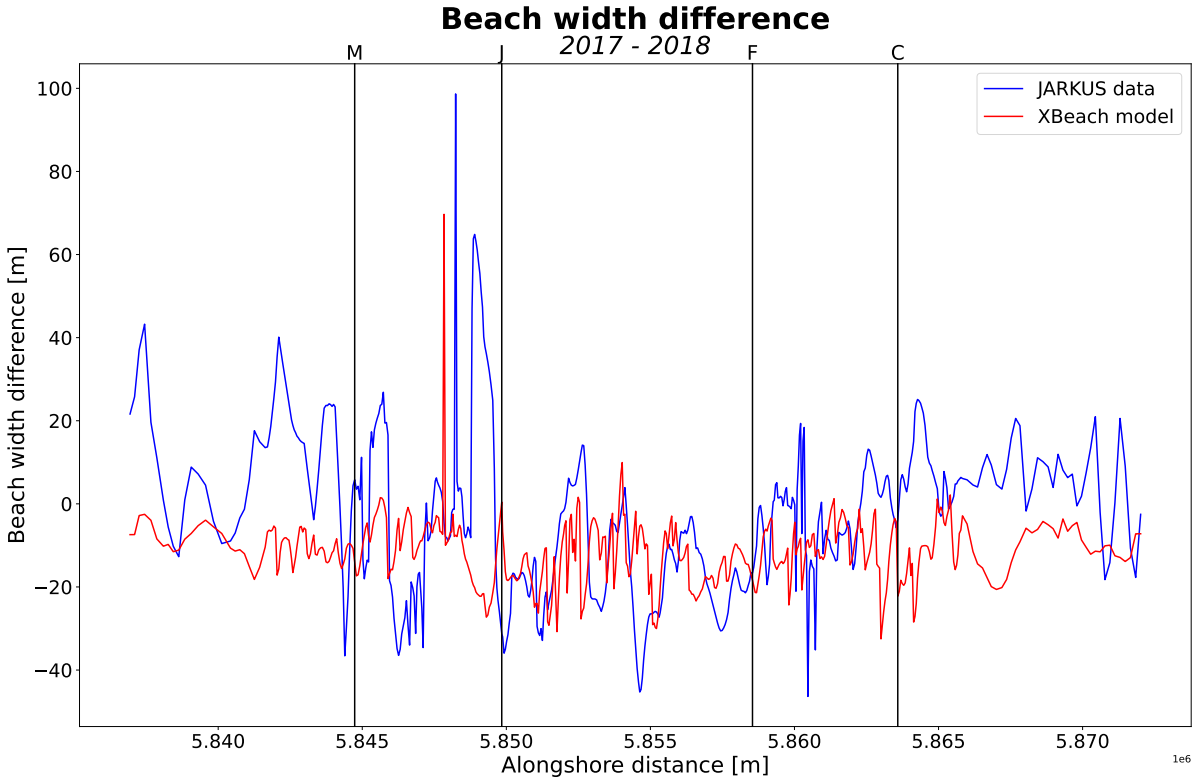

Figure E.8: Comparison between the results of the XBeach model and the measurements. These figures are the results of 2017 - 2018. The black vertical lines indicate the transects as indicated in the figures for the bed level change. A negative beach width difference means a reduction.

The measurements based on the JARKUS data do not match the predictions based on the XBeach model. The predictions show hardly any change in beach width while large variations can be seen in the measurements. Especially between transects J and M, there are large variations in the measurements that are not seen in the predictions. This can be explained by the additional nourishment implemented in 2018, which is included in the results of the measurements but not in the predictions of the model.

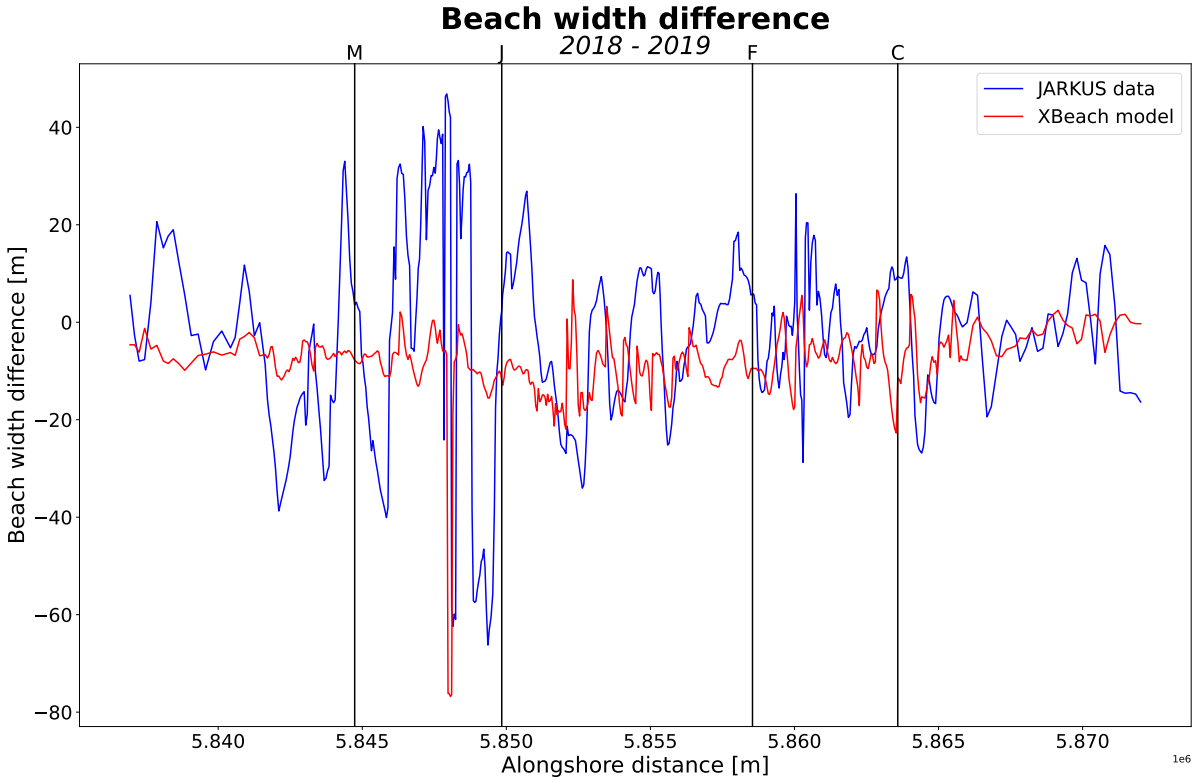

Figure E.9: Comparison between the results of the XBeach model and the measurements. These figures are the results of 2018 - 2019. The black vertical lines indicate the transects as indicated in the figures for the bed level change. A negative beach width difference means a reduction.

In the last year considered in this study, some similarities can be seen, especially in the area between F and J. However, south of transect M, that is, to the left of the first black vertical line, it appears that the predictions do not match the reality. In general, the measurements show larger variations than the predictions based on the XBeach model.

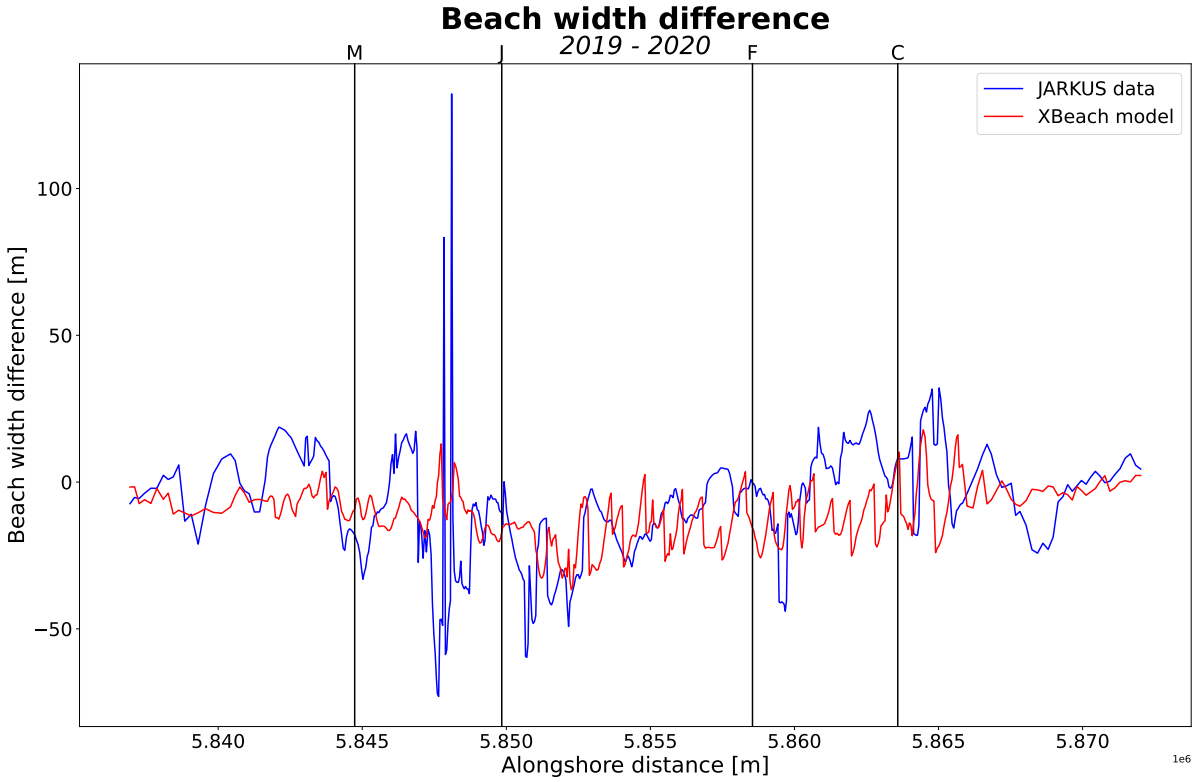

Figure E.10: Comparison between the results of the XBeach model and the measurements. These figures are the results of 2019 - 2020. The black vertical lines indicate the transects as indicated in the figures for the bed level change. A negative beach width difference means a reduction.